NISTIR 3982

QUANTIFYING STANDARD PERFORMANCE OF ELECTROMAGNETIC-BASED MINE DETECTORS

William L. Gans
Richard G. Geyer
Wilfred K. Klemperer

NIST **United States Department of Commerce**
National Institute of Standards and Technology

NISTIR 3982

QUANTIFYING STANDARD PERFORMANCE OF ELECTROMAGNETIC-BASED MINE DETECTORS

William L. Gans
Richard G. Geyer
Wilfred K. Klemperer

Electromagnetic Fields Division
Electronics and Electrical Engineering Laboratory
National Institute of Standards and Technology
Boulder, Colorado 80303-3328

October 1991

U.S. DEPARTMENT OF COMMERCE, Robert A. Mosbacher, Secretary
NATIONAL INSTITUTE OF STANDARDS AND TECHNOLOGY, John W. Lyons, Director

Table of Contents

List of Tables

List of Figures

QUANTIFYING STANDARD PERFORMANCE OF ELECTROMAGNETIC-BASED MINE DETECTORS

William L. Gans, Richard G. Geyer, and Wilfred K. Klemperer
National Institute of Standards and Technology
Boulder, Colorado 80303

This is a final report to sponsor on work performed by National Institute of Standards and Technology (NIST) personnel from January 1, 1985 to December 31, 1990. An overview of the theory of the electromagnetic properties of soils is presented along with a brief review of existing technologies for the detection of buried objects using electromagnetics. The critical electromagnetic performance factors for portable EM mine detectors that NIST has identified are presented, along with a discussion of measurement systems for measuring the constitutive properties of soil and mine-like materials. Recommendations are then presented for a measurement system configuration that should meet most of the Army's requirements. A recommended mine detector testing strategy is then presented along with a set of instructions for specific tests and an alogrithm for comparatively scoring the performance of detectors. The tests and the scoring algorithm are as specific and as detailed as is possible at this stage of development. Last, a section is included that contains NIST's recommendations for the test data that should be archived.

Keywords: buried object; constitutive properties; conductivity; dielectric constant; dielectric loss; elecromagnetic detection; mine; mine detector; permeability; permittivity; remote sensing; sensor; target.

I Introduction

The purpose of this final report is to provide documentation describing the work performed by the National Institute of Standards and Technology (NIST) under two sequential contracts to the U.S. Army Belvoir Research, Development and Engineering Center (BRDEC). The first contract period was from January 1, 1985 to September 30, 1988, and the second period was from January 1, 1989 to December 31, 1990. This introduction summarizes the original and modified work statements and contains a brief description of the contents of the remaining chapters of this report. As closely as possible, the title of this report, the table of contents, and the chapter titles are those requested by BRDEC personnel.

A Work Statement Summaries

The original work statement defining the tasks to be performed over approximately a four year period by NIST for BRDEC is outlined below.

Phase I.

1. Create a joint National Academy of Sciences-NIST-U.S. Army review panel to review annually the work performed by NIST.
2. Review information provided by the Army pertaining to past and present mine detection systems, measurement methods, and standards, as necessary.
3. Provide the Army a suggested selection of standard test targets and soil backgrounds.
4. Provide the Army a preliminary set of definitions, parameters to be controlled, and standard test conditions.
5. Investigate the possibility of developing a performance effectiveness measure for mine detectors.

Phase II.

1. Recommend a final set of standard test targets.
2. Recommend a final set of standard test soils.
3. Recommend a set of measurement methods to ensure replication of test conditions.
4. Formulate (if possible) a definitive set of effectiveness measures.

Phase III.

1. Specify a measurement system to ensure standard test conditions.
2. Provide an uncertainty estimate for the measurement process.

Phase IV.

1. Provide initial guidance, training, technology transfer.

This original work statement covered the first contract period. The documentation that reported the results of NIST's work during this contract period was presented to the Army at Fort Belvoir in September, 1988, and published as a Restricted, National Institute of Standards and Technology Inter-Agency Report in March, 1990 [1.1].

A summary of the second work statement, as modified over the course of the second contract period, is outlined below.

1. Perform engineering studies, with the assistance of an outside contractor, to choose the optimum material(s) to serve as rigid-matrix soil simulation standards.
2. Produce a small number of rigid-matrix soil standard "bricks" as a "proof of concept," and provide the Army with necessary design specifications for these bricks.
3. Provide the Army with a laboratory measurement system for use in measuring the constitutive EM properties of both standard soil materials and standard target materials.

4. Develop a comprehensive set of performance measures (tests) for mine detectors.

This final report contains the documentation for all of the work performed during both contract periods with one exception. The rigid-matrix brick design and specification work will be given to the Army in a separate report because this work is not yet completed. Also, NIST recognizes that more work is required in order to actually translate this research and development into an operational mine detector test range at Fort Belvoir. Therefore, Chapter IX contains an outline of NIST's recommendations for the future work required in order to achieve this goal.

B Report Description

What follows is a brief, chapter-by-chapter description of the contents of this report.

Chapter II contains a review of the existing theoretical relationships between electromagnetic fields and matter.

Chapter III contains a discussion of critical electromagnetic performance factors for portable mine detectors that NIST personnel have identified.

Chapter IV contains a review of past and present methods developed for the measurement of the constitutive properties of materials relevant to electromagnetic mine detection, including the methods used at NIST along with some representative data. Also included in this chapter is a brief description of the measurement system that we have chosen for delivery to the Army.

Chapter V contains a comprehensive review of the existing theory and practices related to the electromagnetic properties of soils, the options for realizing soil or soil-like standards (with advantages and disadvantages discussed for each option), and a description of NIST's recommendations for achieving optimal soil standards by use of rigid-matrix brick soil simulations.

Chapter VI contains a discussion of the desired properties for mine-replica target standards along with NIST's recommendations for both plastic and metal standards. Included is a description of how the standards were fabricated along with possible commercial sources for the required materials.

Chapter VII contains a description of the mine detector testing strategy that has been developed and recommended by NIST, along with our reasons for creating and recommending it. This is followed by a description of seven objective core tests for EM mine detectors that NIST recommends that the Army implement as soon as is practical. The descriptions for these tests are both as general as is possible, allowing the Army to configure them, as requested by the Army, to any of the soil and target standards options discussed in chapters V, and VI, and as detailed as possible considering the fact that the Army has not yet committed to a specific test range configuration. Also included in this chapter are more general descriptions of a set of advanced (more difficult to implement) tests that NIST recommends be implemented after the army has

implemented and gained experience with the first core set. Last, an algorithm for objectively quantifying (scoring) the comparative performance effectiveness of portable, EM mine detectors is presented, along with a recommendation for how to include the required subjective evaluation aspects into the algorithm.

Chapter VIII contains a discussion and a listing of all of the data that NIST has identified which should be permanently recorded in order to maintain adequate records for both individual mine detector tests and the maintenance of the test range as a whole.

Chapter IX contains an outline of NIST's recommendations for future work.

Along with the references cited at the end of each chapter, there is a comprehensive, alphabetized bibliography included at the end of this report. Also included at the end of this report is a brief, alphabetized Glossary of Terms.

References (I)

[1.1] Gans, W. L.; Geyer, R. G.; Klemperer, W. K. Suggested Methods and Standards for Testing and Verification of Electromagnetic Buried Object Detectors. National Institute of Standards and Technology NISTIR 89-3915R; 1990.

II Fundamental Electromagnetic Field-Matter Relationships

A Physical Concepts Governing Electromagnetic Behavior

Any material is electromagnetically characterized by its permittivity ε in F/m, magnetic permeability μ in H/m, and electrical conductivity σ in S/m. Maxwell's equations, together with the constitutive equations relating field quantities in terms of material properties, completely govern electromagnetic wave propagation and behavior in that medium. Therefore, the use of electromagnetic energy to detect buried objects must involve detecting differences between the object and the surrounding medium in one or more of the above quantities.

The constitutive equations for a linear, homogeneous, and isotropic medium may be expressed in the frequency domain as

$$\begin{aligned} \vec{\mathbf{B}} &= \mu \vec{\mathbf{H}}, \\ \vec{\mathbf{J}} &= \sigma \vec{\mathbf{E}}, \\ \vec{\mathbf{D}} &= \varepsilon \vec{\mathbf{E}}, \end{aligned} \tag{2.1}$$

where $\vec{\mathbf{B}}$ is the magnetic flux density (Wb/m^2) related to the magnetic field intensity, $\vec{\mathbf{H}}$ (A/m), by the magnetic permeability; $\vec{\mathbf{J}}$ is the current density (A/m^2) related to the electric field intensity, $\vec{\mathbf{E}}$ (V/m), by the conductivity; and $\vec{\mathbf{D}}$ is the electric flux density, (C/m^2) related to the electric field by the permittivity. Any deviation from linearity is usually included by making ε, μ, or σ field dependent. For anisotropic media, ε, μ, and/or σ become 3×3 tensor matrixes as opposed to constants or scalar functions of frequency.

The solution of Maxwell's equations yields all of the quantities that describe the propagation of electromagnetic waves in terms of the propagation constant, k, where

$$k^2 = \omega\mu(\omega\varepsilon - j\sigma). \tag{2.2}$$

In general, the constituent electrical properties may be written as complex quantities; that is,

$$\begin{aligned} \varepsilon &= \varepsilon' - j\varepsilon'', \\ \sigma &= \sigma' + j\sigma'', \text{ and} \\ \mu &= \mu' - j\mu''. \end{aligned} \tag{2.3}$$

The imaginary part of the propagation constant contains all necessary information about energy loss in a material medium during wave propagation. If, for the moment, magnetic properties are ignored, we may consider only the complex forms of ε and σ in eq (2.2):

$$\omega(\varepsilon' - j\varepsilon'') - j(\sigma' + j\sigma'') = (\sigma'' + \omega\varepsilon') - j(\sigma' + \omega\varepsilon''). \tag{2.4}$$

Here $(\omega\varepsilon' + \sigma'')$ may be considered an effective real permittivity and $(\sigma' + \omega\varepsilon'')$ as an effective conductivity. The $(\sigma' + j\sigma'')$ physically represents carrier transport due to Ohmic and Faradaic diffusion mechanisms, whereas the $(\varepsilon' - j\varepsilon'')$ represents dielectric relaxation mechanisms. The loss tangent is defined from eq (2.4) as

$$\tan\delta = \tan\left(\psi + \frac{\pi}{2}\right) = \frac{\sigma' + \omega\varepsilon''}{\sigma'' + \omega\varepsilon'}, \tag{2.5}$$

where ψ is the phase angle between $\vec{\mathbf{E}}$ and $\vec{\mathbf{J}}$. If there are no dielectric losses, $\varepsilon'' \to 0$. Similarly, if there are no Faradaic diffusion losses, $\sigma'' \to 0$. Hence,

$$\tan\delta = \frac{\sigma'}{\omega\varepsilon'}, \tag{2.6}$$

which physically describes the Ohmic losses.

What follows in this chapter is a detailed discussion of the dielectric and magnetic properties of those materials relevant to this project.

B Dielectric Polarization Mechanisms

We can describe the dielectric properties of a material by the complex dielectric constant, $\varepsilon = \varepsilon' - j\varepsilon''$, where ε' contains all the information about energy storage and ε'' contains all of the information about energy loss (both Ohmic and dielectric losses) in the material during wave propagation. The dialectric constant of a soil is the real effective permittivity of the soil normalized with respect to the permittivity of a vacuum, ε_0.

The quantity ε' is a measure of the amount of polarization in the material. There can be a number of different polarizing mechanisms present; each has a characteristic relaxation frequency and an associated dielectric dispersion centered around this relaxation frequency. Figure 2.1 illustrates the dispersions of dielectric constant and conductivity that are observed in materials in the frequency range of 10^3 to 10^{15} Hz. At the highest frequencies, the polarizing species in a material are the electrons. Electronic polarization occurs when an applied electric field causes a net displacement of the electron cloud of an atom with respect to its nucleus. At frequencies below about 10^{13} Hz, there is also a contribution from atomic polarization. Atomic

polarization occurs in structures (molecules or solutions, for example) in which atoms do not share electrons equally and electric fields displace the electron clouds preferentially towards the stronger binding atoms. It also occurs when charged atoms are displaced with respect to each other. Dipolar polarization, that is, the orientation of polar molecules (molecules with asymmetric charge distributions), occurs at frequencies below about 10^{10} Hz [2.1].

At frequencies below about 10^5 Hz, various types of charge polarizations occur which may be collectively referred to as Maxwell-Wagner mechanisms [2.2, 2.3]. One of these, interfacial (space-charge) polarization, occurs when migrating charge carriers are trapped or impeded in their motion by local chemical or electric potentials, causing local accumulations of charge and a macroscopic field distortion. Another low-frequency mechanism that can occur in soils is due to mixtures of materials that have differing electrical properties (such as conducting spheres embedded in a dielectric). Several different equations are available to describe the resultant properties [2.4, 2.5] for various geometries of the embedded conductor: conducting spheres or rods in a dielectric, alternating layers of dielectrics and conductors, for example. The common cause of these effects is the distributions of charge that occur at conductor-dielectric boundaries and the resultant action under applied electric fields which can yield very large, low-frequency dielectric constants. This mechanism, when we use synthetic soils whose conductivities are controlled by embedded conductors, is very important to examine and to relate to dispersion phenomena normally confronted in natural soil environments. This is true particularly when performance testing of broadband land mine detection systems is done and a relative detector figure of merit is estimated (broadband in this case means that the bandwidth extends into frequencies less than 1 MHz).

Still another dispersion mechanism for dielectric behavior at low frequencies, which is often distinguished from Maxwell-Wagner effects, is that which occurs in colloidal suspensions. Maxwell-Wagner effects are based on the assumption that the charge around conducting particles in a dielectric medium is a thin coating which is much smaller than the particle dimensions [2.5] and that the charge responds to an applied electric field independently of the charge on nearby particles. In colloidal suspensions, on the other hand, the charge layer is on the same order of thickness as or larger than the particle dimensions; hence it is affected by the charge distributions of adjacent particles. The theory of dispersion phenomena in colloidal suspensions is presently a fertile area of research. Dukhin [2.5] has shown that colloidal responses result in far higher low-frequency dielectric constants than those resulting from typical Maxwell-Wagner mechanisms, with dielectric constants on the order of 10^5 not uncommon. This could be an important phenomenon that spectrally increases the visibility of buried plastic land mines when broadband system performance is considered.

C Dielectric Relaxation

Polarization processes occurring in material media as a result of electromagnetic wave propagation are physically damped by relaxation. This relaxation is analogous to a critically damped or overdamped oscillator. In the relaxation process, maximum energy is dissipated at a preferred relaxation frequency, or resonance (which is the reciprocal of the relaxation time constant), with no dissipation at either zero or infinite frequency. Relaxation processes are the only ones observed in the natural soil environment at microwave frequencies and below. Thus, it would be useful to consider some relaxation models (cited in subsequent comments on soil specifications for broadband systems). The following relaxation models are based on the general equation of charge motion

$$\ddot{q} + (\mu\sigma)^{-1}\dot{q} + (\mu\varepsilon)^{-1}q = 0, \tag{2.7}$$

where q is the charge, and $\cdot$ represents differentiation with respect to time. All derivatives are with respect to time. An important current research area is considering diffusion of charged ions whose concentration is spatially variable. For this case, spatial derivatives must be taken in determining diffusion relaxation and this leads to generalized distributed impedances and nonlinear behavior [2.6].

C.1 Debye Relaxation

Debye relaxation occurs in materials that have single relaxation time constants. Relative complex permittivity in a Debye material is given by [2.7, 2.8]

$$\begin{aligned}\varepsilon' - j\varepsilon'' &= \varepsilon_\infty\left[\frac{(\varepsilon_s - \varepsilon_\infty)/\varepsilon_\infty}{1 + j\omega\tau} + 1\right] \\ &= \varepsilon_\infty + \frac{\varepsilon_s - \varepsilon_\infty}{1 + \omega^2\tau^2} - j\frac{(\varepsilon_s - \varepsilon_\infty)\omega\tau}{1 + \omega^2\tau^2},\end{aligned} \tag{2.8}$$

where ε_s is the measured relative real effective permittivity at dc ($\varepsilon_{dc} = \varepsilon_s\varepsilon_0$), ε_∞ is the relative dielectric permittivity at infinite frequency ($\varepsilon_{infinite} = \varepsilon_\infty\varepsilon_0$). τ is the time constant of relaxation, and ε_0 is the free space or vacuum permittivity (8.854×10^{-12} F/m).

C.2 Generalized Relaxation Distributions

Wyllie [2.9] has given an expression for material media in which multiple relaxations or distributions of relaxations are found. Such behavior is more typical of soils at frequencies below 1 MHz than Debye behavior, and the complex dielectric permittivity may be written

$$\varepsilon' - j\varepsilon'' = \varepsilon_\infty + (\varepsilon_s - \varepsilon_\infty)\int_0^\infty \frac{D(\tau)(1 - j\omega\tau)}{1 + \omega^2\tau^2} d\tau, \tag{2.9}$$

where $D(\tau)$ is the time constant distribution function normalized so that

$$\int_0^\infty D(\tau) d\tau = 1.$$

A commonly observed simple relaxation distribution in soils is the Cole-Cole distribution [2.10]. In the Cole-Cole distribution, eq (2.9) reduces to

$$\varepsilon' - j\varepsilon'' = \varepsilon_\infty + \frac{\varepsilon_s - \varepsilon_\infty}{1 + (j\omega\tau)^{1-m}}, \tag{2.10}$$

where $0 \le m \le 1$. The $m = 0$ case corresponds to a Debye material that has a single relaxation. The $m = 1$ case corresponds to an infinitely broad, continuous distribution (one that has no relaxation). Usually $1 - m = c \le 0.25$ for water-saturated soils, and the exact power-law exponential frequency behavior is critically dependent on water saturation, as discussed later in this report. (c is a constant defined in the next section and related to m as above.) This would necessitate methods for keeping c constant (as a function of frequency) in natural (or synthetic water saturated) soils when testing of land mine detectors is performed.

C.3 Non-Debye Behavior of Rocks and Soils

Examples of studies showing the non-Debye behavior of rocks and soils are given by Saint-Amant and Strangway [2.11], Alvarez [2.12], Olhoeft et al. [2.13], Pelton et al. [2.14], Knight [2.15], and Lockner and Byerlee [2.16]. Observed deviations from Debye behavior have led to modifications of the Debye equation [2.12], including the Cole-Cole expression, eq (2.10) and the corresponding Cole-Cole equivalent circuit [2.10]. The significant feature of the Cole-Cole circuit is the inclusion of a constant phase circuit element to model a distribution of relaxation times. The Cole-Cole expression has been found useful in fitting data from lunar soil samples [2.13], and an expression for the complex impedance of a material (as measured in the series mode) that contains a term analogous to the constant phase element in Cole-Cole [2.10] has been used in modeling the impedance of mineralized rocks [2.14, 2.17].

In addition to the Cole-Cole expression, there are three other empirical relations commonly used to describe a non-Debye response. These are the Cole-Davidson [2.18], the combined Cole-Cole, and the Williams-Watts [2.19] expressions. A characteristic feature of all these empirical relations, besides being based on eq (2.7), is that at frequencies away from the relaxation frequency they reduce to expressions showing a power-law dependence on frequency for both ε'

and ε''. This common characteristic led Jonscher [2.20, 2.21] to define this power-law dependence as the "universal dielectric response," that is,

$$\varepsilon'(\omega) = K\omega^{-c}, \tag{2.11}$$

where K and c are constants that depend on the sample material and texture.

D Dielectric Properties of Pure Water

Usually, natural soils contain water, so the way in which dielectric constants combine is important in determining the bulk, or effective, dielectric constant of the soil at hand. The bulk dielectric constant of any soil (whether natural or synthetic) determines the electromagnetic visibility of buried land mines and, therefore, intrinsically affects the performance of any detection system. Before discussion of water saturation of heterogeneous soil mixtures, it is necessary to review fundamental dielectric behavior of pure and saline water.

The frequency dependence of the complex dielectric constant of pure water, ε_w, is well known and is given by the Debye equation [2.1, 2.7],

$$\varepsilon_w(\omega) = \varepsilon_{w\infty} + \frac{\varepsilon_{w0} - \varepsilon_{w\infty}}{1 + j\omega\tau_w}, \tag{2.12}$$

where

$\varepsilon_{w\infty}$ = high frequency (or optical) limit of ε_w (dimensionless),
ε_{w0} = dc dielectric constant of ε_w (dimensionless),
τ_w = relaxation time of pure water (seconds), and
ω = frequency (radians per second).

Equation (2.12) may be simply written

$$\varepsilon_w = \varepsilon'_w - j\varepsilon''_w = \varepsilon'_w(1 - j\tan\delta_w), \tag{2.13}$$

where $\tan\delta_w \equiv \varepsilon''_w/\varepsilon'_w$ is the loss tangent of water.

Rationalization of eq (2.12) yields

$$\varepsilon'_w(\omega) = \varepsilon_{w\infty} + \frac{\varepsilon_{w0} - \varepsilon_{w\infty}}{1 + (\omega\tau_w)^2}, \tag{2.14}$$

and

$$\varepsilon''_w(\omega) = \frac{\omega\tau_w(\varepsilon_{w0} - \varepsilon_{w\infty})}{1 + (\omega\tau_w)^2}, \tag{2.15}$$

The magnitude of the high-frequency dielectric constant $\varepsilon_{w\infty}$ has been determined by Lane and Saxton [2.22] to be

$$\varepsilon_{w\infty} = 4.9 \tag{2.16}$$

and is practically temperature independent. The relaxation frequency of pure water, $f_w = 1/(2\pi\tau_w)$, occurs in the microwave region and is temperature dependent. At 0°C, $f_w \approx 9$ GHz and at 20°C, $f_w \approx 17$ GHz. Equation (2.15) shows that ε''_w has its maximum value at $\omega = 2\pi f_w$. A plot of the frequency variation of ε'_w and ε''_w for pure water at 25°C is shown in figure 2.2 [2.4]. A Cole-Cole plot of ε''_w versus ε'_w, with f as a variable parameter, is shown in figure 2.3 for pure water at T = 0°C [2.23]. This plot is a semicircle with end points defined by $\varepsilon_w = \varepsilon_{w0}$ in the low-frequency limit and by $\varepsilon_w = \varepsilon_{w\infty}$ in the high-frequency limit. The point on the circle at which ε''_w is maximum occurs at the relaxation frequency, $f = f_w$, whose coordinates are simply given by

$$\varepsilon'_w = \frac{(\varepsilon_{w0} + \varepsilon_{w\infty})}{2} \text{ and } \varepsilon''_w = \frac{(\varepsilon_{w0} - \varepsilon_{w\infty})}{2}.$$

The dc dielectric constant of nonconductive water, ε_{w0}, is a function of temperature. Klein and Swift [2.24] have generated a regression fit for $\varepsilon_{w0}(T)$ from dielectric measurements conducted between 1 GHz and 3 GHz,

$$\varepsilon_{w0}(T) = \varepsilon'_{w0}(T) = 88.045 - 0.4147T + 0.6295 \times 10^{-3} T^2, \tag{2.17}$$

where T is in °C, and the loss term, ε''_{w0}, is 0.

E Dielectric Properties of Saline Water

Although the dielectric properties of pure water and ice obey the Debye relaxation equations and are fairly well understood, ionic salts dissolved in water produce an electrolytic solution whose microwave dielectric properties may differ greatly from those of pure water. The salinity S of a solution is defined as the total mass of solid salt in grams dissolved in 1 kg solution. Thus, S is normally expressed in parts per thousand by mass. Little will be said about broadband dielectric characterization of electrolytic solutions, except that the real and imaginary parts of the dielectric constant of a saline water solution are given by [2.24, 2.25]

$$\varepsilon'_{sw} = \varepsilon_{sw\infty} + \frac{\varepsilon_{sw0} - \varepsilon_{sw\infty}}{1 + (\omega\tau_{sw})^2} \tag{2.18}$$

and

$$\varepsilon''_{sw} = \frac{\omega\tau_{sw}(\varepsilon_{sw0} - \varepsilon_{sw\infty})}{1+(\omega\tau_{sw})^2} + \frac{\sigma_i}{\varepsilon_0\omega}, \tag{2.19}$$

where the subscript *sw* refers to saline water and σ_i is the ionic conductivity of the aqueous solution in S/m. The form of the complex permittivity for saline water differs from that of pure water only in the loss term, ε''_{sw}, where the added term, $\sigma_i/\varepsilon_0\omega$, resulting from the ionic conductivity of the aqueous solution is present. The ionic conductivity of saline water has a marked effect on the loss factor ε''_{sw} below 10 GHz. Therefore, high soil salinity will probably significantly affect the dielectric properties of wet soil. As Jedlicka [2.26] notes, few measurements and analyses have been reported relating soil salinity to effective soil dielectric constant. Consequently, the dependence of permittivity on soil salinity is not well understood. We do know, however, that the salinity of (free) pore water within a soil matrix depends directly on the cation exchange capacity of the matrix material. This fact should provide a direct relationship between soil type, amount of volumetric moisture present, and effective soil complex permittivity. Further work will enhance understanding between these physical soil parameters and measured electromagnetic properties.

Stogryn [2.27] points out that there is no evidence to indicate that $\varepsilon_{sw\infty}$ depends on salinity; hence, we are safe to assume that $\varepsilon_{sw\infty} = \varepsilon_{w\infty} = 4.9$. He also empirically determines the dependence of permittivity on both the temperature and salinity of saline water by writing $\varepsilon_{sw\infty}$ as a factorable product, $\varepsilon_{sw0}(T, S) = \varepsilon_{sw0}(T)F(S)$. Polynomial fits to this relation have been obtained [2.24, 2.28] on measurements performed by Ho and Hall [2.29] and Ho, *et al.* [2.30] for $4 < S < 35$ to obtain the following functional (nonmultiplicative) dependence of the dielectric constant of water with respect to salinity,

$$\varepsilon'_{sw0}(T, S) = \varepsilon'_{w0}(T) - 0.1556 - 4.13\times10^{-4}S + 1.58\times10^{-6}S^2 \tag{2.20}$$

and

$$\varepsilon''_{sw0}(T, S) = \varepsilon'_{sw0}\tan\delta_{sw0} = 5.66 + 2.65\times10^{-3}S - 4.5\times10^{-6}S^2. \tag{2.21}$$

Equations (2.17), (2.20) and (2.21) will be used in subsequent development relating effective dielectric constant measurements (real part, ε', and loss tangent, $\tan\delta$) of a lossy fluid-saturated soil mixture to the *in situ* fluid dielectric properties, as well as to the water-filled porosity of the soil mixture.

Several figures are included here to illustrate the relationship between the addition of salts to pure water and the dielectric properties of the resulting solution. Figure 2.4 [2.31] is a plot of dc dielectric constant, ε_{sw0}, versus solution concentration for three different salts. Figure 2.5 [2.31] is a plot of normalized relaxation time for a NaCl solution versus salt concentration at

25°C. Figure 2.6 [2.31] is a plot of the depression (change) of dielectric constant and relaxation time for a NaCl solution versus salt concentration at 0°C, 20°C, and 40°C. These figures show that the presence of salt(s) in water (and thus in damp or wet soils) can drastically change the medium's dielectric constant.

F Heterogeneous Soil Mixtures

By definition, natural soils are mixtures of host matrix mineral(s), air, and water. Generally, the real part of the effective dielectric constant, ε'_{eff}, of the mixture rarely exceeds 8 in the microwave region—as long as there is no liquid water in the mixture. Similarly, the imaginary part ε''_{eff}, usually does not exceed 1 in the absence of liquid water. By way of comparison, we see from figure 2.2 that ε'_w of water is one order of magnitude larger than the relative permittivity of dry materials, whereas ε''_w is two orders of magnitude larger than that of dry materials, particularly at frequencies less than 2 GHz. Because of the large contrast between (complex) ε of the pore water and that of the host matrix in soils, the dielectric constant of the mixture is generally dominated by the dielectric behavior of water. For this reason, many investigators [2.22, 2.27, 2.32, 2.33] have generalized the Debye formulas given by eqs (2.14) and (2.15) to mixtures in the following way,

$$\varepsilon'_{eff} = \varepsilon_{eff\infty} + \frac{(\varepsilon_{eff,0} - \varepsilon_{eff,\infty})}{1+(\omega\tau_{eff})^2}, \tag{2.22}$$

$$\varepsilon''_{eff} = \omega\tau_{eff}\frac{(\varepsilon_{eff,0} - \varepsilon_{eff,\infty})}{1+(\omega\tau_{eff})^2}, \tag{2.23}$$

where $\varepsilon_{eff,0}$, $\varepsilon_{eff,\infty}$, and τ_{eff} are functions of the dielectric constant of the matrix mineral(s), the water saturation, *Sw*, fraction in the pore space of the matrix, and the shape and orientation of the water inclusions. The dielectric constants of the matrix minerals are presumed to be nondispersive (frequency independent or lossless) as well as independent of the applied direction (polarization) of the incident electric field. However, caution must be exercised in the use of eqs (2.22) and (2.23) for soil mixtures over a broad range in frequency, since multiple relaxation phenomena not taken into account by the Debye rules can occur [2.1].

An example of a typical power-law variation of the dielectric constant as a function of water saturation for a consolidated sandstone is shown in figure 2.7 (recalling eq 2.11). As the saturation decreases from full saturation, the power-law exponent, c, increases until at some critical saturation point (usually $Sw \doteq 0.2$ for critical saturation) it drops rapidly to near 0. Most

surface sands would probably fall below critical saturation, whereas most clay soils might fall in the region above critical saturation.

Typical behavior of dielectric constant as a function of both water saturation and frequency is shown in figure 2.8. The observed dependence of ε'_H on *Sw* shows that it increases rapidly up to a critical water saturation, whereupon it increases more gradually and linearly with increasing saturation. For a completely dry soil and one which is only a single component system, ε' goes to some threshold value independent of frequency. For a water saturation above critical saturation, ε' not only changes less with increasing frequency, but also has a lower value, almost by a factor of 4, from 50 kHz to 1 MHz. The significance of this observation is that mine detectors operating at differing frequencies are likely to be observing different contrasts in complex permittivity as long as water saturation (or equivalent metallic concentration in a synthetic soil) stays above critical with a greater dielectric contrast skewed toward lower detection frequencies.

Thus, there may be valid reasons to operate in this low frequency range for enhancing dielectric visibility contrast, even at the expense of spatial target resolution. The purpose of drawing attention to these phenomena is (1) to better compare detection systems that have different operating frequencies (whether fixed or broadband) in terms of the actual electrical contrast, $\varepsilon'_H - \varepsilon'_T$, seen between the host soil environment and buried land mine; and (2) to allow the removal of a variable, nonlinear frequency dependence of the soil's electrical properties in the case of water saturated soils by keeping water saturation above the critical point for differing target size and burial depth parameters.

In summary, the functional dependence of c and ε'_H on water saturation in a porous medium is typified by figures 2.7 and 2.8. The actual power-law exponent observed depends on the texture (microgeometry) of the soil and resultant pore surface water or pore surface area-to-volume ratio.

G Magnetic Susceptibility

Magnetic susceptibility is a fundamental physical property of a material medium. The degree to which a body is magnetized when placed in an external magnetic field is given by

$$\vec{\mathbf{M}} = \chi_m \vec{\mathbf{H}}, \qquad 2.24$$

where $\vec{\mathbf{M}}$ is the magnetization in A/m, $\vec{\mathbf{H}}$ is the applied external magnetic field intensity in A/m, and χ_m is the magnetic susceptibility (dimensionless) relating the applied field to the intensity of magnetization. We will use the International System of Units (SI) here.

For a magnetically linear, isotropic substance, the constitutive equation relating the magnetic flux density in Wb/m^2 within a substance to the external magnetic field $\vec{H}$ due to magnetization is simply expressed by

$$\vec{B} = \mu_0(1+\chi_m)\vec{H} = \mu\vec{H}, \tag{2.25}$$

where μ_0 is the permeability in vacuum ($4\pi \times 10^{-7}$ H/m) and χ_m is the dimensionless magnetic susceptibility defined in eq (2.24).

The magnetic susceptibility of soils depends on the component magnetic minerals derived from chemical and mechanical breakdown of bedrock. Magnetic minerals of importance are few, and those most commonly encountered are the iron and titanium oxides which form several solid solution series in rocks (figure 2.9). Depending on the fractional composition of any solid solution series, the susceptibility may vary widely (figure 2.10). In addition to specific chemical composition, the susceptibility depends on grain size and the intensity of the magnetizing field. Thus, considerable variation in the susceptibility of rocks (and soils) can occur.

References (II)

[2.1] Geyer, R.G. Experimental parameters for land mine detection performance evaluations. NIST Report, Project 7232457, 100 p.; November 1987.

[2.2] Maxwell, J.C. A treatise on electricity and magnetism. Dover Pub.; 1891.

[2.3] Wagner, K.W. Erklarung der dielektrischen Nachwirkungsworgange auf Grund Maxwellscher vorstellungen. Archiv. Electrotechnik. 2: 371; 1914.

[2.4] Hasted, J.B. Aqueous dielectrics. London: Chapman and Hall, 302 p.; 1973.

[2.5] Dukhin, S.S. Dielectric properties of disperse systems, in Surface and colloid science, Vol. 3, Matijevic, E., ed. New York, NY: Wiley Interscience, 83-166; 1969.

[2.6] Sluyters-Rehbach, M.; Sluyters, J.H. Sine wave methods in the study of electrode processes, in Electroanalytical Chemistry, Vol. 4, A.J. Bard, ed. New York, NY: Marcel Dekker, 1-128; 1970.

[2.7] Debye, P. Polar molecules. New York, NY: Chemical Catalog Co.; 1899.

[2.8] Smyth, C.P. Dielectric relaxation times in molecular relaxation processes. London: The Chemical Society, 1-14; 1966.

[2.9] Wyllie, G. Dielectric relaxation and molecular correlation in dielectric and related molecular processes. London; The Chemical Society; 1972.

[2.10] Cole, K.S.; Cole, R.H. Dispersion and absorption in dielectrics. J. Chem. Physics. 9: 341-351; 1941.

[2.11] Saint-Amant, M.; Strangway, D.W. Dielectric properties of dry geologic materials. Geophysics. 35: 624-645; 1970.

[2.12] Alvarez, R. Complex dielectric permittivity in rocks: A method for its measurement and analysis. Geophysics. 38: 920-940; 1973.

[2.13] Olhoeft, G.R.; Frisillo, A.L.; Strangway, D.W. Electrical properties of lunar soil sample 15301, 38. J. Geophys. Res. 79: 1599-1604; 1974.

[2.14] Pelton, W.H.; Ward, S.H.; Hallof, P.G.; Sill, W.R.; Nelson, P.H. Mineral discrimination and removal of inductive coupling with multifrequency IP. Geophysics. 43: 588-609; 1978.

[2.15] Knight, R.J. The use of complex plane plots in studying the electrical response of rocks. J. Geomag. Geoelectr. 35: 767-776; 1983.

[2.16] Lockner, D.A.; Byerlee, J.D. Complex resistivity measurements of confined rock. J. Geophys. Res. 90: 7837-7847; 1985.

[2.17] Madden, T.R.; Cantwell, T. Induced polarization, A review, in Mining Geophysics, Vol. 2, A.W. Musgrove, ed., Soc. Explor. Geophys., 373-400; 1967.

[2.18] Davidson, D.W.; Cole, R.H. Dielectric relaxation in glycerol, propylene glycol, and n-propanol. J. Chem. Phys. 29: 1484-1490; 1951.

[2.19] Williams, G.; Watts, D.C. Non-symmetrical dielectric relaxation behavior arising from a simple empirical decay function. Trans. Faraday. Soc. 66: 80-85; 1970.

[2.20] Jonscher, A.K. The interpretation of non-ideal dielectric admittance and impedance diagrams. Phys. Stat. Solutions (a), 32: 665-676; 1975.

[2.21] Jonscher, A.K. The universal dielectric response, a review of data and their new interpretation. Chelsea Dielectrics Group, University of London; 1979.

[2.22] Lane, J.; Saxton, J. Dielectric dispersion in pure polar liquids at very high radio frequencies, III. The effect of electrolytes in solution. Proc., Roy. Soc. 214(A): 531-545; 1952.

[2.23] Hasted, J.B. Liquid water: dielectric properties - Chapter 7 in Water—a comprehensive treatise, I, the physics and chemistry of water. New York: Plenum Press; 1972.

[2.24] Klein, L.A.; Swift, C.T. An improved model for the dielectric constant of sea water at microwave frequencies. IEEE Trans. Antennas Propag. AP-25: 104-111; 1977.

[2.25] Dobson, M.C.; Ulaby, F.T.; Hallikainen, M.T.; El-Rayes, M.A. Microwave dielectric behavior of wet soil, Part II: dielectric mixing models. IEEE Trans. Geosci. Remote Sensing. GE-23(1): 35-46; 1985.

[2.26] Jedlicka, R.P. Saline soil dielectric measurements. M.S. Thesis, New Mexico State University, NM; 1978.

[2.27] Stogryn, A. Equations for calculating the dielectric constant of saline water. IEEE Trans. Microwave Theory Tech. MTT-19: 733-736; 1971.

[2.28] Wharton, R.P.; Hazen, G.A.; Rau, R.N.; Best, D.L. Electromagnetic propagation logging: advances in technique and interpretation. SPE of AIME Annual Technical Conference and Exhibition (Paper SPE 9267), 21-24; September 1980.

[2.29] Ho, W.; Hall, W.F. Measurements of the dielectric properties of sea water and NaCl solutions at 2.65 GHz. J. Geophys. Res. 78: 6301-6315; 1973.

[2.30] Ho, W.W.; Love, A.W.; Valle, J.J. Measurements of the dielectric properties of sea water at 1.43 GHz. NASA Contractor Report CR-2458. NASA Langley Research Center, Langley, VA; 1974.

[2.31] Debye, P. and Huckel, E.Z., Z. Phys. 24: 133, 305; 1923.

[2.32] Pottel, R. Water: A comprehensive treatise, Vol. II, Ed. F. Franks, Plenum Press, New York-London, ch. 17; 1973.

[2.33] Collie, C.H., Ritson, D.M. and Hasted, J.B. J. Chem. Phys., 16(1); 1948.

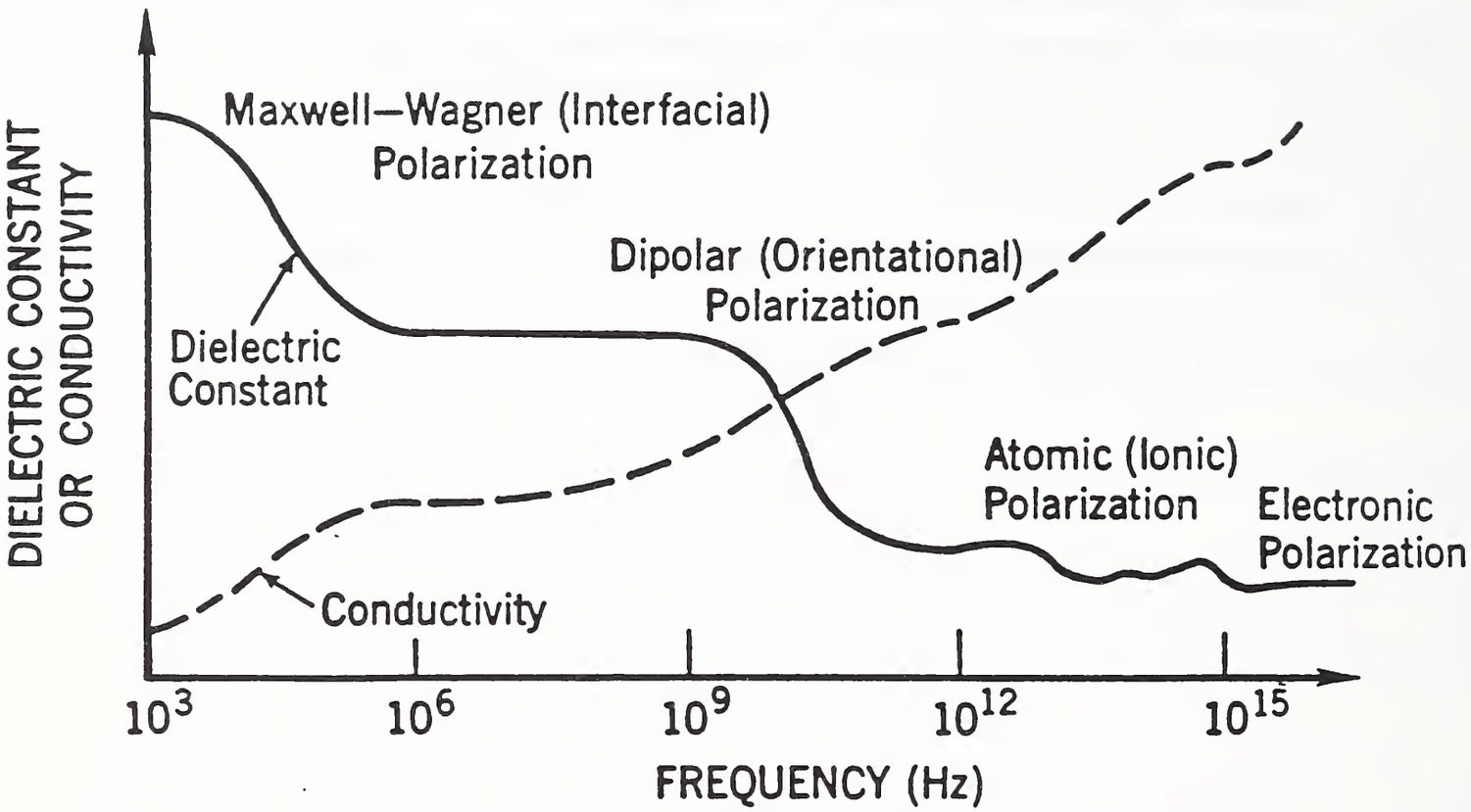

Figure 2.1 Dielectric dispersion for various types of polarization.

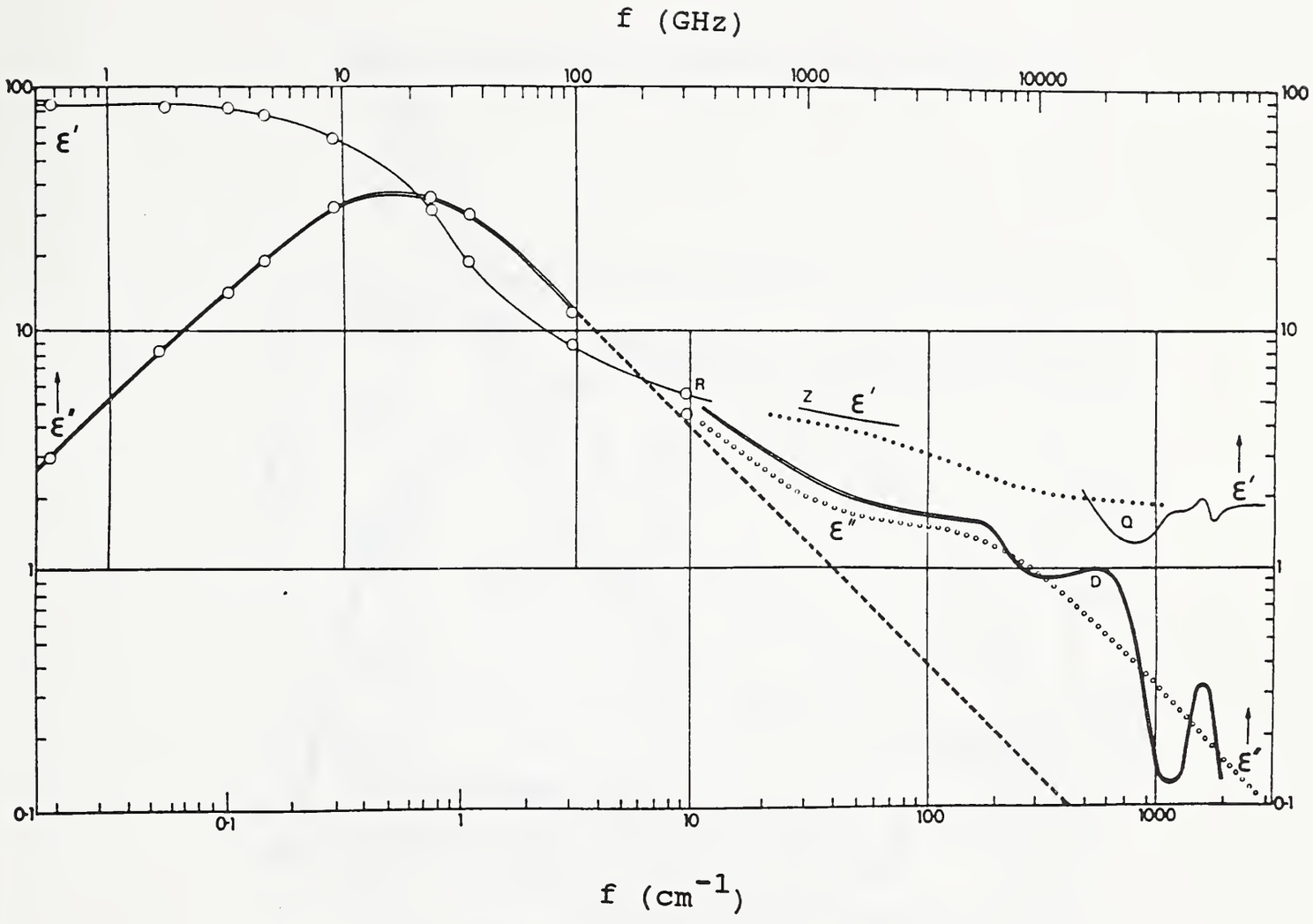

Figure 2.2 Frequency variation of ϵ_w' and ϵ_w'' for pure water at 25°C. Debye equation predicts linear 45° fall-off which appears, above, as the dashed line.

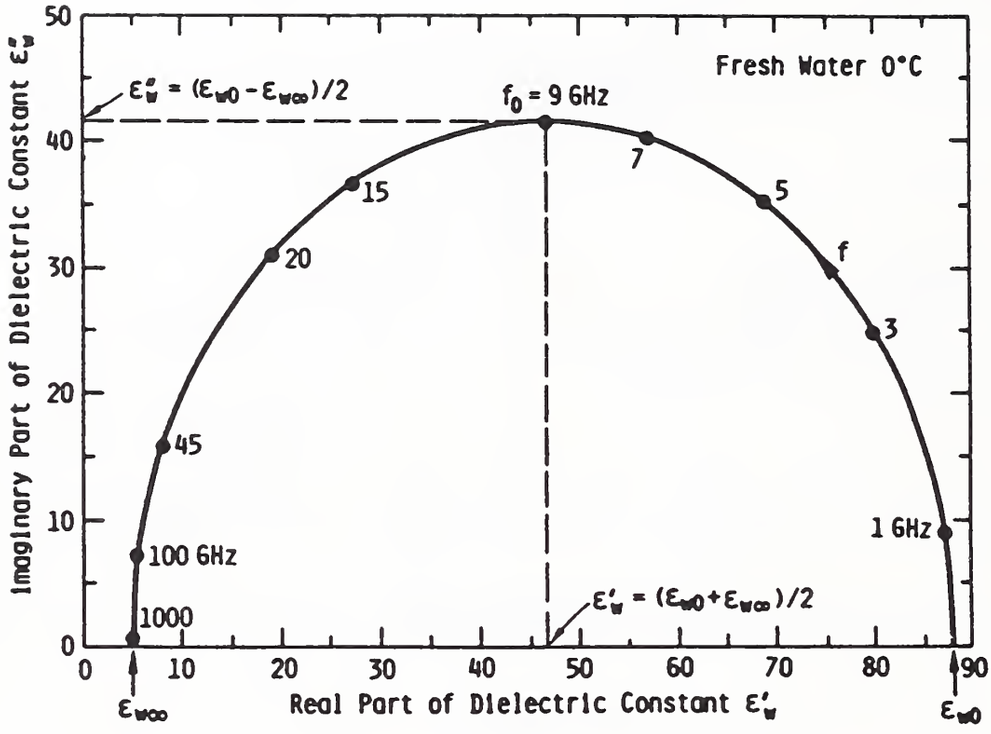

Figure 2.3 Cole-Cole diagram for the dielectric constant of pure water at 0°C.

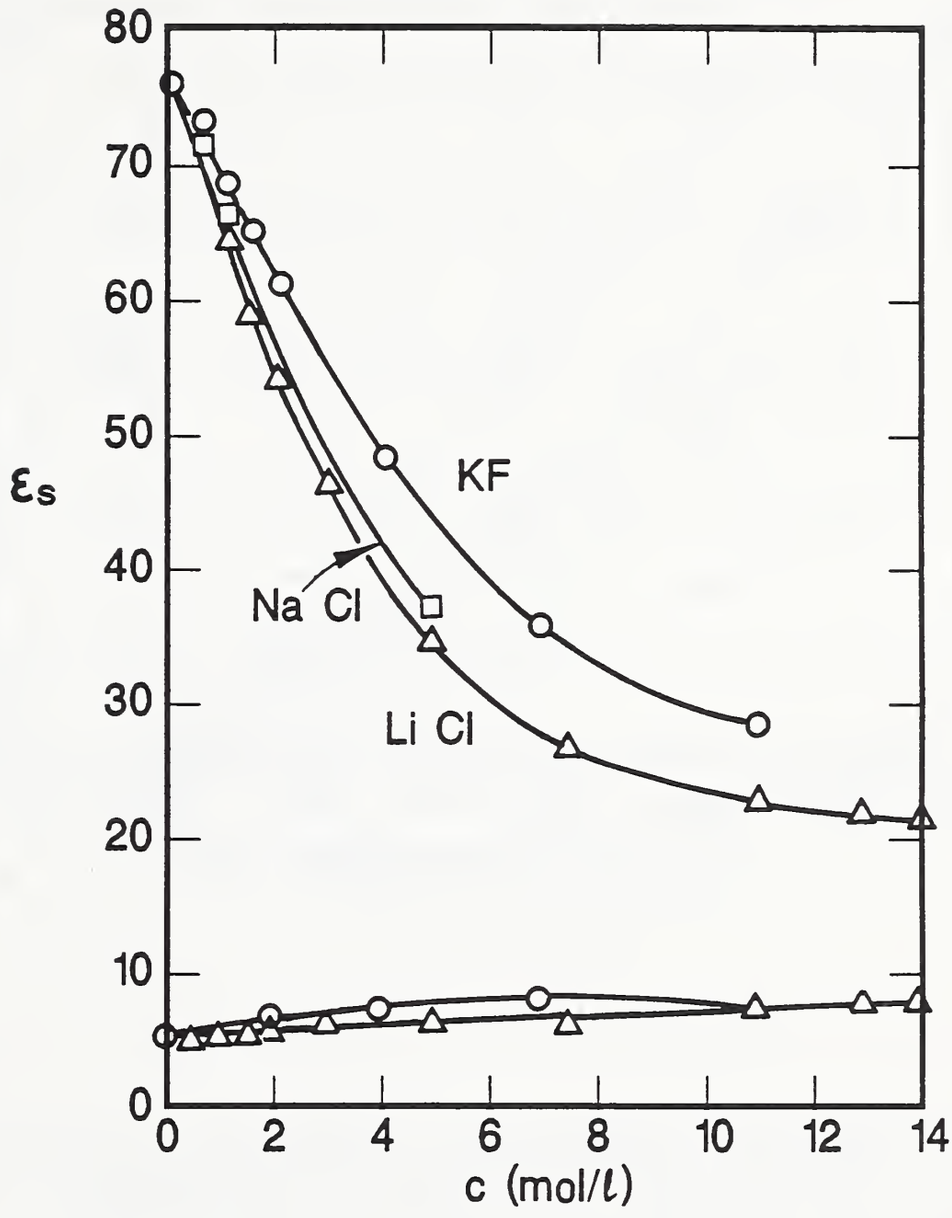

Figure 2.4 Measured concentration dependence of dc dielectric constants for three salts in highly concentrated water solution.

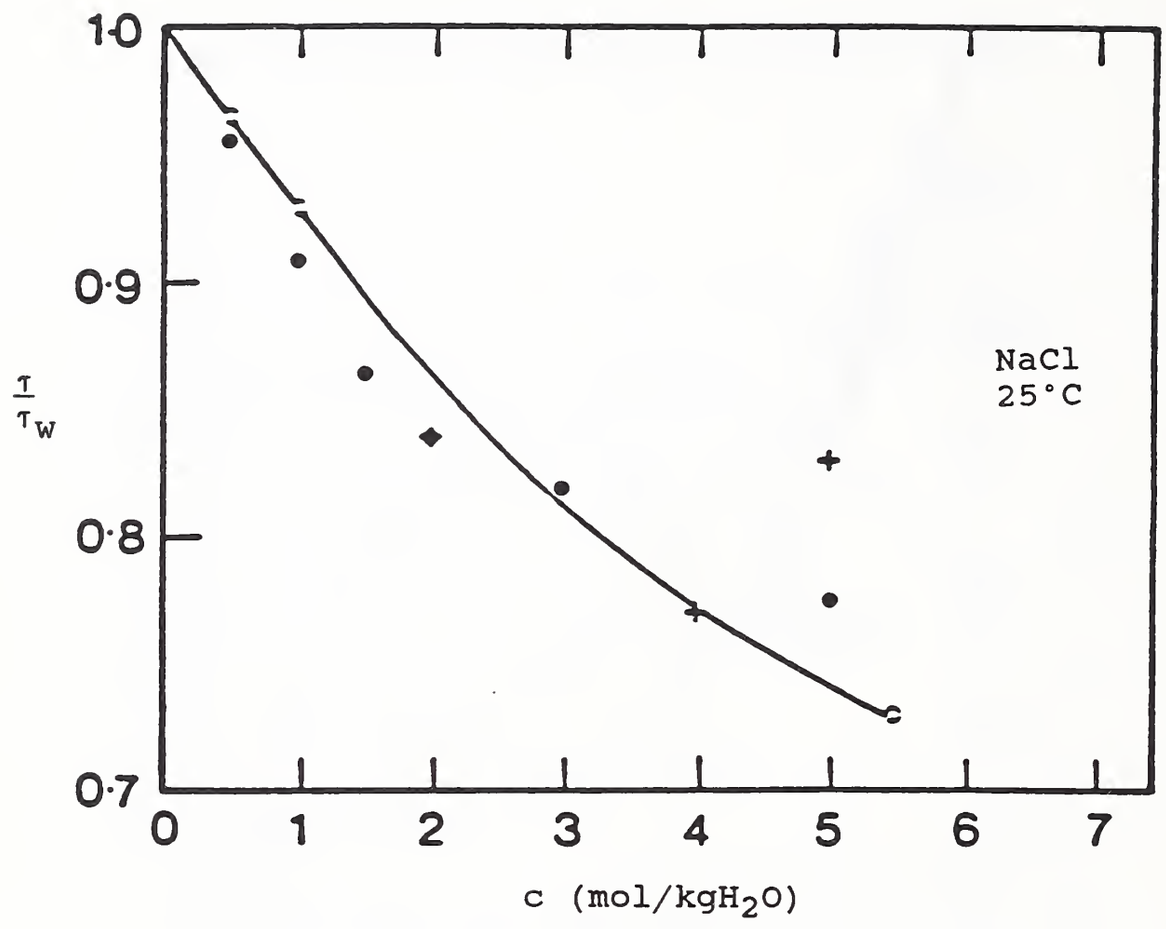

Figure 2.5 Measured concentration dependence of relaxation times of sodium chloride-water solution at 25°C.

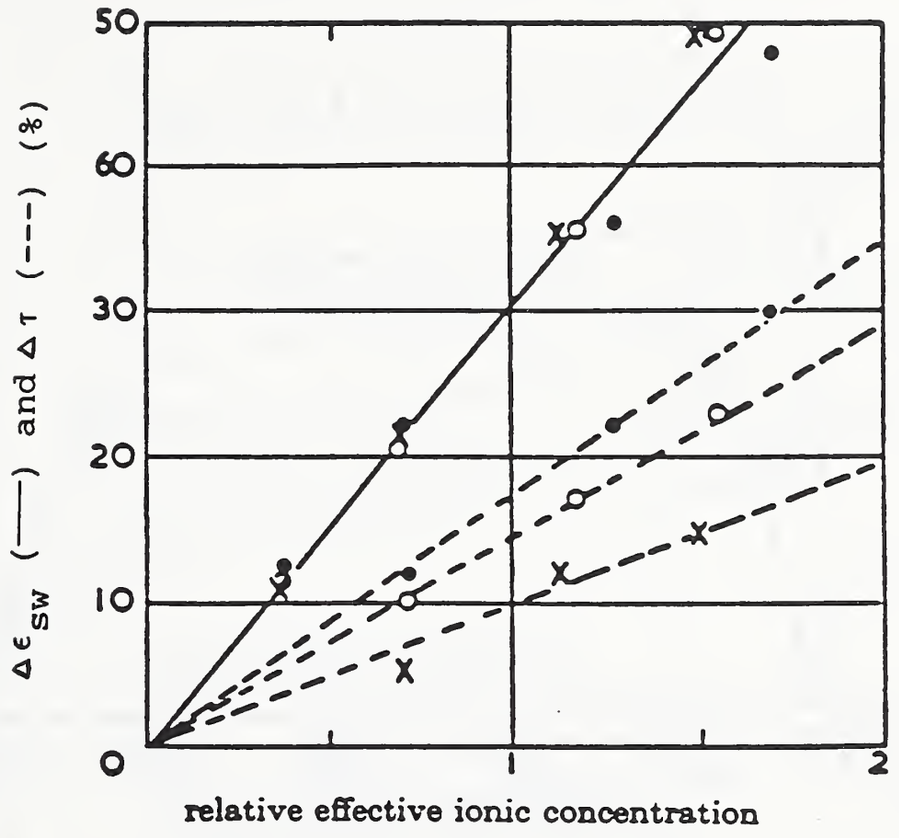

Figure 2.6 Depression of dielectric constant and relaxation time of sodium chloride solutions as a function of ionic concentration. • = 0°C; ◦ = 20°C; x = 40°C.

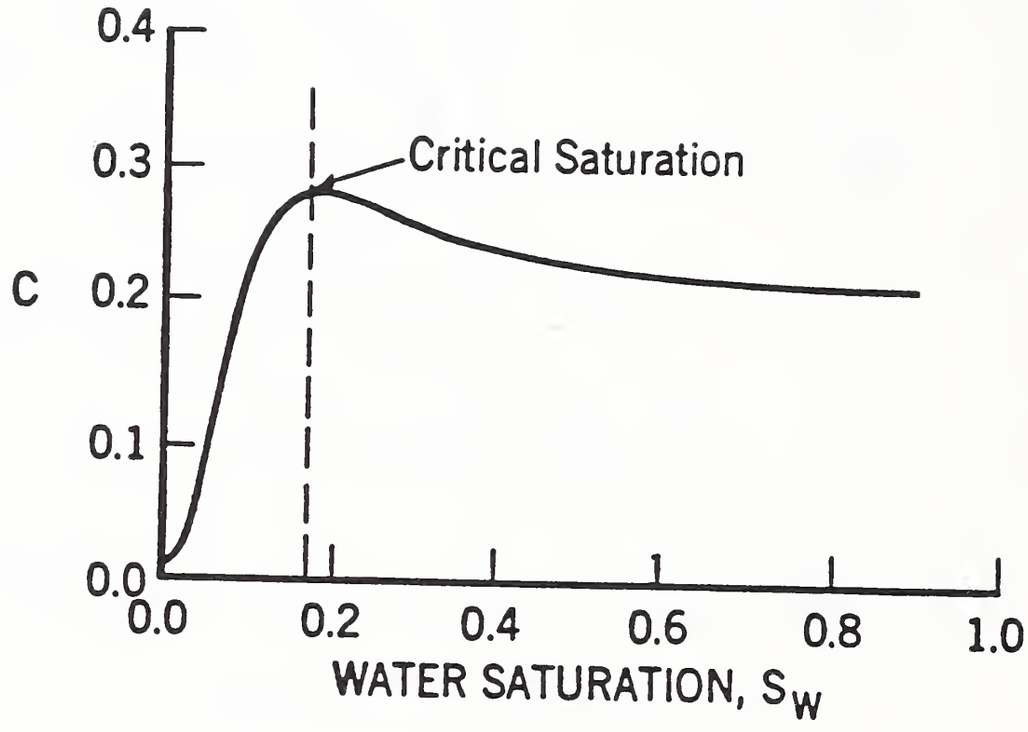

Figure 2.7 Typical power-law exponent variation of dielectric constant as a function of water saturation for a consolidated sandstone.

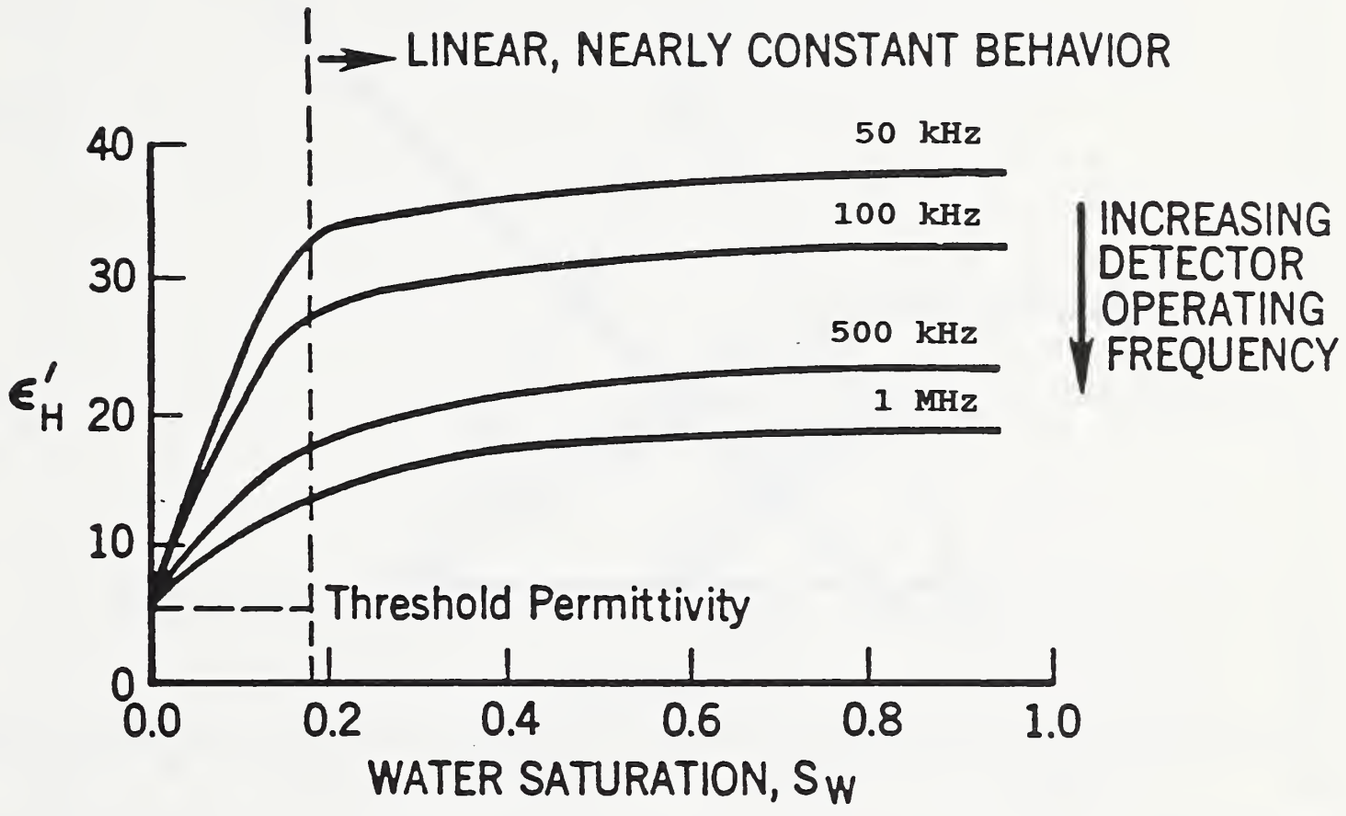

Figure 2.8 Dielectric constant as a function of water saturation for typical sandstone plotted parametrically as a function of frequency.

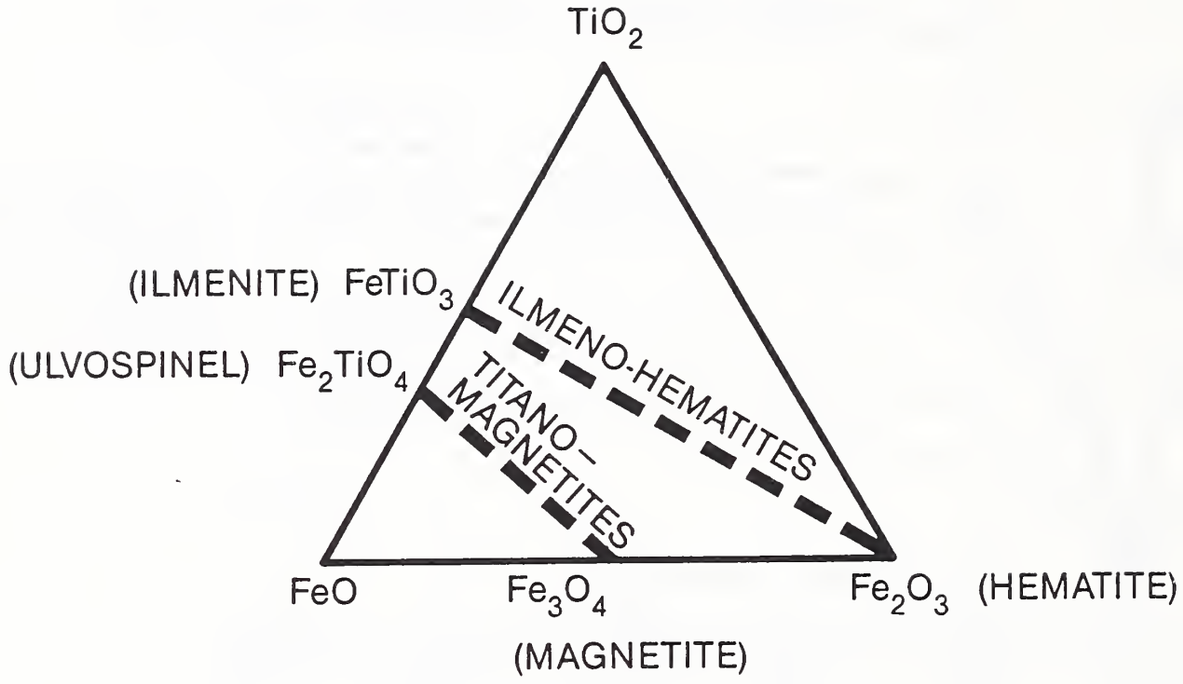

Figure 2.9 **Composition diagram of natural magnetic minerals.**

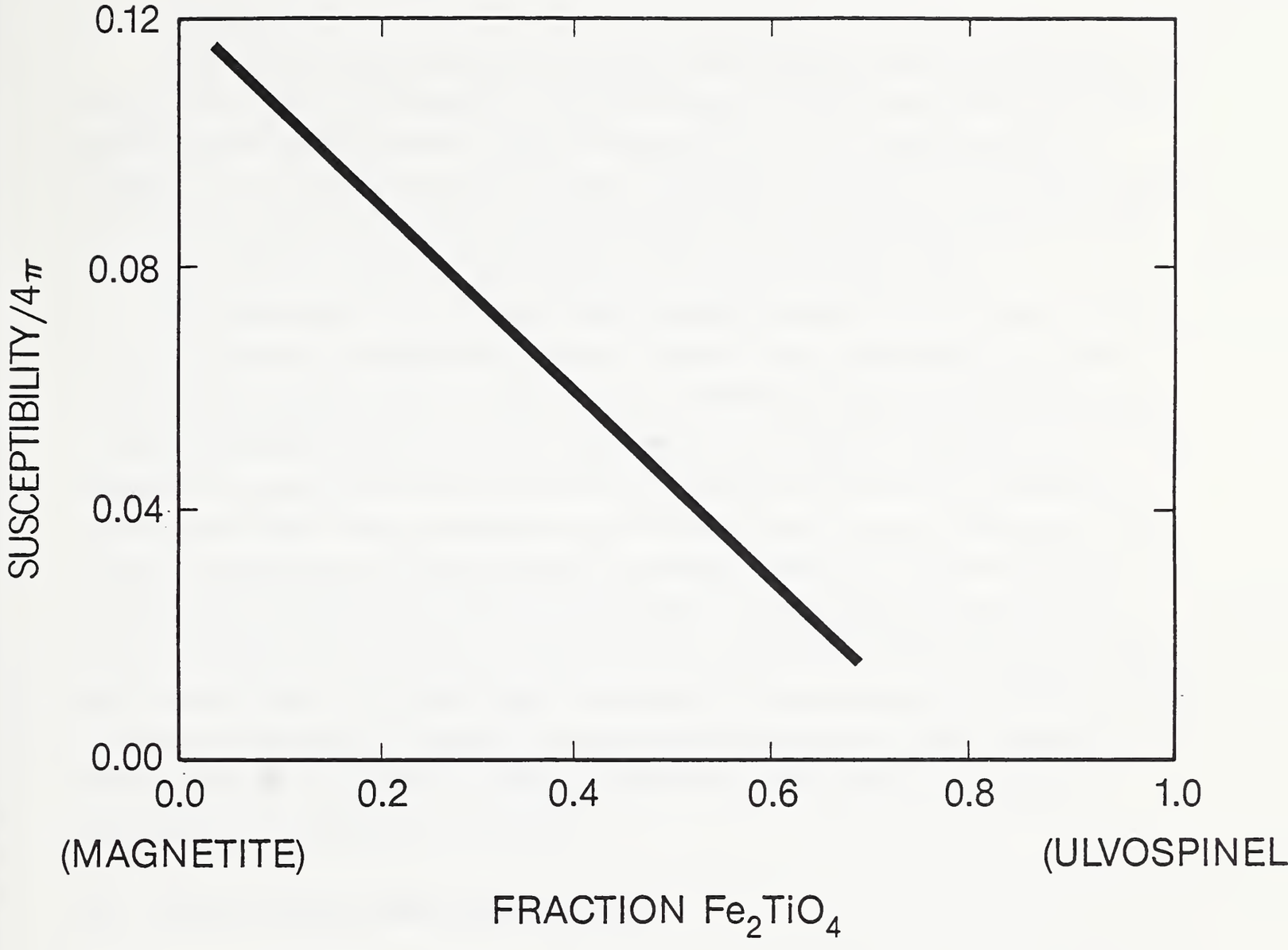

Figure 2.10 Magnetic susceptibility versus fractional composition of magnetite-ulvospinel solid solution.

III Critical Performance Factors

A Introduction

Parameters affecting performance of portable electromagnetic mine detection systems may be divided into three main categories. In the first category are those factors that are not directly related to electromagnetic waves. Some of these parameters are cost, weight, battery life, reliability, ease of operation, and ease of repair. Any attempt to assign an overall figure of merit to a detector system should include weighting factors for this category of parameters, but this task is not within the expertise of NIST personnel and is best left to the Army.

Of the parameters which are directly related to electromagnetic waves, we have chosen to place all of them into two additional categories. The first category discussed in this chapter contains those parameters which we have chosen to call "detector-based." The second category contains those parameters which we call "target-based." The category of detector-based parameters contains *all parameters found above the air/earth interface* such as atmospheric noise; detector noise levels and dynamic range; and sensor height, velocity, and tilt angle. The category of target-based parameters contains *all parameters found at or below the air-earth interface* such as target-soil permittivity, conductivity, and permeability; target-soil contrast ratio; target depth, size, and shape; and ground clutter. What follows in this chapter is a listing and some discussion of all of the detector-based and target-based parameters that NIST personnel have been able to identify. Chapter VII contains detailed descriptions of NIST-suggested performance tests that address a selected set of these parameters, along with a suggested methodology for analysis of the test results.

B Detector-Based Performance Factors

B.1 Noise Factor of Mine Detectors

If there were no noise at the receiver input and none were generated by the receiver, sufficient amplification would result in the detection of any signal, even for a small contrast between the electromagnetic properties of the land mine and host soil. In reality, noise is always present; consequently, amplification of a signal results in amplification of noise as well. Furthermore, the minimum detectable signal power in the receiver is limited by noise which can be attributed to the following internal and external sources: (a) equipment noise (amplifier or sensor noise); (b) cosmic and atmospheric noise picked up by antenna; (c) man-made interference (machinery, other radio transmitters); and (d) ground clutter. If these noise sources

were the only limiting factors affecting mine detection, then a suitable requirement would be that the secondary electromagnetic field due to the presence of a land mine would not be exceeded by these noise sources.

B.1.1 Ideal System Noise Factor

The system noise factor of an ideal receiver may be simply defined as a measure of the degradation of the signal-to-noise ratio as the signal passes through the receiver (which depends on the design of the input stages and frequency of operation of the receiver). The system noise factor, *SNF*, of a mine detector is defined, therefore, as the power ratio of $(S/N)_{in}$ to $(S/N)_{out}$:

$$SNF = 10\log_{10}\frac{(S/N)_{in}}{(S/N)_{out}}. \tag{3.1}$$

For an ideal receiver $(S/N)_{in} = (S/N)_{out}$, so $SNF = 0$ dB. Equation (3.1) is a measurable quantity for evaluating mine detector performance and, in general, depends on both operating frequency and another measurable quantity of the system, its dynamic range.

B.1.2 Overall Operating Noise Factor

For a general receiving system free from the spurious effects of ground clutter, the overall operating system noise factor [3.1-3.3] is given by $f = f_a + f_i$ or

$$f = f_a + (\ell_c - 1)\left(\frac{T_c}{T_0}\right) + \ell_c(\ell_t - 1)\left(\frac{T_t}{T_0}\right) + \ell_c\ell_t(f_d - 1), \tag{3.2}$$

where f_a = the external noise factor defined as

$$f_a = p_n/KT_0b = T_a/T_0\,, \tag{3.3}$$

and

p_n = noise power available from an equivalent loss-free antenna, in W,
K = Boltzmann's constant = 1.38×10^{-23} J/K,
T_o = reference temperature, taken as 288 K,
b = effective noise power bandwidth of the receiving system, Hz,
T_a = effective antenna temperature in presence of external noise, K,
ℓ_c = antenna circuit loss (available input power/available output power),
T_c = actual temperature, K, of the antenna system and nearby ground,
ℓ_t = transmission line loss (available input power/available output power),

T_t = actual temperature, K, of the transmission line,

f_d = noise factor of the receiver.

f_i = internal system noise factor

F_a = the external noise figure defined as

$$F_a = 10 \log f_a (dBW),$$

and F_d = the noise figure of receiver defined as

$$F_d = 10 \log f_d (dBW).$$

If $T_c = T_t = T_o$, eq (3.2) becomes

$$f = f_a - 1 + f_c f_t f_d, \tag{3.4}$$

where

$$f_c = 1 + (\ell_c - 1)\left(\frac{T_c}{T_o}\right) \tag{3.5}$$

is the noise factor associated with the antenna circuit losses and

$$f_t = 1 + (\ell_t - 1)\left(\frac{T_c}{T_o}\right) \tag{3.6}$$

is the noise factor associated with transmission line losses. For no antenna circuit or transmission line losses, f is given by

$$f = f_a - 1 + f_d. \tag{3.7}$$

Internal system noise can be closely controlled by the manufacturer for most mine detection systems. External noise sources are less controllable; of these, atmospheric and ground clutter are the least controllable.

B.2 Sensitivity to Atmospheric Noise

Spaulding [3.3] has given the minimum and maximum external noise figure due to expected atmospheric noise as a function of frequency (from 0.1 Hz to 10^8 Hz). These are shown in figs. 3.1 and 3.2, and take into account the entire earth's surface, all seasons, and times of day. In the frequency range 0.1 Hz to 10 kHz (that of most operating metal mine detection

units), there is very little seasonal, diurnal, or geographic variation. The variability in the 100 to 120 kHz range is principally due to the variability of the earth-ionosphere waveguide cutoff.

Relation (3.3) can be written

$$P_n = F_a + B - 204\ dBW, \tag{3.8}$$

where $P_n = 10 \log p_n$, $B = 10 \log b$, and $10 \log KT_o = -204$. Lauber [3.4] has given the expression for the vertical component of the rms electric field strength for a half-wave dipole in free space:

$$E_n = F_a + 20 \log f_{MHz} + B - 99.0\ dB(\mu V/m). \tag{3.9}$$

If we use a conversion factor of $1\ \mu V/m = 33\ pT$ for relating electric field strengths to orthogonal magnetic field strengths and note that figs. 3.1 and 3.2 may be used for vertical as well as horizontal magnetic field strength noise levels at any frequency and any effective antenna temperature, an approximate value for the magnetic field strength atmospheric noise is given by

$$\begin{aligned} H_n &\doteq 4\pi \times 10^{-9} \sqrt{b} \\ H_n &\doteq 0.1 nT \sqrt{b}. \end{aligned} \tag{3.10}$$

Cohn [3.5] has used this nominal value for H_n to plot primary coil ampere-turns-per-coil diameter required to achieve a specified detection range for a normalized target size of 1 when external atmospheric noise is the only limiting factor. An operating metal detector frequency of 2.5 kHz is close to a local minimum of the external noise figure shown in figure 3.1 (127 dB), which takes into account the entire surface of the earth, all seasons, and all times of day. Therefore, it is an optimal operating frequency with respect to noise figures based on atmospheric sources. Figures 3.1 and 3.2 may be used in specifying the external atmospheric noise figure for any operating frequency and effective antenna temperature.

A report [3.6] on the noise factor for mine detection systems where signals due to ground clutter are specifically excluded has been written. In this paper, an example is taken to show how analytic work may be used with external atmospheric noise measurements to predict whether a given system operating at a specified frequency and effective temperature would allow detection of metal mine targets of specified sizes. In another report [3.7], Geyer has pointed out that there are optimal operating frequencies that maximize the quadrature-induced multipole moments of buried metallic spheres for any permeability and conductivity contrast between the sphere and host soil and for a buried sphere with any diameter. Thus, there is a means in metal-mine detection to choose an operating frequency that maximizes the quadrature response for a given size mine target. Together with the results described here, signal-to-noise ratios could then be

determined to predict whether that size target, at a given depth of burial, would yield a threshold detection signal (signal exceeding overall operating noise factor by at least 2 or 3 dB).

B.3 Detector Dynamic Range

One of the most important measures to be considered in the evaluation of mine detection systems is the mine detection probability that can be ascribed to a given system when the electromagnetic characteristics of the test target and background soil are specified. The detection probability is defined as the probability that the (target) signal, if present, will be detected. Given the electromagnetic characteristics of metallic (or plastic) test standards and background soil(s), as well as the overall operating noise factor of the detection system, a threshold detectability level may be ascertained in principle for any burial depth and size of the test standard.

The function of a mine detection system is to determine the presence or absence of a buried mine. The maximum sensitivity of any system is governed by the threshold of detection. The threshold in turn is set at a level based on a tolerable false alarm rate. A false alarm results from an occasional level of noise exceeding the system threshold. Since system sensitivity is of prime importance, it is necessary to examine the relationship among noise (for the types of noise previously categorized), bandwidth, threshold, and false alarm rate.

Threshold and signal-to-noise requirements for mine detection are reviewed by Geyer [3.6]. The probability of a false alarm can be ascertained once a tolerable false alarm rate and the bandwidth of the detection system are determined. From the estimated false alarm probability and noise variance, a detection threshold may be simply calculated. Finally, minimum acceptable signal-to-noise ratios for any probability of successful detection and any false alarm probability can then be evaluated. Any mine detection system having a high threshold of detection (or low sensitivity) would be given a low figure of merit. Conversely, any detection system that has high sensitivity, or at least variable threshold levels of detection, would be given a higher performance rating. High sensitivity for variable detection thresholds usually means that the system intrinsically has greater dynamic range.

A minimal detection requirement is that the signal output from measured electromagnetic fields perturbed by a land mine (for systems with earphones) be at least 2 or 3 dB above the overall operating noise factor of the system in order to be resolvable. Systems that depend on the normal hearing threshold (approximately a rms sound pressure of 2×10^{-5} N/m^2 at 1 kHz), as well as the smallest discernable change in audible level (2 or 3 dB), are therefore inherently limited in sensitivity. This is a critical systems engineering requirement that should be addressed.

Ensuring signal levels that are at least 2 or 3 dB over the overall operating noise factor of the system (defining signal as that due to the presence of a mine) may or may not always be

possible, even when the mine is electromagnetically visible. Such assurance will demand a thorough broadband analysis of the ground clutter problem, since system internal noise can be controlled and since system engineering considerations can be used to overcome external atmospheric noise sources.

B.4 Sensitivity to Detector Height above Earth's Surface and Pattern Signatures

Smith [3.8] has investigated the directive transmission characteristics of horizontal electric and magnetic dipoles over a dielectric half-space by expressing the field of a general antenna over that half-space as a spectrum of plane waves [3.9]. He then asymptotically evaluates the integrals representing the far field so as to define pattern function, gain, and directivity of the horizontal electric or magnetic dipole antenna as a function of height above the earth.

More recently, Hill [3.10] has considered the specific case of oppositely directed horizontal electric dipole antennas, such as are found in the AN/PRS-7 plastic mine detector (see figure 3.3). A null always exists for the AN/PRS-7 in the directions normal to the air-earth interface from the detector head (midway between the oppositely directed dipole antennas)—in the absence of a lateral change in complex permittivity.

We can, however, examine the effect of antenna height on the field for fixed observation points either in the earth or in the air. This is illustrated in figs. 3.4 and 3.5 which clearly show the desirable and expected increase in subsurface fields (and decrease in the fields in the air), as the antenna is brought closer to the earth's surface. Generally, electromagnetic field enhancement in the earth will always occur as the source antenna is brought closer to the air-earth interface, regardless of the type of source excitation or antenna configuration. The actual enhancement will depend on the specific antenna.

Hill [3.11] has also shown the far-field H-plane multiple-lobe pattern that can occur over a uniform half-space having high dielectric contrast, $\varepsilon'/\varepsilon_0 = 80$ (see figure 3.6). For $1 \le \varepsilon'/\varepsilon_0 \le 4$, this complex pattern does not occur. This H-plane multiple-lobe pattern (more nulls than at $\theta = 0°$, 90°, and 180°) is undesirable in any plastic mine detection system and should be avoided, since it would be difficult to distinguish several closely spaced targets from single buried ones. Any mine detector that has a multiple-lobe signature pattern (more than two side lobes) for the maximum expected ratio of $\varepsilon'/\varepsilon_0$ should be ascribed a lower figure of merit.

The variations in sensor head height over a given sweep time (which are likely to occur in field operations) could lead to signals greater than what might be expected from a buried weak scattering target (such as a plastic mine in dry sand). One seemingly simple systems approach for handling this problem would be to incorporate within the detection head an ultrasonic or infrared range finder that would allow feedback system signal corrections to be made in real time in accordance with theoretical near-field analysis [3.11].

B.5 Sensitivity to Detector Tilt Angle

Depending on a particular detector's antenna configuration and electromagnetic field radiation pattern, the angle between the detector and the earth may be an important parameter. Some configurations might be very sensitive to tilt angle, so that even small deviations from horizontal would seriously degrade the detector's ability to detect targets.

B.6 Sensitivity to Detector Velocity

Depending on a particular detector's antenna configuration, electromagnetic field radiation pattern, and detection electronics circuitry design, the velocity of the detector with respect to the earth may be an important parameter. Again, some configurations might be very sensitive to small deviations from optimal velocity (as specified by the manufacturer) such that the detector's ability to detect targets would be seriously degraded. Inability to respond to rapidly changing signals would severely limit search speed and system utility.

B.7 Sensitivity to Detector Spatial Positioning

Every detector will possess some spatial positioning "sweet spot" through which the detector must pass in order to successfully detect targets. One way to define this spatial positioning problem is to move the detector along lines which have increasing perpendicular distances from the mass center point of the target. For all detectors, there is some distance so defined beyond which the target will not be detected. Also, depending on the rotational orientation of the detector with respect to the axis perpendicular to the earth, this maximum distance from the target may not be constant. As with the detector velocity case mentioned above, the dimensions of this sweet spot will be a function primarily of the detector's antenna configuration, radiated electromagnetic field pattern, and detector electronics circuit design. The effects of variations in this parameter are that some detectors would require very precise positioning of the sensor in order to detect targets while others would be more forgiving.

B.8 Sensitivity to Other Detector-Based Parameters

A large number of other detector-based parameters might play an important role in determining the detector's overall figure of merit. For example, a bistatic detector system, with separate transmit and receive antennas, would require the consideration of antenna spacing. Another example would involve the "intelligence" of the detector system. "Smart" detectors, with otherwise similar designs to "dumb" detectors, could far outperform the latter due to their signal processing, image processing or false-target-rejection capabilities. As will be discussed in chapter VII, NIST recommends that the Army avoid attempting to perform detector-based tests

whenever possible, and instead, require the detector manufacturer to supply this information if so desired.

C Target-Based Performance Factors

C.1 Sensitivity to Specified Complex Permittivity Contrasts

One of the important parameters needed in evaluating the performance of any land mine detection system is that system's sensitivity to specified complex permittivity contrasts. Because mine detectors may have differing operating frequencies or be broadband operationally, it is important to understand dielectric dispersion in test soils so as to be cognizant of various dielectric relaxation processes affecting the validation testing. It is also important to recognize these processes so that standardized test conditions may be properly controlled and so that mine detector performance evaluations are properly made (that is, mine detectors correctly compared) in the light of actual measured electrical contrasts.

C.2 Sensitivity to Target Size

Previous analytic studies performed for BRDEC [3.12, 3.13] have demonstrated that anomalous signals generated by a buried land mine, whether metal or plastic, are proportional to target volume in the frequency range used by most detection systems. Most continuous wave (cw) mine detection systems currently available operate in the Rayleigh scattering region insofar as mine detection is concerned; that is, the electrical size of the target mine is small compared to the wavelength in the surrounding medium. Hence, shape information, which could lead to a reduction in the false alarm rate, cannot be directly ascertained from signals measured by most mine detectors.

Hill [3.13] has used the Born approximation to derive the plane wave scattering matrix [3.9] for objects of low dielectric contrast. He has also considered the shape dependence of scattered (plane wave) electromagnetic fields for the cases of a sphere, a cube, and a cylinder whose electrical properties simulated a plastic nylon land mine. These shapes bracket all those likely to be encountered in land mines. Although some shape dependence in the scattered field was determined (see figure 3.7), it would be difficult to determine and use in the field as a basis for discriminating against unwanted ground clutter signals without a prior knowledge of the target volume itself—even with multiple look-angles of the target with spatially variable transmitter-receiver configurations.

For this reason, we have submitted copper right-circular cylinders that might be used as standards for metallic test objects and both nylon and Teflon spheres that might be used as plastic test objects. These standards can be used in a discriminatory fashion in mine detector

validation tests by parametrically changing the target volume for a given burial depth and host-target electrical property contrast. If a mine detection system is unable to detect the largest standard, it will be unable to detect smaller standards (all other factors being equal). Similarly, if a mine detector cannot sense the presence of a buried land mine where the electrical property contrast is high, it surely will not sense a mine when the contrast is low (all other factors being equal).

C.3 Sensitivity to Burial Depth

One of the more important parameters to be considered in assigning a figure of merit to any mine detection system is its detection sensitivity to a prescribed burial depth of a given land mine. The functional dependence with depth of plane electromagnetic waves traveling in a uniform, isotropic earth is exponential, that is, proportional to $e^{-\gamma z}$ ($+z$ is positive downward), or

$$e^{-\gamma z} = e^{-(1/2)(\pi f \mu \sigma) z} e^{-j(1/2)(\pi f \mu \sigma) z}, \tag{3.11}$$

where μ is the (real) magnetic permeability, σ is the (real) conductivity, and f is the operating frequency. The well-known skin depth, that is, the distance within the earth at which the amplitudes of the electric and magnetic field vectors are attenuated to $1/e = 0.3679$ of their respective values at the surface, is

$$Z_{skin\ depth} \equiv \left(\frac{1}{\pi f \mu \sigma} \right)^{1/2} = \frac{1}{Re(\gamma)}, \sigma >> \omega \varepsilon. \tag{3.12}$$

The plane-wave skin depth gives an effective depth of penetration and can be used as a rule of thumb for effective search depths of a mine detector in conductive soils, even though field excitation is not plane wave.

For a nominal ground conductivity of 0.1 S/m and magnetic permeability approximately equal to that of free space ($4\pi \times 10^{-7}$ H/m), we see that the skin depth is roughly 30 m at 2500 Hz. Hence, highly conducting soils would not be expected to inhibit search depths of most metal mine detectors. However, the effective search depth of a plastic land mine detection unit operating at 250 MHz in the same conductive soil environment would only be about 0.1 m, a depth which is less than the maximum probable depth of mine burial (0.3 m). Effective search depths should at least be 0.3 m in the worst case likely to be encountered—that of an electrically lossy environment—for all cw mine detection systems. The easiest way to control this is to lower the operating frequency.

Dispersion is evident whenever the host medium is lossy. Therefore, two mine detection units operating at widely different frequencies would sense differing electrical property contrasts,

all other factors being equal. It is important to be able to predict when favorable electrical contrast between the mine and the background medium can be expected. Such information allows proper comparisons among various mine detection systems to be made.

Although the expected dielectric contrast and hence visibility of a (plastic or metallic) land mine increases with decreasing frequency (which would increase the detection range performance), spatial resolution and shape definition do not. In this regard, Cohn [3.6] has considered the quasistatic effects of variation in height of the search head on measured signals and detection range, assuming that the attendant signal variations (due to conductive or magnetically permeable ground) remain uncancelled. It would be desirable, if practical, to have as broadband a detection response as possible under the attenuation constraints imposed by a lossy background test medium.

It is advisable to make sensitivity tests of land mine burial depth in a conductive host soil at the maximum probable depth of mine burial. If any mine detection system is unable to sense a given mine at the surface (or in free space), it may be unable to do so when buried in a lossy medium.

C.4 Sensitivity to Target Shape

Anomalous signals generated by a buried land mine, whether metal or plastic, are proportional to target volume in the frequency range used by most detection systems. A means for discriminating among different target shapes (target classification) is vital to reducing the false alarm rate at any given detection threshold and for increasing the detection probability. Such a discrimination capability is closely akin to the susceptibility of that system to unwanted ground clutter in the external noise factor. Any mine detection system having shape discrimination capability would, all other factors being equal, command a higher figure of merit.

Target classification may be viewed as a crude form of inverse scattering that determines which of many body shapes is most consistent with the measured scattered field data. The scattered electromagnetic field produced by either a conducting or dielectric body in the presence of an incident wave is described by Maxwell's equations. Since these fields are determined by the relative positions of the constituent parts of the scattering body surface (the boundary condition), it might be expected that, in general, the characteristics of the scattered field would be different for different object geometries. The most desirable mine classification scheme would produce an image displaying the shape and size of the object being illuminated. Such a detection system would effectively solve the inverse scattering problem, which is determining the boundary conditions from the received waveform.

As expected, there are preferred frequencies for indicating the shape and size of a target. In the theory of scattering, three roughly defined frequency regions are of interest: the Rayleigh,

the resonance, and the optical regions, where the wavelength of the incident field is much larger, of the same order, or much smaller than the size of the target, respectively. With illumination in the Rayleigh region, the scattered field describes the volume of the target [3.14]. The character of the backscattered field in the optical region, on the other hand, is indicative of the principal curvatures of the target's specular points. Illumination in the resonance region gives rise to surface currents that circulate on the body surface of the target (into what would be the optical shadow areas) and re-radiate. Resonance region illumination is generally considered most efficacious for target shape and size determination using multiple frequency measurements.

Chan and Peters [3.15], in an elegant attempt to characterize the effects of buried cultural debris and to distinguish such effects from the expected signals of buried land mines, have examined some resonant phenomena of targets using broadband (short-pulse ground radar) detection systems. Preliminary results suggest that schemes either to eliminate or to process ground clutter will rely on broadband detection systems. The principal limitations in deducing shape information from resonance phenomena are the attenuation constraints imposed by the lossy background test medium when a validation test is performed at the maximum expected depth of burial (0.3 m).

In conclusion, shape discrimination is one of the more important attributes that could give future (broadband) mine detection systems a high figure of merit in validation tests. Because few of the land mine detection systems presently available have demonstrated capability for shape discrimination, however, it will probably have a low weight in any performance effectiveness testing scheme that BRDEC decides upon.

C.5 Sensitivity to Ground Clutter

While it is possible to evaluate the performance of any mine detection system under controlled circumstances having minimal or no ground clutter, it is more difficult to predict the operation of that system on the battlefield. A mine detection system can be tested and shown to have the highest overall figure of merit based on weighted experimental parameters discussed to this point—but could fail to detect a mine in the field where the spurious signals due to ground clutter are high.

Ground clutter includes the natural effects of an inhomogeneous and/or dispersive host medium in which the mine target resides, as well as effects of surface roughness. Other types of ground clutter could stem from surface or buried cultural debris such as spent shells or artillery (see figure 3.8).

Unwanted signals due to ground clutter can be the most important contributor to the overall operating noise factor. This source of noise, which can give large numbers of nuisance or false alarms, is currently difficult to quantify in a meaningful way. Only if there is spatial or temporal

resolvability of the signal in the presence of clutter can there be hope of taking fruitful measures to minimize the effects of interfering signals on target signals. Furthermore, it would be useful to know whether, if any mine detection system incorporated an optimally matched filter as part of its system design, spectral resolvability exists between the mine target signal $S(\omega)$ and unwanted noise signals $N(\omega)$—and, if so, under what conditions. Thus it would be desirable to have a generalized solution to the model illustrated in figure 3.8 which (1) is broadband (not frequency limited); (2) incorporates ground clutter; (3) allows spatially variant and dispersive $\mu_H(r;\omega)$, $\varepsilon_H(r;\omega)$; and (4) can be applied to weak or strong scattering targets.

Such an analysis would provide insight into system design specifications and lead, in general, to the ultimate goal—better detection capability. It is difficult to conceive how present mine detection systems undergoing test validation would perform better in a cluttered environment than in highly controlled, standardized test environments. Consequently, the BRDEC approach of highly controlled validation testing is probably sufficient for comparative performance evaluations of existing detection systems. Geyer [3.7] has outlined an exact deterministic approach to the analysis of ground clutter for an arbitrary dispersive and spatially variant background medium and for an arbitrary incident source field.

One approach to attacking the ground clutter problem and to increasing the detection probability is to know the (near-field) frequency spectrum $S(\omega)$ (or averaged frequency spectrum $\langle S(\omega)\rangle$) of the input target (land mine) signal. Once $S(\omega)$ is given for an ensemble of specified targets, it is not only possible to incorporate adaptive thresholding, but also to design an optimally matched filter transfer function $H(\omega)$ for a mine detection system operating in the presence of white Gaussian noise; that is,

$$H(\omega) \equiv S^*(\omega), \tag{3.13}$$

where $S(\omega)$ is the frequency spectrum of the input (target) signal $s(t)$ and $S^*(\omega)$ is the complex conjugate of $S(\omega)$. A mine detection device that has a system response given by eq (3.13) is the optimal detection system in the sense of maximizing signals relative to average noise power. We could therefore place a higher figure of merit on a mine detector configured such that the output response $O(\omega)$ for a given test standard $S(\omega)$ is given by

$$O(\omega) \equiv S(\omega)S^*(\omega). \tag{3.14}$$

Ground clutter may or may not be white Gaussian in character. If not, it would be possible to design a Wiener-Hopf filter, optimal in the least squares sense; that is,

$$H_{opt}(\omega) = \frac{\Phi_S(\omega)}{\Phi_N(\omega) + \Phi_S(\omega)}, \tag{3.15}$$

when noise is uncorrelated with the desired signal output and where $\Phi_S(\omega)$ and $\Phi_N(\omega)$ are the signal and noise power spectra, respectively. Future detection systems may well incorporate a Wiener-Hopf filter. Such incorporation will await more definitive work on characterizing $\Phi_N(\omega)$.

C.6 Sensitivity to Target Orientation

Detectors may have varying sensitivities to the orientation in the earth of otherwise identical targets. In one orientation the detector may sense the target easily, while in another orientation the detector may fail to detect it. Probably the most important characteristic of a detector that would affect this sensitivity is the polarization of the sensor's electromagnetic field. For example, the magnitude of eddy currents produced by the sensor's exciting field in a target's metal firing pin will depend strongly on the orientation of the pin with respect to the polarization of the field.

C.7 Sensitivity to Soil Stratification

This parameter sensitivity may be considered a special case of ground clutter. If the electromagnetic properties of the soil vary as a function of depth, then it is very possible that the performance of a given detector could be seriously degraded when compared to its performance under uniform soil conditions. Under extreme stratification conditions, a detector could effectively be blinded to targets buried below a particular layer of soil, similar to the blinding of shipboard sonar systems due to different thermal layers in the sea.

C.8 Sensitivity to Target Resolution

The ability of a detector to resolve closely spaced targets could, under certain conditions, become very important. For example, a large vehicle mine could be buried close to a small antipersonnel mine. If only the large mine were to be detected, personnel could be fooled into attempting to disable it with disastrous results to those personnel from the accidental detonation of the small mine.

References (III)

[3.1] Barsis, A. P.; Norton, K. A.; Rice, P. L.; Elder, P. H. Performance predictions for single tropospheric communication links and for several links in tandem. Nat. Bur. Stand. (U.S.) Tech. Note 102; 1961.

[3.2] International Radio Consultative Committee. Characteristics and applications of atmospheric radio noise data; Report No. 3220-2; 1983.

[3.3] Spaulding, D. A. International Radio Consultative Committee. Worldwide minimum external noise levels, 0.1 Hz to 100 GHz; Report No. 670; 1982.

[3.4] Lauber, N. R. Preliminary urban UHF/VHF radio noise intensity measurements in Ottawa, Canada. Proc., 2nd Symp. on EMC; Montreux, Switzerland; 28-30 June, 1977.

[3.5] Cohn, G. I. Low frequency electromagnetic induction techniques; Tech. Essays, Army Countermine Study Report; 1973.

[3.6] Geyer, R. G. Noise factor for mine detection systems: A performance measure; Report to U.S. Army Belvoir Research and Development Center, Fort, Belvoir; 1987.

[3.7] Geyer, R. G. Suggested experimental parameters for land-mine detection performance evaluations; Report to U.S. Army Belvoir Research and Development Center, Fort Belvoir; 1987.

[3.8] Smith, G. S. Directive properties of antennas for transmission into a material half-space. IEEE Trans. Ant. Prop. AP-32(3): 232-246; 1984.

[3.9] Kerns, D. M. Plane-wave scattering-matrix theory of antennas and antenna-antenna interactions; Nat. Bur. Stand. (U.S.) Monogr. 162; 1981.

[3.10] Hill, D. A. Near-field detection of buried dielectric objects, IEEE Trans. Geosci. Remote Sensing; GE-27(4): 364-368; July 1989.

[3.11] Hill, D. A. Fields of horizontal currents located above the Earth. IEEE Trans. Geosci. Remote Sensing; GE-276(6): 726-732; November 1988.

[3.12] Hill, D. A.; Cavcey, K. H. Coupling between two antennas separated by a planar interface. IEEE Trans. Geosci. Remote Sensing; GE-25(4): 422-431; July 1987.

[3.13] Hill, D. A. Electromagnetic scattering by buried objects of low contrast. IEEE Trans. Geosci. Remote Sensing; GE-26(2): 195–203; March 1988.

[3.14] Crispin, J. W.; Siegel, K. M. Methods of radar cross-section analysis. New York, NY: Academic Press; 1968.

[3.15] Chan, L. C.; Peters, L., Jr. Subsurface electromagnetic mine detection and identification; Technical Report, Department of the Army, U.S. Army Mobility Equipment Research and Development Command, Fort Belvoir, VA; 76. p.; 1978.

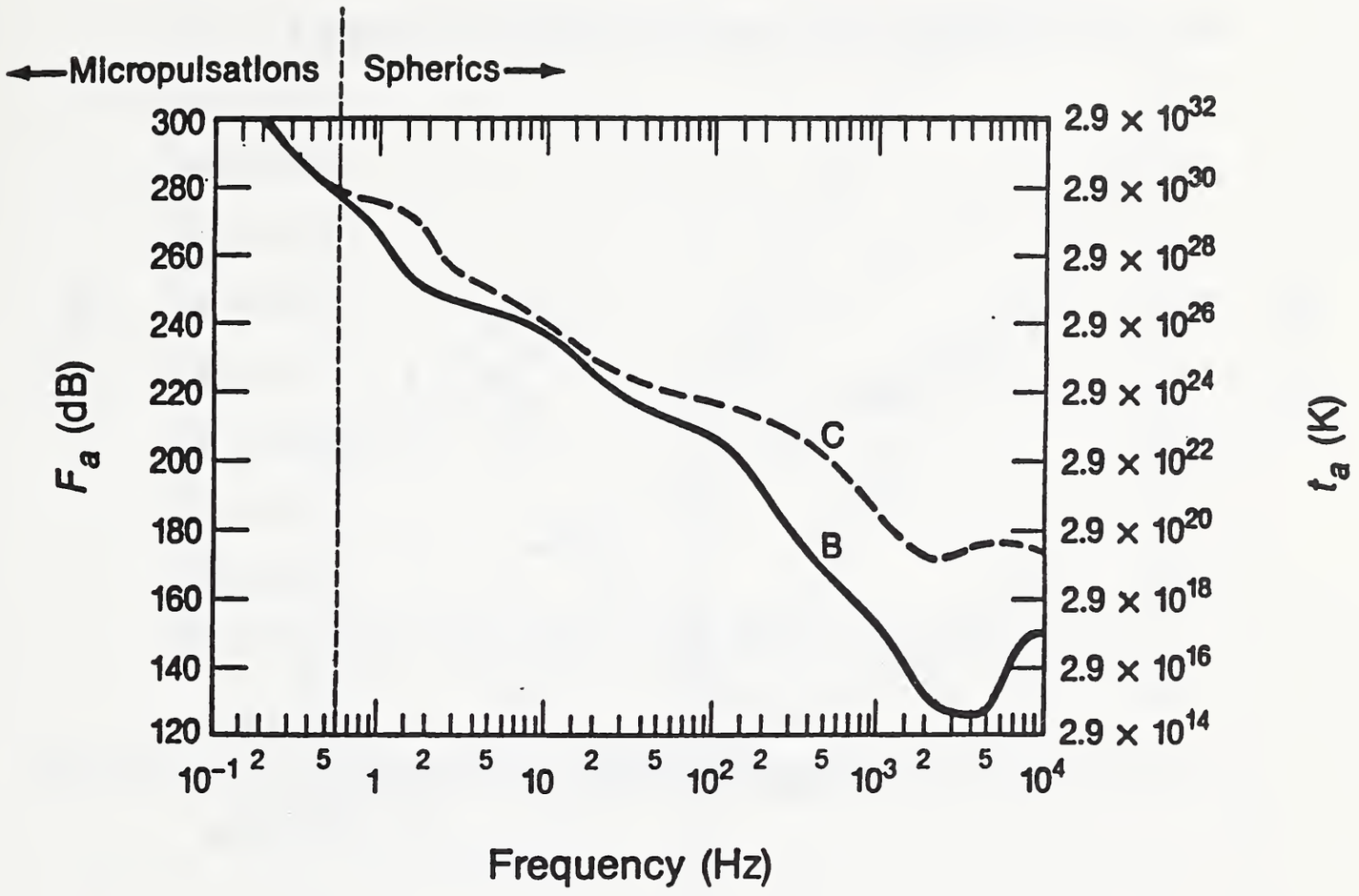

Figure 3.1 Minimum (B) and maximum (C) atmospheric noise figure vs frequency.

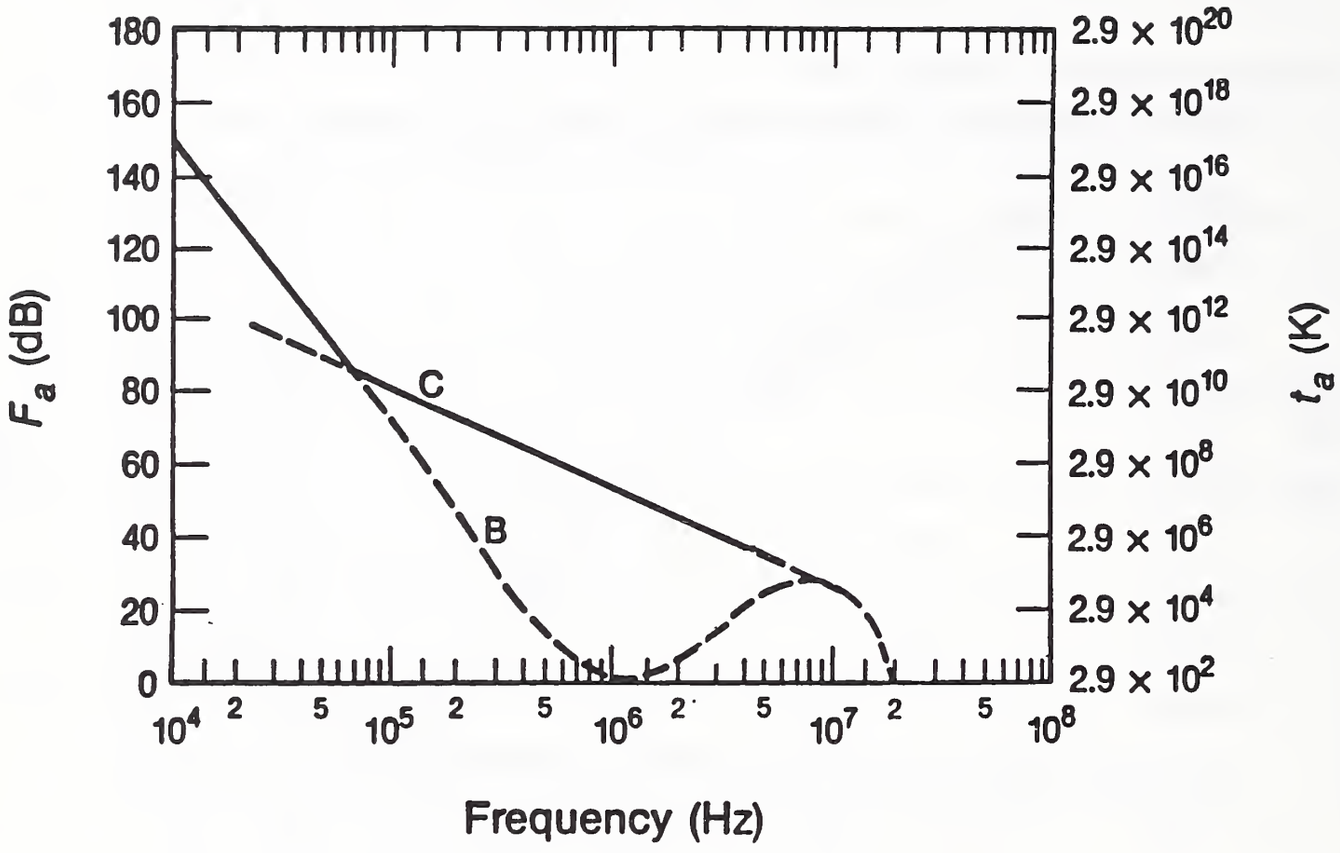

Figure 3.2 Minimum (B) and maximum (C) atmospheric noise figure vs frequency.

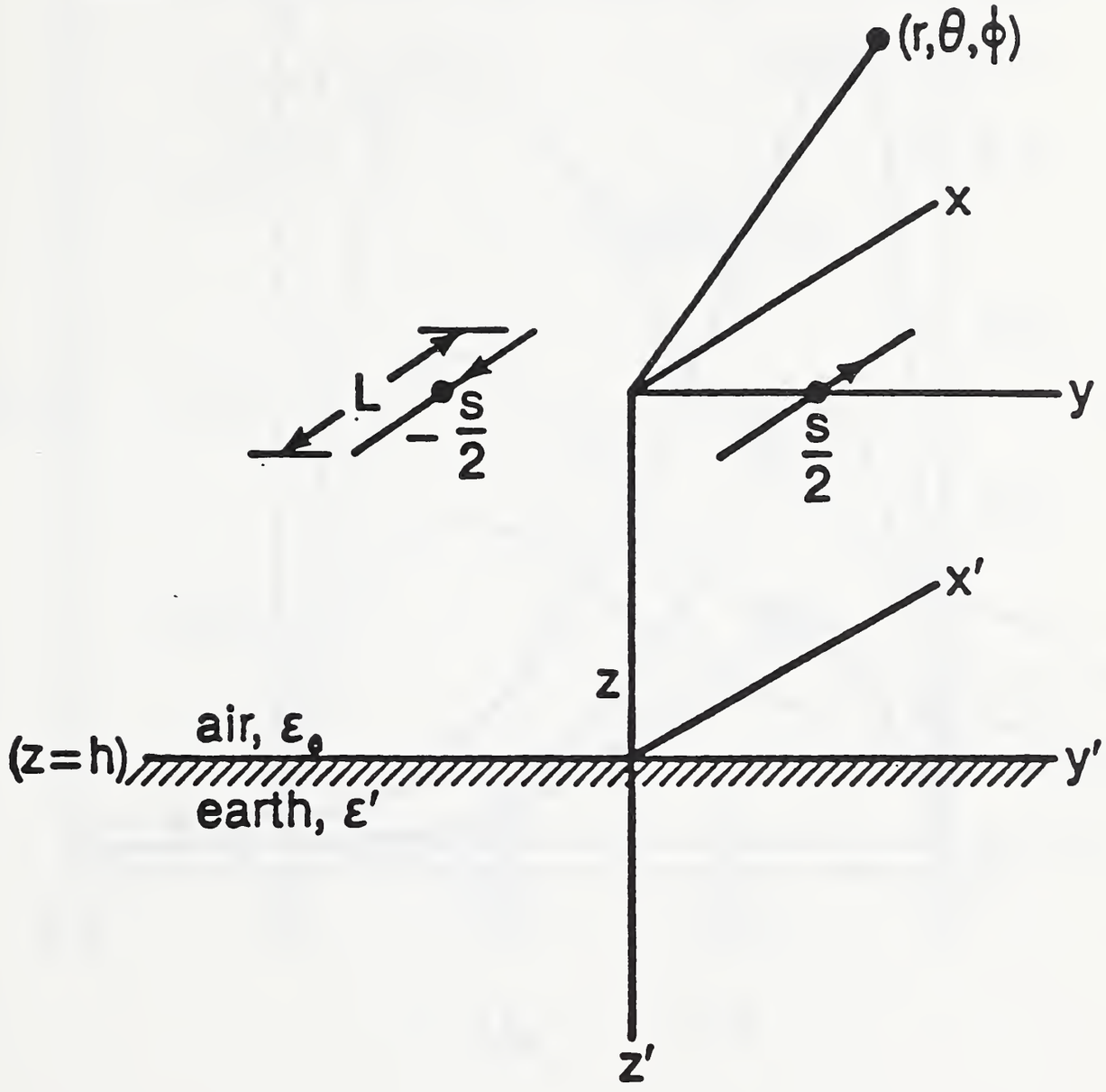

Figure 3.3 Oppositely directed dipoles at height h above the earth.

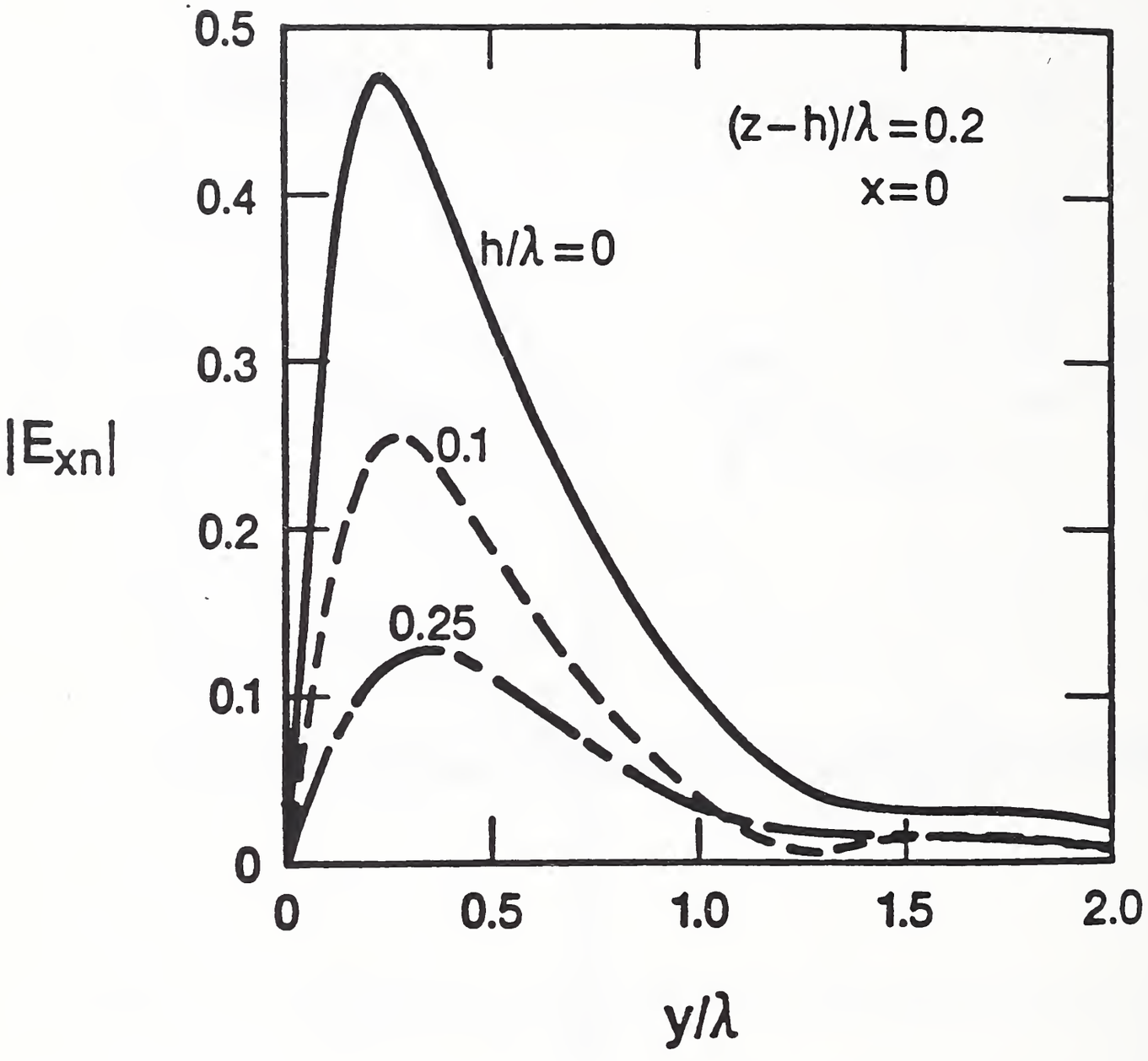

Figure 3.4 Normalized electric field at various heights in air for a fixed observation point in the earth.

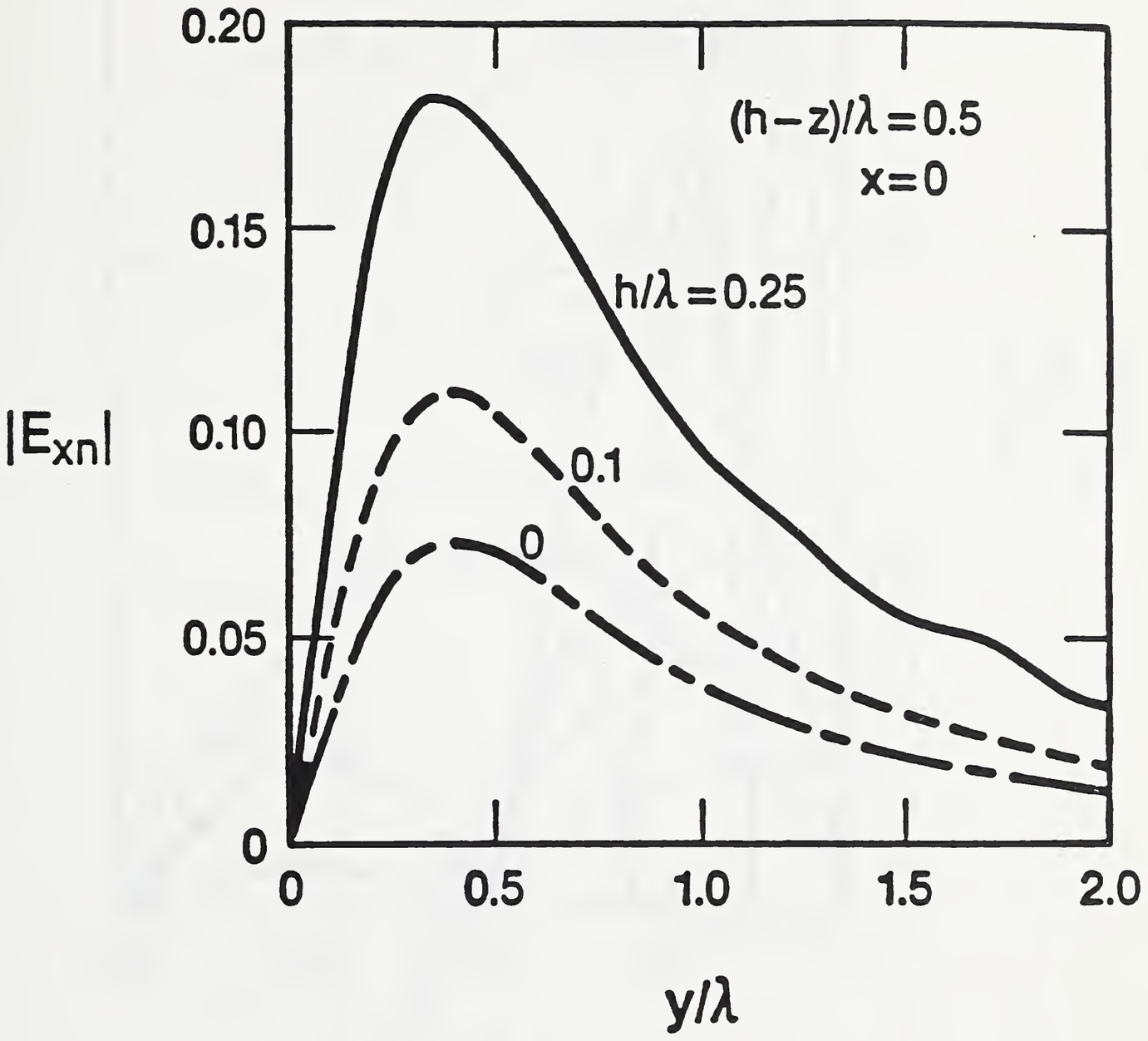

Figure 3.5 Normalized electric field at various heights in air for a fixed observation point in the air.

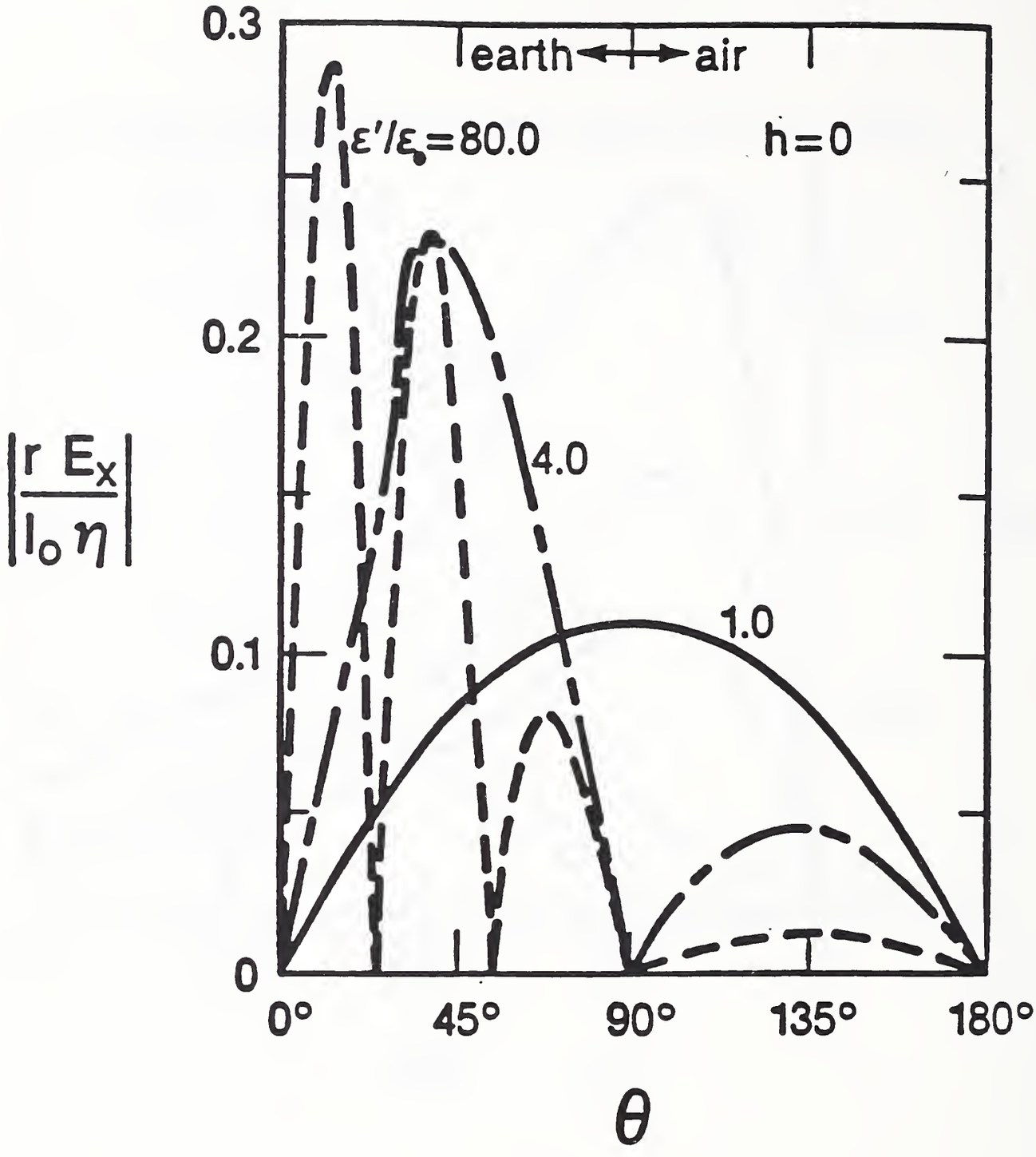

Figure 3.6 H-plane pattern of oppositely directed dipoles located at air/earth interface for various earth permittivities.

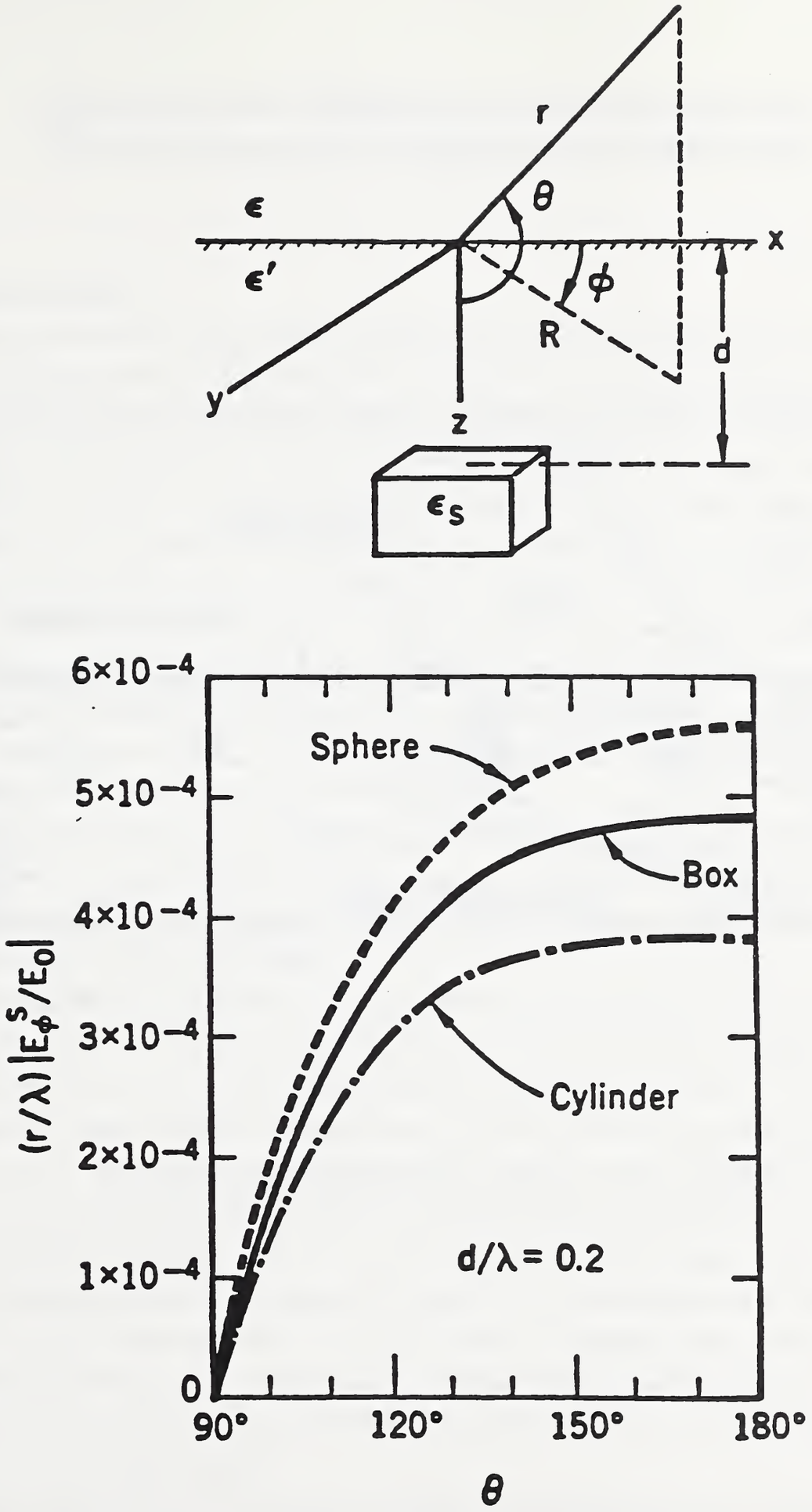

Figure 3.7 Scattered far-field for a cube (side = 0.1 λ), a circular cylinder (height = radius = 0.1084 λ), and a sphere (radius = 0.1241 λ) for normal incidence, TE polarization.

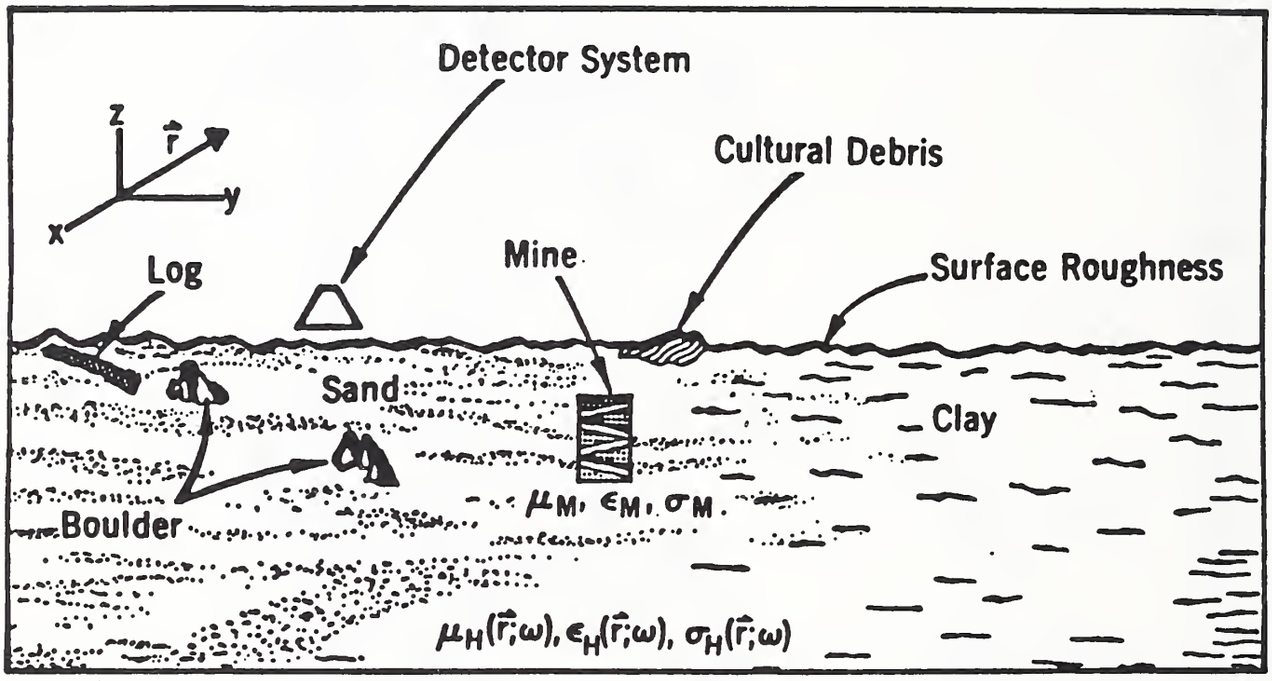

Figure 3.8 Sources of ground clutter.

IV Measurement Methods and Systems for Electromagnetic Properties of Materials

A Introduction

The measurement of mine detector performance generally requires that certain specified tests be carried out with test targets buried in a carefully controlled environment or test lane. For tests of plastic-object detectors that use UHF or microwave frequencies, the returned signals are very much weaker than the transmitted signals. This makes it imperative that the test procedures be designed so that we can obtain consistently similar results for the returns from a given combination of test target and background medium. Unfortunately, test conditions vary over time—especially if the test lane contains damp soil. In this section of the report, we briefly review various laboratory methods for determining the electromagnetic properties of target and background materials. We then describe methods for simulating the electromagnetic properties of damp, sandy soils with dry materials. We also describe methods for accurately determining the electromagnetic properties of such dry materials and for the long-term monitoring of the properties of test lanes composed of such materials.

Dielectric measurement techniques have a long history [4.1–4.3] and will be briefly mentioned here. Afsar, Birch, and Clarke [4.4] give a comprehensive review of techniques developed over the past two decades to measure dielectric properties of materials in the frequency range 1 MHz to 1500 GHz.

Frequency-domain laboratory techniques often employ propagation measurements in a waveguide transmission line containing the dielectric. Measurements of the input admittance of a shielded open-circuited coaxial line filled with the material are common [4.5]. Depending on the frequency range of interest, the admittance at the plane of the sample holder connector is measured by a capacitance bridge (kilohertz range), Schering or twin-T bridges [4.6] (up to 200 MHz), or an Automatic Network Analyzer (ANA) (0.5 MHz to 18 GHz). These admittances are then converted by suitable formulas into complex permittivity, loss tangent, and so on. Closed cavity resonator techniques are also used for permittivity measurements in the microwave region [4.7–4.11]. As the frequency range of interest becomes still higher (greater than 20 GHz) open cavity resonator techniques are used [4.12–4.21], since at the higher frequencies the open resonator can be made fairly small and the high-Q values required for the measurement of low dielectric loss are easily attained.

Time-domain laboratory methods for dielectric spectroscopy are also undergoing rapid development [4.22–4.28]. These methods typically make use of a reflected wave off a length of

air line, part of which is filled with the material to be tested. The complex permittivity is determined from the measured reflection coefficients.

B Laboratory Sample-Holder Measurements of the Electromagnetic Properties of Materials

B.1 Dielectric Measurements Using Terminated Coaxial Lines

Bussey [4.5] and, more recently, Jesch [4.29] have made measurements of the dielectric properties of materials using open, coaxial sample holders. The design of the sample holders, fabricated from precise, 14 mm, 50 Ω coaxial air line and equipped with a 900-BT precision coaxial connector, is shown in figure 4.1. Essentially, soil conductivity and permittivity are determined by the construction of a section of coaxial transmission line, as illustrated in figure 4.1, with the soil serving as the lossy dielectric environment for the electromagnetic fields produced within the transmission line.

The impedance at the input end of a transmission line, having a characteristic impedance z_0 and termination impedance z_e, is given by

$$z_{in} = z_0 \frac{z_e + z_0 \tanh \gamma \ell}{z_0 + z_e \tanh \gamma \ell}, \tag{4.1}$$

where $\gamma = \alpha + j\beta$ is the complex propagation constant of the transmission line, α and β are the respective attenuation and phase constants of the transmission line, and ℓ is the length of the transmission line. When the termination impedance is 0 (short circuit at the termination), eq (4.1) becomes

$$z_{in,\, short\ circuit} = z_0 \tanh \gamma \ell, \tag{4.2}$$

whereas, when the termination is an open circuit we have

$$z_{in,\, open\ circuit} = z_0 (\tanh \gamma \ell)^{-1}. \tag{4.3}$$

Dividing the short circuit input impedance by the open circuit input impedance yields

$$\frac{z_{in,\, short\ circuit}}{z_{in,\, open\ circuit}} = \tanh^2 (\gamma \ell).$$

For simplicity of notation in the following four equations, let

$$A = \frac{z_{in,\,short\ circuit}}{z_{in,\,open\ circuit}}.$$

Then,

$$\gamma = \frac{1}{\ell}\tanh^{-1}\sqrt{A}$$

or

$$\begin{aligned}\gamma &= \frac{1}{2\ell}\ell n\frac{1+\sqrt{A}}{1-\sqrt{A}} \\ &= \frac{1}{2\ell}\ell n\left|\frac{1+\sqrt{A}}{1-\sqrt{A}}\right| + \frac{1}{2\ell}\left(phase\,\frac{1+\sqrt{A}}{1-\sqrt{A}} + 2n\pi\right),\end{aligned} \tag{4.5}$$

n = 0, ±1, ±2, ... Hence the attenuation constant α of the transmission line is

$$\alpha = \frac{1}{2\ell}\ell n\left|\frac{1+\sqrt{A}}{1-\sqrt{A}}\right|, \tag{4.6}$$

and the phase constant β is

$$\beta = \frac{1}{2\ell}phase\,\frac{1+\sqrt{A}}{1-\sqrt{A}} + \frac{n\pi}{\ell}. \tag{4.7}$$

The characteristic impedance z_0 of the coaxial transmission line is

$$z_0 = \sqrt{\frac{j\omega\mu}{\sigma + j\omega\varepsilon}}\,\frac{\ell n(b/a)}{2\pi}, \tag{4.8}$$

where b and a are the outer and inner diameters of the coaxial line, respectively.

From Ampere's law,

$$\nabla\times\vec{\mathbf{H}} = (\sigma + j\omega\varepsilon)\vec{\mathbf{E}}, \tag{4.9}$$

and Faraday's law,

$$\nabla\times\vec{\mathbf{E}} = -j\omega\mu\vec{\mathbf{H}}, \tag{4.10}$$

we see that

$$\gamma^2 = j\omega\mu(\sigma + j\omega\varepsilon), \tag{4.11}$$

so that from measurements of α and β conductivity and permittivity are easily obtained,

$$\sigma(\omega) = 2\alpha\beta/(\omega\mu), \tag{4.12}$$

$$\varepsilon(\omega) = (\beta^2 - \alpha^2)/\omega^2\mu. \tag{4.13}$$

The results of a series of measurements using this open-ended coaxial holder technique are shown in figure 4.2. The technique is well-suited to making measurements of the dielectric properties of granular mixtures. Figure 4.2 shows data obtained at 600 MHz for various mixtures of sand and silicon carbide as the percentage of sand is varied.

B.2 Permittivity and Permeability Measurements with a Two-Port Measurement Technique

As described more fully in Appendix IV.B, the complete electromagnetic properties of materials can be obtained over a wide range of frequencies with a two-port measurement set-up. We made a large number of measurements using an Automatic Network Analyzer (ANA). This system [4.30] is composed of an S-parameter test set, sweep frequency generator, and a control computer. The system is capable of determining S-parameters over the frequency range of 45 MHz to 26.5 GHz. We made all of our measurements between 50 MHz and 1.05 GHz. Before taking any data, calibrations were carried out with three standards: a precision short, an open circuit, and a 50 Ω matched load. These standards were all terminated in 3.5 mm connectors on the S-parameter test set. We used a sample holder made from a 10 cm length of precision beadless 14 mm air line. The holder was terminated with GR-900 connectors. Samples of plastic material were machined on a lathe so that they fitted very precisely between the inner and outer conductors of the holder. Samples of the Teflon and nylon used to make test targets were prepared in this way. To measure the properties of a given sample, one of the GR-900 connectors was removed from the line and the machined sample was then inserted. The distance from the end of the holder to the sample was measured with a depth gauge and recorded before reattaching the GR-900 connector. The holder was then carefully connected to the ANA. See figure 4.3.

Measurements of all four S-parameters were taken over the frequency range from 50 MHz to 1.05 GHz for each material at 5 MHz intervals. This yielded 201 data points per plastic sample. The time required typically did not exceed 15 min per plastic sample—including the time required to store data on a floppy disk. The data are stored as nine numbers for each

frequency: four complex S-parameters (two numbers each) and the frequency (one additional number).

All data are analyzed using a program[1] written in BASIC. The program prompts the user to input the following quantities: (1) the number of data points, (2) the length of the sample holder in meters, (3) the length of the sample, (4) the distance from port 1 of the sample holder to the sample, and (5) the distance from port 2 of the sample holder to the sample. The values given in (2) to (5) above are used to rotate the electrical phases from reference planes located at the GR-900 connectors to corresponding planes located at the S_{11} and S_{22} ends of the sample located inside the holder.

The program asks the user for a file name before retrieving the information from the disk. Values for S_{21} and S_{12} (after reference plane rotation) are displayed on the screen, as well as magnitude and phase differences. Since the system should be symmetrical after phase plane rotation, these differences should be close to 0. A set of differences significantly greater than 0 indicates that one or more of the lengths entered in (2) to (5) above need adjustment, or that various system calibrations have not been properly performed.

The user can request that either the S_{11} and S_{21} products or the S_{22} and S_{12} products be used in the calculations. We used both sets of data; accordingly, there are pairs of overlapping curves for each of the four quantities shown in figures 3.4 and 3.5. The program calculates values of the complex permittivity and permeability for the sample according to formulas given in Appendix IV.B. At this point the program will, at the user's option, print the results before saving them on the disk. The stored values are used later to produce graphs.

B.3 Procedures for Determining EM Properties of Test Soils

Measurements of the permittivity and permeability of granular samples such as dry sand and silicon carbide (SiC) sand mixtures are done with methods similar to those described earlier in the section on plastic test targets. Two thin plastic washers are used to confine the material inside the sample holder. The procedure we have adopted involves first inserting a Teflon washer (14 mm diameter, 1.5 mm thickness) into one end of the beadless air line. A measured volume of the sample is then poured in from the other end while gently tapping the body of the holder to allow the sample to settle. A second 1.5 mm Teflon washer is inserted and pushed firmly into place using a metal tube. The distance from the end of the holder to each of the Teflon washers is then measured with a depth gauge and recorded. The GR-900 precision coaxial connectors are reattached to the sample holder which is subsequently connected to the ANA (using GR-900/SMA adaptors and precision coaxial cables). Figure 4.3 shows the measurement setup.

---

[1] Appendix IV.A, attached.

Examples of the measurements made on dry sand and on a 60 percent/40 percent mixture of dry sand and SiC are shown in figures 4.6 and 4.7.

Errors can be reduced by exercising care in sample preparation. The material between the Teflon washers must be free of voids or air gaps. The washers must be machined so that they present a flat face to the air on one side and to the particulate material on the other side. Washers must be placed correctly in the holder with the plane of the washer perpendicular to the center conductor. We tried to make the washers we used as thin as possible—yet with sufficient material to maintain adequate rigidity. The washers are considered to be a part of the sample by the analysis program; their use may introduce errors if the material under test is electromagnetically very dissimilar. The method used for calculating permittivities and permeabilities also requires that the sample be less than one.quarter of a wavelength long. This limits the length of the sample which can be used or limits the frequency range which can be analyzed for materials of high dielectric constant. Very lossy materials (for which no significant transmission through the sample holder takes place) would also be difficult or impossible to characterize. Finally, for solid samples, care must be taken to insure that the samples fit tightly in the holder to minimize contact resistance.

C *In Situ* Methods

A number of investigators have, with varying degrees of success, attempted to develop probe methods for determining the electromagnetic properties of soils. A report [4.31] outlines the measurement technique and the construction details for a two-frequency, *in situ* probe which can be inserted into holes bored into clay or loose soil. The instrument is reliable and easy to use. It is powered by two 9 V batteries and is portable. Measurements at UHF frequencies should be accurate to within 10 percent for conductivity and permittivity. Dalton *et al.* [4.32] used a parallel electrode probe on the end of a parallel wire transmission line, with time-domain reflectometer equipment for a read-out of soil moisture and electrical conductivity. The analysis assumes that the permittivity and the conductivity are independent of frequency, that the soil has a low loss tangent, and that the end of the parallel-electrode probe is a perfect open circuit at all frequencies. There are conditions (such as in dry, salt-free sand) for which the method might give useful, qualitative information.

There are a number of other methods for determining the electromagnetic properties of materials *in situ* [4.33-4.37]. More recently, Scott and Smith [4.38, 4.39] have shown how to use monopoles and more complicated probes to measure the electromagnetic properties of granular and liquid materials. Another approach, used in the petroleum industry, involves placing cavity-backed antennas on borehole instruments. With this technique, the transit-time and the

attenuation of the electromagnetic waves are measured—from which the complex permittivity can be determined at a fixed frequency.

D Measuring the Electromagnetic Properties of Magnetic Materials

Many techniques for the measurement of the magnetic properties of materials are available [4.40-4.42]. Most techniques for determining magnetic susceptibility involve placing the sample in a weak uniform and time-varying source field (less than 4×10^{-3} A/m) which does not saturate the sample, so the initial susceptibility obtained is independent of the magnetizing field and hysteresis effects are avoided. Measurement techniques often involve balancing a Maxwell inductance bridge with the sample inserted into one solenoidal inductance arm of the bridge (figure 4.8). Another approach is to note the change in mutual reluctance between two coils set up in a coaxial or orthogonal relation to each other when the magnetic sample material is placed near the coils, calibrating the system with a standard of known susceptibility and normalizing sample size to an equivalent half-space composed of material of identical susceptibility to the sample's. One paramagnetic standard often used for calibrating susceptibility bridge measurements is ferrous ammonium sulfate $Fe(NH_4)_2\,(SO_4)_2 \cdot 6H_2O$, with a relative molecular mass of 392.15. The susceptibility of this salt is $32.6 \times 10^{-6} \times 4\pi$.

Figure 4.8 shows a typical susceptibility bridge which detects an inductance change in test coil C_2 by action of the coil's field on a sample having unknown susceptibility. Coils C_1 and C_2 are solenoids carefully matched for inductance. M_1 and M_2 are identical variable inductors. In operation, the bridge is balanced with no specimen in either coil through variable resistor R and inductor M_1. The specimen is then inserted into C_2 (test coil) and the bridge balanced with inductor M_2 where the inductance adjustment is proportional to the susceptibility. Calibration of the inductance M_2 may be achieved by balancing the bridge with a test tube containing a known weight of a paramagnetic compound such as ferrous ammonium sulfate of known susceptibility in the coil C_2. Calibration is simply accomplished by balancing the bridge with inductor M_2 when the test standard is placed in C_2. The test tube is then removed and bridge balanced with variable inductor M_1. The same test tube with the same amount of the same standard substance is again inserted into coil C_2 and the bridge balanced with M_2. This process is repeated throughout the inductance range of C_2 so as to obtain a calibration curve referred to the known standard. If ferrous ammonium sulfate is used, it should be kept in a fresh, sealed bottle since the salt is slightly hygroscopic.

In these techniques, the sample is energized with a low-frequency field. This field must have a low-enough frequency that no conductivity response of the sample will be observed. A model which provides a general rule of thumb for the highest usable ac frequency is that of a conducting permeable sphere in a uniform alternating magnetic field,

$$H = H_0 e^{-j\omega t}, \tag{4.14}$$

as shown in figure 4.9. Ward [4.43] has slightly rewritten (for $e^{-j\omega t}$ time dependence) Wait's [4.44] original results for the in-phase M and out-of-phase N components of the induced dipole moment of a sphere in a uniform alternating magnetic field when the wavelength in the external host medium is much greater than the radius of the sphere ($|\gamma_1 a| << 1$, where $\gamma_1 = [j\omega\mu_1\sigma_1 + \omega^2\mu_1\varepsilon_1]^{1/2}$):

$$M - jN = \left[\frac{2\mu_2(\tan\alpha - \alpha) - \mu_1(\alpha - \tan\alpha + \alpha^2\tan\alpha)}{2\mu_2(\tan\alpha - \alpha) + 2\mu_1(\alpha - \tan\alpha + \alpha^2\tan\alpha)}\right], \tag{4.15}$$

$$\alpha = (j\omega\mu_2\sigma_2)^{1/2} a$$

The in-phase and quadrature components of the induced dipole moment of a sphere are shown plotted as a function of the response parameter of a sphere, $\theta = (\omega\sigma_2\mu_2)^{1/2} a$ in figure 4.10. These components are shown in parametric fashion for $\mu_2/\mu_1 = 1$ (free space) to $\mu_2/\mu_1 = 1000$ (steel sphere).

In order that the conductivity response of the sample be small, figure 4.10 shows that $\theta^2 = (\omega\sigma_2\mu_2)a^2$ should be <<1. In the case of pure magnetite, the permeability μ_2 is approximately $1.5 \times 4\pi \times 10^{-7}$ H/m and the conductivity σ_2 is about 1.5×10^4 S/m. Thus, for a 2.5 cm diameter sphere and the condition that $\theta = 0.1$, we find that the maximum allowable frequency is approximately 400 Hz. The maximum allowable frequency for samples that are considerably less conductive than pure magnetite may be higher while still avoiding sample conductivity response. Wait's work [4.45] can also be used to quantitatively assess detection limits for *both* conductivity and permeability contrasts.

A susceptibility meter was used in measuring the susceptibility of a sample of sand-magnetite mix provided to NIST by Lee Anderson of BRDEC. The sample consists of silica sand and magnetite of about 30 mesh size. The susceptibility meter is quite portable (0.5 kg with dimensions of $190 \times 80 \times 30$ mm, operating on one disposable 9 V battery).

The meter contains two coils placed orthogonally to each other in the detector head, which is mounted in the bottom of the instrument case (circuit diagram shown in figure 4.11). In a nonmagnetic environment the voltage induced in the receiver coil by the transmitter coil is zero. When a sample is brought near the coils, a voltage proportional to the magnetic susceptibility of the sample is induced in the receiver coil. The received signal is detected by a phase-locked amplifier and after rectification is sent to drive an analog panel meter, which is thermally compensated and directly calibrated for susceptibility. Field strengths are less than $4\pi \times 10^{-3}$ A/m at 1000 Hz so that with the phase sensitive receiver circuit the influence of electric

conductivity in most samples is usually eliminated. Calibration is usually done for a half-space geometry, which is convenient when measurements are performed in the field. When laboratory samples are measured, a multiplicative correction factor should be applied according to the soil sample size. A chart indicating this half-space correction factor is given in figure 4.12 from information provided by the manufacturer.

The silica sand-magnetite mixture's susceptibility (~330 g sample, ~50 mm diameter) was measured and found to be approximately 0.175 uncorrected for sample size. Using a correction factor of 2.0 from figure 4.12, the susceptibility of the 330 g sample is about 0.35. For mine detection standards, such measurements can provide the practical property range limits for which detection feasibility of various mine detection systems can be judged. Similar comments can be made about other physical property contrast limits, such as complex permittivity (as a function of frequency), density, and acoustic velocity.

E Recommendations and Conclusions

E.1 Laboratory Measurement System

Over the past two years NIST personnel have carefully analyzed all of the available approaches for the accurate measurement of the electrical permittivity, magnetic permeability, and conductivity of solid and granular materials. In addition to the methods described in this chapter, we also spent much time investigating time-domain approaches to this problem [4.45-4.50].

We have concluded that the time-domain approach, although potentially very accurate and relatively inexpensive when compared to frequency-domain approaches, still requires a great deal of developmental work to be practically useful to the Army. The major drawback at present is the fact that these systems can be calibrated accurately only with the use of at least three different standards, each consisting of a sample of material for which all of the electrical properties are known over the frequency range of interest. Unfortunately, these required standards have not been developed.

We have also concluded that the open-ended coaxial sample holder method described in section IV.B.1 still needs some additional work. Although Bussey [4.5] and Jesch [4.29] were able to perform some fairly accurate measurements using this technique, there are still some unanswered questions on the analysis computer program that they used to extract complex permittivity from the measured data. In particular, there are some numerical constants in the computer software which no one at NIST (including Bussey and Jesch) has been able to explain or justify. As a result, we cannot recommend this approach to the Army at present.

The approach that NIST does recommend is the two-port technique using a vector automatic network analyzer. Over the last two years, personnel at NIST have developed considerable knowledge and expertise with this technique, and we feel that it is the best available approach in terms of cost, adequate accuracy, and ease of use. The superiority of this approach is further enhanced by the fact that the Army already possesses all of the required hardware, and by the fact that the network analyzer manufacturer has recently introduced a comprehensive software product that greatly increases the versatility, ease of use, and accuracy of the method.

Therefore, NIST has placed an order for this software package and, upon its arrival, will configure and test the system at NIST. Then, NIST personnel will deliver this system to the Army as soon as possible. The system will consist of the following components:

BRDEC's existing

a. vector network analyzer system (300 kHz to 3 or 6 GHz);
b. computer controller system (to be delivered);
c. calibration standards kit (to be delivered);
d. all required software for system operation (to be delivered).

E.2 Field Measurement System

NIST has found no measurement system or approach which would meet the Army's needs fully for measurements in the field. The methods reviewed in section III.C all have serious drawbacks; they are not sufficiently proven to yield accurate results over a broad range of frequencies (100 MHz to 5 GHz) and a broad range of soil properties (for example, a dielectric constant range of 2 to 25).

Therefore NIST has the following recommendation; the acquisition of a dielectric probe kit that has recently been introduced by the same manufacturer as that mentioned above for the network analyzer and computer controller. This kit includes all necessary software for operation and data presentation. It is capable of measuring complex permittivity, *in situ,* with a dielectric constant of 2 to 80 and for materials that are solid, liquid, or granular. Its specified operating frequency range is 200 MHz to 20 GHz, and its specified uncertainty is typically ±5 percent.

There are two major drawbacks to this approach. First, the system is not very portable because it must be attached to the network analyzer/computer controller. However, if the latter is placed on a wheeled cart, limited portability would be possible. The second drawback is that the probe accuracy becomes seriously degraded for the combination of low dielectric constant and low frequency. For example, from the manufacturer's data sheets, the probe uncertainty for a dielectric constant of 5 at a frequency of 2 GHz is about ±12 percent. Thus, it would be most useful for the Army in measuring wet soils; its usefulness for performing field measurements of dry soils is, at present, questionable.

Even with these shortcomings, NIST thinks that this probe will meet most of the Army's field measurement needs better than any other known approach. Also NIST thinks that the low frequency limitation is caused by the small dimensions of the probe and could be remedied by building a larger probe. As a subject for future work, we recommend that the Army pursue the design of a larger probe.

NIST has ordered one of these probe kits for delivery to the Army along with the network analyzer system. Before delivery, NIST will perform some laboratory tests on the probe in order to verify its proper operation.

References (IV)

[4.1] von Hippel, Arthur R. Dielectric materials and applications. New York: John Wiley & Sons. 438 p.; 1954.

[4.2] von Hippel, Arthur R. Dielectrics and waves. New York: John Wiley & Sons. 284 p.; 1954.

[4.3] Hill, N. E.; Vaughn, W. E.; Price, A. H.; Davies, M. Dielectric properties and molecular behavior. London: Van Nostrand. 480 p.; 1969.

[4.4] Afsar, M. N.; Birch, J. R.; Clarke, R. N. The measurement of properties of materials. Proc. IEEE; 74(l): 183-199; 1986.

[4.5] Bussey, H. E. Dielectric measurements in a shielded open circuit coaxial line. IEEE Trans. Instrum. Meas.; IM-29(2): 120-124; 1980.

[4.6] Jones, R. N.; Bussey, H. E.; Little, W. E.; Metzker, R. F. Electrical characteristics of corn, wheat, and soya in the 1-200 MHz range; Nat. Bur. Stand. (U.S.) NBSIR 78-897; 1978.

[4.7] Birnbaum, G.; Franeau, J. Measurement of the dielectric constant and loss of solids and liquids by a cavity perturbation method. J. Appl. Phys.; 20: 817-818; 1949.

[4.8] Horner, F. Resonance methods of dielectric measurement at centimeter wavelengths. J. IRE; 93(III): 55-57; 1946.

[4.9] Bethe, H. A.; Schwinger, J. Perturbation theory of resonant cavities; NDRC, Rpt. D2-117; 1943.

[4.10] Cook, R. J. Microwave cavity methods, in high frequency dielectric measurements; J. Chamberlain and G. W. Chantry, ed., IPC Science & Technology Press, pp. 12-27; 1973.

[4.11] Bussey, H. E. Measurement of RF properties of materials: a survey. Proc. IEEE; 55: 1046-1053; 1967.

[4.12] Culshaw, W.; Anderson, M. V. Measurement of permittivity and dielectric loss with a millimeter wave Fabry-Perot interferometer. Proc. IEEE; 109(B), Suppl. 23: 820-826; 1962.

[4.13] Degenford, J.; Coleman, P. D. A quasi-optic perturbation technique for measuring dielectric constants. Proc. IEEE; 54: 520-522; 1966.

[4.14] Degenford, J. A quasi-optic technique for measuring dielectric loss tangents. IEEE Trans. Instrum. Meas.; IM-17: 413-417; 1968.

[4.15] Cullen, A. L.; Yu, P. K. The accurate measurement of permittivity by means of an open resonator. Proc. R. Soc. A; 325: 493-509; 1971.

[4.16] Conbau, G.; Schwering, F. On the guided propagation of electromagnetic wave beams. IRE Trans.; AP-9: 248-256; 1961.

[4.17] Cullen, A. L.; Nagenthiram, P.; Williams, A. D. Improvement in open resonator permittivity measurement. Electron. Letters; Vol. 8: 577-579; 1972.

[4.18] Cullen, A. L.; Nagenthiram, P.; Williams, A. D. A variational approach to the theory of the open resonator. Proc. R. Soc. A.; 329: 153-169; 1972.

[4.19] Kogelnik, H.; Li, T. Laser beams and resonators. Proc. IEEE; 54: 1312-1329; 1966.

[4.20] Cook, R. J.; Jones, R. G.; Rosenberg, C. R. Comparison of cavity and open resonator measurements of permittivity and loss angle at 35 GHz. IEEE Trans. Instrum. Meas.; IM-23: 438-442; 1974.

[4.21] Jones, R. G. Precise dielectric measurements at 35 GHz using an open microwave resonator. Proc. IEEE.; 123(4): 284-290; 1976.

[4.22] Van Gemert, M. J. C. High-frequency time-domain methods in dielectric spectroscopy. Phillips Res. Rpts; 28: 530-572; 1973.

[4.23] Gans, W. L.; Andrews, J. R. Time-domain automatic network analyzer for measurement of rf and microwave components; Nat. Bur. Stand. (U.S.) Tech. Note 672; 1975 September. 165 p.; 1975.

[4.24] Nicolson, A. M.; Ross, G. F. Measurement of the intrinsic properties of materials by time-domain techniques. IEEE Trans. Instrum. Meas.; IM-19 (4): 377-382; 1970.

[4.25] Peyrelasse, J.; Boned, C.; LePetit, J. P. Setting up of a time-domain spectroscopy experiment. Application to the study of the dielectric relaxation of pentanol isomers. J. Phys. Sci. Instr.; 14: 1002-1008; 1981.

[4.26] Nakamura, H.; Mashimo, S.; Wada, A. Precise and easy method of TDR to obtain dielectric relaxation spectra in the GHz region. Japanese J. Appl. Phys.; 21(7): 1022-1024; 1982.

[4.27] Suggett, A. Time-domain methods, dielectric and related molecular processes. Chem. Soc. London; Vol. 1: 101-120; 1972.

[4.28] Bottreau, A. M.; Dutuit, Y.; Moreau, J. On a multiple reflection time domain method in dielectric spectroscopy: Application to the study of some normal primary alcohols. J. Chem. Phys.; 66(8): 3331-3336; 1977.

[4.29] Jesch, R. L. Dielectric measurements of five different soil textural types as functions of frequency and moisture content; Nat. Bur. Stand. (U.S.) NBSIR 78-879; 1978.

[4.30] Measuring Dielectric Constant with the HP 8510 Network Analyzer. Product Note No. 8510-3, Hewlett-Packard Corp., Palo Alto, CA; August 1985.

[4.31] Caldecott, R.; et al. A radio frequency probe to measure solid electrical parameters; Final Report 715616-4; Ohio State University ElectroScience Lab., Columbus, Ohio; January 22, 1985.

[4.32] Dalton, F. N.; et al. Time-domain reflectometry: Simultaneous measurement of soil water content and electrical conductivity with a single probe. Science; 224: 989-990; June 1, 1984.

[4.33] King, R. W.; Smith, G. S. Antennas in matter; fundamentals, theory, and applications. Cambridge, MA: M.I.T. Press; 1981.

[4.34] Smith, G. S.; King, R. W. P. Electric field probes in material media and their application in EMC. IEEE Trans. Electromagn. Compat.; EMC-17: 206-211; 1975.

[4.35] Smith, G. S.; King, R. W. P. Electric field probes in material media and their application in EMC. IEEE Trans. Electromagn. Compat.; EMC-18, p. 130; 1976.

[4.36] Smith, G. S.; Nordgard, J. D. Measurements of the electrical constitutive parameters of materials using antennas. IEEE Trans. Ant. Prop.; 33(7): 783-792; 1985.

[4.37] Scott, W. R. Dielectric spectroscopy using shielded open.circuited coaxial lines and monopole antennas of general length. Ph.D. thesis, Georgia Inst. Tech., 228 p.; 1985.

[4.38] Scott, W. R. and Smith, G. S. Dielectric spectroscopy using monopole antennas of general electrical length. IEEE Trans. Ant. Prop.; AP-34(7): 919-929; July 1986.

[4.39] Smith, G. S. and Scott, W. R. A simple method for the in situ measurement of the electrical properties of the ground. Paper JA02-3, pages 242-245, 1987 IEEE AP-S International Symposium Digest, Virginia Tech. (IEEE Catalog No. CH2435-6/87); June 15-19, 1987.

[4.40] Nagata, T. Rock magnetism. Tokyo: Maruzen Press, 350 p.; 1961.

[4.41] Akimoto, S. Magnetic properties of ferromagnetic oxide minerals as a basis of rock magnetism. Adv. Phys.; 6(288); 1957.

[4.42] Heiland, C. A. Geophysical exploration. Englewood Cliffs, New Jersey: Prentice Hall, pp. 310-314; 1940.

[4.43] Ward, S. H. Electromagnetic theory for geophysical applications. Mining Geophys.; II, p. 78; 1967.

[4.44] Wait, J. R. A conducting sphere in a time varying field. Geophy.; 16, p. 666; 1951.

[4.45] Fellner-Feldegg, H. The Measurement of Dielectrics in the Time Domain. J. Phys. Chem.; 73 (3): 616-623; 1969.

[4.46] Cole, R. H. Evaluation of dielectric behavior by time domain spectroscopy. I. Dielectric response by real time analysis. J. Phys. Chem.; 79 (14): 1459-1469; 1975.

[4.47] Cole, R. H. Evaluation of dielectric behavior by time domain spectroscopy. II. Complex permittivity. J. Phys. Chem.; 79 (14), 1469-1474; 1975.

[4.48] Cole, R. H.; Mashimo, S.; Winsor, P., IV. Evaluation of dielectric behavior by time domain spectroscopy. 3. Precision difference methods. J. Phys. Chem.; 84 (7): 786-793; 1980.

[4.49] Bose, T. K.; Bottreau, A. M.; Chahine, R. Development of a dipole probe for the study of dielectric properties of biological substances in radiofrequency and microwave region with time-domain reflectometry. IEEE Trans. Instrum. Meas.; IM-35 (1): 56-60; 1986.

[4.50] Cole, R H.; Berberian, J. G.; Mashimo, S; Chryssikos, G.; Burns, A.; Tombari, E. Time domain reflection methods for dielectric measurements to 10 GHz. J. Appl. Phys.; 66 (2): 793-802; 1989.

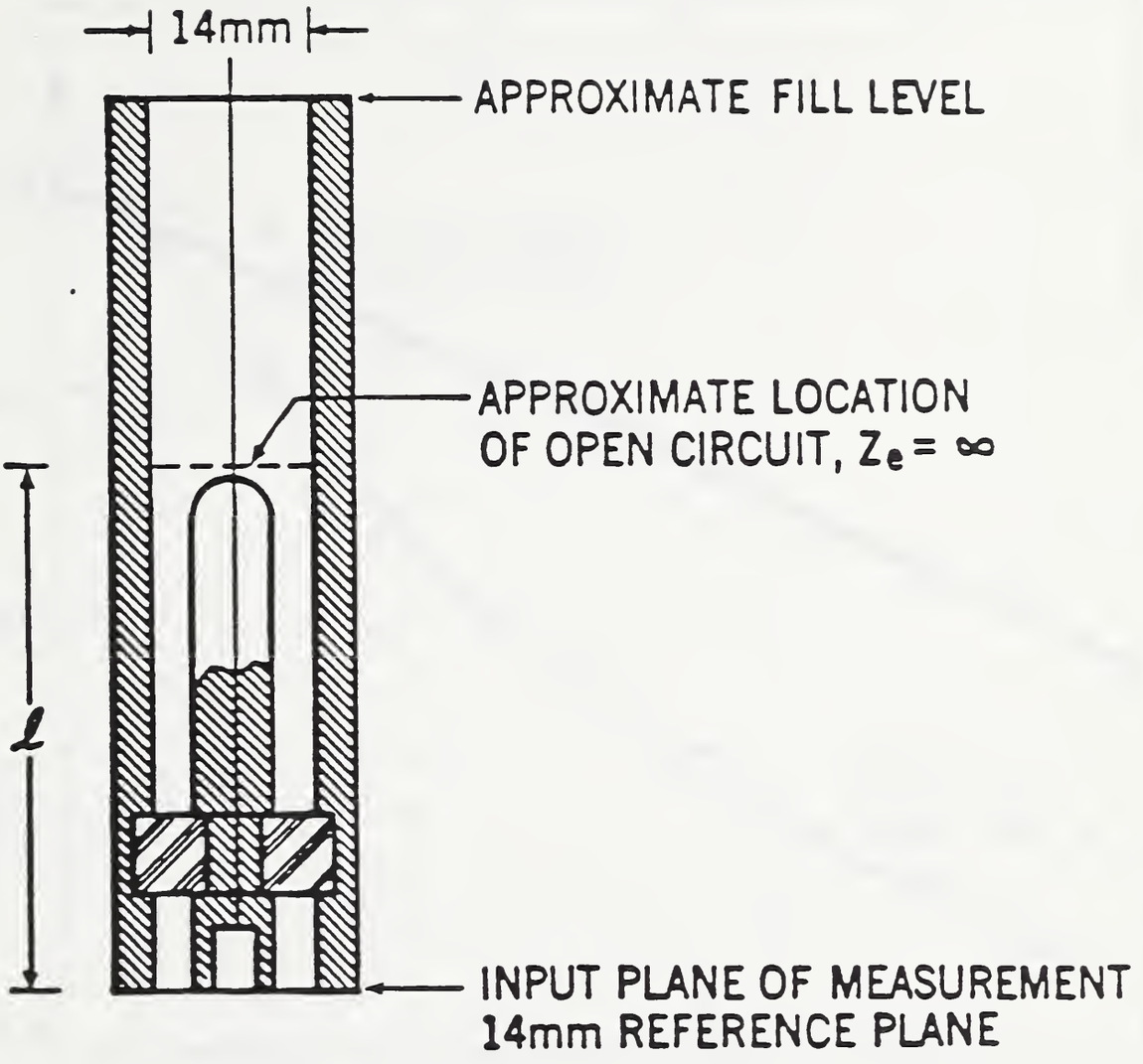

Figure 4.1 Cross-sectional drawing of the coaxial transmission line sample holder for the single-port measurement scheme.

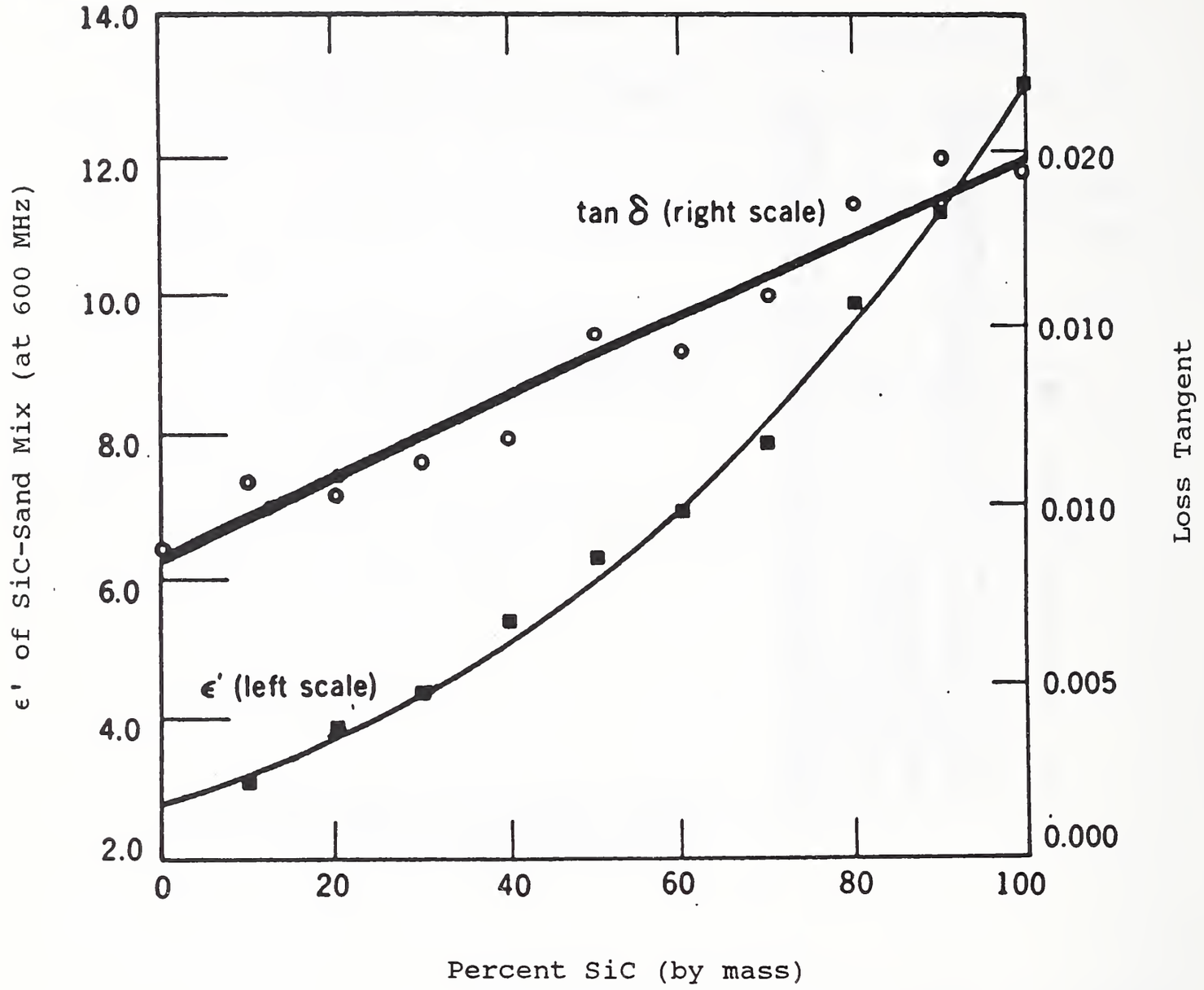

Figure 4.2 Electromagnetic properties (at 600 MHz) of a blend of SiC and silica sand for various percentages (by mass) of SiC.

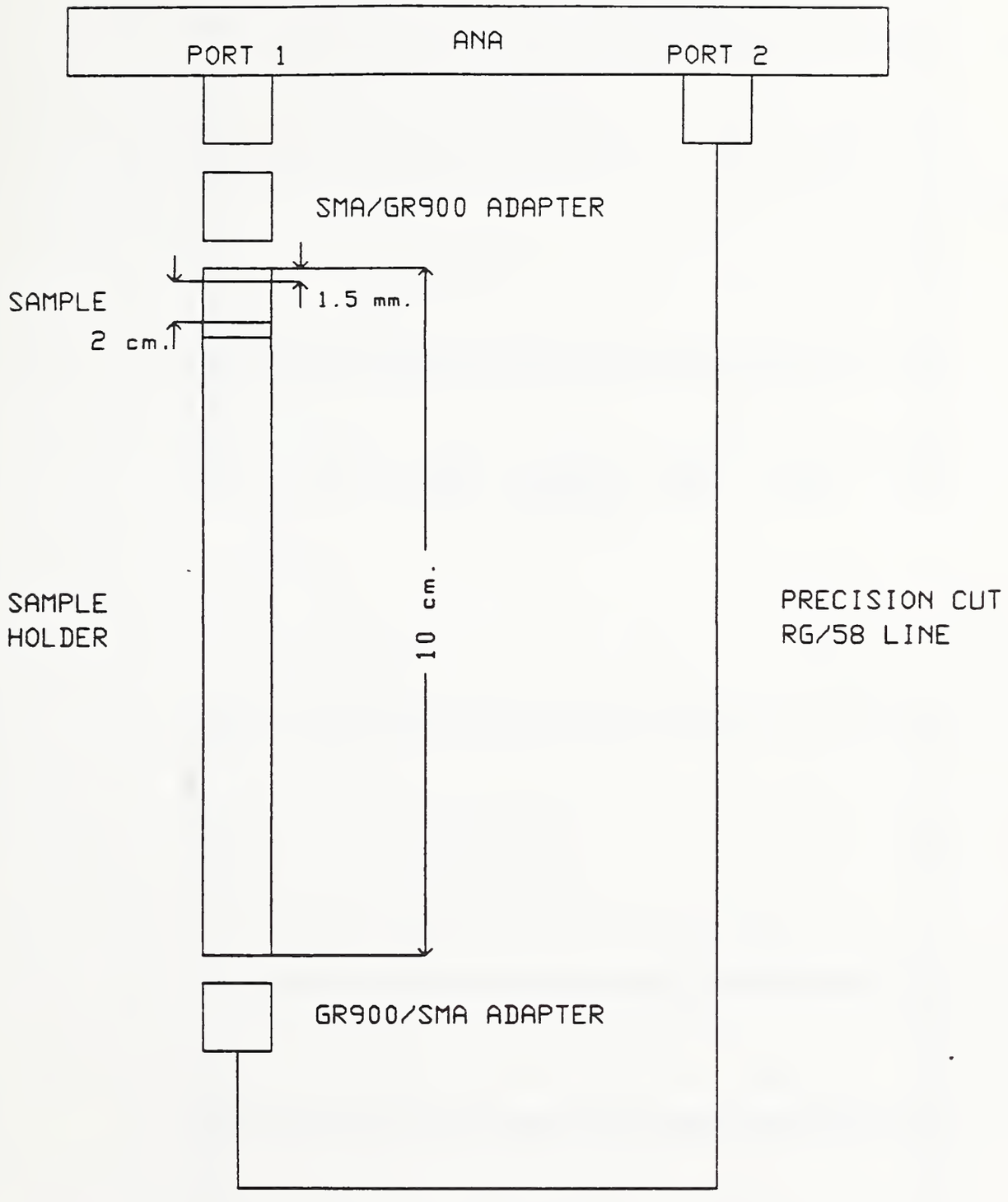

Figure 4.3 Schematic of the ANA materials measurement system.

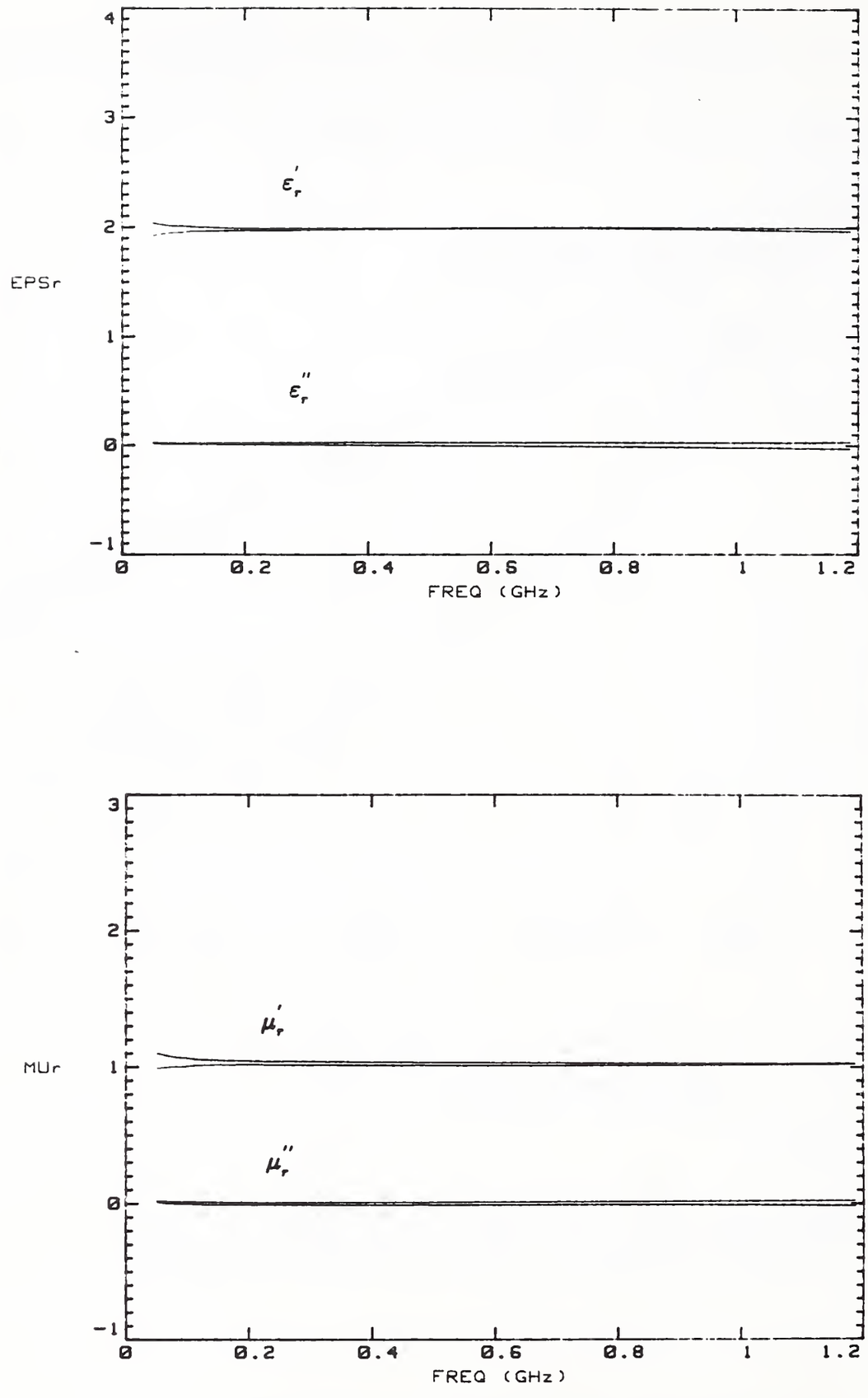

Figure 4.4 Complex relative permittivity and permeability of Teflon as measured with the ANA.

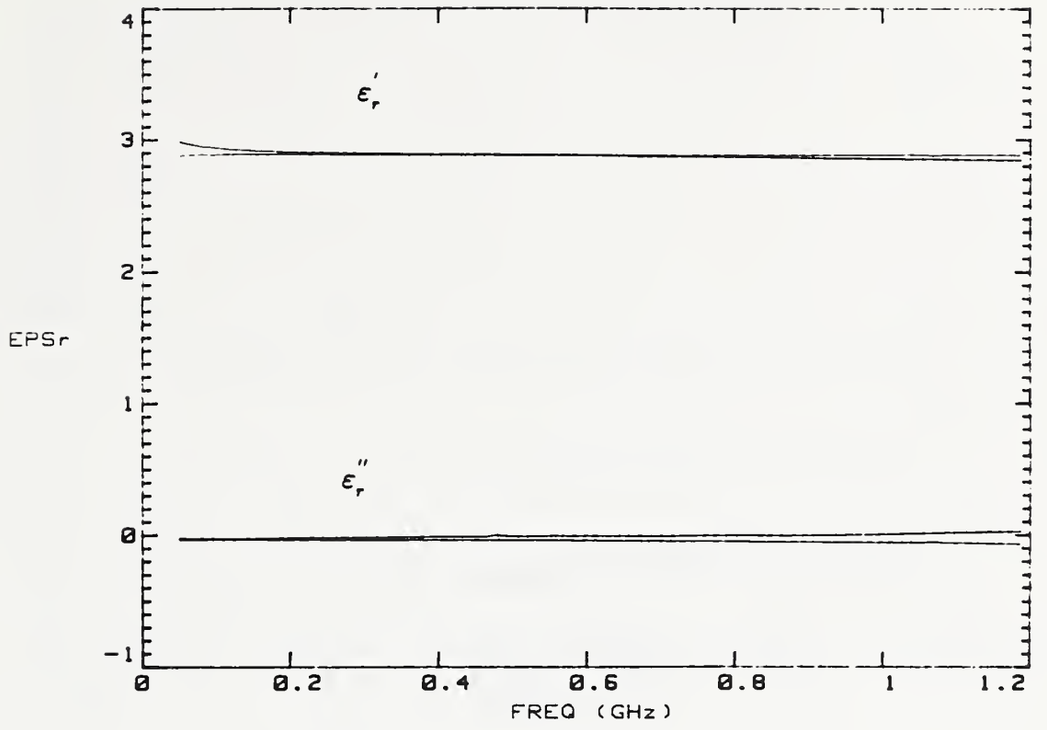

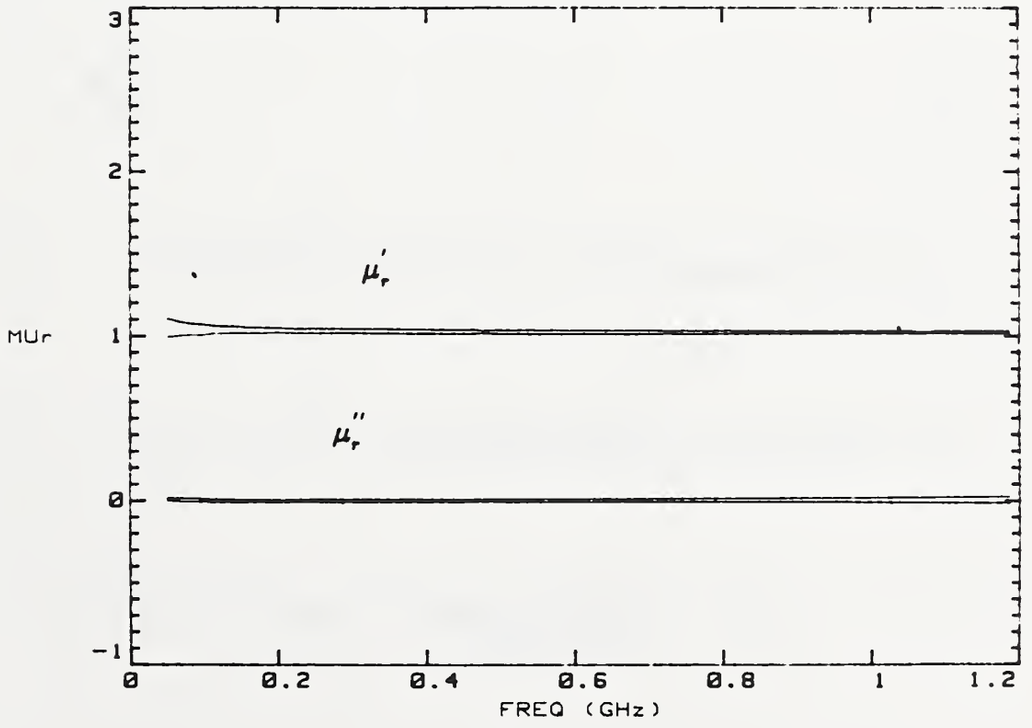

Figure 4.5 Complex relative permittivity and permeability of nylon as measured with the ANA.

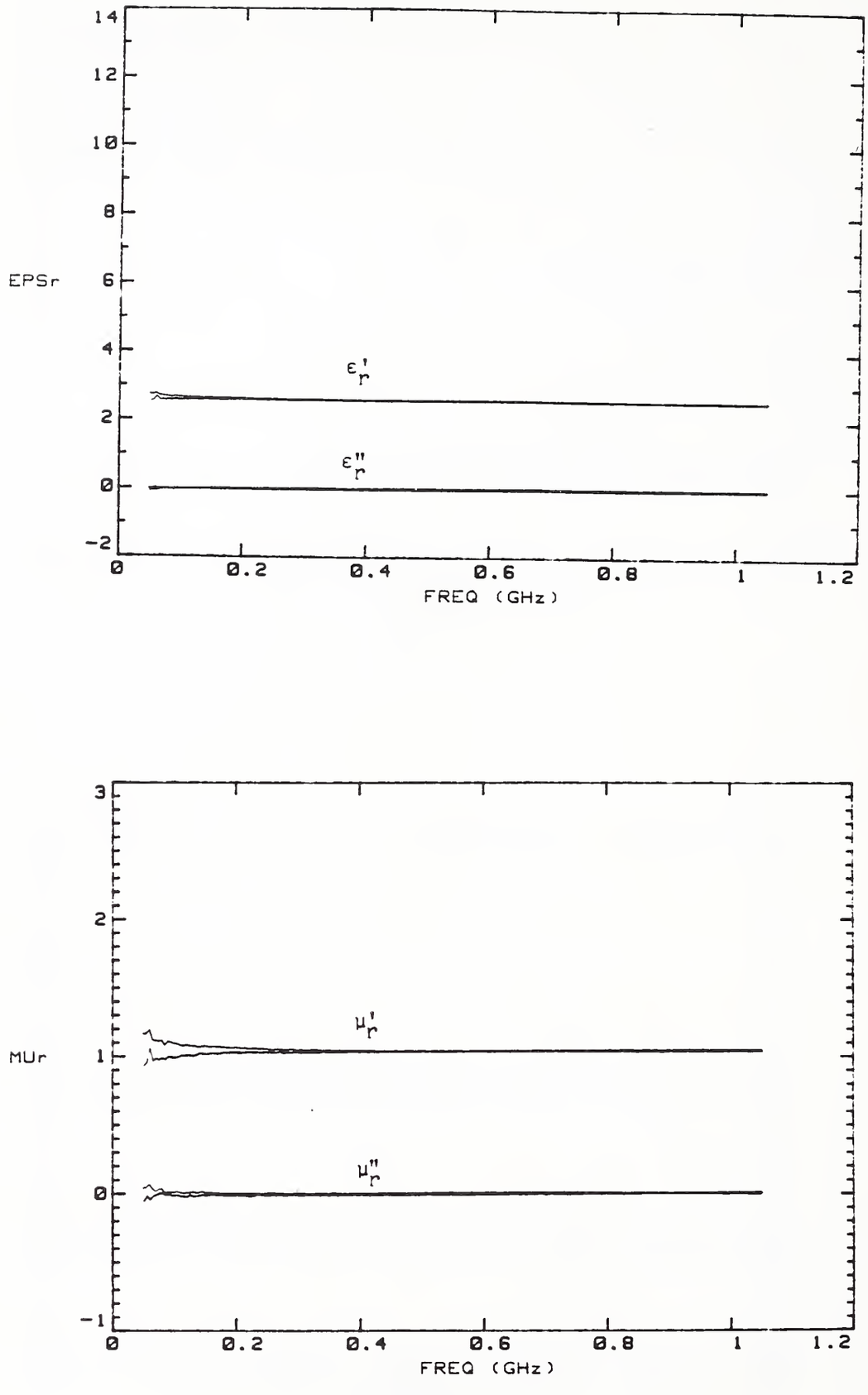

Figure 4.6 Complex relative permittivity and permeability of dry sand as measured with the ANA.

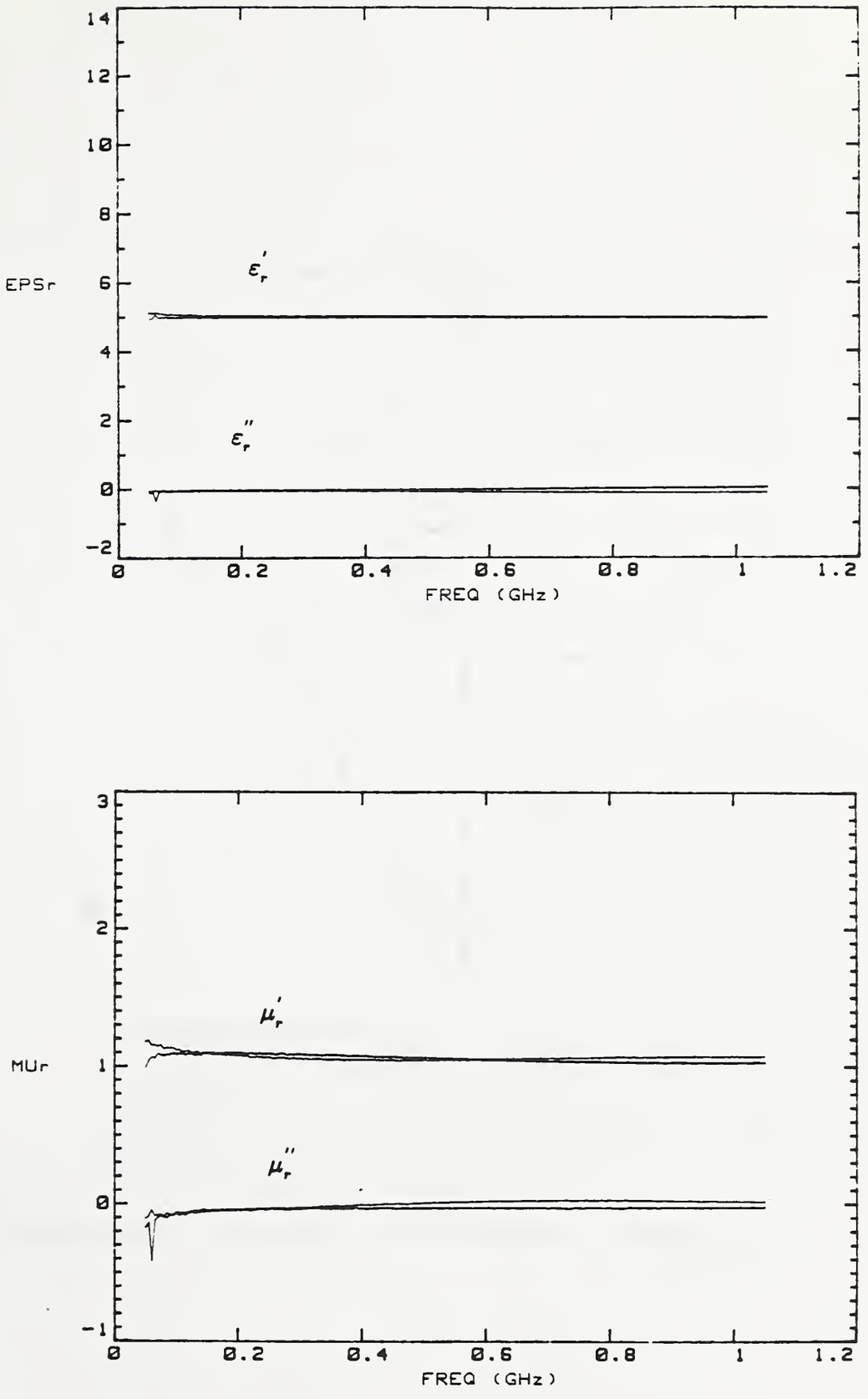

Figure 4.7 Complex relative permittivity and permeability of a 60% dry sand and 40% (by weight) SiC mixture as measured with the ANA.

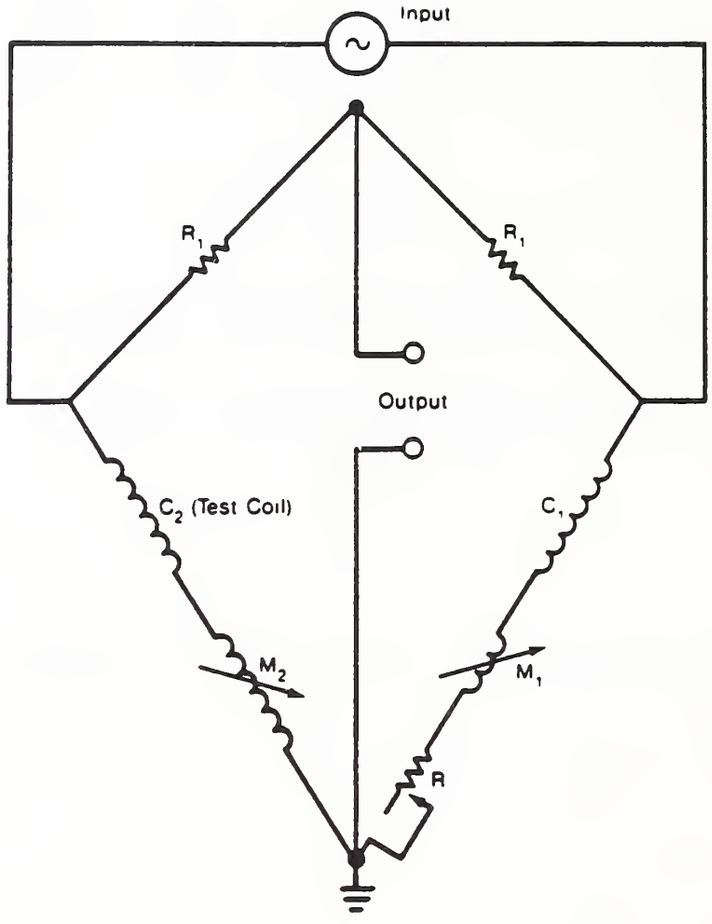

Figure 4.8 Schematic diagram for a typical susceptibility bridge.

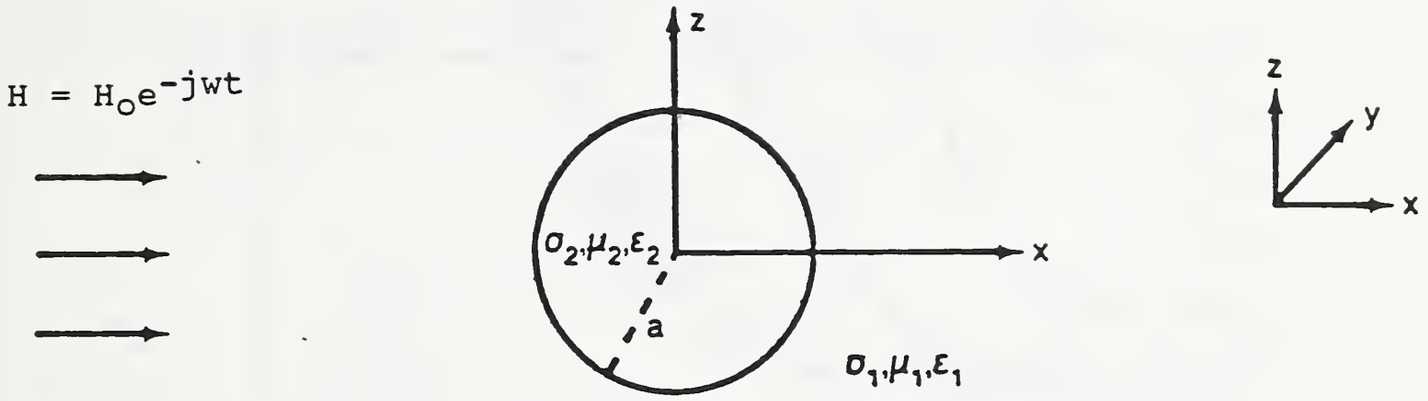

Figure 4.9 Conducting permeable sphere of radius a in a uniform alternating magnetic field. The conductivity, permeability, and permittivity of the host medium are σ_1, μ_1, and ϵ_1, respectively. The conductivity permeability, and permittivity of the sphere are σ_2, μ_2, and ϵ_2, respectively.

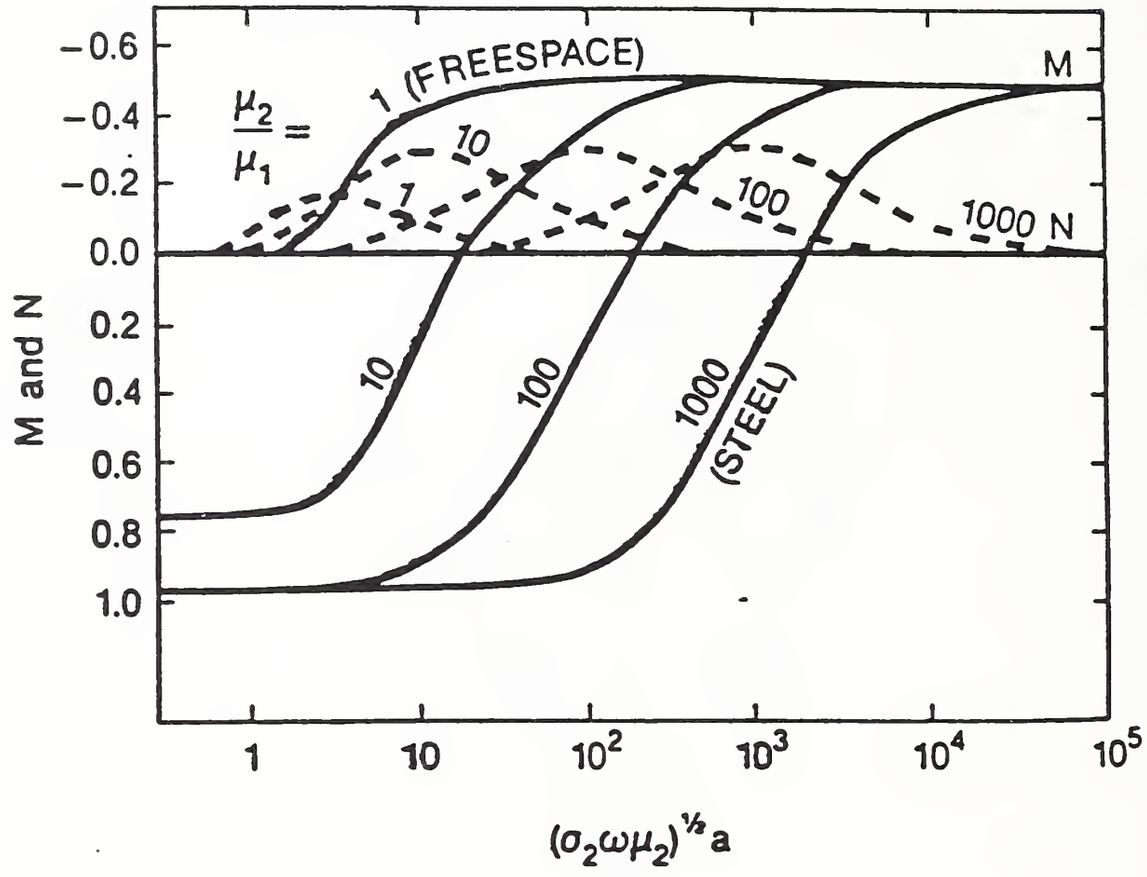

Figure 4.10 In-phase (M) and out-of-phase (N) components of the induced dipole moment for a sphere in a uniform alternating magnetic field for the case $|\gamma_1 a| \ll 1$. See reference [4.43].

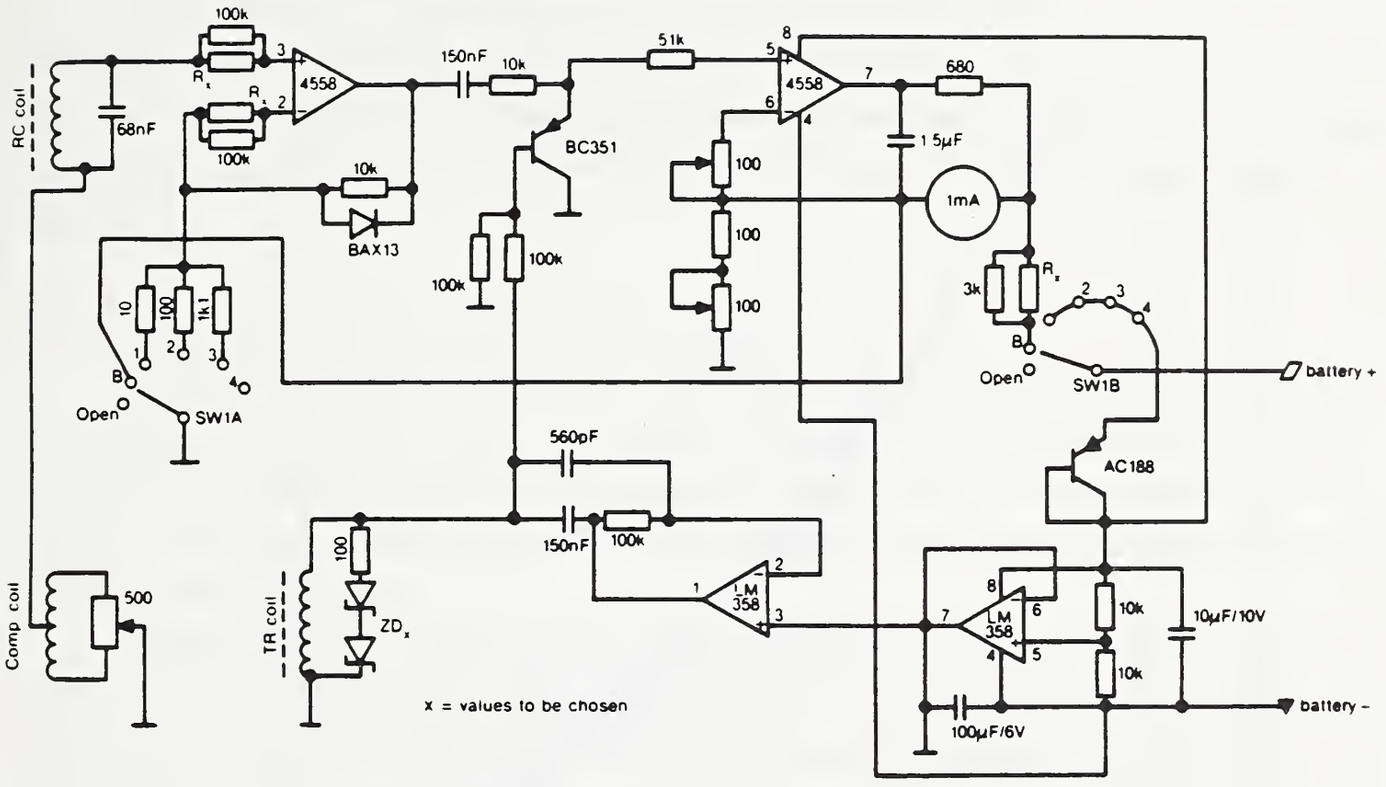

Figure 4.11 Circuit diagram for the susceptibility meter

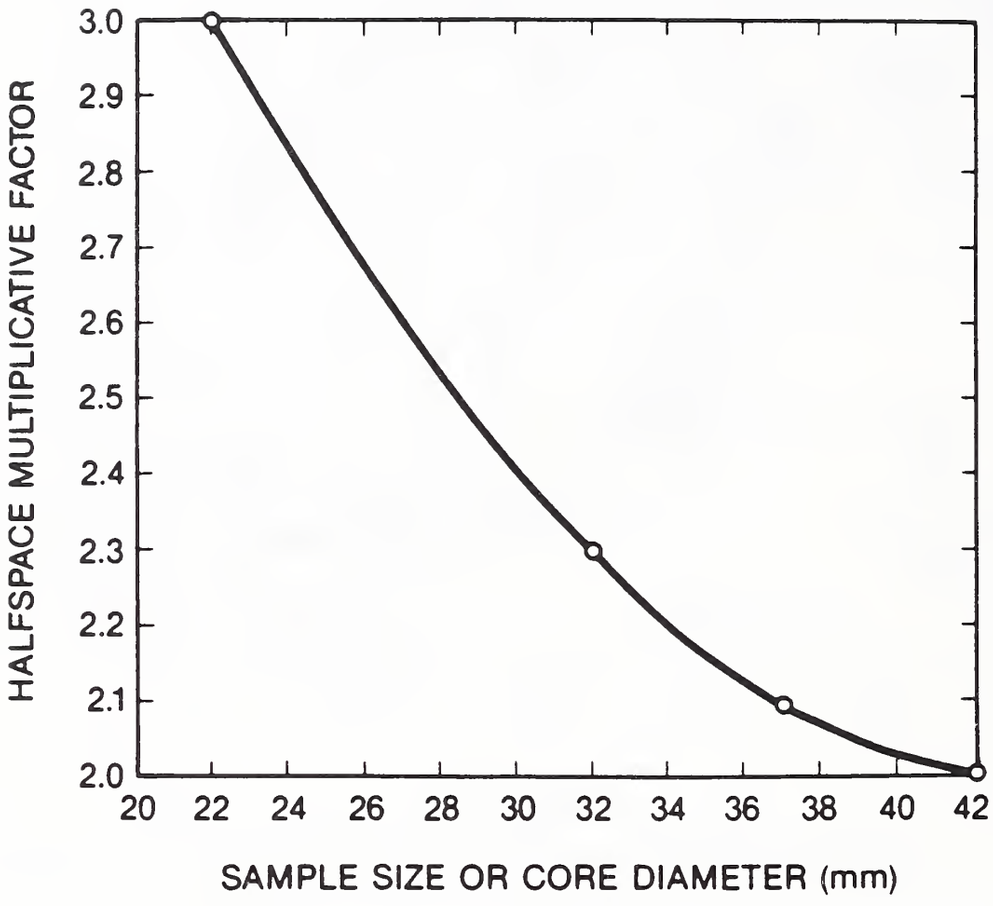

Figure 4.12 Half-space multiplicative correction factor for susceptibility measurements.

V Electromagnetic Properties of the Earth and Options for Standard Media

A Typical Electromagnetic Properties of Real Soils

Knowledge of the electromagnetic properties of typical real soils is necessary before it is possible to identify candidate methods for realizing soil standards. Several cases may be listed and generally characterized in terms of conductivity and permittivity contrasts as representative of the differing electrical environments likely to be encountered in either plastic or metallic mine detection.

Case 1: Dry Beach Sands (Plastic Mine Detection)

One type of host soil environment is that in which either no pore water or very little pore water (water saturation $Sw < 0.01$) exists within a magnetically impermeable, unconsolidated, and electrically resistive soil grain matrix having low cation exchange capacity. Such a situation exists in a dry beach sand or dry gravel host and probably presents the most difficult plastic mine detection test environment.

The host soil conductivity σ_H in this case is generally low ($\sigma_H \leq 10^{-3}$ S/m) and the host dielectric constant, ε'_H, is low and probably less than the target (mine) dielectric constant ($\varepsilon'_H = 2.70$ when referred to dry sand consisting of clean quartz grains having diameters greater than 0.03 mm but less than 0.60 mm where the water saturation, Sw, is 0 and the frequency is 300 MHz). If we take a nylon sphere as representative of our plastic mine target (where the target conductivity, σ_T, is much less than 10^{-3} S/m and the target dielectric constant ε'_T remains fixed at 3.00), then $\varepsilon'_H/\varepsilon'_T \doteq 0.90$ and $\sigma_H/\sigma_T \doteq 1$.

Case 2: Wet, Fresh Water Beach Sands (Plastic Mine Detection)

This situation is characterized by moderately fresh (deionized) pure water saturation ($Sw \doteq 0.14$) in a magnetically impermeable, unconsolidated, and electrically resistive ($\sigma_H \leq 10^{-3}$ S/m) soil grain matrix of low cation exchange capacity. Due to increased water saturation, the host soil dielectric constant at a typical UHF detection frequency of 300 MHz would be approximately 10, leading to dielectric and conductivity ratios of $\varepsilon'_H/\varepsilon'_T \doteq 3.3$ and $\sigma_H/\sigma_T \doteq 1$. Because of the higher permittivity contrast at the chosen operating frequency, this case probably presents a less difficult detection test than Case 1.

Case 3: Wet Clay Soils and Wet Marine Beach Sands (Plastic Mine Detection)

The wet clay soil environment is characterized by highly brackish or saline pore water saturation ($Sw \geq 0.20$) in a magnetically impermeable, unconsolidated, and electrically conductive soil grain matrix of high cation exchange capacity. In such a case, both the measured host soil conductivity and host soil dielectric constant at 300 MHz are relatively high ($0.1 \text{ S/m} \leq \sigma_H < 1 \text{ S/m}$ and $\varepsilon'_H \doteq 20$); this leads to significant dielectric and conductivity ratios where $\varepsilon'_H / \varepsilon'_T \doteq 6.7$ and $\sigma_H / \sigma_T >> 1$ for a nylon spherical target. Such a situation is likely to be that most commonly encountered; therefore, it is one which should be simulated in any validation testing.

These electrical properties would also characterize a magnetically impermeable, unconsolidated, and electrically resistive soil grain matrix of low cation exchange capacity having highly saline pore waters, such as might be encountered in wet marine beach sands. All other factors being equal, target visibility in terms of dielectric contrast is greatest for this case, but because of the conductive (lossy) nature of the host medium, test target detection at increasing depths of burial for UHF operating frequencies is expected to be sharply limited.

Case 4: Magnetically Impermeable Host Soils (Metal Mine Detection)

Because the contrast in conductivity between a metallic mine target in either an electrically resistive dry beach sand or an electrically conductive wet clay remains very high (for analysis purposes, infinite), and because most metal mine detectors operate in the VLF region (affording little attenuation for expected burial depths) and sense secondary magnetic fields due to induced eddy currents within the buried mine, two test soils would seem to bracket those situations commonly encountered in the field. These are a magnetically impermeable or magnetically permeable host medium. The magnetically impermeable host soil may be simulated by quartz sand grains having no magnetite-ilmenite, which are the common naturally occurring magnetic minerals [5.1]. Hence, the host soil medium in this case would have a magnetic permeability μ_H equal to that of free space, μ_0 ($4\pi \times 10^{-7}$ H/m). Conductive losses in the host medium can be controlled either by adding known amounts of saline pore water or aluminum powder.

Case 5: Magnetically Permeable Host Soils (Metal Mine Detection)

Attenuation rates for a plane electromagnetic wave in a uniform, magnetically permeable earth are greater than in a uniform, magnetically impermeable earth—all other factors being equal. In fact, the plane-wave skin depth (distance within the earth at which amplitudes of the electric and magnetic fields are equal to $1/e = 0.3679$ of their respective values at the surface) of a magnetically permeable host soil decreases by $(\mu_r \mu_0)^{-1/2}$ where μ_r is the relative permeability and μ_0 is the permeability of free space or vacuum. The BRDEC already has a test lane

simulating this case that consists of a silica sand magnetite mixture (70 percent dry sand, 30 percent magnetite grains, –30 mesh size) whose relative magnetic permeability was measured and found to be 1.35 [5.1]. Because not all metallic land mine detectors employ ground signal removal techniques, a logical test procedure for evaluating differing systems would be to simulate both Case 4 and 5 in the test lane environment. See table 5.1 (from [5.2]) for a list of the magnetic susceptibility of naturally occurring rocks and minerals.

B Dielectric Mixing Rules

Soils are mixtures of minerals that are the weathered byproducts of rocks. Usually, natural soils contain some water, so the way in which dielectric constants combine is important in determining the bulk, or effective, dielectric constant of the soil at hand. The bulk dielectric constant of any soil (whether natural or synthetic) determines the electromagnetic visibility of buried land mines and, therefore, intrinsically affects the performance of any detection system. Once a range of suitable dielectric background characteristics, relatable to conditions actually encountered in the field, is accepted, mixing rules provide the easiest and most pragmatic approach to specification of standard test soils.

Geyer [5.3] has noted that some mixing rules have little broadband applicability to soils since they are based on systems where little or no conduction takes place. For example, when one of the components in a composite dielectric is conductive, large (frequency-, temperature-, and salinity-dependent) polarizations can occur that can be attributed to interfacial polarizations at the boundaries of the conductive phase. A mixing rule that does not account for these interfacial polarizations has little broadband applicability. Despite the fact that most mixing rules fail in a broadband sense (since they do not account for all relaxation effects), it is nonetheless useful to be able to predict the effective electromagnetic properties of soils of different lithologies and porosities even over narrower frequency ranges—100 MHz to 2 GHz in this case—that affect the signal levels measured by UHF land mine detection systems.

The purpose of a mixing rule is to allow estimation of the dielectric properties of a soil (either test standard or soil encountered in the field) when given measurements of that soil's physical properties only. Its usefulness will be limited by its dependence on adjustable soil- and frequency-specific parameters. An efficacious mixing rule, then, will provide a convenient means for predicting a test soil's dielectric behavior in microwave land mine performance testing and in signal level determination. It will also provide a physically based mixing model that is dependent on measurable soil parameters and can be used for subsequent development and research.

Table 5.1

Magnetic susceptibility of rocks and minerals.

Magnetic minerals	*Susceptibility $\chi_m/4\pi$ (SI)*		
Magnetite crystals	6.3	to	24.0
Magnetite	0.04	to	2.0
Ilmenite	0.03	to	0.14
Franklinite	0.036		
Pyrrhotite	0.007	to	0.028
Specularite	0.003	to	0.004
Chromite	0.002		
Major rock types			
Basic effusive	0.001	to	0.004
Basic plutonics	<0.0001	to	<0.004
Granites and allied rocks	<0.0001	to	<0.001
Gneisses, schists, and slates	<0.0001	to	<0.001
Sedimentaries	<0.0001	to	<0.001
Specific rock types			
Igneous rocks			
Basalt	0.000 68	to	0.006 3
Diabase	0.000 078	to	0.004 2
Gabbro	0.000 44	to	0.004 1
Granite	0.000 03	to	0.002 7
Porphyry	0.000 023	to	0.000 5
Metamorphic rocks			
Serpentine	0.000 25	to	0.014
Slate	0.000 039	to	0.003 0
Gneiss	0.000 01	to	0.002 0
Schist	0.000 026	to	0.000 24
Sedimentary rocks			
Shale	0.000 04	to	0.000 5
Clay	0.000 2		
Sandstone	0.000 005	to	0.000 017
Dolomite	0.000 000 9	to	0.000 014
Limestone	0.000 004		
Iron ores and minerals			
Siderite	0.000 1	to	0.003
Limonite	0.000 1	to	0.000 2
Hematite	0.000 04	to	0.000 1
Ankerite	0.000 02	to	0.000 1

Table 5.1

Magnetic susceptibility of rocks and minerals, continued.

Typical sulfide minerals			
Arsenopyrite	0.000 005	to	0.000 2
Chalcopyrite	0.000 005	to	0.000 2
Chromite	0.000 005	to	0.000 2
Markasite	0.000 005	to	0.000 2
Pyrite	0.000 005	to	0.000 2
Diamagnetic minerals and rocks			
Anhydrite	–0.000 001 1	to	–0.000 01
Quartz	–0.000 001 1	to	–0.000 001 2
Sylvite	–0.000 000 9	to	–0.000 001 1
Calcite	–0.000 000 6	to	–0.000 001 0
Rock salt	–0.000 000 4	to	–0.000 001 3

Generally, all materials can be classified into one of three dielectric groups. The first of these, to which pure water and ice belong, is homogeneous substances. A second group, in which ionic salts are dissolved in solution (usually water) is electrolytic solutions. The third group, heterogeneous mixtures, includes that of wet, lossy soils or multicomponent (lossy or nonlossy) media of interest here for test soil lanes. The merits of any chosen background material (standard) for mine test lanes depend not only on correlation with actual field conditions likely to be encountered but also on the ease with which its (complex) dielectric properties can be predicted and controlled for the operational frequency range of interest.

B.1 Function-Theoretic Rules

In general, the average dielectric constant of a heterogeneous mixture consisting of two or more substances is related to the dielectric constants of the individual substances, their volume fractions, their spatial distributions, and their orientations relative to the direction of the incident electric field vector [5.4]. In order to determine the functional dependence of the average dielectric constant of a mixture on these variables, the average electric field within the mixture as a whole must be related to the electric fields within the inclusions [5.5]. The problem is that if the inclusions are randomly dispersed throughout the host medium, it is not generally possible to derive an exact solution for the fields within the inclusions since the mutual electromagnetic interactions of the inclusions are dependent on their positions with respect to each other. Tinga [5.6] gives a review of various approximations that have been proposed for solving the interaction problem. These approximations vary from those that ignore short-range interactions between inclusions (by restricting the validity of the dielectric mixing model to only those

mixtures characterized by a low concentration of inclusions) to relations that account for first-order inclusion interactions by the solution of Maxwell's equations and appropriate boundary conditions [5.6, 5.7]. In all cases, the dimensions of the inclusions are much smaller than the propagation wavelength in the host medium. Bottcher [5.8] gives a comprehensive review of dielectric mixing models that includes both empirical (or semi-empirical) formulations for specific mixtures as well as theoretical models developed for highly specialized media that contain either ellipsoidal particle inclusions (spheres, disks, needles) or confocal ellipsoidal spheroids.

B.2 Generalized Heuristic Rules for Soil Mixtures

Natural soils are mixtures of matrix minerals, air, and water. As noted in [5.3], water in the pore spaces of surface soils consists of two phases. One of these phases is the bulk (free) pore water. The other is adsorbed water that is adjacent to the matrix grain surfaces and usually several molecular layers thick. This adsorbed water is called surface (or bound) water. The saturation at which the dielectric constant becomes less sensitive to water saturation is entirely a function of the amount of surface water in soil pore spaces; this explains the dependence of the dielectric constant on soil texture types (particle size and shape distributions) as well as on the intrinsic porosity of the soil mixture. Of course, the porosity is simply related to the bulk density, and the degree of conductive loss responsible for electromagnetic wave attenuation is dependent on the salinity of the pore water which, in turn, depends quite naturally on both the matrix cation exchange capacity and the soil temperature. The fact that the electrical properties of water-saturated soils are frequency dependent is also not physically surprising since we expect polarization, that is, the orientation of polar molecules (molecules with asymmetric charge distributions), to occur in an applied electric field. The mobility of any polar molecule (such as water) will always depend on the time rate of variation of that field.

Bound water adsorbed to a solid surface has a dielectric response significantly different from that of free water. This is so because the molecular mobility of the water molecules has been reduced by physical bonding to the matrix grain surfaces [5.9, 5.10, 5.11]. Most of the measurement evidence to date seems to indicate that the restricted mobility causes a reduction of the static dielectric constant of water adsorbed to the surface from 80 for free water to about 6 for sorbed water [5.10] which is greater than an order-of-magnitude reduction. Furthermore, surface-bound water exhibits a relaxation frequency of about 10^4 Hz instead of 100 GHz, which is seven orders of magnitude lower than that of bulk water [5.3, 5.12].

Such observations have led McCafferty and Zettlemayer [5.11] to suggest that dielectric dispersion in the VLF region in systems composed of a solid and adsorbed water may principally be due to relaxation of the adsorbed water. However, an equally plausible explanation is that

conductivity inhomogeneities in a soil matrix are responsible for dielectric dispersion and it is not the rotational mobility of water molecules in the surface water that is important, but rather the conductivity of the surface layer [5.13, 5.14].

Thus the most general form of a heuristic, predictive dielectric mixing rule that might be used for soil specifications would separate the volumetric percentages of bound and free water. The soil mixture is then described electrically as a four-component system whose constituent components are linearly combined in terms of the respective volume fractions as

$$\varepsilon_{soil}^{\alpha} = \mathrm{v}_m \varepsilon_m^{\alpha} + \mathrm{v}_a \varepsilon_a^{\alpha} + \mathrm{v}_{bw} \varepsilon_{bw}^{\alpha} + \mathrm{v}_{fw} \varepsilon_{fw}^{\alpha}, \tag{5.1}$$

where v represents volume fraction; the subscripts m, a, bw, and fw represent soil matrix, air, bound water, and free water, and α is a constant.

Here we recognize that

$$\Phi = \text{total porosity} = (\rho_m - \rho_b)/\rho_m = 1 - \rho_b/\rho_m,$$

where ρ_m and ρ_b denote the matrix (solid material) and bulk (air, water, material mixture) density, respectively, and

$$\begin{aligned} \mathrm{v}_m &\equiv 1 - \phi, \\ \mathrm{v}_a &\equiv \phi - Sw, \\ Sw &= \mathrm{v}_{bw} + \mathrm{v}_{fw}. \end{aligned} \tag{5.2}$$

The two terms involving bound and free water are often combined into a single term with an empirically determined multiplicative factor of the free water permittivity in the soil [5.15]. That is,

$$\mathrm{v}_{bw} \varepsilon_{bw}^{\alpha} + \mathrm{v}_{fw} \varepsilon_{fw}^{\alpha} \doteq Sw^{\nu} \varepsilon_{fw}^{\alpha}, \tag{5.3}$$

where the exponent ν of total water saturation Sw is empirically derived.

Substituting eqs (5.2) and (5.3) into (5.1) and recognizing that $\varepsilon_a^{\alpha} \equiv 1$ yields the following relation in terms of porosity and water saturation:

$$\varepsilon_{soil}^{\alpha} = (1 - \phi)\varepsilon_m^{\alpha} + \phi - Sw + Sw^{\nu} \varepsilon_{fw}^{\alpha}, \tag{5.4}$$

In terms of the bulk and soil matrix densities, eq (5.4) may be written

$$\varepsilon_{soil}^{\alpha} = 1 + \frac{\rho_b}{\rho_m}(\varepsilon_m^{\alpha} - 1) + (Sw^{\nu} \varepsilon_{fw}^{\alpha} - Sw), \tag{5.5}$$

where $\rho_b/\rho_m = \mathrm{v}_m/\mathrm{v}_b$ is the soil matrix volume fraction.

For $\alpha = 1$, eq (5.5) is known as a *linear* model; for $\alpha = 1/2$ as a *refractive* model (since $\varepsilon^{1/2} \equiv n$ is the refractive index); and for $\alpha = 1/3$ as the *cubic* model.

The results of over 500 measurements made by Dobson et al. [5.15], on five differing soil types at nine frequencies (from 4.0 GHz to 18 GHz) and for volumetric moistures Sw ranging from 0.01 to total saturation gave values of v between 1.0 and 1.16 and suggested a refractive model ($\alpha = 1/2$) as most suited for soil-water mixtures. This was observed earlier by Shutko and Reutov [5.16]. Hence $Sw^v \doteq Sw$ and

$$\varepsilon_{soil}^{1/2} \doteq 1 + \frac{\rho_b}{\rho_m}(\varepsilon_m^{1/2} - 1) + Sw(\varepsilon_{fw}^{1/2} - 1). \tag{5.6}$$

Combining the effects of bound and free water into one term (eq (5.3)) reduces the implicit dependence of ε_{soil} on soil type (5.4); this is not surprising since clays are expected to have more bound water than, say, sand grains. In general, however, ε_{soil} and ε_{fw} in eq (5.6) are complex quantities, since attenuative loss due to electrolytic conduction is fundamentally implicit in natural soils and therefore must be incorporated into test lane soils for realistic performance testing. In fact, the loss tangent of soil pore water, which depends on salinity (and temperature), is essentially an *in situ* parameter and cannot be ascertained correctly by pore fluid extraction. These complicating facts will be addressed below.

B.2.1 Dry Soil Mixture

For a dry soil mixture, eq (5.6) simplifies to

$$\varepsilon_{soil}^{1/2} = 1 + \frac{\rho_b}{\rho_m}(\varepsilon_{matrix}^{1/2} - 1) \tag{5.7}$$

since $Sw \equiv 0$. Or, in terms of the porosity ϕ of the soil mixture

$$\varepsilon_{soil}^{1/2} = (1 - \phi)\varepsilon_{matrix}^{1/2} + \phi\varepsilon_{air}^{1/2} \tag{5.8}$$

or

$$\varepsilon_{soil}^{1/2} = (1 - \phi)\varepsilon_{matrix}^{1/2} + \phi,$$

since $\varepsilon_{air}^{1/2} = 1 - j0$. In this case, the soil mixture will have a real dielectric constant (or exhibit no conductive losses). Therefore, essentially no electromagnetic attenuation will be imposed on field behavior by the background soil medium in the frequency range of interest and detection systems operating at higher relative frequencies would be expected to perform best, all other

factors being equal [5.3]. Examples of dielectric, nonlossy test soils are dry sands ($Si0_2$ or SiC). Frequency-domain measurements of the dielectric constant on these soils have been reported previously [5.3].

B.2.2 Lossy, Fluid-Saturated Soils

For lossy, fluid-saturated soils the dielectric mixing rule becomes more complicated since both the bulk soil mixture and the pore water become electrically lossy and attenuate electromagnetic fields. In this case the electromagnetic fields of a mine detection system operating at a higher relative frequency would suffer greater attenuation. If the effective skin depth is too small relative to the burial depth of a buried mine, the detection system would perform more poorly than a system operating at a lower frequency. There are two cases to consider: one where background soils are only partially water saturated and the other where soils are fully saturated.

B.2.2.1 Partially Saturated Soil Mixtures

The complex dielectric constant of the soil may be written

$$\varepsilon_{soil}^{1/2} = (1-\phi)\varepsilon_{matrix}^{1/2} + (\phi - Sw)\varepsilon_{air}^{1/2} + Sw\varepsilon_{water}^{1/2}, \tag{5.9}$$

where

$$\begin{aligned}
\varepsilon_{matrix}^{1/2} &= \sqrt{\varepsilon'_{matrix}} && \text{(nonlossy)},\\
\varepsilon_{air}^{1/2} &\equiv 1 && \text{(nonlossy)},\\
\varepsilon_{water}^{1/2} &= \left[\varepsilon'_{water} - j\varepsilon''_{water}\right]^{1/2} && \text{(lossy)},\\
&= \left[\varepsilon'_{water}(1 - j\tan\delta_{water})\right]^{1/2},\ \tan\delta_{water} \equiv \frac{\varepsilon''_{water}}{\varepsilon'_{water}}, && (5.10)
\end{aligned}$$

and

$$\begin{aligned}
\varepsilon_{soil}^{1/2} &= \left[\varepsilon'_{soil} - j\varepsilon''_{soil}\right]^{1/2} && (lossy),\\
&= \left[\varepsilon'_{soil}(1 - j\tan\delta_{soil})\right]^{1/2},\ \tan\delta_{soil} \equiv \frac{\varepsilon''_{soil}}{\varepsilon'_{soil}}.
\end{aligned}$$

Use of the half-angle relation

$$\tan\delta = \frac{2\tan\delta/2}{1-\tan^2\delta/2}$$

allows a complex dielectric constant $\varepsilon = \varepsilon'(1 - j\tan\delta)$ to be written as

$$\varepsilon^{1/2} = \frac{\sqrt{\varepsilon'}}{\left(1 - \tan^2\frac{\delta}{2}\right)^{1/2}}\left(1 - j\tan\frac{\delta}{2}\right). \tag{5.11}$$

Use of eqs (5.11) and (5.10) in (5.9) then yields

$$\frac{\sqrt{\varepsilon'_{soil}}}{\left(1 - \tan^2\frac{\delta_{soil}}{2}\right)^{1/2}}\left(1 - j\tan\frac{\delta_{soil}}{2}\right) = (1-\phi)\sqrt{\varepsilon'_{matrix}} + (\phi - Sw) + \frac{Sw\sqrt{\varepsilon'_{water}}}{\left(1 - \tan^2\frac{\delta_{water}}{2}\right)^{1/2}}\left[1 - j\tan\frac{\delta_{water}}{2}\right].$$

Separating real and imaginary parts yields

$$\frac{\sqrt{\varepsilon'_{soil}}}{\left(1 - \tan^2\frac{\delta_{soil}}{2}\right)^{1/2}} = \sqrt{\varepsilon'_{matrix}} + \phi\left(1 - \sqrt{\varepsilon'_{matrix}}\right) - Sw + \frac{Sw\sqrt{\varepsilon'_{water}}}{\left(1 - \tan^2\frac{\delta_{water}}{2}\right)^{1/2}} \tag{5.12}$$

and

$$\frac{\sqrt{\varepsilon'_{soil}}\tan\frac{\delta_{soil}}{2}}{\left(1 - \tan^2\frac{\delta_{soil}}{2}\right)^{1/2}} = \frac{Sw\sqrt{\varepsilon'_{water}}\tan\frac{\delta_{water}}{2}}{\left(1 - \tan^2\frac{\delta_{water}}{2}\right)^{1/2}}. \tag{5.13}$$

Both eqs (5.12) and (5.13) must be satisfied simultaneously. ε'_{soil}, $\tan\delta_{soil}$ and ε'_{matrix} are known from measurements. The total porosity ϕ and water and air saturations, Sw, and $\phi - Sw$ may be determined by using a value for the water salinity S which is based on the cation exchange capacity of the matrix soil type. The dielectric constant ε'_{water} of the pore water is computed from eqs (2.17) and (2.20). The loss tangent of the pore water is then calculated from eq (2.21). Substituting these values and the measured ε'_{soil} and $\tan\delta_{soil}/2$ into eq (5.13) allows the determination of Sw from which the total porosity is computed (eq (5.12)).

B.2.2.2 Saturated Soil Mixtures

A more expedient approach is to relate the complex dielectric constant of the soil mixture to the water-filled porosity ϕ_w so that we may write

$$\varepsilon_{soil}^{1/2} = (1 - \phi_w)\varepsilon_{matrix}^{1/2} + \phi_w\varepsilon_{water}^{1/2}. \tag{5.14}$$

Use of eqs (5.10) and (5.11) now yields

$$\frac{\sqrt{\varepsilon'_{soil}}}{\left(1-\tan^2\frac{\delta'_{soil}}{2}\right)^{1/2}} = (1-\phi_w)\sqrt{\varepsilon'_{matrix}} + \frac{\phi_w\sqrt{\varepsilon'_{water}}}{\left(1-\tan^2\frac{\delta_{water}}{2}\right)^{1/2}} \tag{5.15}$$

and

$$\frac{\varepsilon'_{soil}\tan\frac{\delta_{soil}}{2}}{\left(1-\tan^2\frac{\delta_{soil}}{2}\right)^{1/2}} = \frac{\phi_w\sqrt{\varepsilon'_{water}}\tan\frac{\delta_{water}}{2}}{\left(1-\tan^2\frac{\delta_{water}}{2}\right)^{1/2}} \tag{5.16}$$

Again, ε'_{soil}, $\tan\delta_{soil}$, and ε'_{matrix} are known from measurements. A value for the salinity S of the pore water is then taken. The real part of the pore water permittivity ε'_{water} at temperature T, °C, is then computed from

$$\varepsilon'_{water} = \varepsilon'_{wo}(T) - 0.1556 - 4.13\times10^{-4}S + 1.58\times10^{-6}S^2 \tag{5.17}$$

where

$$\varepsilon'_{wo}(T) = 88.045 - 0.4147T + 6.295\times10^{-4}T^2. \tag{5.18}$$

Next the loss tangent of the pore water is calculated from

$$\tan\delta_{water} = [\varepsilon'_{water}]^{-1}[5.66 + 2.65\times10^{-3}S - 4.5\times10^{-6}S^2]. \tag{5.19}$$

This initial value of $\tan\delta_{water}$ obtained above is substituted into eq (5.15) to determine ϕ_w. A corrected value of $\tan\delta_{water}/2$ is determined from eq (5.16), which is then used to determine a new value for the water salinity and porosity ϕ_w until they converge to constant values. This approach is one commonly used in geophysics and reservoir engineering to determine both the water-filled porosity and pore water salinity of rocks from *in situ* dielectric measurements. For our purposes here, these are the fundamental parameters that allow us to predict, from a mixing relationship, how attenuative a background soil is. The important point is that the complex permittivity (both lossless and lossy parts) of the background test medium be the same in performance evaluations of mine detector systems operating at the same frequency. While various synthetic substances can be thought of that can simulate the real field situation of water-saturated soils in terms of the complex permittivity at a single frequency, there are few synthetics which, in combination, can simulate the dielectric behavior of water-saturated soils over a broad range in frequency.

B.3 Application to Granular Soil Mixtures

As an application to dielectric property prediction of soil mixtures, consider a two-phase mixture of air and dry sand, where sand consists of washed quartz grains that have diameters ranging from 0.027 and 0.60 mm. Recalling eq (5.7) we write

$$\varepsilon_{soil}^{1/2} = 1 + \frac{\rho_b}{\rho_m}(\varepsilon_{matrix}^{1/2} - 1).$$

For this mixture, Geyer [5.3] and Jesch [5.17] have reported a measured mean relative dielectric constant, ε'_{soil}, of 2.702 at 300 MHz and for a mean bulk density, ρ_b, of 1.540 g/cm^3. Standard deviations for the dielectric constant and mean bulk density were 0.0486 and 0.022 g/cm^3, respectively. Bussey [5.18, 5.19] has reported ε' of silica equal to 3.822, measured at 9 GHz with the use of cavity resonators. Von Hippel [5.20] has reported ε' of (fused) silica at 25°C and at 300 MHz equal to 3.78. Von Hippel's results show fused silica essentially dispersionless over the frequency range of 100 Hz to 25 GHz, with $\tan\delta_{silica} = 0.5 \times 10^{-4}$ at 300 MHz. Clark [5.21] and Morey [5.22] give the matrix density of pure silica, ρ_m, to be 2.203 g/cm^3.

In summary, use of the two-phase refractive dielectric mixing rule yields a predicted dielectric constant

$$\varepsilon_{soil,predicted} = [1 + 0.699(\varepsilon_{matrix}^{1/2} - 1)]^2 = 2.756.$$

This result differs by 2.1 percent from observed measurements using an open-ended transmission line with a vector automatic network analyzer. This difference is probably due to impurities in the quartz sand, which would affect both ρ_m and ε_{matrix}.

B.4 NIST Measurements of Electromagnetic Soil Properties

B.4.1 Natural Soils

A large number of dielectric measurements on soils have been made by NIST over the past decade. Jesch [5.17], using frequency-domain open-circuit coaxial transmission line techniques (described in detail in Chapter IV), has made dielectric measurements of five different natural soil types. The textural types were sand, sandy loam, silt loam, clay loam, and clay. Sand is defined as washed quartz grains having diameters from 0.027 mm to 0.60 mm, whereas silt is washed quartz grains having diameters between 0.0033 mm and 0.021 mm. The clay used was inorganic (kaolin or bentonite) with plate diameters less than 0.0033 mm.

The soils used by Jesch [5.17] were constructed as follows:

Sand texture	9.5 parts sand, 0.5 parts clay, 0.3 parts silt;
Sandy loam	6.4 parts sand, 3.6 parts clay, 2.5 parts silt;
Silt loam	2 parts sand, 8 parts clay, 6.8 parts silt;
Clay loam	3.2 parts sand, 6.8 parts clay, 3.3 parts silt; and
Clay	2 parts sand, 8 parts clay, 2 parts silt.

These soil types, which are classified according to particle size and distribution, are illustrated in figures 5.1 and 5.2.

The natural soil measurements for the above five soil types were accomplished for moisture levels ranging from 0 to 48 percent and for test frequencies from 300 to 9300 MHz. A small but representative sample of the results is shown in tables 5.2, 5.3, 5.4, 5.5, and 5.6. Little dispersion is observed for all soils when $Sw \doteq 0$. However, as water saturation increases, greater dispersion in ε' occurs, particularly as the matrix particle diameters decrease. From previous discussion, this is expected, since the ratio of surface water to bulk pore water dramatically increases by several orders of magnitude.

B.4.2 Synthetic Soils

A further extensive study of permittivity measurements has recently been accomplished at NIST for synthetic soil materials that might be used in land mine validation testing. These measurements were also performed in the frequency domain, using open-circuit coaxial transmission-line techniques. Data were collected for wetted sands and various silicon carbide (60-grit) and sand mixtures, as well as for silicon carbide and aluminum powder mixtures, over the frequency range of 50 to 750 MHz. A brief summary of the results is given here.

Initially, the coaxial line was filled with tap water at 20°C in order to verify the experimental procedure and calculations. Calculated relative permittivity and loss tangent from 50 MHz to 1.20 GHz are shown in figure 5.3, validating laboratory procedures.

Dielectric dispersion curves for wetted sand samples (water saturations varying from 4 percent to 14 percent) are given in figures 5.4, 5.5, and 5.6. The dielectric constant predictably increases as water saturation increases, with dispersion evident principally at frequencies less than 150 MHz. In addition, the relative permittivities at 600 MHz of a 5 cm section of various water-saturated sands were measured as a function of drying time at approximately 20°C. These results, illustrated in figure 5.7, show that host soil relative permittivities can vary by as much as a factor of 2 over a 72 h drying time. Hence, if wetted soils are used for test beds, the host relative permittivity should be measured at the time of validation testing so as to properly compare different detection systems.

Various mixtures of silicon carbide and sand were also examined and the results are given in figures 5.8, 5.9, 5.10, 5.11, and 5.12. The loss tangent increases slightly with increasing

Table 5.2

Experimental results of dielectric measurements on sand as a function of water saturation *Sw* and frequency *f* [5.17].

Sand

f	*Sw = 0* ε'		*Sw = 0.04* ε'		*Sw = 0.14* ε'	
(MHz)	*(Mean)*	*(Std. Dev.)*	*(Mean)*	*(Std. Dev.)*	*(Mean)*	*(Std. Dev.)*
300	2.702	0.0486	4.225	0.168	10.458	0.413
500	2.694	0.0492	4.079	0.162	10.641	0.415
1000	2.693	0.0515	4.019	0.165	11.179	0.349
2000	2.695	0.0515	3.940	0.142	9.951	0.334
4000	2.656	0.0419	3.946	0.148	10.544	0.441
9300	2.737	0.0660	3.373	0.198	10.179	1.140

Table 5.3

Experimental results of dielectric measurements on sandy loam as a function of water saturation *Sw* and frequency *f* [5.17].

Sandy loam

f	*Sw = 0* ε'		*Sw = 0.06* ε'		*Sw = 0.24* ε'	
(MHz)	*(Mean)*	*(Std. Dev.)*	*(Mean)*	*(Std. Dev.)*	*(Mean)*	*(Std. Dev.)*
300	2.650	0.040	5.967	0.076	24.527	0.326
500	2.642	0.047	5.407	0.062	24.328	0.185
1000	2.660	0.079	4.909	0.028	22.705	0.625
2000	2.680	0.102	4.408	0.035	21.156	1.072
4000	2.691	0.125	4.301	0.019	15.549	1.560
9300	2.663	0.027	3.813	0.084	9.884	2.400

frequency as opposed to the case of wetted sands, where the loss tangent either remained constant or decreased with frequency. Provided these silicon carbide mixtures have little conductive (lossy) material in them, almost no dispersion is evident. Therefore, by controlling the sand-silicon carbide mix, we may simulate a host medium whose effective permittivity ranges from 3 to 13 but remains constant over the 50 to 750 MHz range (for any given mix) for plastic land mine validation tests.

The addition of conductive aluminum powder to silicon carbide yielded expected dispersion, as seen in figure 5.13. In fact, addition of even 5 percent aluminum powder (by mass) caused dispersion to be evident. Hence, if conductive constituents such as aluminum

Table 5.4

Experimental results of dielectric measurements on silt loam as a function of water saturation *Sw* and frequency *f* [5.17].

Silt loam

f	*Sw = 0* ε'		*Sw = 0.05* ε'		*Sw = 0.10* ε'	
(MHz)	*(Mean)*	*(Std. Dev.)*	*(Mean)*	*(Std. Dev.)*	*(Mean)*	*(Std. Dev.)*
300	2.340	0.049	4.453	0.097	9.151	0.186
500	2.321	0.051	4.038	0.083	8.083	0.182
1000	2.318	0.059	3.692	0.078	7.458	0.343
2000	2.343	0.085	3.391	0.080	5.573	0.157
4000	2.325	0.044	3.319	0.108	5.275	0.048
9300	2.408	0.094	3.170	0.092	4.065	0.268

Table 5.5

Experimental results of dielectric measurements on clay loam as a function of water saturation *Sw* and frequency *f* [5.17].

Clay loam

f	*Sw = 0* ε'		*Sw = 0.06* ε'		*Sw = 0.12* ε'	
(MHz)	*(Mean)*	*(Std. Dev.)*	*(Mean)*	*(Std. Dev.)*	*(Mean)*	*(Std. Dev.)*
300	2.775	0.024	5.667	8.719	0.183	0.186
500	2.760	0.027	5.108	0.168	8.083	0.182
1000	2.773	0.037	4.649	0.101	7.363	0.223
2000	2.771	0.051	4.151	0.065	5.702	0.018
4000	2.758	0.048	4.024	0.156	5.682	0.005
9300	2.708	0.076	3.826	0.122	4.657	0.418

powder are added to host test lanes, the dispersion characteristics of the lossy test media should be known *a priori* so that detection systems operating at different frequencies may be compared properly (just as for wetted soils).

C Loose Matrix Synthetic Soils for Narrowband or Fixed Frequency Test Lanes for Nonmetallic Buried Objects

The point of the discussion on polarization mechanisms and relaxation processes is to provide insight into the dielectric frequency dependence. Because the dielectric frequency dependence for most soil materials is generally flat from 1 MHz to 1 GHz, there is valid

Table 5.6

Experimental results of dielectric measurements on clay as a function of water saturation *Sw* and frequency *f* [5.17].

	Clay					
	Sw = 0		*Sw = 0.06*		*Sw = 0.12*	
f	*ε′*		*ε′*		*ε′*	
(MHz)	*(Mean)*	*(Std. Dev.)*	*(Mean)*	*(Std. Dev.)*	*(Mean)*	*(Std. Dev.)*
300	2.717	0.052	6.030	6.034	10.676	0.204
500	2.703	0.053	5.399	0.015	9.402	0.186
1000	2.721	0.065	4.952	0.058	9.871	0.807
2000	2.721	0.068	4.187	0.005	6.294	0.124
4000	2.732	0.105	4.289	0.085	5.642	0.823
9300	2.677	0.052	3.754	0.053	5.185	0.950

Table 5.7

Preliminary set of standard background media for plastic mine detector validation testing.

Background medium	*Dielectric constant, ε′*	*Loss tangent, σ/ω ε′*
Dry silica sand	2.8 ± 0.05	0.01
Mixture: 40% SiC, 60% dry sand	5.0 ± 0.2	0.013 ± 0.002
Mixture: 80% SiC, 20% dry sand	10.0 ± 0.4	0.018 ± 0.003

justification for specifying synthetic test soils since their constituent electromagnetic properties may be more controllable. A preliminary suggested set of standard background media is given in table 5.7 for plastic mine detector validation testing.

In the natural soil environment encountered in the field, both conduction and dielectric mechanisms influence mine detector signals. The common factor affecting both conduction and dielectric mechanisms is the water saturation, *Sw*. Thus, in standard background test media it is critical to control and/or to know water saturations. As a matter of test procedure, mine lanes for UHF detectors should not only be enclosed in an electromagnetically anechoic environment (to avoid spurious noise reflections off metallic objects), but also one which is shielded from the varying influences of outside weather that affect *Sw*.

D Loose Matrix Natural Soils for Test Lanes for Metallic Buried Objects and Broadband Systems

The use of synthetic soils for test lanes for single-frequency metal land mine detectors may also be justified in terms of greater control of constituent properties governing detector signals. Since these detectors generally operate at a frequency around 2500 Hz, there are usually no significant attenuation problems in sensing metallic mine signals at burial depths that may be as great as 1 m, even for a relatively conductive ($\sigma_H \doteq 0.1$ S/m) soil or for that which is magnetically permeable ($\mu_H = 1.4\mu_0$). Suggested background media for single-frequency metal mine detectors are given in table 5.8. Because the conductivity contrast between a metallic mine and almost any conceivable natural soil is so high (effectively infinite for analysis purposes), requirements on testing environments for metal mine detectors are much less stringent. That is, test lanes for VLF or ELF single-frequency metal mine detectors need not be in an anechoic environment nor do they need to be shielded from the influences of outside weather.

Signals measured by both single-frequency plastic mine UHF and metal mine VLF detectors are sensitive only to the volume of the buried land mine. In order to gain shape information (and therefore minimize false alarms due to ground clutter), future detectors must be developed that are broadband in design and measurement—a fact well recognized in radar work. As such development proceeds, the sensitivity to complex permittivity contrasts (mine visibility), affected by dielectric relaxation processes, becomes relevant in understanding detector performance and in specifying optimal system bandwidth.

The use of synthetic or natural soils in test lanes for broadband system validation should be approached with caution. Natural soils often depart drastically from Debye behavior (single relaxation dielectric dispersion) at frequencies less than 1 MHz. Furthermore, broadband dispersive characteristics of synthetic soils (in the ELF or VLF frequency range) may not compare to that of natural soils commonly encountered by the field soldier.

Thus, although it would be desirable to have background test material that is electromagnetically analogous to those commonly encountered in the field, it is equally desirable to have test soils that can be accurately specified, and whose properties can be closely controlled and measured. On account of these two requirements, it is expedient to examine in more detail the dielectric characteristics of water saturated soils with a view toward understanding those parameters that can be controlled and are responsible for governing electromagnetic field behavior. At the very least, such an examination should provide insight into how natural soils might be used in performance testing of broadband mine detection systems or in predicting how they may differ from the suggested set of standard background media given in tables 5.7 and 5.8.

Table 5.8

Preliminary set of standard background media for metal detector validation testing.

Background medium	*Relative magnetic permeability,* μ/μ_0
Dry sand	1.00
Mixture: Dry sand with 30% magnetite	1.35

E NIST Recommendations and Conclusions

Considering the choice of a test range configuration, whether to use actual soils, simulations formulated with liquids or loose granular materials, or rigid-matrix "brick" soil simulations, any one of these possibilities could be used for target-based testing. Our recommendation is to use the rigid-matrix brick approach because it is the most versatile and allows the tightest control of all test range parameters. Also, several of the proposed tests described in chapter VII could not be performed well, if at all, with the other approaches. Those tests are explicitly identified in chapter VII. What follows in this chapter is a discussion of the advantages and disadvantages of the different approaches for test range soil media mentioned above. (It should be noted here that NIST's work on developing the technology required for the rigid-matrix brick approach is not yet complete and will be reported to BRDEC separately.)

E.1 Natural Soil Test Range

Although utilizing natural soils in the test range would be the best approach in terms of approximating realistic test conditions, there are many disadvantages to this scheme.

(a) *Water/Soluble Salt Content Variation.* The complex relative permittivity of soils, expressed as $\varepsilon_s' - j\varepsilon_s''$, is heavily dependent on the soil's water and soluble salt content. The magnitude of the permittivity of dry soils $\left|\varepsilon_s' - j\varepsilon_s''\right|$ is usually in the range of 2 to 3, even with soluble salts present, but if the soil contains water, the magnitude of the permittivity can rise to 20 or greater, depending on the water content and the frequency of the EM excitation. This is due primarily to the fact that the permittivity of pure water is about 80. Also, the soil's attenuation of EM energy, directly proportional to the imaginary part ε_s'' of its permittivity, is a strong function of water/salt content. The attenuation of most dry soils is in the range of very nearly zero to about 1 dB/cm, depending on the soil type and the frequency. Adding water to the soil can cause this attenuation to rise as high as 40 dB/cm or greater in the

extreme case of water saturation, high salt content, and high frequency. Much of this high loss is caused by the highly conductive electrolytes formed by the addition of water to the salts present in the soil.

More than any other variable, the permittivity and attenuation of soils is controlled by their water/soluble salt content. Therefore, it is crucial to control the value of this variable if accurate, repeatable detector tests are desired. Unfortunately, the use of natural soils makes this control practically impossible. Water evaporation and changes in relative humidity will cause the soil's water content to vary continuously. Even if a means were developed to continuously monitor the permittivity and attenuation of the test range soil, the interpretation of comparative detector test results would be extremely difficult. Also, attempts to both control and continuously monitor the permittivity and attenuation of natural soils in a test range would undoubtedly be time-consuming and expensive.

(b) *Water Gradient Variation.* The use of natural soils would also make it very difficult to control the gradient of water content as a function of soil depth. Gravity and evaporation will cause the soil's water content to increase with increasing depth under most conditions. (An exception, of course, would be if the soil were completely saturated, as in a swamp.) The main point here is that it would be impossible to control this gradient, and thus, the soil's permittivity as a function of soil depth. Although it could be argued that water content gradients certainly exist "in the field," it may be desirable in the future to analyze detector test results with the assumption that the soil permittivity is uniform throughout the test range soil volume. In any event, the most versatile test range configuration would allow the control of this variable.

(c) *Soil Density Variation.* The use of natural soils in a detector test range would inevitably lead to variations in the soil density, and therefore, in its permittivity. Compaction over time would occur and the localized soil density would be changed whenever the range was disturbed, say, by walking on the soil or by burying a new target. Although the permittivity changes would not be as great as in the case of water content, they still could be on the order of tens of percent. As in the water content case, it would be very difficult and expensive to both control and monitor the soil density.

(d) *Soil Density Gradient Variation.* Similar to the water content gradient problem, the effects of gravity cause a soil density gradient problem, with the density of the soil increasing with increasing depth. Again, there may be analysis considerations that

would make it desirable to be working with test range soils that are uniform in density.

(e) *Soil Reproducibility.* Finding and/or preparing natural soils that would be suitable for use in a detector test range would be very difficult. Variations in the distributions of grain size, grain shape, and mineral content would almost certainly occur, leading to nonuniformities in the soil's permittivity and attenuation. This problem would also make it difficult for any other laboratories to duplicate the Army's test range. However, this reproducibility problem does not, in itself, preclude the use of natural soils. It simply increases the testing uncertainties.

(f) *Target Position and Orientation Variations.* The use of natural soils would allow for wide variations in the repeatibility of target placement. Small variations would probably occur even if the targets were never moved. Removing and reburying targets would cause still larger variations.

(g) *Soil Surface Variations.* The amount of EM energy entering the soil from the air above, along with its spatial distribution is a strong function of the air-soil interface profile. Variations in this profile would almost certainly occur over time with the use of natural soils, making it very difficult to ensure that each detector is being tested under the exact same conditions.

(h) *Soil Contamination Variations.* Over time, it would be very difficult to see to it that no contaminating materials were ever introduced into a natural soil test range. Even more difficult would be trying to identify any observed variations in test results as being caused by range contamination, rather than by variations in one of the other variables previously mentioned.

E.2 Loose Granular Material Test Range

Another approach to configuring the detector test range is the use of mixtures of loose, granular materials in place of natural soils. The advantage to this approach, as compared to using natural soils, is that the sources of parameter variation described in (a), (b), and (e), above, could be eliminated. Mixtures of different granular materials could be formulated which would possess the same permittivities and attenuations as those occurring in natural soils. No water would be required because its effects would be included in the mixture. Also, there would be no reproducibility problem because the EM properties of the mixtures would presumably be constant as long as the ratios of constituent materials were held constant. Therefore, we believe that using loose granular materials in place of natural soils for a test range would be a better approach.

However, similar to the case of natural soils, there are many disadvantages to this scheme as well. The parameter variation problems listed above in (c), (d), and (f) through (h), would still exist. In addition, two new problems would be created. First, the permittivity and attenuation of natural soils, especially with water present, is a strong and generally nonlinear function of frequency. Although it is possible to formulate mixtures of dry, granular materials that would simulate the EM properties of various natural soils, this simulation would be accurate only over a narrow band of frequencies. We know of no mixtures which would simulate water-containing natural soils over the frequency band of, say, 100 MHz to 5 GHz, a useful band for detectors. Thus, different mixtures would have to be formulated for testing detectors that possess different operating frequencies. Also, the testing of broadband detectors, for example, swept-frequency or pulse-type detectors, would necessarily have to be done under unrealistic conditions.

Second, there would be problems in terms of temperature dependence of the permittivities of the loose granular mixtures. The variation in permittivity for damp or wet natural soils, as a function of temperature, is of the same order as the variation as a function of frequency. Therefore, the same problems as those posed by frequency variation, mentioned above, would exist.

E.3 Liquid Material Test Range

Still another approach to configuring the detector test range is to simulate natural soil media with a liquid phase material, such as an emulsion of oil and water, or oil and salt water. If water were one of the main constituents of the liquid mixture, then this method would be superior to using either natural soils or loose granular materials. Smith and Scott [5.23] are presently doing some work on this approach at the Georgia Institute of Technology. Essentially, their reported work consists of mixing mineral oil and water or salt water into emulsions that possess electromagnetic properties that closely approximate those of natural soils. As part of their approach, they have incorporated frequency scaling in order to reduce the necessary sizes of the range and test components.

All of the disadvantages stated above, in principle, would not exist with this approach. However, there would be some restrictions and disadvantages. First, it would not be possible to simulate water or soil density gradients. Second, it would be very difficult, if not impossible, to incorporate surface profile variations into the range. Third, the benefits of frequency scaling would not be applicable for mine detector testing because it is not feasible for the Army to scale detectors, that is, reduce their size and increase their operating frequency proportionately. And last, there could be a problem with stability of the properties of the liquid mixture. Emulsions tend to separate, generally, on a time scale of minutes to weeks, so a means would be necessary for re-emulsifying the mixture periodically. Depending on the size and configuration of the test

range, this problem could easily become practically overwhelming. There are other potential problems with this approach, such as cost and ease of detector testing, but we should not rule out this approach.

E.4 Rigid-Matrix Brick Test Range

The last test range approach to be considered here is one using rigid-matrix bricks as a natural soil simulation. This is the approach that we recommend because it is the most versatile and allows the tightest control of all conceivable test range parameters.

This approach is quite similar to the liquid emulsion approach, discussed above, in the sense that both methods involve the use of water or salt water solutions as one of the material constituents. Thus, the dominating effects of water/salt water on the permittivity of natural soils could be accurately and faithfully reproduced, with none of the parameter control problems that would exist with the use of natural or loose granular material simulations.

The principal advantages of using rigid-matrix bricks, as opposed to liquid emulsions, are as follows: First, although bricks can be constructed with negligible property gradients, it also would be possible to build gradient simulations into the bricks if so desired. That is, by constructing the bricks in layers, with slightly different permittivities in each layer, naturally occurring water or soil density gradients could be simulated. Second, irregular surface profiles could be built into the top layer of bricks allowing the testing of detectors under conditions where the air-earth interface is not a flat plane. The built-in surface irregularities would remain constant, thus ensuring repeatable detector tests. Third, target position and orientation variations would be held to a minimum because the targets could be embedded in the bricks. Fourth, a wider variation in permittivity contrast between the targets and the soil medium would be possible because targets could be formulated from the same materials used to make the bricks. And last, the range would be very versatile because changing its testing configuration would only involve moving a small number of bricks.

The disadvantages of this approach are few. As with the case of liquid emulsion approaches, insufficient work has been done on this approach to identify and quantify the real disadvantages. However, potential problem areas can be identified. First, like the liquid emulsion approach, this brick approach could be quite expensive to implement due to brick material costs and brick manufacturing costs. We cannot estimate these costs until our brick development work is complete. Second, there is a potential problem with unwanted electromagnetic wave reflections from brick interfaces and from the boundaries of the range. (Reflections from the range boundaries are a problem that affects all four of the approaches discussed here and must be dealt with in the actual range design.) The measurement and analysis of brick-interface reflections is one of the tasks for future work by NIST. A third potential

problem is ease of range operation. Repeated moving of the bricks must be minimized because the process would be time consuming and arduous, and it would reduce the operating life of the range due to damage and contamination. In this regard, NIST has also proposed that a computer-controlled detector-positioning system be employed on the range in order to eliminate the need for personnel to walk on it.

References (V)

[5.1] Geyer, R.G. Magnetic susceptibility measurements for mine detection: Some general comments. NIST Report, U.S. Army Belvoir Research Development and Engineering Center, Fort Belvoir, VA, 10 p.; 1987.

[5.2] Heiland, C.A. Geophysical Exploration. Englewood Cliffs, New Jersey: Prentice Hall, pp. 310-314; 1940.

[5.3] Geyer, R.G. Experimental parameters for land mine detection performance evaluations. NIST Report, U.S. Army Belvoir Research Development and Engineering Center, Fort Belvoir, VA, (Proj. 7232457), 100 p.; November 1987.

[5.4] Ulaby, F.T.; Moore, R.K.; Fung, A.K. Microwave remote sensing, Vol. III: From theory to applications. London, England: Addison-Wesley Publishing Co.; 1982.

[5.5] Hasted, J.B. Liquid water: Dielectric properties. Chapter 7 Water—A comprehensive treatise, I, The physics and chemistry of water. New York: Plenum Press; 1972.

[5.6] Tinga, W.R. Generalized approach to multiphase dielectric mixture theory. J. Appl. Phys. 44: 3897-3902; 1973.

[5.7] Ho, W.W.; Love, A.W.; VanMelle, M.J. Measurements of the dielectric properties of sea-water at 1.43 GHz. NASA Contractor Report CR-2458. NASA Langley Research Center, Langley, VA; 1974.

[5.8] Bottcher, C.J.F. Theory of electric polarization. Amsterdam: Elsevier; 1952.

[5.9] Kurosaki, S. The dielectric behavior of water sorbed in silica gel. J. Phys. Chem. 58: 320-324; 1954.

[5.10] Bockris, J.; Gileady, E.; Huller, K. Dielectric relaxation in the electric double layer. J. Chem. Physics. 44: 1445-1456; 1966.

[5.11] McCafferty, E.; Zettlemayer, A.C. Adsorption of water vapor on discussions, Vol. 52: 239-254; 1971.

[5.12] Hasted, J.B. The dielectric properties of water *in* Progress in Dielectrics, Vol. 3., J.B. Birks and J. Hart, eds. New York: John Wiley & Sons; 1961, 101-149.

[5.13] Nair, N.K.; Thorp, J.M. Dielectric behavior of water sorped in silica gels, Part 1, commercial silica gels and the elimination of dielectric hysteresis. Trans. Faraday Soc. 61: 962-974; 1965.

[5.14] Kenyon, W.E. Texture effects on megahertz dielectric properties of calcite rock samples. J. Appl. Phys. 55: 3151-3159; 1984.

[5.15] Dobson, M.C.; Ulaby, F.T.; Hallikainen, M.T.; El-Rayes, M.A. Microwave dielectric behavior of wet soil, Part II: Dielectric mixing models. IEEE Trans. Geosci. Remote Sensing. GE-23(1): 35-46; 1985.

[5.16] Shutko, A.M.; Reutov, E.M. Mixture formulas applied in estimation of dielectric and radiative characteristics of soils and grounds at microwave frequencies, IEEE Trans. Geosci. Remote Sensing. GE-20: 29-32; 1982.

[5.17] Jesch, R.L. Dielectric measurements of five different soil textural types as functions of frequency and moisture content. Nat. Bur. Stand. (U.S.) NBSIR 78-896, 26 p.; 1978.

[5.18] Bussey, H.E. International comparison of complex permittivity measurement at 9 GHz. IEEE Trans. Instrum. Meas. IM-23(3): 235-239; 1974.

[5.19] Bussey, H.E.; Gray, J.E.; Bamberger, E.C.; Rushton, E.; Russel, G.; Petley, B.W.; Morris, D. International comparison of dielectric measurements. IEEE Trans. Instrum. Meas. IM-13: 305-311; 1964.

[5.20] Von Hippel, A.R. Dielectric materials and applications. New York: The Technology Press of M.I.T. and John Wiley & Sons, 438 p.; 1954.

[5.21] Clark, S.P. Handbook of physical constants. Geol. Soc. Amer. Memoir 97, 587 p.; 1966.

[5.22] Morey, L. Properties of glass. New York: Reinhold Press; 1954.

[5.23] Smith, G.S.; Scott, W.R., Jr. The use of emulsions to represent dielectric materials in electromagnetic scale models. IEEE Trans. Ant. Prop., vol. 38, No. 3: 323-334; March, 1990.

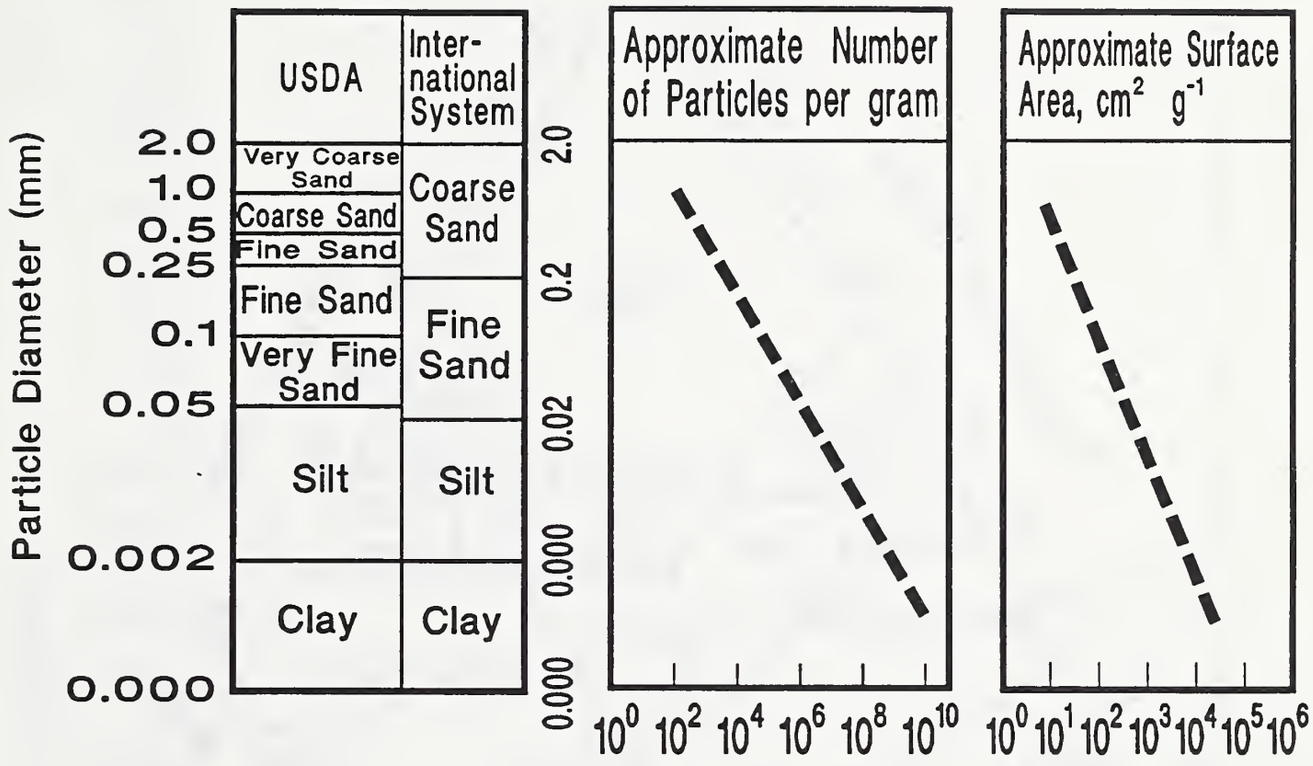

Figure 5.1 Particle properties for different soil types.

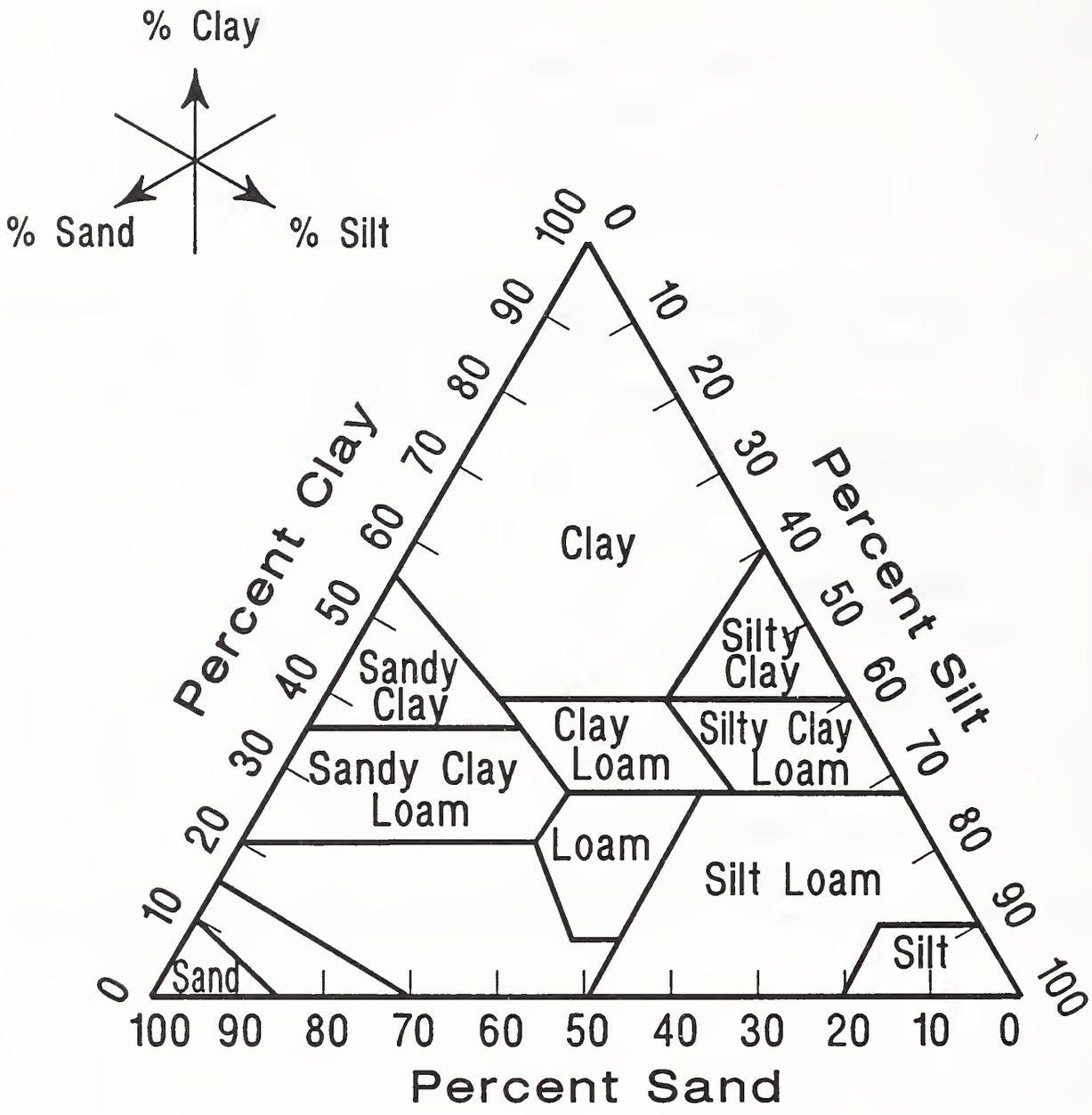

Figure 5.2 Particle distribution for different soil types.

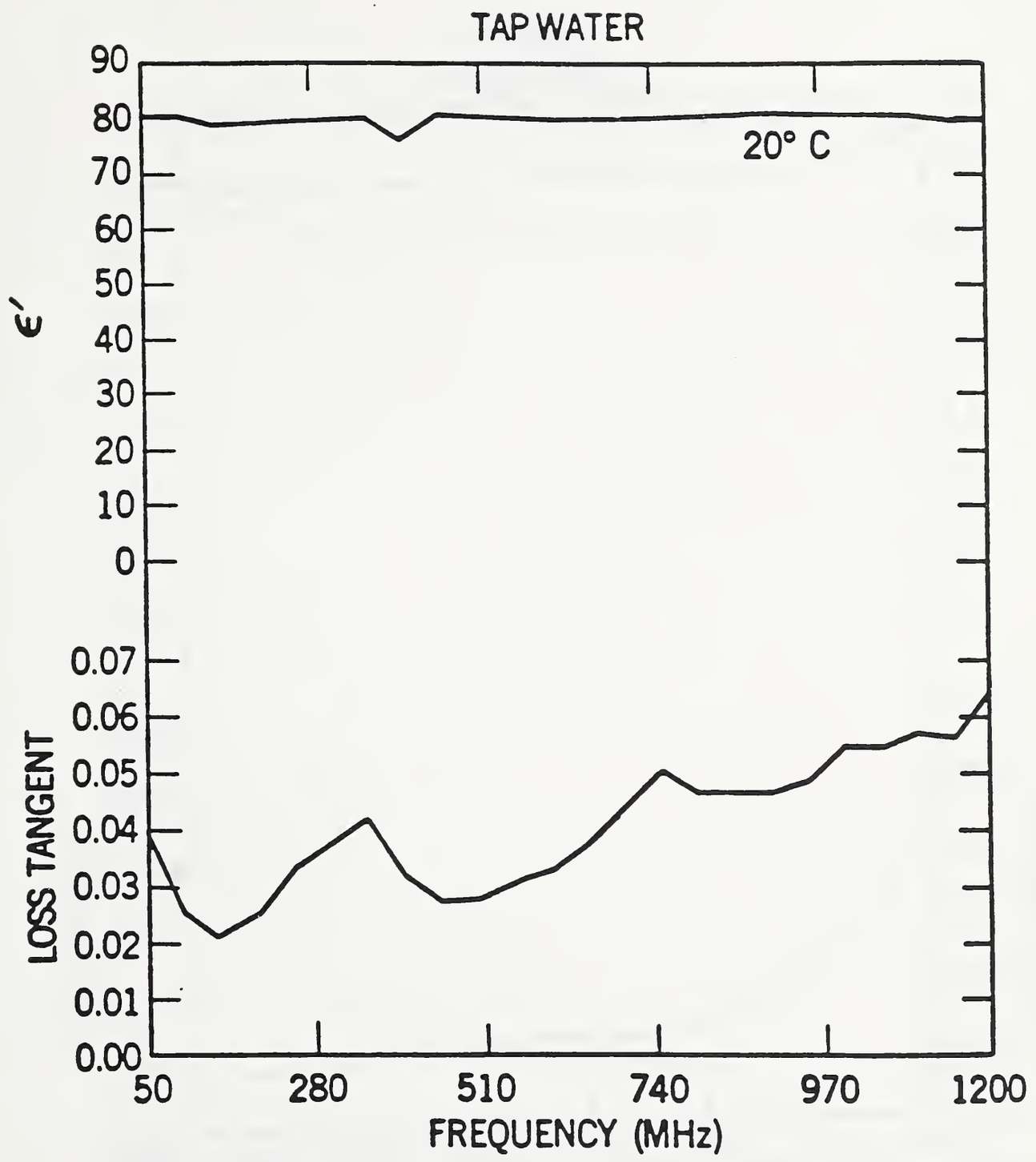

Figure 5.3 Measured permittivity and loss tangent vs frequency for tap water at 20°C.

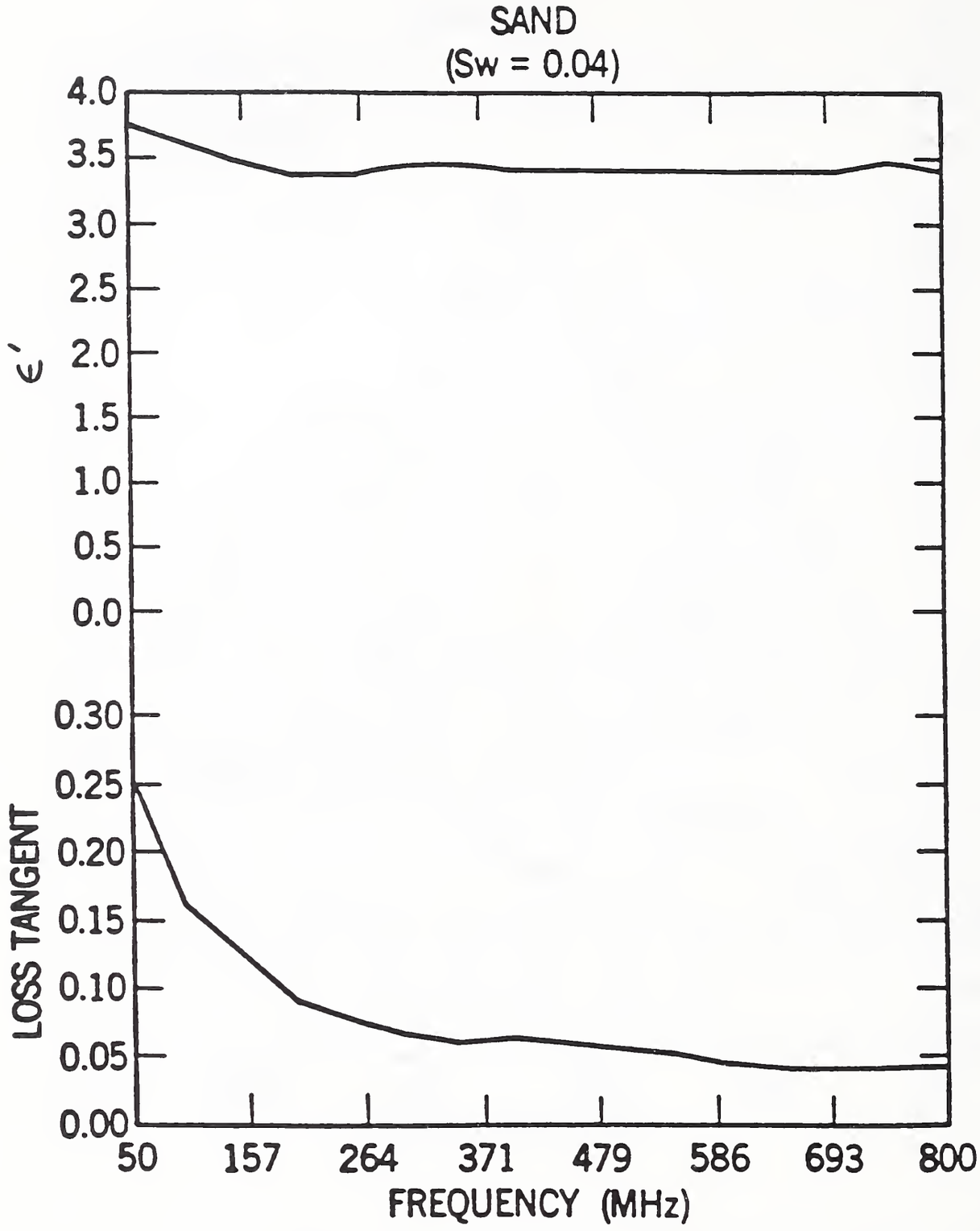

Figure 5.4 Measured permittivity and loss tangent vs frequency for sand with 4% water.

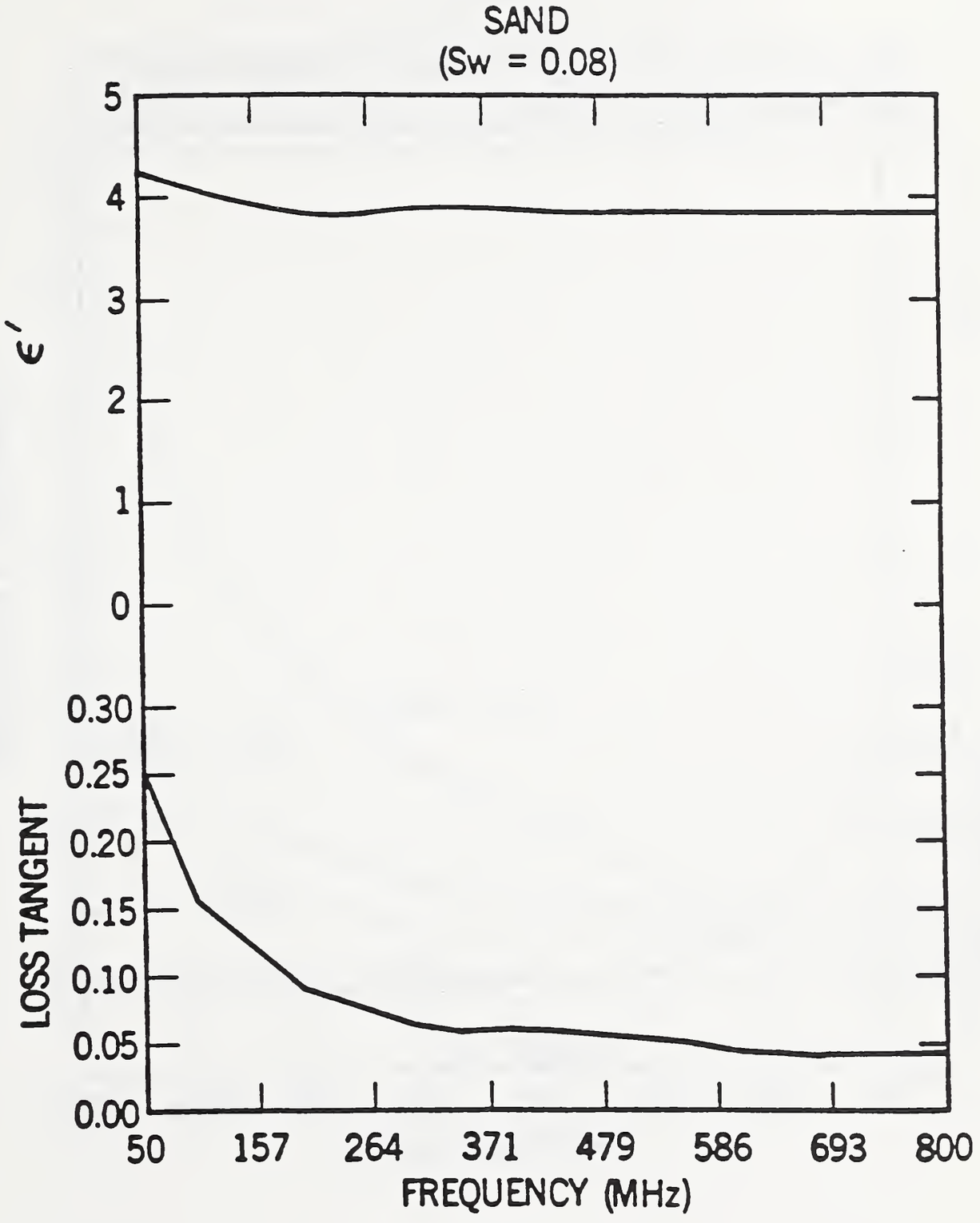

Figure 5.5 Measured permittivity and loss tangent vs frequency for sand with 8% water.

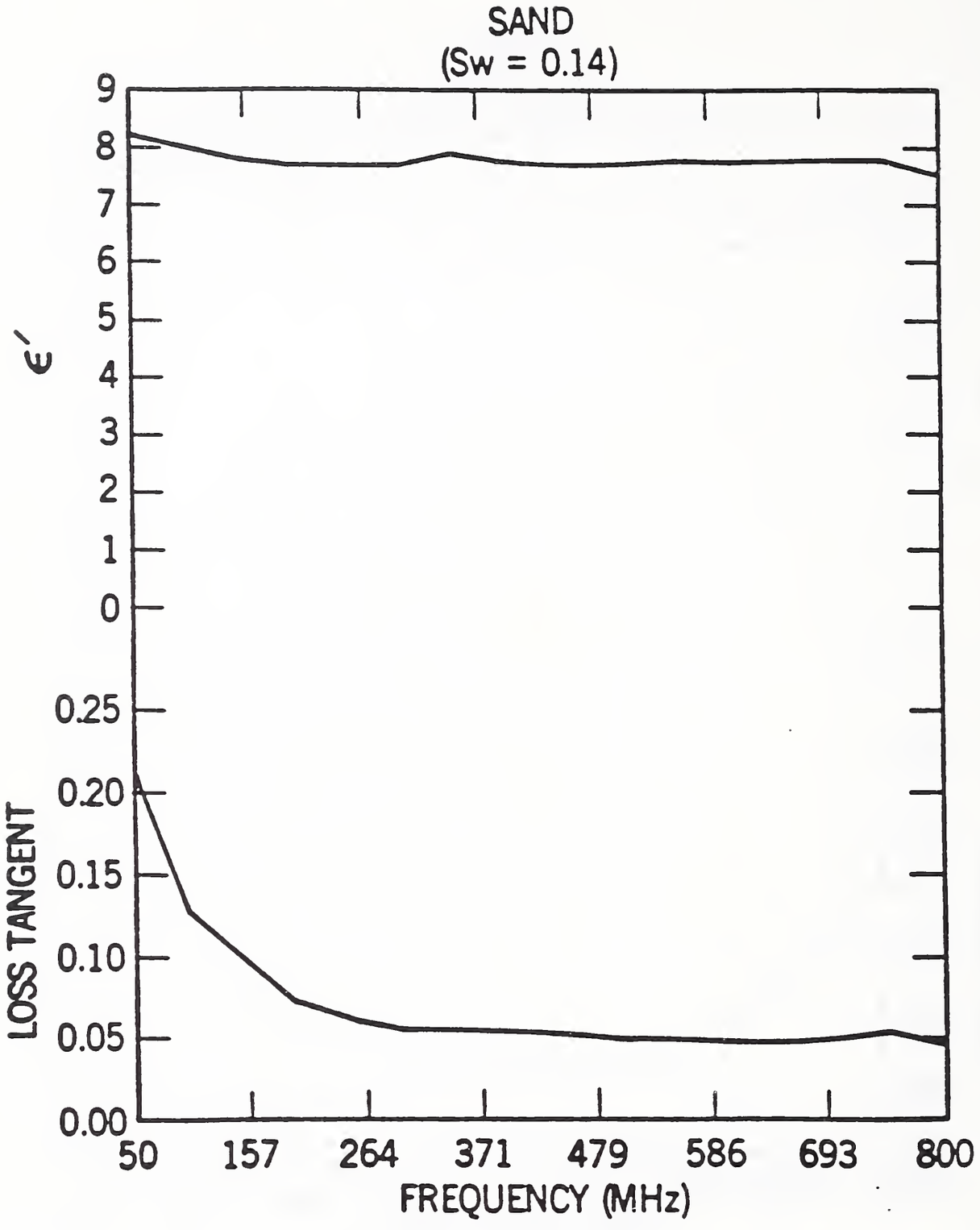

Figure 5.6 Measured permittivity and loss tangent vs frequency for sand with 14% water.

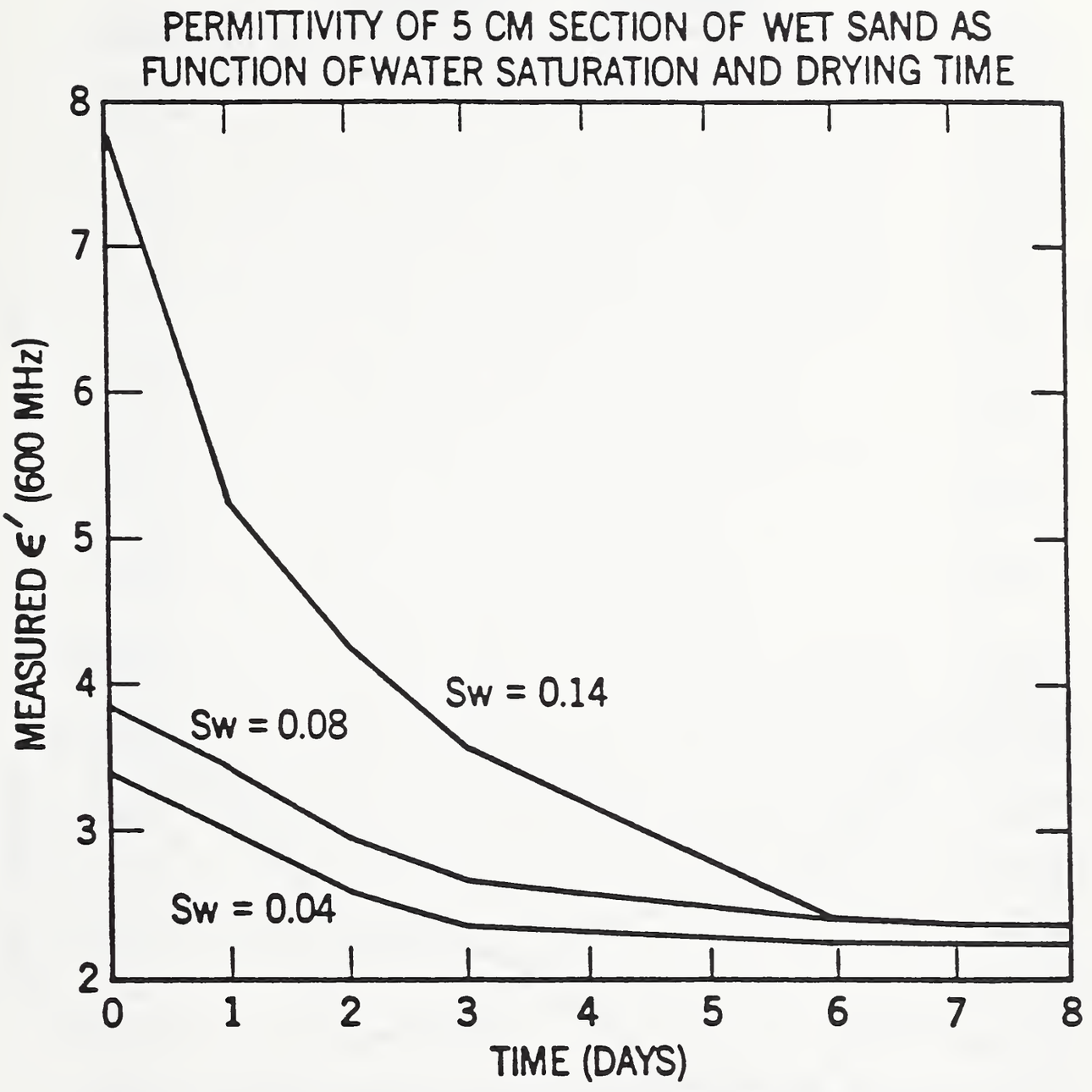

Figure 5.7 Measured permittivity at 600 MHz vs drying time at 20°C for various sand and water mixtures.

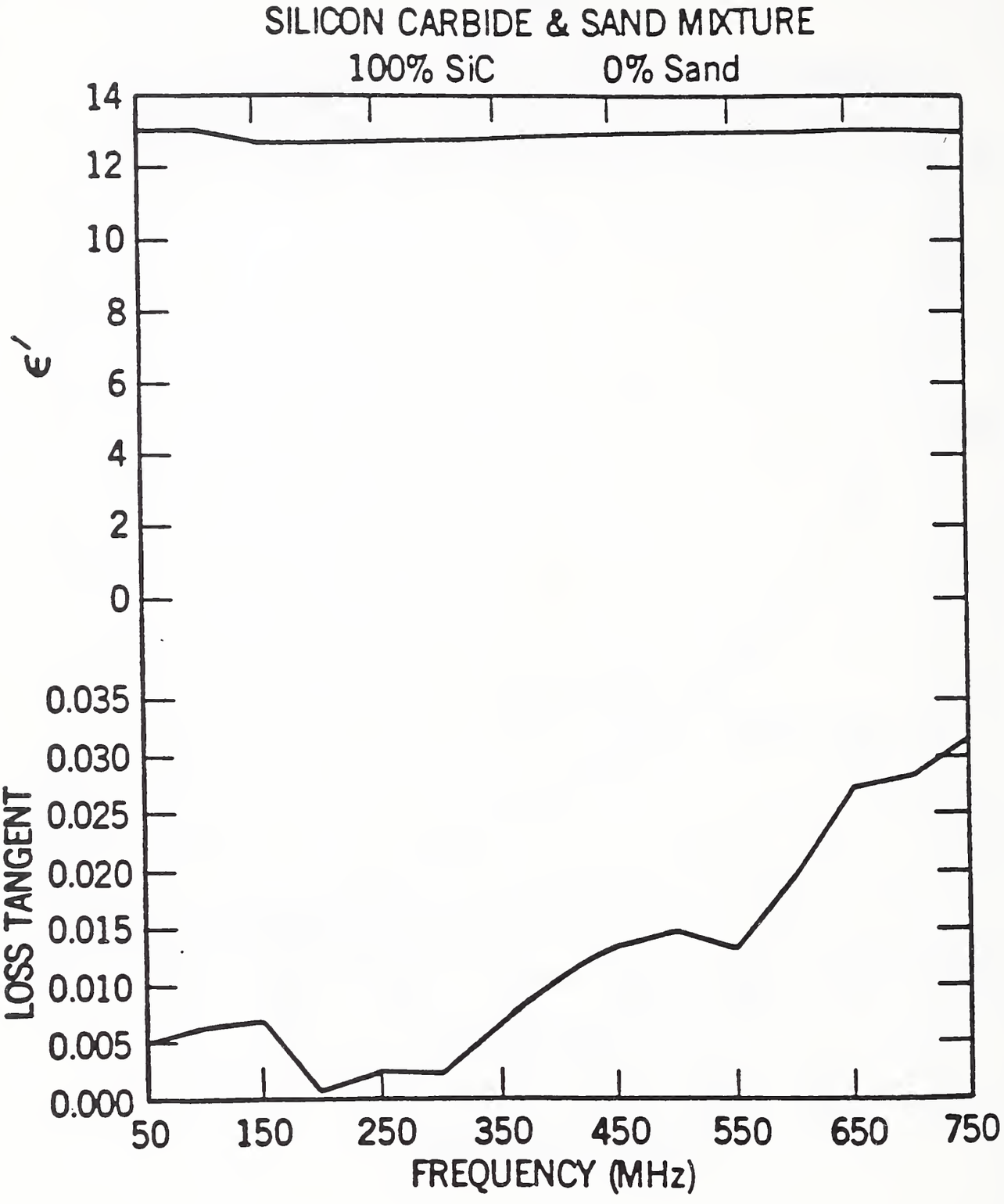

Figure 5.8 Measured permittivity and loss tangent vs frequency for 100% silicon carbide.

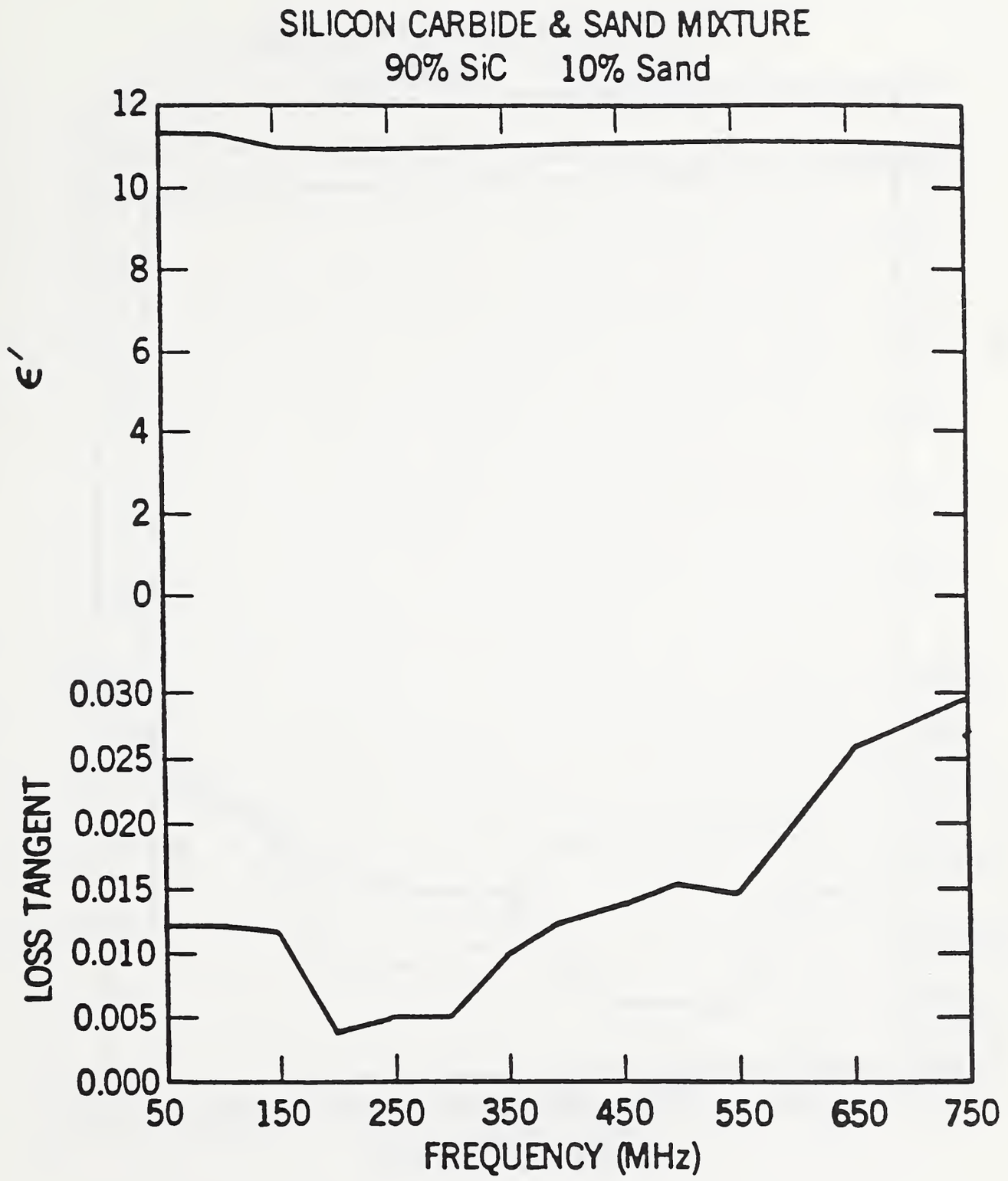

Figure 5.9 Measured permittivity and loss tangent vs frequency for 90% silicon carbide 10% sand mixture.

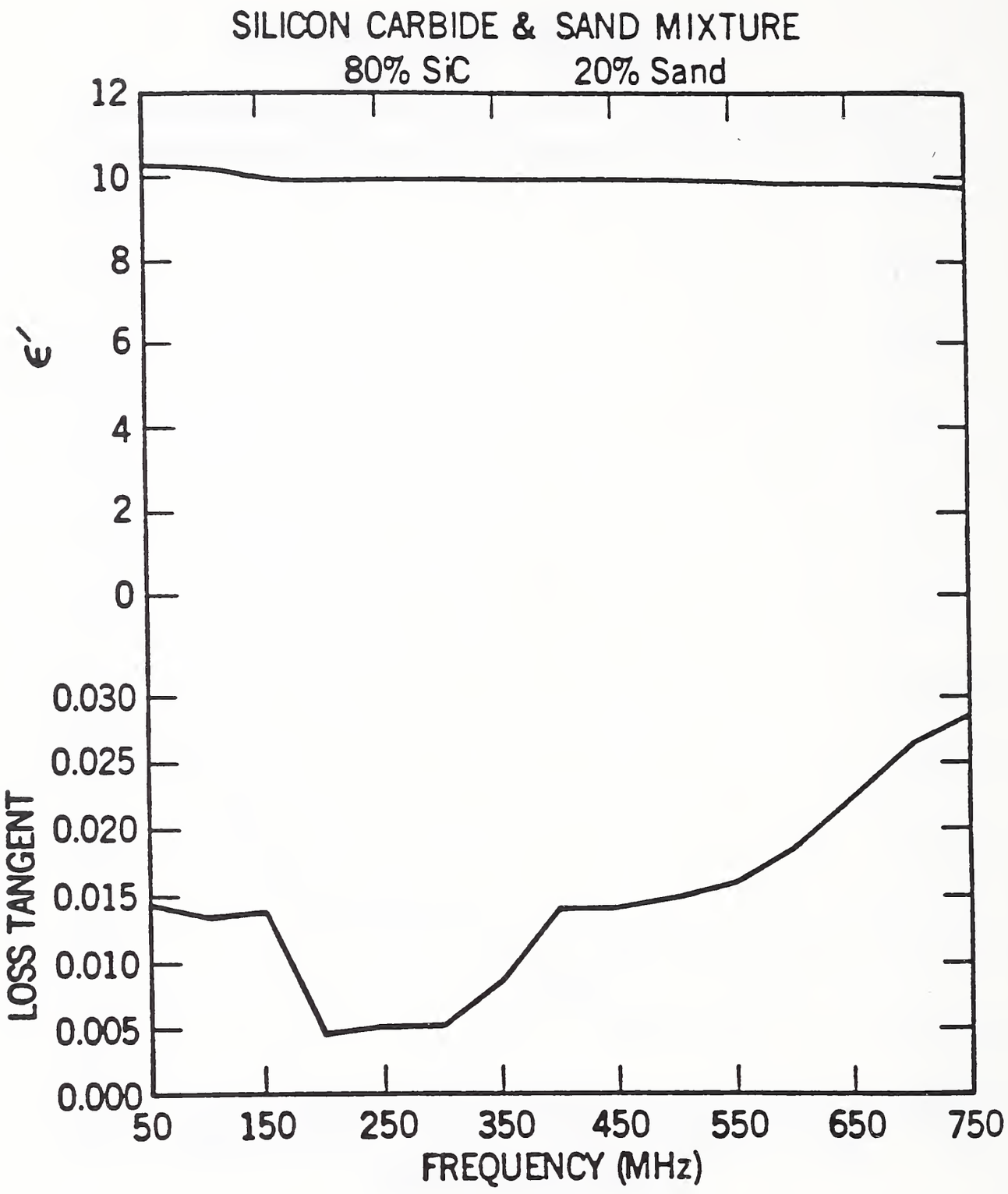

Figure 5.10 Measured permittivity and loss tangent vs frequency for 80% silicon carbide 20% sand mixture.

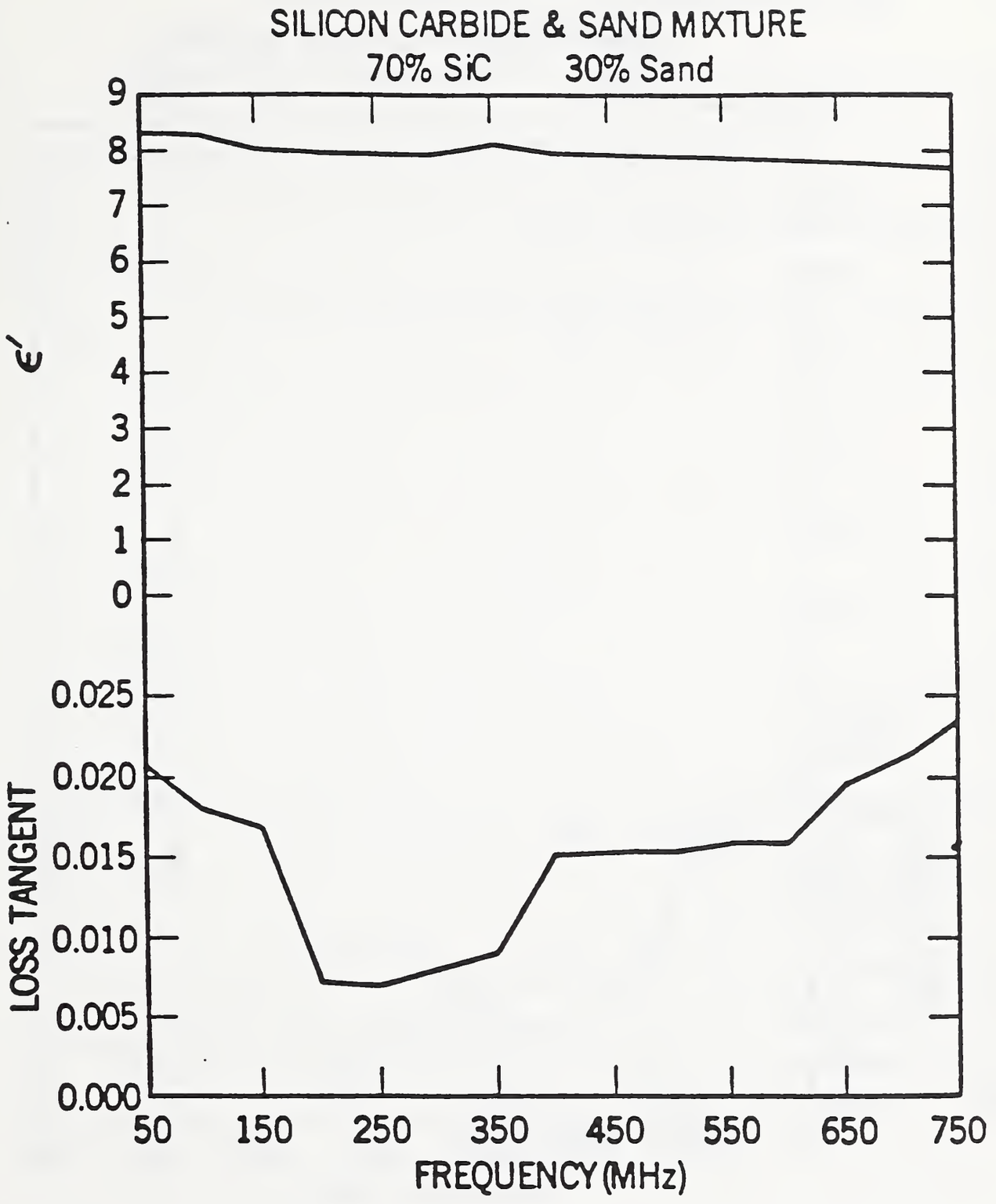

Figure 5.11 Measured permittivity and loss tangent vs frequency for 70% silicon carbide 30% sand mixture.

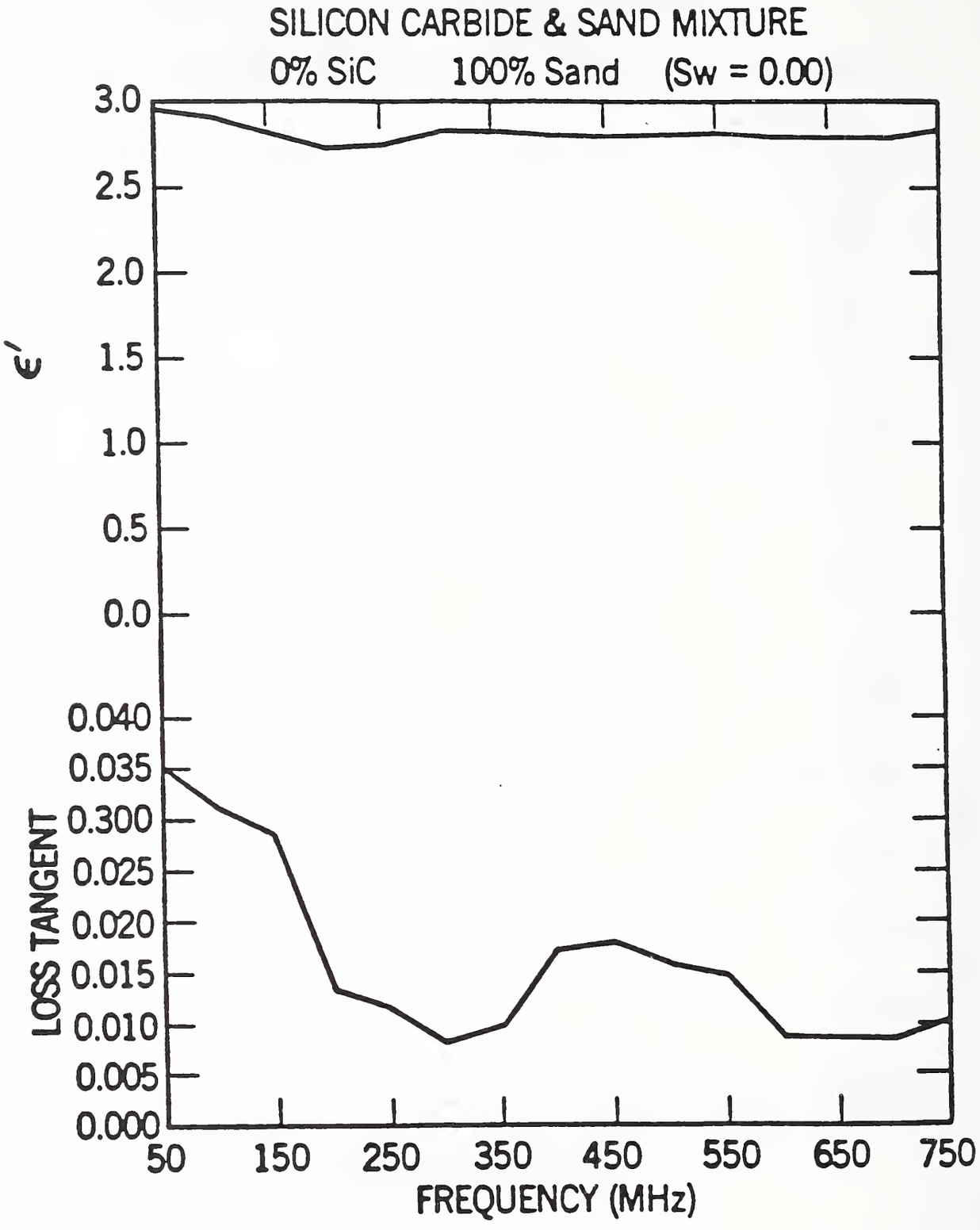

Figure 5.12 Measured permittivity and loss tangent vs frequency for 100% sand.

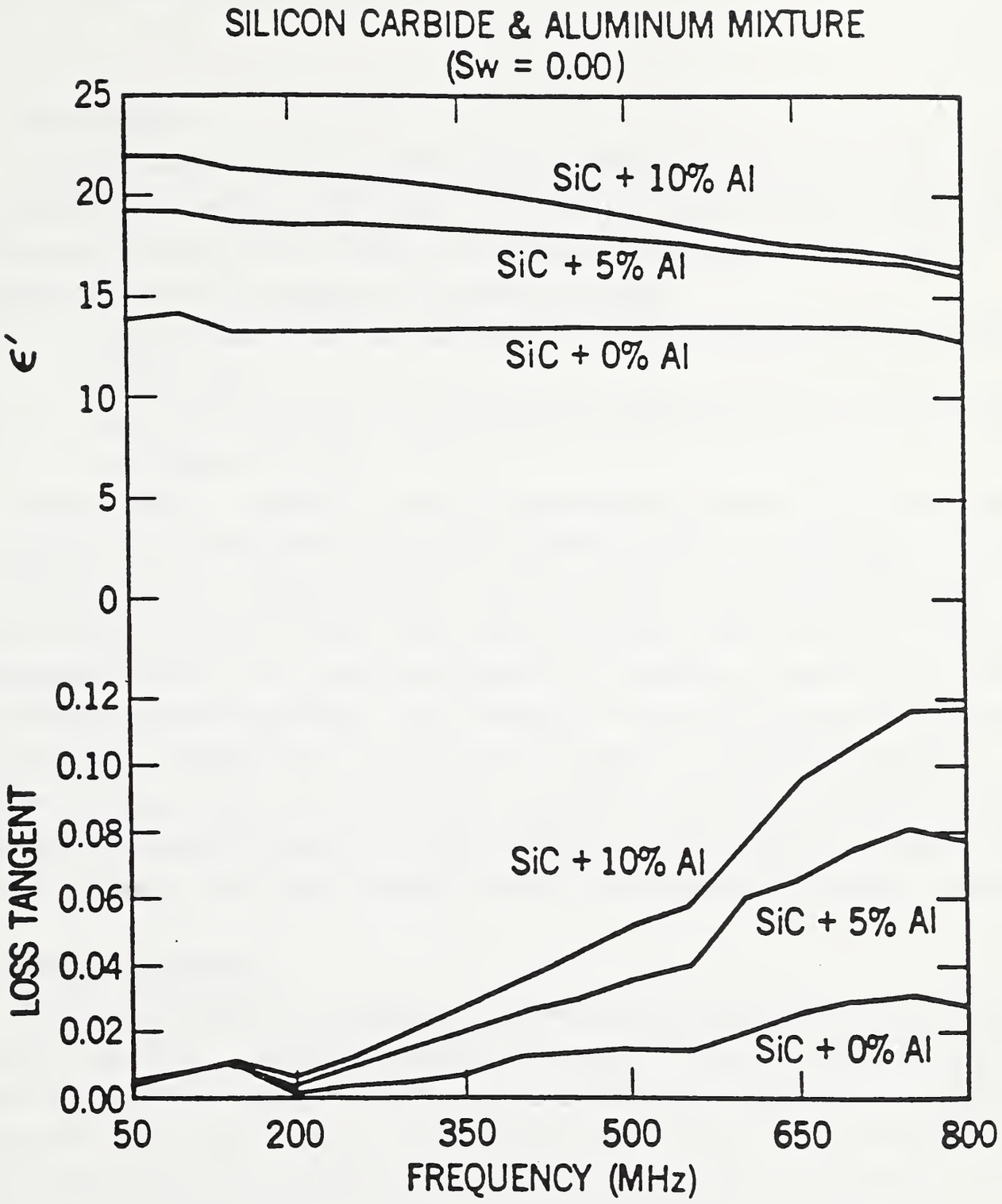

Figure 5.13 Measured permittivity and loss tangent vs frequency for various silicon carbide and aluminum powder mixtures.

VI Target Standards

A Introduction

"Standard" targets should have certain desirable characteristics—such as stability over time, reproducibility, and ease of fabrication. Unfortunately, some approaches to standardization involve particularly high costs; this tends to limit the use of good standards to a few well equipped laboratories. We distinguish two classes of standards:

(1) standards based on some well established theory or on known, immutable physical properties, and

(2) artifact standards which are reproducible and stable but for which a good theoretical model does not yet exist.

Where possible, we specify that testing of mine detectors be carried out with metallic and nonmetallic targets fabricated from pure or well analyzed materials. We also suggest that targets have simple cylindrical or spherical shapes. When, for purposes of realistic modeling, other target shapes and components must be used, at least the primary standards should be cylindrical or (preferably) spherical. Good theoretical models for the scattering of electromagnetic waves are available for these simple shapes. Also, the detection of spherical targets does not depend on target orientation. Furthermore, we suggest that the primary standard targets be molded or machined of single component materials without voids or simulated firing mechanisms. This can aid in further reducing the number of variables. Oxidation, water adsorption, and any surface or dimensional changes of the targets should be carefully monitored or entirely avoided if possible.

B Metallic Standards

Testing metal detectors has traditionally involved checking whether they can succeed in finding an ordinary U.S. one-cent coin buried in various soils. This nicely illustrates one of the pitfalls of using artifact standards. The Government started minting copper-clad zinc pennies in October 1982. The weight of the coin decreased from approximately 3.1 g to approximately 2.55 g. To our knowledge, the copper alloy used is chosen on the basis of its durability—its conductivity is not controlled. For careful work, we should avoid using ordinary coins as standard targets.

Objective testing of metal detectors can best be carried out with a set of known, repeatable metallic targets. Low frequency metal detectors transmit in the kilohertz range and sense eddy currents induced in buried metallic objects. The magnitude of these eddy currents varies as the $-1/2$ power of the conductivity of the target material and is directly proportional to target

volume for simple shapes such as cylinders or spheres [6.1]. It is important, when describing how these targets are made or copied, to specify the conductivity of the material. Certain materials, such as brass or aluminum alloys, exhibit very different conductivities depending on their composition and heat treatment. Highly purified elemental metals, especially those with the highest conductivity, show very little variation in conductivity from lot to lot. A further advantage is that their conductivity varies only slightly with changes in room temperature so this effect can be neglected when testing metal detectors. Accordingly, suitable standard test objects should have high conductivity. In increasing order of conductivity, this means gold, copper, or silver. We chose copper since it is the least expensive. "Five nines" purity electro-refined copper is readily available. The American Society of Metallurgists (ASM) of Metals Park, Ohio, lists the properties of various grades of wrought copper in the 8th edition of the *Metals Handbook* [6.2]. Oxygen-free, electro-refined copper has a conductivity of 5.977×10^{-7} S/m at 20°C.

Copper corrodes easily. We spray our copper test objects with a thin coating of spray lacquer. If considerable wear and handling are likely to take place, a hard chromium plating over a nickel plating would be appropriate for these targets.

A set of seven copper cylindrical test objects was provided to BRDEC in July 1986. These copper test objects were all machined from right-circular cylinder bar stock on a precision lathe at NIST. Electro-refined copper is commercially available. The weights and other specifications are given in table 6.1.

The smaller objects are suitable for calibrating the response of metal detectors (those operating at frequencies in the kilohertz range) to objects as small as firing pins. The other objects in this set were provided to test the response of low-frequency metal detectors to significantly larger amounts of metal. Large metal objects (such as unexploded ordnance) must often be located using mine detectors optimized for very small metal objects. Eddy currents die out slowly for the case of the large copper targets. Tests of target detectibility with the 32 g and larger cylinders should be performed with due regard for the long time constants involved (on the order of one-half second or more).

In addition to the copper cylinders, which we consider the primary targets for testing purposes, we have fabricated a small set of stainless steel pins. We consider the pins to be secondary standards, useful for simulating the properties of firing pins in mines. Because of the difficulty of specifying the composition of stainless steel, results using these objects may show greater variability than those using the copper cylinders. The pins should, however, prove useful in tests of the detectors for plastic mines where the orientation of such pins may be important. These pins can simply be cut from existing right-circular cylinder bar stock, also commercially available. Specifications for the pins are given in table 6.2.

Table 6.1

Copper test objects.

Material:	Copper, electro-refined, 99.999% pure
Shape:	Right-circular cylinders, diameter twice the height
Density:	8.96 g/cm^3

Mass (g)	*Diameter (mm)*	*Height (mm)*
1	6.58	3.29
2	8.28	4.14
4	10.44	5.22
8	13.15	6.58
32	20.87	10.44
128	33.14	16.57
512	52.60	26.30

All American Iron and Steel Institute (AISI) type 300 series steels are chromium-nickel austenitic steels in grades having up to 30% chromium and up to 20% nickel. Type 304 contains the following percentages:

Cr..... 18 to 20 %
Ni..... 8 to 12 %
C ..... 0.08 % (max)
Mn ..... 2 % (max)
Si ..... 1 % (max)

The composition range is based on ladle analysis for standard AISI Type 304 as of 1959. It is not a specification. It is a classification which has been agreed upon and used by producers in the United States for grades which have attained an arbitrary annual minimum tonnage [6.2]. We do not recommend 304 stainless steel for the standard targets, although it is useful for secondary standards and for estimating the performance of mine detectors in locating objects such as firing pins.

C Nonmetallic Standards

NIST fabricated Teflon and nylon spheres as calibration targets for nonmetallic mine detectors and delivered these to BRDEC in July 1986. The masses and diameters for these objects are listed in table 6.3.

Table 6.2

Stainless steel test objects.

Material: Type 304 stainless steel
Shape: Cylindrical pins or narrow rods
Density: Approximately 7.9 g/cm^3

Mass (g)	*Diameter (mm)*	*Height (mm)*
1.56	3.175	25.4
0.39	1.5875	25.4
0.096	0.7938	25.4

Table 6.3

Spherical plastic test objects.

Material: Nylon
Shape: Spherical
Density: 1.15 g/cm^3
Relative dielectric constant: 3.0

Material: Teflon
Shape: Spherical
Density: 2.2 g/cm^3
Relative dielectric constant: 2.1

Mass (g)	*Diameter (mm)*	*Mass (g)*	*Diameter (mm)*
36.8	39.0	68.4	39.0
72.0	49.2	136.8	49.2
144.0	62.0	273.6	62.0
288.0	78.2	547.2	78.2
576.0	98.5	1094.4	98.5

Teflon and nylon were chosen for these reasons:

(1) nylon and Teflon are relatively impervious to moisture as well as to common alkaline, acidic, or salt components likely to be found in ordinary soils;

(2) these materials are readily available commercially in shapes and sizes suitable for further machining; and

(3) their relative dielectric constants (2.1 and 3.0) nicely bracket known values for many common explosives.

We decided to systematically vary the parameter of target volume rather than target mass, specifying five different sizes in each of the two materials. The volumes increase by an approximate factor of 2 for each step up in size.

Table 6.4

Cylindrical plastic test objects.

Quantity	*Diameter (in mm)*	*Height (in mm)*	*Material*
2	76.2	25.4	Nylon
2	152.4	50.8	Nylon
2	304.8	76.2	Nylon
2	76.2	25.4	Teflon
2	152.4	50.8	Teflon
2	304.8	76.2	Teflon

Discussions about the procedures for plastic mine detectors have focussed on two additional points: (1) the need for still larger test objects, and (2) whether the shape of the test objects could be made to conform more closely to that of known, real mines. We think that small spheres are most likely to give the best, most repeatable results. Spherical targets do not require careful alignment with the surface of the ground—only the depth matters. Spherical targets have a well defined radar cross section which does not depend on target orientation. They are also preferred on theoretical grounds, since the EM scattering cross section is well known even when the illuminating wavelength is much smaller than the diameter of the sphere [6.3]. A theoretical paper by Hill [6.4] outlines a method for calculating the scattering cross section for buried spheres, cylinders, and rectangular parallelopipeds when the dielectric contrast between the target material and the background medium is low.

We have fabricated both nylon and Teflon cylindrical targets of various sizes for use as secondary standards. They are similar to the dummy mines of Type I, class B, sizes 1, 2, and 3 [6.5]. However, they do not have air voids or replicas of firing mechanisms installed. All of the plastic targets, both spherical and cylindrical, were machined on a precision lathe at NIST. Numerical control of the lathe was required for the spherical shapes. All were cut from right-circular cylinder bar stock which is commercially available. Quantities delivered to the Army in August, 1988, and dimensions for these mine replicas are given in table 6.4.

D Relationship of Standards to Realistic Targets

D.1 Metallic Objects Relationships

For low-frequency treasure finders and metallic mine detectors, the tests with the cylindrical copper targets are more than adequate to establish detector sensitivity and other performance requirements. The response of low-sensitivity equipment (operating in the kilohertz range) shows little if any dependence on target orientation even for targets which are highly

acicular (needlelike). The situation is very different for equipment operating at microwave frequencies, where polarization effects become important. When testing the ability of plastic object detectors to locate, say, metallic firing pins, target orientation must be carefully controlled for the resulting data to be useful and repeatable. In particular, the targets listed in table 6.2 are likely to exhibit very different radar cross sections when placed parallel or perpendicular to the E-field of an operating AN/PRS-7 plastic object detector.

D.2 Nonmetallic Object Relationships

The materials from which these targets were machined were chosen to approximate the range of dielectric constants likely to be encountered in real mines. These targets (perfectly spherical or perfectly cylindrical) scatter electromagnetic waves in a very predictable fashion. An analytic solution for spherical objects is well known [6.3, 6.6]. Good approximations are available for the scattered fields from cylindrical objects [6.4]. The targets we have provided cover the range from anti-tank to smaller than anti-personnel. However, these standards do not mimic all features of real mines. Typical mines and mine replicas contain air voids, firing mechanisms, pull rings, and other accessories which significantly modify the radar cross section. BRDEC has made arrangements for the manufacture of a number of mine-like targets to address this issue [6.5]. Such targets cannot simultaneously satisfy two divergent requirements: (a) complete properties of real mines, and (b) precision in detector performance measurement and test repeatability. Realistic mine replicas possess radar cross sections which vary with changes in temperature and barometric pressure. Their nonuniform filler separates into layers or even deteriorates over time. Air voids (and light-weight foam inserts to simulate voids) distort or change shape permanently. Nevertheless, they are interesting test objects which certainly *look* like mines; it should be possible to use them as secondary or tertiary standards so long as their radar cross sections are frequently compared with those of the primary standards.

The detection of buried, nonmetallic objects is a difficult task [6.7]. Their typically low-contrast ratio in sandy soil or loam leads to their becoming nearly invisible to electromagnetic waves. Because of their small size, carefully made anti-personnel mines (those without air voids or metal pins) are often completely undetectable with present-day equipment.

E NIST Recommendations and Conclusions

Accurate testing of treasure finders and mine detectors is notoriously difficult. When performance tests are carried out, the degree to which meaningful, repeatable data can be obtained is critically dependent on the targets being used. At UHF and higher frequencies, target orientation must also be carefully established unless the targets are spherical. What follows are

NIST's recommendations for target standards that should be used to test metal detectors and nonmetallic object detectors.

E.1 Targets for Metal Detector Testing

It is difficult or impossible to obtain consistent results with mine replicas for coins. The coated pure copper standards that NIST has provided to the Army should be used as primary standard targets for the testing of low-frequency metal detectors; their permeability and conductivity are known very accurately and their masses and volumes have been carefully controlled. For more realistic target detection testing, the Type 304 stainless steel cylinders that have also been provided to the Army should be used. Although the permeability and conductivity are not known to the accuracy of the copper standards, they should prove sufficiently accurate and repeatable for all but the most demanding tests.

E.2 Targets for Nonmetallic Object Detector Testing

Sets of standard spherical and/or cylindrical nylon and Teflon targets should be utilized for the most accurate tests of nonmetallic object detectors. The spherical standards should be used whenever errors due to target orientation must be avoided in the tests. The cylindrical standards, being somewhat more realistic in shape, should suffice for the majority of the tests as described in chapter VII. The principal reason that NIST recommends the use of these targets for most of the tests is that they are homogeneous, have well known constituent electromagnetic properties, and, most important for theoretical modeling purposes, have known scattered electromagnetic field signatures. As is stated in chapter VII, these standards do not preclude using more realistic mine replicas as targets for other tests.

For a more robust testing strategy, NIST recommends fabricating targets using the same rigid-matrix technology as is being studied for soil standards. The results of these studies on rigid-matrix technology, being done under contract by NIST for BRDEC, are not yet available and will be reported in a second document. With little additional effort, standard targets can be molded with known electromagnetic properties that can cover a wide range of values. Thus, for example, targets for a set of tests to measure permittivity contrast ratio could be constructed with incrementally varying permittivity. Using the nylon or Teflon targets, on the other hand, would require varying the permittivity of the soil standards which would be more difficult and expensive as well as less realistic. In addition, using this technology would allow the fabrication of extremely realistic mine replica targets with such features as air gaps, inhomogeneities (explosives with a plastic shell, for example), and firing pins.

References (VI)

[6.1] Wait, J.R. A conducting sphere in a time-varying magnetic field. Geophysics; 16(4): 666-672; 1951.

[6.2] Metals Handbook, 8th Edition, American Society of Metallurgists; 1980.

[6.3] Mie, G. Beiträge Zur Optik Trüber Medien, Speziell Kolloidaler Metallosungen. Annalen der Physik 25, p. 377; 1908.

[6.4] Hill, D. A. Electromagnetic scattering by buried objects of low contrast. IEEE Trans. Geosci. Remote Sensing GE-26, pp. 195-203; 1988.

[6.5] Brown, D.; Tanner, John D.; Paca, Francis B. Mine detector targets: Metallic and nonmetallic, generic set, development efforts. VSE Corp. Report ASD/0047-87/35RD; October 1987.

[6.6] Van deHulst, H. C. Light scattering by small particles. N.Y.: J. Wiley & Sons, 1957.

[6.7] Pear, Robert. Returning Afghan refugees face peril of millions of land mines. NY Times; 13 August, 1988.

VII Standard Measures of Effectiveness

A Introduction

This chapter contains NIST's recommended strategy for testing and comparing portable, electromagnetic-based mine detectors. The next section contains a description of this strategy and our reasons for recommending it. Section VII.C contains detailed instructions on how to perform a recommended core set of tests, and section VII.D contains general descriptions for an advanced set of tests. And last, section VII.E contains a recommended approach for comparatively rating each detector tested.

B Test Strategy

The test strategy that we recommend is predominantly a *target-based* strategy, as opposed to a *detector-based.* (See Chapter III, p. 3-1, for NIST's definitions of *target-based* and *detector-based.*) The method proposed, which we call the "eye-chart" method, is patterned after the physician's eye chart. This chart consists of rows of letters or other characters, with the characters of each row smaller than those of the previous row. The physician's test consists of having the patient read the characters from a fixed distance until they are too small for the patient to see. The physician can thus determine the patient's visual acuity.

In a like manner, by carefully selecting a set of targets and embedding them in a soil or soil-like medium, we can create a test range wherein each succeeding target is more difficult to detect than the last in some sense. For a particular detector test, we would simply determine how many of the targets the detector could find from the complete set when the detector is operated according to the manufacturer's instructions. Then, by conducting tests on an ensemble of different target sets, each one designed to test for a different parameter sensitivity, we could determine an overall "score" for each detector. This in turn, would allow us to comparatively rate each manufacturer's detector(s) in order to determine which one exhibits the "best" performance.

Probably the best way to illustrate this target-based approach to detector testing is with an example. Let us assume we wish to perform a "target depth" test with which we want to determine the detector's ability to find identical targets buried at different depths in the surrounding soil medium. The test range configuration for this test would consist of a number of identical targets, buried at increasing depths and suitably separated from each other in order to assure target isolation. All other variables, such as target rotational orientation, target ε_t, μ_t and σ_t, and soil medium ε_s, μ_s and σ_s, would be held constant. Then, the detector under test would be

operated according to the manufacturer's instructions in an attempt to have it detect each of the targets in the set. The raw "score" for the detector for this test would simply be the number of targets detected.

The resolution of this test is a function of the number of buried targets just as the resolution of the physician's eye chart is a function of the number of rows of characters. The range of difficulty for this test is a function of the maximum depth at which a target is buried, just as the range of difficulty for the physician's eye chart is determined by the size of the characters in the bottom row. The *absolute* accuracy of this test is a function of our ability to control all of the pertinent target/soil parameters, but here it should be noted that the *relative* accuracy of the test, for purposes of comparing two or more detectors, is a function only of the stability in time of the pertinent target/soil parameters. Their absolute values are only of secondary importance.

There are many advantages to this method. First is its *simplicity*. Since each test is designed to observe the detector's sensitivity to only one parameter at a time, then analysis of each detector's weak and strong points will be relatively easy.

Second, this approach is relatively *easy*. It does not require the Army to perform difficult, expensive, and time consuming detector-based tests. Although NIST recommends a few detector-based tests in this report, none of them requires performing any measurements on the detector itself. NIST believes that it is not necessary to know such details about the detector as its electromagnetic antenna field pattern, its bandwidth, or its signal-to-noise ratio, in order to determine its ability to detect mines. In general, the *design* and *modeling* of detectors should be left to industry whenever possible, and the Army, as the end user of detectors, should be concerned only with their functionality. The test strategy presented in this report reflects this philosophy.

The third advantage of this strategy is its *generality*. Practically any portable EM-based mine detector can be tested using this strategy. Any test strategy that requires development of new tests for each new detector technology that evolves is inferior.

A fourth advantage of this strategy is its *realism*. Rather than an approach which uses a set of detector-based parameters to *predict* the detector's ability to find mines, this approach involves the actual quantitative measurement of a detector's ability to find mines under varying conditions. No mathematical modeling, predictions, or extrapolations are necessary.

The last advantage of this strategy is its *versatility*. NIST has made a number of recommendations in this report concerning optimal target standards (nylon and Teflon spheres and cylinders) and soil standards (rigid-matrix bricks). However, this test strategy will also work using practically any type of target soil. The strategy, itself, imposes no restrictions on the actual test range design chosen by the Army.

C Recommended Core Tests

Contained in this section are detailed descriptions of seven core tests that we recommend the Army implement as soon as is practical. NIST has chosen these particular tests as a core set because they are relatively easy to implement and because they offer a substantial challenge to any portable, EM-based mine detector. The next section contains less-detailed descriptions of seven more tests that the Army may choose to implement in the future. However, we recommend that these seven core tests be implemented first. With the experience gained from performing these core tests over a period of time, NIST believes that the Army will be in a much better position to decide what additional tests may be required and what the test designs should include.

In the detailed descriptions of each recommended test that follow, we have chosen numerical values for each of the relevant variables that we believe are realistic. However, these values should be considered to be only examples; the final choice of such parameters as the number of targets and the range of variables for each test should be decided by Army personnel, using their superior knowledge of actual field conditions that are desired for simulation. For each test, five elements are presented; the objective of the test, the test's requirements, test restrictions, a description of the recommended test technique, and test variations that the Army may wish to try.

In order to implement these tests, any one of the test range configurations and target sets discussed in chapters V and VI can be used. However, we note under "Restrictions" those range configurations that would make that particular test extremely difficult.

We recommend that, at minimum, two different soil media be used for each test in the case of *nonmetallic* detectors, and one soil medium in the case of kilohertz range *metallic* detectors. The two different media for nonmetallic detectors should have relative permittivities (at 500 MHz, 23°C) of $(2.7 - j0.02)$ (dry sand approximation) and $(10 - j12)$ (wet clay/loam approximation). The relative permeability for these two media should be $(1 - j0)$. The relative permeability for the metallic detector medium should be approximately 1.35, the value of the sand/magnetite mixture now present in the Army's existing test range at Fort Belvoir. The successful detection of targets in these media we believe would be a minimally robust indication that the detector could be expected to perform well in the field. Of course, the range could always be expanded at a later date to provide testing capabilities for other soil types. (NIST's recommendations on how to create these soil simulations in a rigid-matrix brick formulation will be delivered to the Army in a separate report.)

Before describing these tests in detail, we must mention a few other caveats here. First, we recommend that each of the detectors be operated exactly according to the manufacturer's instructions. If the instructions are faulty, we believe that this fact should be part of the test; it

should be the manufacturer's responsibility to provide instructions for its use that optimize its performance. Also, we must make the assumption that the detection of a target by a detector is very clear cut; it either detects a target or it doesn't and there is no gray area allowed. If there is gray area, then we recommend that the Army insist to the manufacturer that it be removed. A third caveat concerns target separation in the test range. It is important to know that nearby targets are not interfering with a particular test in spite of the fact that nothing is known about the detector's radiated EM field pattern. To alleviate this problem we recommend that the Sensor Active Envelope Test be performed first. The results of this test will indicate what the minimum target spacing should be. To begin testing, and with no *a priori* knowledge of required target separation, we arbitrarily recommend a spacing of 1 m. If the Sensor Active Envelope Test indicates that this distance is too small then the targets can be spread out. The last caveat concerns choice of targets for each test. Except for the Target Shape Test and the Target Orientation Test, we recommend that, at minimum, both the nylon and the Teflon spheres, described in chapter VI, be used for the reasons stated there. If the Army wishes, however, practically any targets [7.1] may be used in addition to these. Restrictions, if any, are listed for each test. (In our forthcoming report on rigid-matrix brick formulations, we will specify a method for making targets with variable permittivities, suitable for use in the Target-Earth Contrast Tests.)

In the test discriptions which follow, procedures are given for nonmetallic-target tests using the dry sand and wet clay/loam media approximations, as well as metallic-target tests using the sand/magnetite medium approximation. NIST considers this to be minimal set of required tests. As a first step toward increasing the robustness of the testing strategy, we recommend that the nonmetallic-target tests be repeated in the sand/magnetite medium approximation, and the metallic-media approximations. Regardless of which medium is used, the testing procedure and scoring system for each target set remains unchanged.

C.1 Sensor Active Envelope Tests

(1) *Objective:* To determine the size of the area beneath the sensor in which targets are detected.

(2) *Requirements:* Bury a target, separated from any other targets in the surface plane by enough distance to ensure target isolation. The target burial depth should be 0 m, as measured from the top of the target, and this test need only be performed in the "dry sand" medium.

(3) *Restrictions:* This is the only test for which a "score" is not explicitly recorded. Rather, it is necessary to record the perpendicular distances between the center of the target and the center of the sensor at which target detection *just* fails.

(4) *Recommended Techniques:*

a. *Dry Sand:* We recommend the use of two spherical targets for this test, one of Teflon and one of nylon, each with a diameter of 15.24 cm. Bury each of the targets to a depth of 0 m measured from the top of the target such that there are no other targets within 3 m. For each of the targets, move the detector sensor along a straight line such that the center of the sensor moves over the center of the target. The height of the sensor must be at the optimal height recommended by the manufacturer, and must be kept constant above the surface of the earth. Also, the rotational orientation of the detector must be recorded and kept constant. Verify that the detector detects the target. (If not, since this is the easiest of all challenges for the detector, the test is complete and the detector's score is 0.) Then, move the detector sensor along another straight line that is parallel to but displaced by 3 cm from the first line. Again, verify detection. Continue this test along displaced, parallel sensor paths until the displacement reaches 1.5 m. Record the displacement distances for which detection occurs, stops, and reoccurs. (Detection may stop at a given distance due to a null in the radiated field, and then reoccur when the target appears in a side lobe of the radiation.) Now, rotate the sensor about the vertical axis by an angle of 30° clockwise and repeat the above scans, again recording the distances. Continue this rotation in 30° steps until the sensor has been rotated a full 360°. Now, a chart may be sketched showing the sensor active envelope(s). For all subsequent tests for this detector, adequate target isolation, when required, can be achieved based on these test results. (If the Army wishes, they may also devise a numerical score for this test, similar to the scores obtained for all the other tests. NIST personnel do not have enough information to specify this score, but it is clear that a sensor active envelope that is too small would be disadvantageous, as would be one that were not centered under the physical sensor.)

b. *Wet Clay/Loam:* Same as that for dry sand.

c. *Magnetite/Sand:* We recommend the use of two right-circular cylinder metallic targets for this test, one of pure copper and one of Type 304 stainless steel. The height of the copper target should be 4.14 mm and its diameter should be 8.28 mm. The height of the stainless steel target should be 25.4 mm, and its diameter, 1.5875 mm. (NIST has supplied the Army with samples of the "standard" and "realistic" targets under a previous contract; they are described in chapter VI.) Each of these targets should be buried in an upright orientation

(flat sides parallel to the earth surface) at a depth of 0 m measured from the top of each target. Then, the test should be performed as described above for the plastic targets.

(5) *Variations:* This test may be conducted with a Teflon sphere, nylon or Teflon cylinder, or with a more realistic target such as one of the mine replicas supplied to the Army by others. Also, this test can be repeated for different detector sensor heights above the earth in order to estimate a three-dimensional sensor active envelope.

C.2 Target Burial Depth Tests

(1) *Objective:* To determine a detector's ability to detect targets at increasing burial depths in the surrounding soil.

(2) *Requirements:* Bury a set of *identical* targets at increasing depths in the medium, separated from each other in the surface plane by enough distance to ensure target isolation. The parameters that must be held constant for this test are target and soil constitutive EM properties, and target orientation if the chosen targets are not spherical in shape.

(3) *Restrictions:* None.

(4) *Recommended Techniques:*

a. *Dry Sand:* We recommend the use of two target sets for this test, the first set consisting of nine Teflon spheres with a diameter of 7.62 cm, and the second set consisting of nine nylon spheres with the same diameter. The targets should be buried at depths of 0, 2.5, 5, 7.5, 10, 12.5, 15, 20, and 25 cm, measured from the top of the targets. Each target should be positioned at least 1 m from a range boundary or any other target, or at a greater distance if the results of the Sensor Active Envelope Test so indicate. Operating the detector according to the manufacturer's instructions, count and record the number of targets detected for each set. Two scores will result, each with a range of 0 to 9, 9 indicating that all targets were detected in the set.

b. *Wet Clay/Loam:* Same as that for dry sand, above.

c. *Magnetite/Sand:* For the burial depth testing of metallic detectors we recommend two sets of targets. The "standard" set consists of pure copper right-circular cylinders with a height of 4.14 mm and a diameter of 8.28 mm. the "realistic" set consists of Type 304 stainless steel right-circular cylinders with a height of 25.4 mm and a diameter of 1.5875 mm. (NIST has supplied the Army with samples of these "standard" and "realistic" targets under a previous

contract; they are described in Chapter VI.) The targets should be buried in an upright orientation (flat sides parallel to the earth surface) at the same depths, measured from the top of the targets, as those stated above for the plastic targets. The testing method is also the same as for the plastic targets; again, the possible scores for each target set will range from 0 to 9, with 9 signifying that all targets were detected.

(5) *Variations:* The Army may wish to perform these tests with other targets in addition to those recommended.

C.3 Target Volume Tests

(1) *Objective:* To determine the detector's ability to detect targets of decreasing size (volume.)

(2) *Requirements:* Bury a set of targets with differing volumes at *identical* depths in the medium, separated from each other in the surface plane by enough distance to ensure target isolation. The parameters that must be held constant for these tests are target and soil constitutive EM properties, target burial depth, and target orientation.

(3) *Restrictions:* None.

(4) *Recommended Techniques:*

a. *Dry Sand:* We recommend the use of two target sets for this test, the first set consisting of six Teflon spheres, and the second set, consisting of six nylon spheres. In both cases, their diameters should be 2.54, 5.08, 7.62, 10.16, 12.7, and 15.24 cm. The targets should all be buried at a depth of 10 cm, measured from the top of each target. Each target should be positioned at least 1 m from a range boundary or any other target, this distance, again, depending on the results of the Sensor Active Envelope Test. Operating the detector according to the manufacturer's instructions, count and record the number of targets detected for each set. Two scores will result, with a range of 0 to 6 for both the Teflon targets and the nylon targets.

b. *Wet Clay/Loam:* Same as that for dry sand.

c. *Magnetite/Sand:* For the target volume testing of metallic detectors we recommend two sets of targets. The "standard" set consists of pure copper right-circular cylinders, and the "realistic" set consists of Type 304 stainless steel right-circular cylinders. Five copper targets (coated with a thin layer of lacquer to resist corrosion) are recommended, with dimensions as follows: (1) h = 3.29 mm, d = 6.58 mm; (2) h = 4.14 mm, d = 8.28 mm; (3) h = 5.22 mm, d = 10.44 mm; (4) h = 6.58 mm, d = 13.15 mm; and (5) h = 10.44 mm,

d = 20.87 mm. All of these cylinders have a diameter-to-height ratio of 2:1, and their weights are 1, 2, 4, 8, and 32 g. Three stainless steel targets are recommended, all with a height of 25.4 mm (1 in). Their diameters and weights are as follows: (1) d = 0.7938 mm, w = 0.096 g; (2) d = 1.5875 mm, w = 0.39 g; and (3) d = 3.175 mm, w = 1.56 g. (These dimensions were chosen because they are realistic and available, as mentioned in chapter VI.) The same burial and testing procedures should be followed as those for the dry sand case described above, except that the cylinders should be buried in an upright orientation with their flat sides parallel to the earth surface.

(5) *Variations:* The Army may choose different target sets in addition to the ones recommended by NIST.

C.4 Target-Earth Contrast Tests

(1) *Objective:* To determine the detector's ability to detect targets as the permittivity of the target approaches that of the surrounding soil.

(2) *Requirements:* Bury a set of spherical targets with increasing permittivities (but otherwise identical) in the medium, separated from each other in the surface plane by enough distance to ensure target isolation. The target-to-medium permittivity ratios should be centered around 1, with an equal number of targets possessing permittivities above and below this value. The parameters that must be held constant for these tests are the soil constitutive EM properties, target burial depth, and target orientation.

(3) *Restrictions:* We recommend that this test only be undertaken for the case of dry sand. All available evidence indicates that there is never a contrast ratio problem, either with permittivity or permeability, if the soil is wet or contains magnetic material. Also, NIST recommends that the targets be constructed from the rigid-matrix formulations of polyester and glass microballoons, as described in our forthcoming report. We know of no other simple way to manufacture targets with the required permittivities.

(4) Recommended Techniques:

a. *Dry Sand:* We recommend the use of one target set for this test, consisting of six spheres, each with a diameter of 7.62 cm. The target-to-medium permittivity ratios should be 0.9, 0.94, 0.98, 1.02, 1.06, and 1.1. With the assumption that the magnitude of the permittivity of dry sand is 2.7, then the target permittivity magnitudes should be 2.43, 2.54, 2.65, 2.75, 2.86, and 2.97, and the imaginary part of the permittivity, ε_t'', should be on the order of 0.02 to

match the loss characteristics of dry sand. The targets should all be buried at a depth of 10 cm, measured from the top of each target. Each target should be positioned at least 1 m from a range boundary or any other target, again, depending on the outcome of the Sensor Active Envelope Test. Operating the detector according to the manufacturer's instructions, count and record the number of targets detected. The resulting score will have a range of 0 to 6, with 6 being perfect.

(5) *Variations:* The Army may wish to perform this test with other target volumes, shapes, or burial depths, in addition to the ones recommended by NIST.

C.5 Target Shape Tests

(1) *Objective:* To determine the detector's ability to detect targets with varying shapes.

(2) *Requirements:* Bury a set of targets with varying shapes (but otherwise identical) in the medium, separated from each other in the surface plane by enough distance to ensure target isolation. The parameters that must be held constant for these tests are target burial depth, target volume, and target orientation.

(3) *Restrictions:* None

(4) *Recommended Techniques:*

a. *Dry Sand:* We recommend the use of two target sets for this test, the first set consisting of five Teflon right-circular cylinders, and the second set consisting of five nylon right-circular cylinders. For both sets, all should possess equal *volumes*, and diameters of 2.54, 5.08, 7.62, 10.16, and 12.7 cm, respectively. Since we wish to have a diameter-to-height ratio of 3:1 for the middle target in each set, then, in order to maintain equal volumes for all targets, their respective heights must be 22.86, 5.71, 2.54, 1.43, and 0.91 cm. The targets should all be buried at a depth of 10 cm, measured from the top of each target. Each target should be buried with its flat sides as parallel as possible to the air-earth interface, and be positioned at least 1 m from a range boundary or any other target, again, depending on the results of the Sensor Active Envelope Test. Operating the detector according to the manufacturer's instructions, count and record the number of targets detected. The resulting scores for each set will have a range of 0 to 5, with 5 being perfect.

b. *Wet Clay/Loam:* Same as that for dry sand.

c. *Magnetite/Sand:* We recommend the use of one target set for this test, consisting of five lacquer-coated pure copper right-circular cylinders, all with equal volumes, and with diameters of 3, 6, 8.28, 10, and 13 mm. Since we wish

to have a diameter-to-height ratio of 2:1 for the middle target in the set, then, in order to maintain equal volumes for all targets, their respective heights must be 31.54, 7.88, 4.14, 2.84, and 1.68 mm. The same burial and testing procedures should be followed as those for the dry sand case described above.

(5) *Variations:* The Army may choose to perform these tests with targets of different shapes or volumes than those recommended by NIST. (These shapes were chosen because, as mentioned in chapter VI, their scattered fields are computable.)

C.6 Target Orientation Tests

(1) *Objective:* To determine the detector's ability to detect targets with varying orientations in the soil.

(2) *Requirements:* Bury a set of identical targets (nonspherical) in the medium with varying orientations with respect to the air-earth interface plane. The targets should be separated from each other in the surface plane by enough distance to ensure target isolation. The parameters that must be held constant for these tests are target and soil constitutive EM properties, target burial depth, and target volume.

(3) *Restrictions:* None

(4) *Recommended Techniques:*

a. *Dry Sand:* We recommend the use of two target sets for this test, the first consisting of five Teflon right-circular cylinders, and the second consisting of five nylon right-circular cylinders. All should possess a diameter of 7.62 cm and a height of 2.54 cm. The targets should be buried such that the vector normal to the cylinders' flat surface subtends angles of 10°, 20°, 30°, 40°, and 50°, respectively, with respect to the vector normal to the air-earth interface plane. The targets should all be buried at a depth of 10 cm, measured from the uppermost point of each target, and should be positioned at least 1 m from a range boundary or any other target, again, depending on the results of the Sensor Active Envelope Test. Operating the detector according to the manufacturer's instructions, count and record the number of targets detected. The resulting scores for each set will have a range of 0 to 5, with 5 being perfect.

b. *Wet Clay/Loam:* Same as that for dry sand.

c. *Magnetite/Sand:* For the target orientation testing of metallic detectors we recommend the use of one target set, consisting of five lacquer-coated pure copper right-circular cylinders, all with a diameter of 3 mm and a height of 31.54 mm. The targets should be buried such that the vector normal to the

cylinders' flat surface subtends angles of 0°, 22.5°, 45°, 67.5°, and 90°, respectively, with respect to the vector normal to the air-earth interface plane. The same burial and testing procedures should be followed as those for the dry sand case described above.

(5) *Variations:* In addition to the targets recommended by NIST as a minimum set, the Army may wish to repeat this test with other targets of differing shape and/or constitutive EM properties.

C.7 Sensor Height Tests

(1) *Objective:* To determine the heights above the air-earth interface plane at which the detector sensor functions properly.

(2) *Requirements:* Bury a target, separated from any other targets in the surface plane by enough distance to ensure target isolation. The parameters that must be held constant for this test are target and soil constitutive EM properties, target burial depth, shape, volume, and orientation.

(3). *Restrictions:* This test is recommended only for hand-held detectors where normal operation would be expected to involve variations in the height of the sensor above the earth.

(4) *Recommended Techniques:*

a. *Dry Sand:* We recommend the use of two spherical targets for this test, one of Teflon and one of nylon, each with a diameter of 7.62 cm. The targets should be buried to a depth of 10 cm, measured from the top of each target. Each target should be positioned at least 1 m from a range boundary or any other target, again, depending on the results of the Sensor Active Envelope Test. Move the detector sensor along a straight line such that the center of the sensor moves over the center of the target. The height of the sensor must be at the optimal height recommended by the manufacturer, and must be kept constant above the surface of the earth. Verify that the detector detects the target. (If not, this test is complete and the detector's score for this test is zero.) Then, repeat the straight-line scan for increasing sensor heights of from 0.5 cm above the earth to the height at which detection ceases, in step sizes of 0.5 cm. Record the heights at which detection both commences and ceases, and then compute the height range for which detection is successful. Compute the score for the detector as follows: If the height range is less than or equal to 0.5 cm, the score is 0; if the range is between 0.5 cm and 1.0 cm, the score is 1; if the range is between 1 cm and 2 cm, the score is 2; if the range is between 2 cm and 4 cm, the score is 3; if

the range is between 4 cm and 8 cm, the score is 4; and if the range is greater than 8 cm, the score is 5. Thus, a score of 5 is considered perfect.

b. *Wet Clay/Loam:* Same as that for dry sand, above.

c. *Magnetite/Sand:* We recommend the use of two right-circular metallic cylinders for this test, one or pure copper and the other of Type 304 stainless steel. The copper target should have a height of 4.14 mm and a diameter of 8.28 mm, while the stainless steel target should have a height of 25.4 mm and a diameter of 1.5875 mm. Both should be buried in an upright orientation at a depth from the top of each target of 10 cm. Then, follow the procedure described for the dry sand/plastic targets, above.

(5) *Variations:* The Army may wish to perform these tests using additional targets to the ones NIST recommends. Also different target burial depths may be desired. And possibly, the Army may want to combine this test with the Sensor Active Envelope Test (VII.C.1) in order to measure an estimate for the three-dimensional sensor active area.

D Future Tests

In this section we describe, in general terms, a set of advanced tests which the Army may choose to develop and implement at a later date. For various reasons, stated in the test descriptions, they would be more difficult to implement than the core set of tests. Therefore, NIST recommends that the Army should develop the core set first, gain some months of experience in performing the core set, make modifications as necessary, and then consider adding more advanced tests.

D.1 Sensor Velocity Test

In order to determine the target detection sensitivity to variations in the velocity of the detector sensor, it may be desirable to develop a test for this. The test would consist of moving the sensor along a straight line over a buried target at varying velocities and determining the minimum and maximum velocities for which successful detection occurs. A raw score could then be derived as a function of the range of velocity for which the detector performs successfully. Detectors with a very narrow sensor velocity range would receive a lower score than those that exhibited a wider range. The reason that this test is more difficult to implement is that it would require an overhead positioning system that would be capable of moving the sensor over the earth at variable and known velocities.

D.2 Sensor Tilt Angle Tests

The sensor tilt angle test would involve moving the detector sensor along a straight line over a buried target with the sensor rotated to increasing angles about its horizontal axes. At minimum, the sensor would be rotated about both the x and y horizontal axes separately. The angle at which the detector no longer detects the target would then be recorded, indicating the detector's sensitivity to sensor tilt. There would almost certainly be a relationship between the results of this test and the Sensor Active Envelope and Sensor Height tests, all of which should yield a good estimate of the sensor's radiated EM beam pattern. This test would be more difficult to implement because it would also require an overhead positioning system.

D.3 Target Resolution Test

The objective of this test would be to measure the minimum distance between two buried targets for which the detector successfully detects the presence of each target, individually. The two targets need not be the same. This test would be designed to test for the possibility that, for example, a large anti-vehicle mine were buried close to a smaller anti-personnel mine. This two-target test would be more difficult to implement because of its spatial complexity and number of degrees of freedom.

D.4 Surface Clutter Tests

These tests would involve placing objects at or embedded in the air-earth surface above a buried target in order to test for the detector's ability to "see through" the surface object clutter and successfully detect the buried target. These objects could be, for example, pieces of rock, wood or other vegetation, and/or metal fragments, and they could be either uniform or random in both size and positioning. These tests also could involve simply varying the surface profile of the earth. The reasons that these tests are more difficult are that, first, there are practically an infinite number of possibilities for configuring the clutter, and, second, it would be difficult to maintain the exact configuration of the clutter over time. The use of the rigid-matrix brick approach, recommended by NIST in chapter V, would eliminate the latter difficulty because it would be possible to either glue or partially embed the clutter objects in one or more bricks.

D.5 Volume Clutter Tests

These tests would be very similar to the Surface Clutter Tests; the major difference is that the clutter object(s) would be completely buried in the medium in close proximity to the target. Again, such objects could be rocks, wood or other vegetation, and/or metal fragments.

D.6 Earth Stratification Test

These tests would be designed to measure the detector's ability to find targets when the constitutive EM properties of the soil are not constant functions of soil depth. This type of test may be considered a special case of the Volume Clutter Test. As one example of this type of test, a target could be buried in dry sand (relative dielectric constant = 2.70) at a depth of 10 cm, and in which a 1 cm layer of wet soil (relative dielectric constant = 10) is located between the air-earth surface and the target, say at a depth of 5 cm. The detector would then be operated according to the manufacturer's instructions to see if it could detect the target. The reasons that these tests are more difficult are, first, like all of the clutter tests, the number of possible tests is practically infinite, and second, this test is probably possible only if dry, granular soil simulations or rigid-matrix bricks are used for the soil medium.

D.7 False Alarm Tests

All of the tests presented so far have been some sort of measure of a detector's ability to detect targets. It may also be important to the Army to measure a detector's ability to avoid detecting innocuous objects that are buried in the earth. These tests would involve burying such objects as rocks, wood or other vegetation, and/or metal fragments, with no real targets present, to measure the detector's ability to differentiate between these objects and real targets. These tests would be more difficult to implement, again, because of the enormous number of innocuous objects that would need to be considered.

E Test Result Analysis

In this section a NIST-recommended method is presented for reducing the raw scores from each test performed into an overall score. This overall score for each detector will then allow the Army to rate competing detectors. It is important for the Army to understand that the soil and target standards, the core test instructions, and the following data reduction method, recommended by NIST, are as *objective* as possible. That is to say, if our recommendations are followed closely, then the score that each detector receives should be based on sufficiently accurate and precise measurements, and that score should be quite repeatable over time.

However, the *analysis* of the test results is necessarily a *subjective* task that only the Army can perform. As described below, we have attempted to build this subjectivity into the data reduction method in the form of *weighting factors*. In the process of the Army assigning numerical values to these weighting factors they will automatically be factoring in the relative importance to the Army of the results of each test. As an example of this process, the Army may decide that since a particular detector's ability to detect targets is strongly inhibited by the fact that the sensor height must be maintained within too small a range (say ±3 mm), it must assign a

lower overall score, even though this detector otherwise out-performs all other candidates. By a judicious choice of weighting factor values, this decision by the Army can be incorporated into the scoring method. NIST personnel, with their primary area of expertise lying in the area of electromagnetic measurements, are not as qualified as Army personnel to assign values to these subjective weighting factors.

By design, the raw scores that result from each of the core tests described in VII.C are in the form of positive integer numbers. If numerical weighting factors are assigned to each test then the raw score total for each detector may be expressed as

$$RST = \sum_{i=1}^{N} W_i S_i , \tag{7-1}$$

where RST is the raw score total, W_i is the weighting factor for the ith test, S_i is the positive integer score for that test, and N is the total number of tests performed. This raw score total may be normalized to cover the range 0 to 100 by the following,

$$NST = \frac{100.0}{RST_{MAX}} \sum_{i=1}^{N} W_i S_i \tag{7-2}$$

where NST is the normalized score total, and

$$RST_{MAX} = \sum_{i=1}^{N} W_i S_{i(MAX)} \tag{7-3}$$

where $S_{i(MAX)}$ are the maximum scores possible for each of the N tests.

As an example, assume that the tests described in VII.C.2 through VII.C.7 (dry and and wet clay/loam only) were performed on a detector with the following results.

Test No.	*Dry Sand Result*	*Perfect Score*	*Weighting Factor*	*Clay/Loam Result*	*Perfect Score*	*Weighting Factor*
C.2.	7	9	10	5	9	10
C.3.	5	6	5	4	6	5
C.4.	4	6	8	N/A	N/A	N/A
C.5.	5	5	3	5	5	3
C.6.	4	5	3	5	5	3
C.7.	4	5	7	3	5	7

N, the total number of tests is 11, and,

RST = 70 + 25 + 32 + 15 + 12 + 28 + 50 + 20 + 15 + 15 + 21

= 303.

RST_{MAX}, the maximum possible raw score, is

$$RST_{MAX} = 90 + 30 + 48 + 15 + 15 + 35 + 90 + 30 + 15 + 15 + 35$$
$$= 418.$$

Therefore, *NST*, the normalized score for this detector, is

$$NST = \frac{100}{418}(303) = 72.5.$$

This algorithm is open-ended and may be used for any number of tests, including non-EM based tests such as for ease of operation, detector mass, and battery life. It will always yield a score of between 0 and 100 so competing detectors will be compared on an equal footing as long as the same tests are performed on each detector in the same manner.

Another point that needs to be mentioned about this algorithm is that, in general, neither the tests themselves nor the weighting factors are required to be constants or linear functions; they may each be nonlinear. For example, the Target Depth Test, described in C.2, is inherently nonlinear because the increase in depth, from one target to the next, is not constant. Thus, there is not a linear relationship between a detector's numerical score for this test and the maximum depth at which it can detect targets. Similarly, the Army may wish to make one or more weighting factors a nonlinear function of the numerical score achieved. NIST's recommendation, for future test development, is for the Army to build desired nonlinearities into the tests, themselves, and to try to keep the weighting factors constant whenever possible.

References (VII)

[7.1] Brown, D.; Tanner, J. D.; Paca, F. B. Mine Detector Targets: Metallic and Nonmetallic, Generic Set, Development Efforts. Report No. VSE/ASD/0047-87/35RD, VSE Corporation, Alexandria, VA; 1987.

VIII Archival Record Requirements

As a part of this study, the Army has asked NIST to identify those data that should be permanently recorded for each test. We recommend that for each individual test the following items be recorded, on paper, into an electronic data base with backup, or both.

(1) The title of the test.
(2) The test date.
(3) The test start time.
(4) The test finish time.
(5) The test start ambient temperature to ±0.5°C.
(6) The test finish ambient temperature to ±0.5°C.
(7) The test start ambient relative humidity to ±5.0%.
(8) The test finish ambient relative humidity to ±5.0%.
(9) The test start barometric pressure to ±50 Pa.
(10) The test finish barometric pressure to ±50 Pa.
(11) The identification number(s) of the target(s) used.
(12) The identification number(s) of the soil medium or (media) used.
(13) The exact position of each target in the range (*x, y, z* coordinates.)
(14) The target(s) relative permittivity to ±5% (real) and ±10% (imaginary) from either NIST-supplied data (Teflon and nylon) or measured data.
(15) The target(s) relative permeability to ±5% (real) and ±10% (imaginary) from either NIST-supplied data (Teflon and nylon) or measured data.
(16) The soil medium (or media) relative permittivity to ±5% (real) and ±10% (imaginary) from measured data.
(17) The soil medium (or media) relative permeability to ±5% (real) and ±10% (imaginary) from measured data.
(18) All measured depths, angles, velocities, and so on, as appropriate for each test. (These variables must be kept as constant as possible.)
(19) The numerical values measured from the Sensor Active Envelope Test, both detection start and stop distances and their associated sensor rotation angles.
(20) The integer numerical score for the DUT for that test.
(21) The identity of the person(s) conducting the test.

In addition to this recorded data for each individual test, it is recommended that the Army keep a continuing record of test range data (Range Log). This log should be used to record all of the pertinent history of the range including the following.

(1) Dates and times of range usage.

(2) Identities of all persons using the range at those times.

(3) Dates and times of range parameter measurements, such as soil medium relative permittivity and permeability. (We recommend that they be measured and recorded at least monthly.)

(4) Numerical results of those measurements and measurement technique(s) and system(s) used, including relevant software.

(5) Identity of person(s) performing the range measurements.

(6) The dates, times, and exact nature of *all* modifications to the range.

(7) The identity of the person(s) performing those modifications.

(8) The dates, times, and exact nature of any accidents that occur which could conceivably change the range parameters.

(9) The dates, times, and exact nature of any electromagnetic interference (EMI) problems that are observed. (The sources of these problems should be located and eliminated as soon as possible.)

(10) Any other remarks that the range user believes are appropriate to maintaining the integrity of the range.

These are all of the data that NIST has been able to identify, both for individual tests and for overall range integrity. As experience is gained in utilizing the range, the Army may discover that there are other variables or facts that they wish to record. Space should be allowed, either on paper forms or within electronic data base fields, for additional data to be recorded in the future.

IX Conclusion

The first section of this chapter contains a brief summary of the key conclusions that NIST has drawn from our work for the Army from January 1, 1985 to December 31, 1990. In the second section, we present NIST's recommendations for the future work required in order for the Army to realize an actual, functional mine detector test range.

A Key Conclusions

There were three key tasks for which the U.S. Army Belvoir Research, Development, and Engineering Center requested NIST's assistance. Drawing upon NIST's expertise in electromagnetic measurements and metrology, they asked us to perform the following tasks:

1. Specify "standard" materials and configurations that the Army could use for test targets and background soil media for the laboratory testing of portable, electromagnetic-based mine detectors. The key objective was to specify target and soil standards that possess constitutive electromagnetic properties as close in values to actual mines and soil backgrounds as possible, and whose properties are well defined and stable over time.
2. Specify measurement methods for constitutive electromagnetic properties of the materials specified above, and measurement systems that the Army can use for periodically verifying the numerical values of those properties. The approximate accuracy of these measurements requested by the Army was ±10%.
3. Specify measurement methods for determining the performance effectiveness of portable, electromagnetic-based mine detectors in the laboratory.

Chapters V and VI contain our recommendations for soil standards and target standards, respectively. For the reasons stated there, we have recommended the use of Teflon and nylon spheres for standard targets which simulate plastic mines, and copper and stainless steel right-circular cylinders for standard targets which simulate mines containing metal. A small number of each of these standards has been fabricated at NIST and delivered to the Army. We have also recommended the use of rigid-matrix bricks, presently being designed by NIST and an outside contractor, as the optimum approach for realizing soil standards. For the reasons stated in chapter V, we believe that the rigid-matrix bricks will prove superior to natural soils, loose, granular mixture soil simulations, or liquid soil simulations. (The results of NIST's design efforts for rigid-matrix bricks will be presented to the Army in a separate report.)

Chapter III contains our recommendations for measurement methods and systems which the Army can use for periodically measuring the electromagnetic properties of relevant target and

soil materials. The methods and systems finally chosen by NIST possess state-of-the-art accuracy, and are commercially available, versatile, and easy to operate. These systems will be assembled and tested at NIST, and delivered to the Army upon manufacturer's delivery of the ordered equipment.

Chapter VI contains NIST's recommendations for a portable, electromagnetic-based mine detector test strategy. Briefly, this "eye-chart" strategy consists of designing objective tests that test for detector sensitivity to only one critical parameter at a time. For each test, all the critical parameters except the tested one are held as constant as possible. In the test range, each parameter is varied over a range of "easy" to "difficult" and the detector is scored on how many targets in each test it can detect. We have described in as much detail as possible seven "core" tests which clearly illustrate the test strategy, and which we recommend be implemented first. We then present, in less detail, seven "advanced" tests which we recommend that the Army implement later, after gaining experience from actual performance of the first set. Also presented in this chapter is a simple, objective algorithm which can be used to provide the Army an overall performance effectiveness rating for each tested detector.

B Recommendations for Future Work

With the information supplied in this report, the report on the rigid-matrix brick design, and the measurement systems, we believe that the Army's next effort should be devoted to actually implementing our recommendations for a mine detector test range. Practically all of the remaining work to be done to complete this range lies outside the primary area of expertise of NIST personnel. However, we present here a listing of the remaining tasks that we believe must be accomplished to realize this goal. This listing represents a phased approach with the objective of verifying the efficacy of each step before continuing on to the next step. In this manner, the maximum cost-effectiveness should be realized.

1. The Army should provide a temperature-controlled, relative humidity-controlled, and enclosed space for the construction of the first test range. We recommend that this first range be dedicated to the testing of mine detectors for plastic objects in a dry sand medium. Our reasons for this choice are that it provides a very difficult challenge for mine detectors and that it should be the easiest of the ranges to implement.
2. The Army should pursue the actual design of this range, using outside contractors as necessary. This design must include further studies on the optimal methods and configurations for the manufacture of rigid-matrix bricks, their placement and manipulation in the range, and the required range boundaries to minimize electromagnetic wave reflections. For this range, we recommend that the rigid-matrix

brick depth be at least 80 cm, and that the surface area be large enough to allow the positioning of at least 10 targets, each positioned at least 1 m from range side boundaries and from each other. As part of this design, we recommend that actual radiated electromagnetic field tests be performed on ensembles of bricks in order to determine the manufacturing methods and configuration which minimize unwanted wave reflections from brick surfaces. Also as part of this design process, manufacturing methods should be developed for embedding standard and other targets into the bricks.

3. Based on the actual design plans produced in Step 2, above, the Army should construct this range with the assistance of outside contractors, as necessary.
4. The Army should pursue the design of an accurate, three-dimensional, computer-controlled positioning system for installation above the rigid-matrix brick test range. Attaching detectors under test to this positioning system will allow much more accurate control of the detector motion during tests than if the detectors were to be human-operated. We recommend that the same computer system as that delivered to the Army as part of the measurement system be used for this automated positioning function.
5. Upon completion of the first test range construction, the Army should implement the seven "core" tests described in chapter VII of this report. It is anticipated that some experimentation will be required in order to optimize the range and step size of each of the critical measurement parameters.
6. After gaining experience with this range for a satisfactory time (perhaps one year), the Army should consider the design and construction of several other ranges, each one designed around a different set of realistic soil electromagnetic constitutive properties. We recommend that future test ranges should be designed and built, based on the information provided by NIST in this and the brick report, for the simulations of damp soils, salty wet soils, and magnetic soils as a minimum set.

X Glossary of Terms

The following is a selected alphabetized listing of terms used in this report. Whenever possible, the definitions have been taken from References [10.1] or [10.2].

clutter. Any deviation from geometric or material uniformity in the constitutive properties of the earth. Clutter will cause undesired scattering of radiated electromagnetic energy and may be caused by (1) an irregular (non-plane) air-earth surface profile or (2) any variations in the constitutive properties of the earth at or below the surface.

complex dielectric constant. The complex permittivity of a physical medium in ratio to the permittivity of free space [10.1].

complex conductivity. For isotropic media, at a particular point, and for a particular frequency, the ratio of the complex amplitude of the total electric current density to the complex amplitude of the electric field strength. **Note:** The electric field strength and total current density are both expressed as phasors, with the latter composed of the conduction current density plus the displacement current density [10.1].

complex permeability. For isotropic media, the ratio of the magnetic flux density to the magnetic field intensity. In anisotropic media, complex permeability becomes a matrix [10.1].

complex permittivity. For isotropic media the ratio of the electric flux density to the electric field, in which the displacement current density represents the total current density. **Note:** This term is used to describe both the conductive and dielectric properties of a medium [10.1].

conductivity (material). A factor such that the conduction-current density is equal to the electric-field intensity in the material multiplied by the conductivity. **Note:** In the general case it is a complex tensor quantity [10.1].

constitutive relations (radio wave propagation). Constraints imposed by the medium on the relationships between electric and magnetic field intensity vectors and their respective flux density vectors [10.1].

dielectric constant. That property which determines the electrostatic energy stored per unit volume for unit potential gradient [10.1].

dielectric loss tangent. A measure of the energy loss in a dielectric medium. It is expressed as $\tan\delta$ and is the power loss in the medium divided by its reactive power at a sinusoidal voltage of specified frequency.

magnetic susceptibility (isotropic medium). The (unitless) ratio of the magnetization to the magnetic field intensity.

mine. An encased explosive designed to destroy enemy personnel or equipment [10.2].

mine detector (electromagnetic). A device for the indication of the presence of mines that senses that presence by means of electromagnetic fields.

permeability. A general term used to express various relationships between magnetic flux density and magnetic field intensity. These relationships are either (1) absolute permeability, that in general is the quotient of a change in magnetic flux density divided by the corresponding change in magnetic field intensity: or (2) relative permeability, which is the ratio of the absolute permeability to the permeability of a vacuum.

permittivity. A general term used to express various relationships between electric flux density and electric field intensity. These relationships are either (1) absolute permittivity, that in general is the quotient of a change in electric flux density divided by the corresponding change in electric field intensity: or (2) relative permittivity, which is the ratio of the absolute permittivity to the permittivity of a vacuum.

sensor (test, measurement and diagnostic equipment). A transducer that converts a parameter at a test point to a form suitable for measurement by the test equipment [10.1].

standard (test, measurement and diagnostic equipment). A laboratory type device which is used to maintain continuity of value in the units of measurement by periodic comparison with a higher echelon or national standards. They may be used to calibrate a standard of lesser accuracy or to calibrate test and measurement equipment directly [10.1].

target (radar). (A) Specifically, an object of radar search or tracking; (B) Broadly, any discrete object which reflects energy back to the radar [10.1].

transducer. A device that is actuated by power from one system and supplies power in any other form to a second system [10.2].

References (X)

[10.1] Jay, F., Editor in Chief. IEEE Standard Dictionary of Electrical and Electronics Terms. ANSI/IEEE Std. 100-1984, Third Edition; 1984.

[10.2] Webster's Seventh New Collegiate Dictionary. G. & C. Merriam Company, Springfield, MA; 1967.

Appendix IV.A BASIC Program to Print Out Values of μ and ε

```
110!Last Revision August 7, 1987  11:21
115!This program calculates the relative mu and epsilon of a
116!     material from
120!S-parameter results obtained from the HP8510 network analyzer.
125!Written by Eric J. Vanzura (303) 497-5752   6/26/1987
130     GOSUB Init
135     GOSUB Load_matrix
140     GOSUB Calc_rotation
145     GOSUB Calc_dielectric
150     GOSUB Print_results
155     GOSUB Save_results
160     GOTO End
165!
170! ////////////////////////////////////////////////////////////
175!
180 Init:!
185     OUTPUT KBD USING "#,K";"SCRATCH KEY"&CHR$(255)&CHR$(69)
190     DEG
195     OPTION BASE 1
200     INTEGER I,J,Use_s11,Datacount,Bad_number
205     REAL Samplelength,L1,L2,Rot1,Rot2,Lairline,Test
210     DIM Test$[160]
215     Datacount=201
220     Samplelength=.095     !METERS
225     Lairline=.0994
230     L2=.002
235     L1=Lairline-Samplelength-L2
240     GOSUB Init_expt
245     ALLOCATE A(Datacount,9),B(Datacount,2),Lam0(Datacount),
                Prompt$[40],Id$[40]
250     ALLOCATE OPTION S11(Datacount),S12(Datacount),S21(Datacount),
                S22(Datacount)
255     ALLOCATE OPTION Gam1(Datacount),Gam2(Datacount),
        Gam(Datacount),K(Datacount),Lam(Datacount),T(Datacount)
260     ALLOCATE OPTION Mu(Datacount),Eps(Datacount)
265*
270     COM /Files/ Sourcedisk$[20],Diskout$[20],Diskdrive$[20],
        Filename$[10]
275     COM /Bugs/ INTEGER Bug1,Bug2,Bug3,Printer,Printer_on
280     Printer=701
285     Printer_on=0
290     Prty=VAL(SYSTEM$("SYSTEM PRIORITY"))+1
295     DISP CHR$(129);" DO YOU WANT TO USE (S11,S21) DATA OR
        (S22,S12) DATA? ";
300     DISP CHR$(128)
305     ON KEY 4 LABEL "S11,S21 DATA",Prty GOSUB Use_s11_yes
310     ON KEY 5 LABEL "S22,S12 DATA",Prty GOSUB Use_s11_no
315     Done=0
320     LOOP
325     EXIT IF Done
330     END LOOP
335     RETURN
340 !
```

```
355 Init_expt:!
360 Enter_datacount:OUTPUT KBD USING "#,K";Datacount
365    LINPUT "ENTER number of frequencies in datafile",Test$
370    CALL Test_real(Test,Test$,51.,401.,Bad_number)
375    IF Bad_number THEN GOTO Enter_datacount
380    Datacount=INT(Test)
385 Enter_airline:!
390    OUTPUT KBD USING "#,K";Lairline
395    LINPUT "ENTER length of airline (meters)",Test$
400    CALL Test_real(Test,Test$,.01,.5,Bad_number)
405    IF Bad_number THEN GOTO Enter_airline
410    Lairline=Test
415 Enter_sample:!
420    OUTPUT KBD USING "#,K";Samplelength
425    LINPUT "ENTER sample length (meters)",Test$
430    CALL Test_real(Test,Test$,.001,Lairline,Bad_number)
435    IF Bad_number THEN GOTO Enter_sample
440    Samplelength=Test
445 Enter_l1:!
450    OUTPUT KBD USING "#,K";L1
455    LINPUT "ENTER distance from Port 1 interface to
       sample (meters)",Test$
460    CALL Test_real(Test,Test$,0.,.5,Bad_number)
465    IF Bad_number THEN GOTO Enter_l1
470    L1=Test
475 Enter_l2:!
480    OUTPUT KBD USING "#,K";L2
485    LINPUT "ENTER distance from Port 2 interface to
       sample (meters)",Test$
486    CALL Test_real(Test,Test$,0.,.5,Bad_number)
490    IF Bad_number THEN GOTO Enter_l2
495    L2=Test
500    RETURN
505 !
510 ! ////////////////////////////////////////////////////////////
515 !
520 Use_s11_yes:OFF KEY
525    Use_s11=1
530    Done=1
535    RETURN
540 !
545 ! ////////////////////////////////////////////////////////////
550 !
555 Use_s11_no:OFF KEY
560    Use_s11=0
565    Done=1
570    RETURN
575 !
580 ! ////////////////////////////////////////////////////////////
585 !
590 Load_matrix:!
595    Prompt$="8510 S-PARAMETER DATA"
600    CALL Select_disk(Prompt$)
605    CALL Enterfilename("CAT",Prompt$)
610    IF Filename$="" THEN
```

```
615         CAT Diskdrive$
620         CALL Enterfilename("ABORT",Prompt$)
625         IF Filename$="" THEN
630             BEEP
635             DISP "PROGRAM ABORTED"
640             STOP
645         END IF
650     END IF
655     DISP CHR$(129);" GETTING DATA FROM DISK ";CHR$(128)
660     ASSIGN @Datapath TO Filename$&Diskdrive$
665     ENTER @Datapath;A(*)
670     ASSIGN @Datapath TO *
675     FOR I=1 TO Datacount
680*
685*
690*
695*
700     NEXT I
705     IF Printer_on THEN PRINTER IS Printer
710     PRINT "FREQ          S11            S21            S22
         S12"
715     FOR I=1 TO Datacount STEP INT(Datacount/10)
720         PRINT USING "2D.2D,4X,4(2(SD.3D),2X)";A(I,1),S11(I),
            S21(I),S22(I),S12(I)
725     NEXT I
730     PRINTER IS 1
735     RETURN
740 !
745 ! ////////////////////////////////////////////////////////////
750 !
755 Calc_rotation:!
760     DISP CHR$(129);" CALCULATING PHASE ROTATIONS L1=";L1;" ";
        CHR$(128)
765     FOR I=1 TO Datacount
770         Lam0(I)=.29979/A(I,1)     !METERS
775         Rot1=360*L1/Lam0(I)
780         Rot2=360*L2/Lam0(I)
785*
790*
795         S11(I)=S11(I)*(Phase1^2)
800         S21(I)=S21(I)*(Phase1*Phase2)
805         S12(I)=S12(I)*(Phase1*Phase2)
810         S22(I)=S22(I)*(Phase2^2)
815     NEXT I
820     DISP " S11 AND S22 SHOULD NOW BE VERY CLOSE TO EQUAL ";
              CHR$(128)
825     IF Printer_on THEN PRINTER IS Printer
830     PRINT "FREQ (GHz)         S11                S22
           S11-S22       ANGLE(S11-S22)"
835     FOR I=1 TO Datacount STEP INT(Datacount/30)
840*
845     NEXT I
846     PRINT " S11 AND S22 SHOULD NOW BE VERY CLOSE TO EQUAL ";
          CHR$(128)
850     PRINTER IS 1
```

```
855     RETURN
860 !
865 ! ////////////////////////////////////////////////////////
870 !
875 Calc_dielectric:!
880 Cd:!
885     DISP CHR$(129);" CALCULATING COMPLEX MU AND EPSILON ";
        CHR$(128)
890     FOR I=1 TO Datacount
895         IF Use_s11 THEN
900             K(I)=(S11(I)^2-S21(I)^2+1)/(2*S11(I))
905         ELSE
910             K(I)=(S22(I)^2-S12(I)^2+1)/(2*S22(I))
915         END IF
920*
925*
930         IF ABS(Gam1(I))<1 THEN
935             IF ABS(Gam2(I))<1 THEN
940                 BEEP
945                 DISP "GAM1(";I;") AND GAM2(";I;") ARE BOTH LESS
                        THAN 1 !?"
950                 PAUSE
955             ELSE
960                 Gam(I)=Gam1(I)
965             END IF
970         ELSE
975             IF ABS(Gam2(I))>1 THEN
980                 BEEP
985                 DISP "GAM1(";I;") AND GAM2(";I;") ARE BOTH
                        GREATER THAN 1 !?"
990                 PAUSE
995             ELSE
1000                Gam(I)=Gam2(I)
1005            END IF
1010        END IF
1015        IF Use_s11 THEN
1020        T(I)=(S11(I)+S21(I)-Gam(I))/(1-(S11(I)+S21(I))*Gam(I))
1025        ELSE
1030        T(I)=(S22(I)+S12(I)-Gam(I))/(1-(S22(I)+S12(I))*Gam(I))
1035        END IF
1040*
1045        Mu(I)=Lam0(I)*(1+Gam(I))/(Lam(I)*(1-Gam(I)))
1050        Eps(I)=Lam0(I)^2/(Lam(I)^2*Mu(I))
1055    NEXT I
1060    RETURN
1065!
1070! ////////////////////////////////////////////////////////
1075!
1080 Print_results:!
1085    Prty=VAL(SYSTEM$("SYSTEM PRIORITY"))+1
1090    DISP CHR$(129);" DO YOU WANT A PRINTOUT OF MU AND
        EPSILON DATA? ";CHR$(128)
1095    ON KEY 5 LABEL "PRINT TO SCREEN",Prty GOSUB Prnt_to_screen
1100    ON KEY 7 LABEL "PRINT TO PRINTER",Prty GOSUB Prnt_to_printer
1105    ON KEY 6 LABEL "NO",Prty GOSUB Done_return
```

```
1110    Done=0
1115    LOOP
1120    EXIT IF Done
1125    END LOOP
1130    OFF KEY
1135    RETURN
1140!
1145! ////////////////////////////////////////////////////////
1150!
1155 Prnt_to_screen:OFF KEY
1160    PRINTER IS 1
1165    GOSUB Prnt_results
1170    RETURN
1175!
1180! ////////////////////////////////////////////////////////
1185!
1190 Prnt_to_printer:OFF KEY
1195    PRINTER IS Printer
1200    GOSUB Prnt_results
1205    RETURN
1210!
1215! ////////////////////////////////////////////////////////
1220!
1225 Prnt_results:OFF KEY
1230    PRINT "Freq (GHz)   Mu                          Epsilon"
1235    IF Printer_on THEN
1240        FOR I=1 TO Datacount
1245            PRINT USING "2D.4D,2(4X,2(S3D.4D,2X))";A(I,1),
                            Mu(I),Eps(I)
1250        NEXT I
1255    ELSE
1260        FOR I=1 TO Datacount STEP INT(Datacount/20)
1265            PRINT USING "2D.4D,2(4X,2(S3D.4D,2X))";A(I,1),
                            Mu(I),Eps(I)
1270        NEXT I
1275    END IF
1280    PRINTER IS 1
1285    Done=1
1290    RETURN
1295!
1300! ////////////////////////////////////////////////////////
1305!
1310 Save_results:!
1315    FOR I=1 TO Datacount
1320        B(I,1)=A(I,1)
1325    NEXT I
1330    Prty=VAL(SYSTEM$("SYSTEM PRIORITY"))+1
1335    DISP "SAVE MU (PERMEABILTY) RESULTS?"
1340    ON KEY 5 LABEL "YES",Prty GOSUB Save_mu
1345    ON KEY 6 LABEL "NO",Prty GOSUB Done_return
1350    Done=0
1355    LOOP
1360    EXIT IF Done
1365    END LOOP
1370    OFF KEY
```

```
1375   DISP "SAVE EPSILON (PERMITTIVITY) RESULTS?"
1380   ON KEY 5 LABEL "YES",Prty GOSUB Save_eps
1385   ON KEY 6 LABEL "NO",Prty GOSUB Done_return
1390   Done=0
1395   LOOP
1400   EXIT IF Done
1405   END LOOP
1410   OFF KEY
1415   RETURN
1420!
1425! ////////////////////////////////////////////////////////
1430!
1435 Save_mu:OFF KEY
1440   Prompt$="REAL PART OF MU RESULTS"
1445   CALL Select_disk(Prompt$)
1450   IF Diskdrive$="NO DISK" THEN GOTO Save_im_mu
1455   Id$=""
1460   CALL Enter_id(Id$,Prompt$)
1465   IF Id$="" THEN GOTO Save_im_mu
1470   CALL Enterfilename("ABORT",Prompt$)
1475   IF Filename$="" THEN GOTO Save_im_mu
1480   FOR I=1 TO Datacount
1485*
1490   NEXT I
1495   CALL Save_file(B(*),Datacount,Id$)
1500   PRINT "REAL PART OF MU SAVED"
1505 Save_im_mu:!
1510   Prompt$="IMAGINARY PART OF MU RESULTS"
1515   !CALL Select_disk(Prompt$)
1520   IF Diskdrive$="NO DISK" THEN GOTO Save_mu_rtn
1525   !Id$=""
1530   !CALL Enter_id(Id$,Prompt$)
1535   IF Id$="" THEN GOTO Save_mu_rtn
1540   CALL Enterfilename("ABORT",Prompt$)
1545   IF Filename$="" THEN GOTO Save_mu_rtn
1550   FOR I=1 TO Datacount
1555*
1560   NEXT I
1565   CALL Save_file(B(*),Datacount,Id$)
1570   PRINT "IMAGINARY PART OF MU SAVED"
1575 Save_mu_rtn:Done=1
1580   RETURN
1585!
1590! ////////////////////////////////////////////////////////
1595!
1600 Save_eps:OFF KEY
1605   Prompt$="REAL PART OF EPSILON RESULTS"
1610   !CALL Select_disk(Prompt$)
1615   IF Diskdrive$="NO DISK" THEN GOTO Save_im_eps
1620   !Id$=""
1625   !CALL Enter_id(Id$,Prompt$)
1630   IF Id$="" THEN GOTO Save_im_eps
1635   CALL Enterfilename("ABORT",Prompt$)
1640   IF Filename$="" THEN GOTO Save_im_eps
1645   FOR I=1 TO Datacount
```

```
1650*
1655    NEXT I
1660    CALL Save_file(B(*),Datacount,Id$)
1665    PRINT "REAL PART OF EPSILON SAVED"
1670 Save_im_eps:!
1675    Prompt$="IMAGINARY PART OF EPSILON RESULTS"
1680    !CALL Select_disk(Prompt$)
1685    IF Diskdrive$="NO DISK" THEN GOTO Save_ep_rtn
1690    !Id$=""
1695    !CALL Enter_id(Id$,Prompt$)
1700    IF Id$="" THEN GOTO Save_ep_rtn
1705    CALL Enterfilename("ABORT",Prompt$)
1710    IF Filename$="" THEN GOTO Save_ep_rtn
1715    FOR I=1 TO Datacount
1720*
1725    NEXT I
1730    CALL Save_file(B(*),Datacount,Id$)
1735    PRINT "IMAGINARY PART OF EPSILON SAVED"
1740 Save_ep_rtn:Done=1
1745    RETURN
1750!
1755! ////////////////////////////////////////////////////////////
1760!
1765 Done_return:!
1770    Done=1
1775    RETURN
1780!
1785! ////////////////////////////////////////////////////////////
1790!
1795 End:!
1796    DISP "Program finished. Have a nice day."
1800    END
1805!
1810! ************************************************************
1815!
1820    SUB Enterfilename(Ac$,OPTIONAL Prompt$)
1825 Enterfilename:      !
1830        COM /Files/ Sourcedisk$,Diskout$,Diskdrive$,Filename$
1835        INTEGER I,Ascii_num
1840        DIM Test$[160]
1845        SELECT NPAR
1850        CASE 1
1855            DISP " ENTER the FILE NAME ";
1860        CASE 2
1865            DISP " ENTER the FILE NAME for ";Prompt$;
1870        END SELECT
1875        SELECT Ac$
1880        CASE "CAT"
1885            DISP " ... (ENTER alone to CAT) ";
1890        CASE "ABORT"
1895            DISP " ... (ENTER alone to ABORT) ";
1900        CASE "VALID"
1905        END SELECT
1910        LINPUT Test$
1915        Test$=TRIM$(Test$)
```

```
1920        IF LEN(Test$)=0 THEN
1925            SELECT Ac$
1930            CASE "VALID"
1935                DISP "You MUST enter the FILE NAME now."
1940                BEEP
1945                WAIT 1.8
1950                GOTO Enterfilename
1955            CASE "ABORT","CAT"
1960                GOTO Abortline
1965            CASE ELSE
1970                DISP "Ac$=";Ac$;" in SUB Enterfilename"
1975                BEEP
1980                PAUSE
1985            END SELECT
1990        END IF
1995        IF LEN(Test$)>10 THEN
2000            BEEP
2005            DISP "ERROR in NAME ENTRY--up to 10 chars, you have ";
2010            DISP LEN(Test$);" "
2015            WAIT 1.8
2020            OUTPUT 2 USING "#,K,K";"?#";Test$
2025            GOTO Enterfilename
2030        END IF
2035        Filename$=Test$
2040        FOR I=1 TO LEN(Filename$)
2045            Ascii_num=NUM(Filename$[I])
2050            SELECT Ascii_num
2055            CASE 65 TO 90,95,97 TO 122,48 TO 57
2060                !Allowed characters
2065            CASE ELSE
2070                BEEP
2075                DISP "ERROR in NAME ENTRY--ILLEGAL CHARACTERS,
                          TRY AGAIN."
2080                WAIT 1.8
2085                OUTPUT 2 USING "#,K,K";"?#";Filename$
2090                GOTO Enterfilename
2095            END SELECT
2100        NEXT I
2105        SUBEXIT
2110 Abortline:Filename$=""
2115        SUBEXIT
2120    SUBEND
2125    !
2130    ! ************************************************************
2135    !
2140    SUB Select_disk(OPTIONAL Prompt$)
2145 Select_disk:OFF KEY
2150        COM /Files/ Sourcedisk$,Diskout$,Diskdrive$,Filename$
2155        INTEGER Prty
2160        Prty=VAL(SYSTEM$("SYSTEM PRIORITY"))+1
2165        IF NPAR=1 THEN
2170            DISP " SELECT DISK DRIVE for ";Prompt$;" ... NO
                      DISK to abort. "
2175        ELSE
2180            DISP " SELECT DISK DRIVE .... NO DISK to abort. "
```

```
2185        END IF
2190        ON KEY 0 LABEL "NO DISK",Prty GOSUB No_disk
2195        ON KEY 1 LABEL "9133H  V0 ^V1",Prty GOSUB Hard9133h0
2200        ON KEY 11,Prty GOSUB Hard9133h1
2205        ON KEY 2 LABEL "9133H  Floppy",Prty GOSUB Floppy9133h
2210        ON KEY 3 LABEL "9133XV Hard",Prty GOSUB Hard9133xv
2215        ON KEY 4 LABEL "9133XV Floppy",Prty GOSUB Floppy9133x
2220        IF Sys_id$[1,4]<>"S300" THEN
2225        ON KEY 5 LABEL "LEFT Internal",Prty GOSUB Left_internal
2230        ON KEY 6 LABEL "RIGHT Internal",Prty GOSUB Right_internal
2235        END IF
2240        ON KEY 7 LABEL "9125   Floppy",Prty GOSUB Floppy9125
2245        ON KEY 8 LABEL "9122   Left",Prty GOSUB Floppy9122l
2250        ON KEY 9 LABEL "9122   Right",Prty GOSUB Floppy9122r
2255        LOOP
2260        EXIT IF Done
2265        END LOOP
2270        SUBEXIT
2275 Left_internal:Diskdrive$=":HP9153,700,0"
2280        GOTO Diskselected
2285 Right_internal:Diskdrive$=":INTERNAL,4,0"
2290        GOTO Diskselected
2295 Hard9133xv:Diskdrive$=":HP9133,700,0"
2300        GOTO Diskselected
2305 Floppy9133x:Diskdrive$=":HP9133,702,0"
2310        GOTO Diskselected
2315 Hard9133h0:Diskdrive$=":,700,0,0"
2320        GOTO Diskselected
2325 Hard9133h1:Diskdrive$=":,700,0,1"
2330        GOTO Diskselected
2335 Floppy9133h:Diskdrive$=":,700,1"
2340        GOTO Diskselected
2345 Floppy9122r:Diskdrive$=":,707,1"
2350        GOTO Diskselected
2355 Floppy9122l:Diskdrive$=":,707,0"
2360        GOTO Diskselected
2365 Floppy9125:Diskdrive$=":,704,0"
2370        GOTO Diskselected
2375 No_disk:Diskdrive$="NO DISK"
2380 Diskselected:OFF KEY
2385        Done=1
2390        RETURN
2395   SUBEND
2400   !
2405   ! ***************************************************8
2410   !
2415    SUB Enter_id(Id$,OPTIONAL Return_test$)
2420 Enter_id:!
2425    !
2430   !LAST REVISION  30/SEPT/86
2435        OPTION BASE 1
2440        COM /Bugs/ INTEGER Bug1,Bug2,Bug3,Printer,Printer_on
2445    !
2450        DIM Test$[160]
2455        INTEGER N
```

```
2460        N=LEN(Id$)
2465        Test$=Id$
2470        SELECT Id$
2475        CASE ""
2480            !OUTPUT NOTHING
2485        CASE ELSE
2490            OUTPUT 2 USING "K,#";Test$
2495        END SELECT
2500        SELECT NPAR
2505        CASE 1    !NO Return_test$ given
2510        DISP CHR$(129);"Please ENTER a description (<= 40 chrs).";
2515        DISP CHR$(128);
2520        CASE ELSE
2525        DISP CHR$(129);"Please ENTER a description (<= 40 chrs) ";
2530        DISP CHR$(128);
2535            SELECT Return_test$
2540            CASE Id$
2545                DISP " for THIS ID";
2550            CASE "ABORT"
2555                DISP " CLR LN/ ENTER to ABORT."
2560            CASE ELSE
2565                DISP " for ";Return_test$;
2570            END SELECT
2575        END SELECT
2580        LINPUT Test$
2585        DISP ""
2590        Test$=TRIM$(Test$)
2595        N=LEN(Test$)
2600        SELECT N
2605        CASE >40
2610        DISP "Length of data_id$ too long. You entered ";N;
2615        DISP " characters. Try again."
2620            BEEP
2625            WAIT 1.5
2630            IF NPAR=2 THEN
2635                IF Id$<>Return_test$ THEN
2640                    OUTPUT 2 USING "#,K";Test$
2645                END IF
2650            END IF
2655            GOTO Enter_id
2660        CASE =0
2665            IF NPAR>1 THEN
2670                IF Return_test$="ABORT" THEN
2675                    Id$=Test$   !=""
2680                    SUBEXIT
2685                END IF
2690            END IF
2695            DISP "You must ENTER SOMETHING or you'll ";
2700            DISP "never get out of this."
2705            BEEP 1000,.3
2710            WAIT 1.8
2715            GOTO Enter_id
2720        CASE ELSE
2725             !Everything ok
2730        END SELECT
```

```
2735        Id$=Test$
2740    SUBEND
2745 !
2750 ! ************************************************
2755 !
2760    SUB Save_file(T_f(*),INTEGER Datacount,Id$)
2765 Save_file:   !
2770        COM /Files/ Sourcedisk$,Diskout$,Diskdrive$,Filename$
2775        ON ERROR CALL Errortrap
2780        Diskspace=INT((3500+(Datacount*16))/256)+1
2785        CREATE BDAT Filename$&Diskdrive$,Diskspace,256
2790!       CREATE ASCII Filename$&Diskdrive$,Diskspace*2
2795        ASSIGN @Datapath TO Filename$&Diskdrive$
2800        OUTPUT @Datapath;"N"
2805        OUTPUT @Datapath;TRIM$(Id$)
2810        OUTPUT @Datapath;Datacount
2815        OUTPUT @Datapath;Datacount
2820        OUTPUT @Datapath;T_f(*)
2825        ASSIGN @Datapath TO *
2830        OFF ERROR
2835    SUBEND
2840!
2845! ********************************************************
2850!
2855    SUB Errortrap
2860 Errortrap:       !Trap disk errors here
2865        COM /Files/ Sourcedisk$,Diskout$,Diskdrive$,Filename$
2870        DIM File$[20],Test$[160],What$[20],Ac$[5]
2875        BEEP 400,.6
2880        SELECT ERRN
2885        CASE 54
2890            DISP "DUPLICATE FILE NAME:  ";Filename$;
2895            DISP "....PURGE old one? (Y/N)";
2900            LINPUT What$
2905            SELECT What$[1,1]
2910            CASE "Y","y"
2915                PURGE Filename$&Diskdrive$
2920            CASE ELSE
2925                Ac$="VALID"
2930                Prompt$=""
2935                CALL Enterfilename(Ac$)
2940            END SELECT
2945        CASE 52,53
2950            DISP "Improper FILE NAME --- ENTER NEW FILE NAME";
2955            OUTPUT 2 USING "#,K,K";"?#";Filename$
2960            LINPUT Filename$
2965            Filename$=TRIM$(Filename$)
2970        CASE 56
2975            DISP "FILE:  ";Filename$;" is not on this disk,
                      please insert";
2980            DISP " correct disk"
2985            PAUSE
2990        CASE 64
2995            DISP "This disk is full, PLEASE insert clean disk"
3000            PAUSE
```

```
3005        CASE 56
3010            DISP "DATA INPUT disk must be in drive!!  ";
3015            DISP "...CONTINUE when ready."
3020            PAUSE
3025        CASE 72,73,76
3030            DISP Diskdrive$;
3035            DISP " is not available, type correct";
3040            DISP " unit specifier (ie. ':,707,0').";
3045            OUTPUT 2 USING "K,#";Diskdrive$
3050            LINPUT Diskdrive$
3055        CASE 80
3060            DISP "CHECK DISK drive door!"
3065            PAUSE
3070        CASE ELSE
3075            DISP ERRM$;" 'CONTINUE' when fixed"
3080            PAUSE
3085        END SELECT
3090        DISP CHR$(12)
3095        SUBEXIT
3100    SUBEND
3105    !
3110    ! ********************************************************
3115    !
3120    SUB Test_real(Test,Test$,Low,High,INTEGER Bad_number)
3125 Test_real:!
3130        Bad_number=0
3135        ON ERROR GOSUB Trap_bad_number
3140        IF Bad_number THEN RETURN
3145        Test=VAL(TRIM$(Test$))
3150        OFF ERROR
3155        SELECT Test
3160        CASE <Low
3165            BEEP 1000,.3
3170            DISP " Number entered is TOO LOW. ";
3175            DISP " LOWEST allowable number is ";Low
3180            WAIT 2.1
3185            Bad_number=1
3190        CASE >High
3195            BEEP 1000,.3
3200            DISP " Number entered is TOO HIGH. ";
3205            DISP " HIGHEST allowable number is ";High
3210            WAIT 2.1
3215            Bad_number=1
3220        CASE ELSE
3225            Bad_number=0
3230     ! Number within limits
3235        END SELECT
3240        SUBEXIT
3245!
3250! ////////////////////////////////////////////////////////
3255 !
3260 Trap_bad_number:!
3265        SELECT ERRN
3270        CASE 15,32
3275  DISP CHR$(129);"What you ENTERED is not a number! Try again. ";
```

```
3280            DISP CHR$(128)
3285            Bad_number=1
3290            WAIT 1.7
3295            LINPUT "Please ENTER the number you wish",Test$
3300        CASE ELSE
3305            DISP ERRN,ERRM$
3310            BEEP 850,.5
3315            Bad_number=1
3320            PAUSE
3325        END SELECT
3330        RETURN
3335    SUBEND
```

Appendix IV.B: Automatic Network Analyzer System for Measuring ε and μ

The ANA approach is based on measuring reflection S_{11} and transmission S_{21} from and through a section of material-filled air line. These S parameters are then mathematically inverted to determine ε and μ. The analysis is straightforward and is repeated here for convenience. We follow the notation used in [3.30].

In terms of the normal plane-wave reflection (Γ) and transmission (T) coefficients, S_{11} and S_{21} are given by

$$S_{11}(\omega) = \frac{(1-T^2)\Gamma}{1-T^2\Gamma^2}, \tag{4B.1}$$

and

$$S_{21}(\omega) = \frac{(1-\Gamma^2 T)}{1-T^2\Gamma^2}$$

where

$$\Gamma = \frac{Z - Z_0}{Z + Z_0}, \tag{4B.2}$$

and

$$T = e^{-\gamma d}.$$

Inverting eq (4B.1) yields

$$\Gamma = K \pm (K^2 - 1), \tag{4B.3}$$

where

$$K = \frac{\left[S_{11}^2(\omega) - S_{21}^2(\omega)\right] + 1}{2S_{11}(\omega)}, \tag{4B.4}$$

and

$$T = \frac{\left[S_{11}(\omega) - S_{21}(\omega)\right] - \Gamma}{1 - \left[S_{11}(\omega) + S_{21}(\omega)\right]\Gamma}.$$

We find that

$$\mu_r/\varepsilon_r = \left(\frac{1+\Gamma}{1-\Gamma}\right)^2 = x\,, \tag{4B.5}$$

and

$$\mu_r\varepsilon_r = \left[\frac{1}{k_0 d}\ell n\left(\frac{1}{T}\right)\right]^2 = y\,, \tag{4B.6}$$

It follows that

$$\varepsilon_r = (y/x)^{1/2}, \tag{4B.7}$$

and

$$\mu_r = (yx)^{1/2}.$$

Bibliography

Afsar, M. N.; Birch, J. R.; Clarke, R. N. The measurement of properties of materials. Proc. IEEE; 1986; 74(l), pp. 183-199.

Akimoto, S. Magnetic properties of ferromagnetic oxide minerals as a basis of rock magnetism. Adv. Phys.; 1957; 6(288).

Alvarez, R. Complex dielectric permittivity in rocks: A method for its measurement and analysis. Geophysics. 38: 920-940; 1973.

Barringer, A. R. The use of audio and radio frequency pulses for terrain sensing. Proc., 2nd Symposium on Remote Sensing of Environment, Center for Remote Sensing Information and Analysis, Willow Run Laboratories; University of Michigan; 1963: 201–214.

Barsis, A. P. Performance predictions for single tropospheric communication links and for several links in tandem. International Radio Consultative Committee worldwide minimum external noise levels, 0.1 Hz to 100 GHz; 1983. Report No. 3220-2.

Barsis, A. P.; Norton, K. A.; Rice, P. L.; Elder, P. H. Performance predictions for single tropospheric communication links and for several links in tandem; 1961; Nat. Bur Stand. (U.S.) Tech. Note 102.

Beckman, P. Probability in communication engineering. New York, NY: Harcourt, Brace and World, Inc.; 1967

Bethe, H. A.; Schwinger, J. Perturbation theory of resonant cavities; 1943; NDRC, Rpt. D2-117.

Birnbaum, G.; Franeau, J. Measurement of the dielectric constant and loss of solids and liquids by a cavity perturbation method. J. Appl. Phys.; 1949; 20, pp. 817-818.

Bockris, J.; Gileady, E.; Huller, K. Dielectric relaxation in the electric double layer. J. Chem. Physics. 44: 1445-1456; 1966.

Bose, T. K.; Bottreau, A. M.; Chahine, R. Development of a dipole probe for the study of dielectric properties of biological substances in radiofrequency and microwave region with time-domain reflectometry. IEEE Trans. Instrum. Meas.; 1986; IM-35 (1), pp. 56-60.

Bottcher, C.J.F. Theory of electric polarization. Amsterdam: Elsevier; 1952.

Bottreau, A. M.; Dutuit, Y.; Moreau, J. On a multiple reflection time domain method in dielectric spectroscopy: Application to the study of some normal primary alcohols. J. Chem. Phys.; 1977; 66(8), pp. 3331-3336.

Broadhurst, M. G.; et al. A dielectric phantom material for electromagnetic radiation; 1986; NBS Report for the Div. of Medical Engineering, Center for Devices and Radiological Health, Food and Drug Administration; 60 p.

Brown, D.; Tanner, J. D.; Paca, F. B. Mine Detector Targets: Metallic and Nonmetallic, Generic Set, Development Efforts. Report No. VSE/ASD/0047-87/35RD, VSE Corporation, Alexandria, VA, 1987.

Brumley, S. A.; et al. Far field electromagnetic principles applied to mine detection. U.S. Army Belvoir R & D Center, Contract No. DAAK 70-86-C-0072; June, 1987; Final Report.

Burrell, G. A.; Munk, B. A. The array scanning method and applying it to determine the impedance of linear antennas in a lossy half space. The Ohio State University ElectroScience Lab. Dept. of Electrical Engineering (prepared under Contract DAAG53-76-C-0179 for U.S. Army Mobility Equipment Research and Development Command, Ft. Belvoir, VA 22060); Technical Report 4460-1.

Burrell, G. A.; Peters, Jr., L.; Terzuoli, Jr., A. J. The propagation of electromagnetic video pulses with application to subseurface radar for tunnel application. The Ohio State University ElectroScience Lab. Dept. of Electrical Engineering (prepared under Contract DAAG53-76-C-0179 for U.S. Army Mobility Equipment Research and Development Command, Ft. Belvoir, VA 22060); Technical Report 4460-2.

Burrell, G. A.; Peters, Jr., L. Pulse propagation in lossy media using the low-frequency window for video pulse radar application. Proc. IEEE 67: 1979; No. 7.

Burrell, G. A.; Richmond, J. H.; Peters, Jr., L.; Tran, H. B.; Acoustic, electromagnetic and elastic wave scattering—Focus on T-matrix approach. A scattering model for detection of tunnels using video pulse radar in systems. New York, Pergamon Press; 1979: 667–683.

Bussey, H. E. Dielectric measurements in a shielded open circuit coaxial line. IEEE Trans. Instrum. Meas.; 1980; IM-29(2), pp. 120-124.

Bussey, H. E. Measurement of RF properties of materials: a survey. Proc. IEEE; 1967; 55, pp. 1046-1053.

Bussey, H.E. International comparison of complex permittivity measurement at 9 GHz. IEEE Trans. Instrum. Meas. IM-23(3): 235-239; 1974.

Bussey, H.E.; Gray, J.E.; Bamberger, E.C.; Rushton, E.; Russel, G.; Petley, B.W.; Morris, D. International comparison of dielectric measurements. IEEE Trans. Instrum. Meas. IM-13: 305-311; 1964.

Caldecott, R.; et al. A radio frequency probe to measure solid electrical parameters; January 22, 1985; Final Report 715616-4; Ohio State University ElectroScience Lab., Columbus, Ohio.

Chan, L. C. Subsurface electromagnetic target characterization and identification. The Ohio State University; 1979; Ph.D. dissertation.

Chan, L.C.; Moffat, D. L.; and Peters, Jr., L. A characterization of subsurface radar targets. Proc. IEEE 67; 1979; No. 7: 991–1001.

Chan, L.C.; Moffat, D. L.; and Peters, Jr., L. Estimation of the complex natural resonances from a class of subsurface targets. Acoustic, electromagnetic, and elastic wave scattering—focus on T-matrix approach. New York: Pergamon Press; 1979: 453–463.

Chan, L.C.; Moffat, D. L.; and Peters, Jr., L. Improved performance of a subsurface radar target identification system through antenna design. IEEE Trans. Ant. Prop.; 1981; AP-29 (No. 2): 307–312.

Chan, L.C.; Moffat, D. L.; and Peters, Jr., L. Subsurface radar target imaging estimates. IEEE Trans. Ant. Prop.; 1981; AP-29 (No. 2); 413–418.

Chan, L. C.; Peters, L., Jr. Subsurface electromagnetic mine detection and identification; 1978; Technical Report, Department of the Army, U.S. Army Mobility Equipment Research and Development Command, Fort Belvoir, VA; 76. p.

Clark, S.P. Handbook of physical constants. Geol. Soc. Amer. Memoir 97, 587 p.; 1966.

Cohn, G. I. Low frequency electromagnetic induction techniques; 1973; Tech. Essays, Army Countermine Study Report.

Cole, K.S.; Cole, R.H. Dispersion and absorption in dielectrics. J. Chem. Physics. 9: 341-351; 1941.

Cole, R. H. Evaluation of dielectric behavior by time domain spectroscopy. I. Dielectric response by real time analysis. J. Phys. Chem.; 1975; 79 (14), pp. 1459-1469.

Cole, R. H. Evaluation of dielectric behavior by time domain spectroscopy. II. Complex permittivity. J. Phys. Chem.; 1975; 79 (14), pp. 1469-1474.

Cole, R H.; Berberian, J. G.; Mashimo, S; Chryssikos, G.; Burns, A.; Tombari, E. Time domain reflection methods for dielectric measurements to 10 GHz. J. Appl. Phys.; 1989; 66 (2), pp. 793-802.

Cole, R. H.; Mashimo, S.; Winsor, P., IV. Evaluation of dielectric behavior by time domain spectroscopy. 3. Precision difference methods. J. Phys. Chem.; 1980; 84 (7), pp. 786-793.

Collie, C.H., Ritson, D.M. and Hasted, J.B. J. Chem. Phys., 16(1); 1948.

Conbau, G.; Schwering, F. On the guided propagation of electromagnetic wave beams. IRE Trans.; 1961; AP-9, pp. 248-256.

Cook, R. J. Microwave cavity methods, in high frequency dielectric measurements; 1973; J. Chamberlain and G. W. Chantry, ed., IPC Science & Technology Press, pp. 12-27.

Cook, R. J.; Jones, R. G.; Rosenberg, C. R. Comparison of cavity and open resonator measurements of permittivity and loss angle at 35 GHz. IEEE Trans. Instrum. Meas.; 1974; IM-23, pp. 438-442.

Crispin, J. W.; Siegel, K. M. Methods of radar cross-section analysis. New York, NY: Academic Press; 1968.

Cullen, A. L.; Nagenthiram, P.; Williams, A. D. A variational approach to the theory of the open resonator. Proc. R. Soc. A.; 1972; 329, pp. 153-169.

Cullen, A. L.; Nagenthiram, P.; Williams, A. D. Improvement in open resonator permittivity measurement. Electron. Letters; 1972; Vol. 8, pp. 577-579.

Cullen, A. L.; Yu, P. K. The accurate measurement of permittivity by means of an open resonator. Proc. R. Soc. A; 1971; 325, pp. 493-509.

Culshaw, W.; Anderson, M. V. Measurement of permittivity and dielectric loss with a millimeter wave Fabry-Perot interferometer. Proc. IEEE; 1962; 109(B), Suppl. 23, pp. 820-826.

Dalton, F. N.; et al. Time-domain reflectometry: Simultaneous measurement of soil water content and electrical conductivity with a single probe. Science; June 1, 1984; 224, pp. 989-990.

Davenport, W. B.; Root, W. L. Random signals and noise. New York, NY: McGraw-Hill Book Co.; 1970.

David, J. L. Relative permittivity measurements of a sand and clay soil *in situ*. Geological Survey of Canada; 1975; Paper 75-1C: 361–363.

Davidson, D.W.; Cole, R.H. Dielectric relaxation in glycerol, propylene glycol, and n-propanol. J. Chem. Phys. 29: 1484-1490; 1951.

Davis, C. W.; Peters, Jr., L. Characteristics of a video pulse radar system operating in the high-frequency window at the Hazel A. mine near Gold Hill, Colorado. The Ohio State University ElectroScience Lab., Dept. of Electrical Engineering; 1979; Technical Report 784460-8.

Davis, C. W.; Peters, Jr., L. Application of a video pulse radar system to detect tunnels at the Curtis School Yard in Trumbull County, Ohio. The Ohio State University ElectroScience Lab., Dept. of Electrical Engineering; 1979; Technical Report 78440-7.

Davis, III, G. W. A computational model for subsurface propagation and scattering for antennas in the presence of a conducting half space. The Ohio State University ElectroScience Lab., Dept. of Electrical Engineering; 1979; Technical Report 479X-7.

Davis, J. L.; Topp, G. C.; Omran, O. P. Measuring soil water content *in situ* using time-domain reflectometry techniques. Geological Survey of Canada; 1977: Paper 77-1B; 33–36.

Debye, P. and Huckel, E.Z., Z. Phys. 24: 133, 305; 1923.

Debye, P. Polar molecules. Dover Publications: New York; 1929.

Debye, P. Polar molecules. New York, NY: Chemical Catalog Co.; 1899.

Degenford, J. A quasi-optic technique for measuring dielectric loss tangents. IEEE Trans. Instrum. Meas.; 1968; IM-17, pp. 413-417.

Degenford, J.; Coleman, P. D. A quasi-optics perturbation technique for measuring dielectric constants. Proc. IEEE; 1966; 54, pp. 520-522.

Dines, A.; Lytle, R. J. Computerized geophysical tomography. Proc. IEEE; 1979; 67: No. 7.

Dobson, M.C.; Ulaby, F.T.; Hallikainen, M.T.; El-Rayes, M.A. Microwave dielectric behavior of wet soil, Part II: Dielectric mixing models. IEEE Trans. Geosci. Remote Sensing. GE-23(1): 35-46; 1985.

Dukhin, S.S. Dielectric properties of disperse systems, in Surface and colloid science, Vol. 3, Matijevic, E., ed. New York, NY: Wiley Interscience, 83-166; 1969.

Falls, Bernard, A. Apparatus for measuring the electromagnetic impedance of soils; 1977.

Fall, R. A.; et al. EM soil properties in the VHF/UHF range. U.S. Army R & D Center; May 1972; Report 2030.

Fellner-Feldegg, H. The measurement of dielectrics in the time domain. J. Phys. Chem.; 1969; 73 (3), pp. 616-623.

Fountain, L. S. Evaluation of the EM properties of soil materials; December 1984; Final Report, VSE Corp., Alexandria, VA.

Gabillard, R.; Degauge, P.; Wait, J. R. Subsurface electromagnetic telecommunication—review. IEEE Trans. Communication Technology; Com-19: 1217–1228.

Gans, W. L.; Andrews, J. R. Time-domain automatic network analyzer for measurement of rf and microwave components; 1975; Nat. Bur. Stand. (U.S.) Tech. Note 672; 1975 September. 165 p.

Gans, W. L.; Geyer, R. G.; Klemperer, W. K. Suggested Methods and Standards for Testing and Verification of Electromagnetic Buried Object Detectors. National Institute of Standards and Technology NISTIR 89-3915R; 1990.

Gelegnse, M.; Barringer, A. R. Recent progress in remote sensing with audio and radio frequency pulses. Proc., 3rd Annual Symp. on Remote Sensing of the Environment; 469–494.

Geyer, R. G. Noise factor for mine detection systems: A performance measure; 1987; Report to U.S. Army Belvoir Research and Development Center, Fort, Belvoir.

Geyer, R. G. Suggested experimental parameters for land-mine detection performance evaluations; 1987; Report to U.S. Army Belvoir Research and Development Center, Fort Belvoir, VA 22060-5606. Project No. 7232457.

Geyer, R.G. Experimental parameters for land mine detection performance evaluations. NIST Report, Project 7232457, 100 p.; November 1987.

Geyer, R.G. Experimental parameters for land mine detection performance evaluations. NIST Report, U.S. Army Belvoir Research Development and Engineering Center, Fort Belvoir, VA, (Proj. 7232457), 100 p.; November 1987.

Geyer, R.G. Magnetic susceptibility measurements for mine detection: Some general comments. NIST Report, U.S. Army Belvoir Research Development and Engineering Center, Fort Belvoir, VA (Project No. 7232457) 10 p.; 1987.

Goldman, S. Information theory. New York, NY: Prentice-Hall, Inc.; 1953.

Hancock, J. C.; Wintz, P. A. Signal detection theory. New York, NY; Prentice-Hall, Inc.; 1953.

Hasted, J. B. Aqueous dielectrics. London: Chapman and Hall, 302 p.; 1973.

Hasted, J. B. Liquid water: Dielectric properties. Chapter 7 Water—A comprehensive treatise, I, The physics and chemistry of water. New York: Plenum Press; 1972.

Hasted, J. B. The dielectric properties of water *in* Progress in Dielectrics, Vol. 3., J.B. Birks and J. Hart, eds. New York: John Wiley & Sons; 1961, 101-149.

Hayes, P. K. An on-site method for measuring the dielectric constsnt and conductivity of soils over a one gigahertz bandwidth. The Ohio State University ElectroScience Lab., Dept. of Electrical Engineering; Technical Report 582X-1.

Heiland, C. A. Geophysical exploration. Englewood Cliffs, New Jersey: Prentice Hall; 1940, pp. 310-314.

Hill, D. A. Electromagnetic scattering by buried objects of low contrast. IEEE Trans. Geosci. Remote Sensing; March 1988; GE-26(2), 195-203.

Hill, D. A. Fields of horizontal currents located above the Earth. IEEE Trans. Geosci. Remote Sensing; November 1988; GE-276(6); 726-732.

Hill, D. A. Near-field detection of buried dielectric objects, IEEE Trans. Geosci. Remote Sensing; July 1989; GE-27(4); 364-368.

Hill, D. A.; Cavcey, K. H. Coupling between two antennas separated by a planar interface. IEEE Trans. Geosci. Remote Sensing; July 1987; GE-25(4); 422-431.

Hill, N. E.; Vaughn, W. E.; Price, A. H.; Davies, M. Dielectric properties and molecular behavior. London: Van Nostrand; 1969. 480 p.

Ho, W.; Hall, W.F. Measurements of the dielectric properties of sea water and NaCl solutions at 2.65 GHz. J. Geophys. Res. 78: 6301-6315; 1973.

Ho, W.W.; Love, A.W.; Valle, J.J. Measurements of the dielectric properties of sea water at 1.43 GHz. NASA Contractor Report CR-2458. NASA Langley Research Center, Langley, VA; 1974.

Ho, W.W.; Love, A.W.; VanMelle, M.J. Measurements of the dielectric properties of sea-water at 1.43 GHz. NASA Contractor Report CR-2458. NASA Langley Research Center, Langley, VA; 1974.

Hoekstra, P.; Delany, A. Dielectric properties of soils at UHF and microwave frequencies. J. Geophys. Res. 79; 1974; (No. 11): 1699–1708.

Hogg, R. V.; Craig, A. T. Introduction of mathematical statistics. New York, NY: Macmillan Co.; 1970.

Horner, F. Resonance methods of dielectric measurement at centimeter wavelengths. J. IRE; 1946; 93(III), pp. 55-57.

Horner, F.; Harwood, J. An investigation of atmospheric radio noise at very low frequencies. J. IRE, 1956; 103B(743).

Izadian, J. An underground near-field antenna pattern range. The Ohio State University ElectroScience Lab., Dept. of Electrical Engineering; 1980.

Izadian, J. S. Two dimensional EM-scattering by buried penetrable noncircular cylinders using the method of moments. The Ohio State University; Ph.D. dissertation.

Jay, F., Editor in Chief. IEEE Standard Dictionary of Electrical and Electronics Terms. ANSI/IEEE Std. 100-1984, Third Edition, 1984.

Jedlicka, R.P. Saline soil dielectric measurements. M.S. Thesis, New Mexico State University, NM; 1978.

Jesch, R.L. Dielectric measurements of five different soil textural types as functions of frequency and moisture content. Nat. Bur. Stand. (U.S.) NBSIR 78-896, 26 p.; 1978.

Jones, R. G. Precise dielectric measurements at 35 GHz using an open microwave resonator. Proc. IEEE.; 1976; 123(4), pp. 284-290.

Jones, R. N.; Bussey, H. E.; Little, W. E.; Metzker, R. F. Electrical characteristics of corn, wheat, and soya in the 1-200 MHz range; 1978; Nat. Bur. Stand. (U.S.) NBSIR 78-897.

Jonscher, A.K. The interpretation of non-ideal dielectric admittance and impedance diagrams. Phys. Stat. Solutions (a), 32: 665-676; 1975.

Jonscher, A.K. The universal dielectric response, a review of data and their new interpretation. Chelsea Dielectrics Group, University of London; 1979.

Kennaugh, E. M. The K-pulse concept. IEEE Trans. Ant. Prop.; 1981; AP-29(No. 2).

Kenyon, W.E. Texture effects on megahertz dielectric properties of calcite rock samples. J. Appl. Phys. 55: 3151-3159; 1984.

Kerns, D. M. Plane-wave scattering-matrix theory of antennas and antenna-antenna interactions; 1981; Nat. Bur. Stand. (U.S.) Monogr. 162.

King, R. W.; Smith, G. S. Antennas in matter; fundamentals, theory, and applications. Cambridge, MA: M.I.T. Press; 1981.

Klein, L.A.; Swift, C.T. An improved model for the dielectric constant of sea water at microwave frequencies. IEEE Trans. Ant. Prop. AP-25: 104-111; 1977.

Knight, R.J. The use of complex plane plots in studying the electrical response of rocks. J. Geomag. Geoelectr. 35: 767-776; 1983.

Kogelnik, H.; Li, T. Laser beams and resonators. Proc. IEEE; 1966; 54, pp. 1312-1329.

Kottenstette, J. P.; Steffen, D. A. Planning for short pulse radar experiments; September 30, 1987; Final report for U.S. Army Belvoir Research and Development Center, Fort Belvoir, VA 22060-5606; 109 p.

Kouyoumjian, R. G.; Peters, Jr., L.; Thomas, D. T. A modified geometrical optics method for scattering by dielectric bodies. IEEE Trans.; 1963; LAP-11: 690–703.

Kurosaki, S. The dielectric behavior of water sorbed in silica gel. J. Phys. Chem. 58: 320-324; 1954.

Lane, J.; Saxton, J. Dielectric dispersion in pure polar liquids at very high radio frequencies, III. The effect of electrolytes in solution. Proc., Roy. Soc. 214(A): 531-545; 1952.

Lauber, N. R. Preliminary urban UHF/VHF radio noise intensity measurements in Ottawa, Canada. Proc., 2nd Symp. on EMC; 28-30 June, 1977; Montreux, Switzerland.

Lentz, R. R. Microwave detection of buried objects. Dept. of Electrical & Electronic Engineering, Queen Mary College, Mile End Road, London; May 1976; Contract Report AT-2042-059-RL.

Lentz, R. R. Detection of shallowly buried objects. Electr. Ltrs.; 1976; 12(22): 594–595.

Lerner, R. M. Ground Radar system; 1974; U.S. Patent No. 3,831,173.

Lockner, D.A.; Byerlee, J.D. Complex resistivity measurements of confined rock. J. Geophys. Res. 90: 7837-7847; 1985.

Lundien, J. R. Terrain analysis by EM means: radar responses to laboratory prepared soil samples. U.S. Army Engineer Waterways Experiment Station, Vicksburg, MS; September 1966; Technical Report No. 3-693, Report 2.

Lytle, Jeffrey, R. Mearurement of earth medium electrical characteristics; Techniques, results, and applications; Lawrence Livermore National Laboratory; 1974.

Madden, T.R.; Cantwell, T. Induced polarization, A review, in Mining Geophysics, Vol. 2, A.W. Musgrove, ed., Soc. Explor. Geophys., 373-400; 1967.

Maxwell, J.C. A treatise on electricity and magnetism. Dover Pub.; 1891.

McCafferty, E.; Zettlemayer, A.C. Adsorption of water vapor on α-Fe_2O_3. Faraday Soc. Discussions, Vol. 52; 1971, 239-254.

McWane, P. D. A look at the antenna radiation problem in the time domain. Ohio State University; 1972, Ph.D. dissertation.

Metals Handbook, 8th Edition, (1980), American Society of Metallurgists.

Mie, G. Beiträge Zur Optik Trüber Medien, Speziell Kolloidaler Metallosungen. Annalen der Physik 25, p. 377, (1908).

Morey, 1974; U.S. Patent No. 3,806,795.

Morey, L. Properties of glass. New York: Reinhold Press; 1954.

Nagata, T. Rock magnetism. Tokyo: Maruzen Press; 1961, 350 p.

Nair, N.K.; Thorp, J.M. Dielectric behavior of water sorped in silica gels, Part 1, commercial silica gels and the elimination of dielectric hysteresis. Trans. Faraday Soc. 61: 962-974; 1965.

Nakamura, H.; Mashimo, S.; Wada, A. Precise and easy method of TDR to obtain dielectric relaxation spectra in the GHz region. Japanese J. Appl. Phys.; 1982; 21(7), pp. 1022-1024.

Nicolson, A. M.; Ross, G. F. Measurement of the intrinsic properties of materials by time-domain techniques. IEEE Trans. Instrum. Meas.; 1970; IM-19 (4), pp. 377-382.

Nolan, R. V.; et al. MERADCOM mine detection program: 1960–1980. U.S. Army, Fort Belvoir; May, 1980; Report No. 2294.

Olhoeft, G.R.; Frisillo, A.L.; Strangway, D.W. Electrical properties of lunar soil sample 15301, 38. J. Geophys. Res. 79: 1599-1604; 1974.

Owens, T.E. Cavity detection using VHF hole-to-hole electromagnetic techniques. Paper presented at Symposium on Tunnel Detection, Colorado School of Mines, Golden, CO; 1981.

Pear, Robert. Returning Afghan refugees face peril of millions of land mines. NY Times, 13 August, 1988.

Pelton, W.H.; Ward, S.H.; Hallof, P.G.; Sill, W.R.; Nelson, P.H. Mineral discrimination and removal of inductive coupling with multifrequency IP. Geophysics. 43: 588-609; 1978.

Peters, Jr., L.; Richmond, J. H. Scattering from cylindrical nonhomogeneities in a lossy medium. Radio Science 17; 1982; (No. 5): 973–987.

Peters, Jr., L.; Burrell, G. A.; Tran, H. B. A scattering model for detection of tunnels using video pulse systems. The Ohio State University ElectroScience Lab. Dept. of Electrical Engineering; 1977; Technical Report 4460-3.

Peyrelasse, J.; Boned, C.; LePetit, J. P. Setting up of a time-domain spectroscopy experiment. Application to the study of the dielectric relaxation of pentanol isomers. J. Phys. Sci. Instr.; 1981; 14, pp. 1002-1008.

Probeck, Charles. R & D of a single-channel search head. U.S. Army Fort Belvoir, Contract No. DA-44-009 ENG-1666: (Cook Electric Co., Chicago, IL); February 1956; Tech. Report.

Pottel, R. Water: A comprehensive treatise, Vol. II, Ed. F. Franks, Plenum Press, New York-London, ch. 17; 1973.

Rubin, W. L.; DiFranco, J. B. Radar detection. Electro-technology; April 1964.

Saint-Amant, M.; Strangway, D.W. Dielectric properties of dry geologic materials. Geophysics. 35: 624-645; 1970.

Scott, W. R.; Smith, G. S. Dielectric spectroscopy using monopole antennas of general electrical length. IEEE Trans. Ant. Prop.; July 1986; AP-34(7), pp. 919-929.

Scott, W. R. Dielectric spectroscopy using shielded open.circuited coaxial lines and monopole antennas of general length. Ph.D. thesis, Georgia Inst. Tech.; 1985, 228 p.

Scott, Jr., W. R.; Smith, G. S. Error analysis for dielectric spectroscopy using shielded open-circuited coaxial lines of general length. Ph.D. thesis, School of Electrical Engineering, Georgia Institute of Technology: Atlanta, GA: October, 1985.

Scott, Jr., W. R.; Smith, G. S. Error analysis for dielectric spectroscopy using shielded open-circuited coaxial lines of general length. IEEE Trans. Instrum. Meas.; June 1986; IM-35(2): 130–137.

Shutko, A.M.; Reutov, E.M. Mixture formulas applied in estimation of dielectric and radiative characteristics of soils and grounds at microwave frequencies, IEEE Trans. Geosci. Remote Sensing. GE-20: 29-32; 1982.

Skolnik, M. I. Introduction to radar systems. New York, NY: McGraw-Hill Book Co., Inc.; 1962.

Sluyters-Rehbach, M.; Sluyters, J. H. Sine wave methods in the study of electrode processes, in Electroanalytical Chemistry, Vol. 4, A.J. Bard, ed. New York, NY: Marcel Dekker, 1-128; 1970.

Smith, G. Antenna pattern performance near the interface of a dielectric medium. IEEE APS: 1983.

Smith, G. S. Directive properties of antennas for transmission into a material half-space. IEEE Trans. Ant. Prop. AP-32(3), 1984, pp. 232-246.

Smith, G. S.; King, R. W. P. Electric field probes in material media and their application in EMC. IEEE Trans. Electromagn. Compat.; 1975; EMC-17, pp. 206-211.

Smith, G. S.; King, R. W. P. Electric field probes in material media and their application in EMC. IEEE Trans. Electromagn. Compat.; 1976; EMC-18, p. 130.

Smith, G. S.; Nordgard, J. D. Measurements of the electrical constitutive parameters of materials using antennas. IEEE Trans. Ant. Prop.; 1985; 33(7), pp. 783-792.

Smith, G. S.; Scott, Jr., W. R. The use of emulsions to represent dielectric materials in electromagnetic scale models. IEEE Trans. Ant. Prop. vol. 38, No. 3, March, 1990, pp. 323-334.

Smith, G. S.; Scott, W. R. A simple method for the in situ measurement of the electrical properties of the ground. Paper JA02-3, pages 242-245, 1987 IEEE AP-S International Symposium Digest, June 15-19, 1987, Virginia Tech. (IEEE Catalog No. CH2435-6/87).

Smyth, C.P. Dielectric relaxation times in molecular relaxation processes. London: The Chemical Society, 1-14; 1966.

Spaulding, D. A. International Radio Consultative Committee. Worldwide minimum external noise levels, 0.1 Hz to 100 GHz; 1982; Report No. 670.

Stogryn, A. Equations for calculating the dielectric constant of saline water. IEEE Trans. Microwave Theory Tech. MTT-19: 733-736; 1971.

Suggett, A. Time-domain methods, dielectric and related molecular processes. Chem. Soc. London; 1972; Vol. 1, pp. 101-120.

Tinga, W. R. Generalized approach to multiphase dielectric mixture theory. J. Appl. Phys. 44: 3897-3902; 1973.

Tribuzi, C. A. An antenna for use in an underground (HFW) radar system. The Ohio State University ElectroScience Lab. Dept. of Electrical Engineering; 1977; Technical Report 4460-4.

Tricoles, G.; et al. Near-field electromagnetic detection of mines. General Dynamics Electronics Div. Report No. R-87-013; August 1987, Final Report.

Ulaby, F.T.; Moore, R.K.; Fung, A.K. Microwave remote sensing, Vol. III: From theory to applications. London, England: Addison-Wesley Publishing Co.; 1982.

Van deHulst, H. C. Light scattering by small particles. N.Y.: J. Wiley & Sons, 1957.

Van Gemert, M. J. C. High-frequency time-domain methods in dielectric spectroscopy. Phillips Res. Rpts; 1973; 28, pp. 530-572.

Volakis, J., and Peters, Jr., L. Elimination of undesired natural resonances for improved target identification. Paper presented at International Union of Radio Science, Quebec; 1980.

Volakis, J., and Peters, Jr., L. Improved identification of underground targets using video pulse radars by elimination of undesired natural resonances. IEEE Trans. Ant. Prop.; 1983; AP-31 (No. 2).

Volakis, J. Improved identification of underground targets using video-pulse radars by elimination of undesired natural resonances. M.Sc. thesis, Ohio State University.

von Hippel, A.R. Dielectric materials and applications. New York: The Technology Press of M.I.T. and John Wiley & Sons, 438 p.; 1954.

von Hippel, Arthur R. Dielectrics and waves. New York: John Wiley & Sons; 1954. 284 p.

Wagner, K.W. Erklarung der dielektrischen Nachwirkungsworgange auf Grund Maxwellscher vorstellungen. Archiv. Electrotechnik, 2: 371; 1914.

Wait, J. R. A conducting sphere in a time varying field. Geophy.; 1951; 16, p. 666.

Wait, James R. Mutual electromagnetic coupling of loops over a homogeneous ground. Geophysics XX; 1955; (No. 3): 630–637.

Wald, L. W. Modification of the HFW underground antenna based on experimental studies. The Ohio State University ElectroScience Lab. Dept. of Electrical Engineering: Technical Report 4460-6.

Ward, S. H. Electromagnetic theory for geophysical applications. Mining Geophys.; 1967; II, p. 78.

Watt, A. D.; Maxwell, E. L. Characterization of atmospheric noise from 1 to 100 kHz. Proc. IRE; June 1957: 787.

Webster's Seventh New Collegiate Dictionary. G. & C. Merriam Company, Springfield, MA, 1967.

Wharton, R.P.; Hazen, G.A.; Rau, R.N.; Best, D.L. Electromagnetic propagation logging: advances in technique and interpretation. SPE of AIME Annual Technical Conference and Exhibition (Paper SPE 9267), 21-24; September 1980.

Williams, G.; Watts, D.C. Non-symmetrical dielectric relaxation behavior arising from a simple empirical decay function. Trans. Faraday. Soc. 66: 80-85; 1970.

Williams, W. H.; et al. Elf: Computer automation and error correction for a microwave network analyzer. IEEE Trans. Instrum. Meas.; March 1988; 37(1): 95–100.

Wmyth, C. P. Dielectric relaxation times in molecular relaxation processes. London, the Chemical Society; 1966.

Woodward, P. M. Probability and information theory with application to radar. New York, NY: McGraw-Hill Book Co., Inc.; 1955.

Wyllie, G. Dielectric relaxation and molecular correlation in dielectric and related molecular processes. London; The Chemical Society; 1972.

Young, J. D.; Caldecott, R.; 1976; U.S. Patent No. 3,967,282.

Young, J. D.; Caldecott, R.; 1977; U.S. Patent No. 4,062,010.

International Radio Consultative Committee. Characteristics and applications of atmospheric radio noise data; 1983; Report No. 3220-2.

International Radio Consultative Committee. Worldwide minimum external noise levels, 0.1 Hz to 100 GHz; 1982; Report No. 670.

Measuring Dielectric Constant with the HP 8510 Network Analyzer. Product Note No. 8510-3, Hewlett-Packard Corp., Palo Alto, CA; August 1985.

BL-114A
(5-90)

U.S. DEPARTMENT OF COMMERCE
NATIONAL INSTITUTE OF STANDARDS AND TECHNOLOGY

BIBLIOGRAPHIC DATA SHEET

1. PUBLICATION OR REPORT NUMBER
NISTIR 3982

2. PERFORMING ORGANIZATION REPORT NUMBER
B91-0305

3. PUBLICATION DATE
October 1991

4. TITLE AND SUBTITLE

Quantifying Standard Performance of Electromagnetic-Based Mine Detectors

5. AUTHOR(S)

William L. Gans, Richard G. Geyer, and Wilfred K. Klemperer

6. PERFORMING ORGANIZATION (IF JOINT OR OTHER THAN NIST, SEE INSTRUCTIONS)

U.S. DEPARTMENT OF COMMERCE
NATIONAL INSTITUTE OF STANDARDS AND TECHNOLOGY
BOULDER, COLORADO 80303-3328

7. CONTRACT/GRANT NUMBER

8. TYPE OF REPORT AND PERIOD COVERED

9. SPONSORING ORGANIZATION NAME AND COMPLETE ADDRESS (STREET, CITY, STATE, ZIP)

U.S. Army Belvoir Research, Development, and Engineering Center
Ft. Belvoir, VA 22060-5606

10. SUPPLEMENTARY NOTES

11. ABSTRACT (A 200-WORD OR LESS FACTUAL SUMMARY OF MOST SIGNIFICANT INFORMATION. IF DOCUMENT INCLUDES A SIGNIFICANT BIBLIOGRAPHY OR LITERATURE SURVEY, MENTION IT HERE.)

This is a final report to sponsor on work performed by National Institute of Standards and Technology (NIST) personnel from January 1, 1985 to December 31, 1990. An overview of the theory of the electromagnetic properties of soils is presented along with a brief review of existing technologies for the detection of buried objects using electromagnetics. The critical electromagnetic performance factors for portable EM mine detectors that NIST has identified are presented, along with a discussion of measurement systems for measuring the constitutive properties of soil and mine-like materials. Recommendations are then presented for a measurement system configuration that should meet most of the Army's requirements. A recommended mine detector testing strategy is then presented along with a set of instructions for specific tests and an algorithm for comparatively scoring the performance of detectors. The tests and the scoring algorithm are as specific and as detailed as is possible at this stage of development. Last, a section is included that contains NIST's recommendations for the test data that should be archived.

12. KEY WORDS (6 TO 12 ENTRIES; ALPHABETICAL ORDER; CAPITALIZE ONLY PROPER NAMES; AND SEPARATE KEY WORDS BY SEMICOLONS)

buried object; constitutive properties; conductivity; dielectric constant; dielectric loss; electromagnetic detection; mine; mine detector; permeability; permittivity; remote sensing; sensor; target

13. AVAILABILITY

[X] UNLIMITED

[ ] FOR OFFICIAL DISTRIBUTION. DO NOT RELEASE TO NATIONAL TECHNICAL INFORMATION SERVICE (NTIS).

[ ] ORDER FROM SUPERINTENDENT OF DOCUMENTS, U.S. GOVERNMENT PRINTING OFFICE, WASHINGTON, DC 20402.

[X] ORDER FROM NATIONAL TECHNICAL INFORMATION SERVICE (NTIS), SPRINGFIELD, VA 22161.

14. NUMBER OF PRINTED PAGES
184

15. PRICE
A09

ELECTRONIC FORM

IR 3983

UNAVAILABLE FOR BINDING


AMERICAN BINDERY
2
5-94